UNIVERSIDAD DE CÓRDOBA

Junta de Andalucía
Consejería de Agricultura, Ganadería, Pesca y Desarrollo Sostenible
INSTITUTO DE INVESTIGACIÓN Y FORMACIÓN AGRARIA Y PESQUERA

DESARROLLO DE METODOLOGÍAS ANALÍTICAS PARA LA CARACTERIZACIÓN DE LA CALIDAD Y LA TRAZABILIDAD ALIMENTARIA

DEVELOPMENT OF ANALYTICAL METHODOLOGIES FOR FOOD QUALITY CHARACTERIZATION AND TRACEABILITY

Autor:

José Manuel Muñoz Redondo

Directores:

Dr. José Manuel Moreno Rojas

Dra. Gema Pereira Caro

Programa de Ingeniería Agraria, Alimentaria, Forestal y de Desarrollo Rural Sostenible por la Universidad de Córdoba y la Universidad de Sevilla

Fecha de depósito en el Idep: 28/06/2021

TITULO: *DESARROLLO DE METODOLOGÍAS ANALÍTICAS PARA LA CARACTERIZACIÓN DE LA CALIDAD Y LA TRAZABILIDAD ALIMENTARIA*

AUTOR: *José Manuel Muñoz Redondo*

Campus de Rabanales
Ctra. Nacional IV, Km. 396 A
14071 Córdoba

https://www.uco.es/ucopress/index.php/es/
ucopress@uco.es

TÍTULO DE LA TESIS: Desarrollo de metodologías analíticas para la caracterización de la calidad y la trazabilidad alimentaria

DOCTORANDO: José Manuel Muñoz Redondo

INFORME RAZONADO DE LOS DIRECTORES DE LA TESIS

La tesis doctoral llevada a cabo por D. José Manuel Muñoz Redondo supone un avance en el estudio de una temática de actualidad: la calidad y trazabilidad alimentaria. Las metodologías analíticas que se desarrollan y sus aplicaciones en casos reales pueden suponer un beneficio para el sector agroalimentario.

En este trabajo de investigación se desarrollan, por un lado, herramientas analíticas avanzadas para caracterizar la calidad aromática de bebidas con gran relevancia en el sector industrial español, como son el vino y el Brandy de Jerez. Estas técnicas se aplican a casos reales para estudiar el impacto de etapas específicas del proceso de producción sobre el perfil aromático del producto final, tales como la maceración pre-fermentativa, el tiempo de crianza o el uso de distintas estrategias de fermentación. Los conocimientos generados en este campo ayudan a comprender mejor los complejos mecanismos detrás de la experiencia sensorial de estas bebidas.

Asimismo, se desarrollan herramientas analíticas y estadísticas para estudiar la trazabilidad de frutas tropicales (mango y aguacate) producidas en Andalucía, cuyo propósito es acogerse a una Indicación Geográfica Protegida (IGP). Los positivos resultados obtenidos en esta investigación ponen de manifiesto el potencial de las técnicas desarrolladas, basadas en isótopos estables y análisis multi-elemental, para distinguir el producto nacional del producido en otros países, proporcionando mecanismos para asegurar su origen y proteger la producción andaluza.

Los resultados de esta investigación han dado lugar a diversas comunicaciones a congresos internacionales y la publicación de 6 artículos científicos en revistas internacionales de alto índice de impacto y 3 en revisión. Además, una parte de la investigación de esta tesis se desarrolló mediante una estancia internacional de 3 meses en la Fondaziones E. Mach (Italia).

Por todo ello, se autoriza la presentación de la tesis doctoral.

En Córdoba, 28 de Junio de 2021

MORENO ROJAS JOSE MANUEL - 80146931G
Firmado digitalmente por MORENO ROJAS JOSE MANUEL - 80146931G
Fecha: 2021.06.28 10:26:22 +02'00'

Fdo.: José Manuel Moreno Rojas

PEREIRA CARO MARIA GEMA - 77337783F
Firmado digitalmente por PEREIRA CARO MARIA GEMA - 77337783F
Fecha: 2021.06.28 11:40:07 +02'00'

Fdo.: Gema Pereira Caro

TÍTULO DE LA TESIS:

Desarrollo de metodologías analíticas para la caracterización de la calidad y la trazabilidad alimentaria

DOCTORANDO:

José Manuel Muñoz Redondo

INFORME RAZONADO DEL TUTOR DE LA TESIS

(se hará mención a la evolución y desarrollo de la tesis, así como a trabajos y publicaciones derivados de la misma).

Dña. María Isabel López Infante, profesora asociada del Departamento de Bromatología y Tecnología de los Alimentos, del Área de Tecnología de los Alimentos, como tutora del mencionado doctorando:

INFORMA

Que el presente trabajo de investigación titulado “Desarrollo de metodologías analíticas para la caracterización de la calidad y la trazabilidad alimentaria” realizado por el doctorando D. José Manuel Muñoz Redondo, bajo la dirección del Dr. José Manuel Moreno Rojas y la Dra. Gema Pereira Caro, reúne los requisitos para ser presentado para su exposición y defensa como Tesis Doctoral de la Universidad de Córdoba y ratifico la consideración favorable emitida por los Directores de la tesis doctoral a tal efecto.

Por todo ello, se autoriza la presentación de la tesis doctoral.

Córdoba, 22 de Junio de 2021

Firma del tutor de la Universidad de Córdoba

Fdo.: María Isabel López Infante

Mención de doctorado internacional

La presente Tesis Doctoral cumple con los requisitos establecidos por la Universidad de Córdoba para la obtención del título de Doctor con Mención Internacional, concurriendo las siguientes circunstancias de obligado cumplimiento:

- Estancia internacional de 3 meses llevada a cabo durante el periodo de formación de doctorado, entre el 1 de octubre y el 31 de diciembre de 2018, en el departamento de calidad alimentaria y nutrición del centro de investigación e innovación Fondazione Edmund Mach, bajo la supervisión de la Dra. Federica Camin. El trabajo de investigación de dicha estancia se desarrolló bajo el título “Isotopic characterization to assure the origin of tropical food".

- Parte de la Tesis Doctoral se ha redactado y presentado en inglés, lengua habitual para la comunicación científica en el campo de investigación de la presente tesis.

- La Tesis Doctoral ha sido informada por dos expertos doctores pertenecientes a alguna institución de educación superior o instituto de investigación no española:

    - Dra. Nives Ogrinc (Eslovenia)
    - Dr. José Sousa Câmara (Portugal)

- Un miembro del tribunal de la tesis es un doctor vinculado a una institución de educación superior o centro de investigación no español: Luana Bontempo (Italia)

- La Tesis Doctoral incluye 6 artículos publicados en revistas de alto impacto JCR, todas situadas en el primer cuartil de su categoría, indicados en la sección siguiente.

El doctorando

Fdo.: José Manuel Muñoz Redondo

Publicaciones incluidas en la tesis doctoral

Journal	Título	Año	Categoría	Índice de impacto	Cuartil
Food Chemistry	The influence of pre-fermentative maceration and ageing factors on ester profile and marker determination of Pedro Ximenez sparkling wines	2017	Food Science & Technology	4.946	Q1 (2017): 7/133 (95.11 %)
Journal of Agricultural and Food Chemistry	Quantitative Profiling of Ester Compounds Using HS-SPME-GC-MS and Chemometrics for Assessing Volatile Markers of the Second Fermentation in Bottle	2017	Agriculture, Multidisciplinary	3.412	Q1 (2017): 2/57 (97.37 %)
Talanta	Multivariate optimization of headspace solid-phase microextraction coupled to gas chromatography-mass spectrometry for the analysis of terpenoids in sparkling wines	2019	Chemistry, Analytical	5.339	Q1 (2019): 10/81 (87.79 %)
Journal of Agricultural and Food Chemistry	Impact of Sequential Inoculation with the Non-*Saccharomyces T. delbrueckii* and *M. pulcherrima* Combined with *Saccharomyces cerevisiae* Strains on Chemicals and Sensory Profile of Rosé Wines	2021	Agriculture, Multidisciplinary	4.192	Q1 (2019): 4/58 (93.97 %)
Food Control	Tracing the geographical origin of Spanish mango (Mangifera indica L.) using stable isotopes ratios and multi-element profiles	2021	Food Science & Technology	4.258	Q1 (2019): 19/139 (86.69 %)
Fermentation	A Statistical Workflow to Evaluate the Modulation of Wine Metabolome and Its Contribution to the Sensory Attributes	2021	-	Disponible en 2021	-
Food Chemistry (bajo revisión)	Multi-element and stable isotopes characterization of commercial avocado fruit (Persea americana Mill) with origin authentication purposes	2021	Food Science & Technology	6.306	Q1 (2019): 6/139 (96.04 %)
Food Chemistry (enviado)	Multivariate optimization of headspace solid-phase microextraction coupled to gas chromatography-mass spectrometry for the analysis of esters in brandies	2021	Food Science & Technology	6.306	Q1 (2019): 6/139 (96.04 %)
Journal of Agricultural and Food Chemistry (enviado)	Influence of cold stabilization and filtration in the ester profile of Brandy de Jerez	2021	Agriculture, Multidisciplinary	4.192	Q1 (2019): 4/58 (93.97 %)

Financiación

La presente Tesis Doctoral ha sido realizada en el Instituto Andaluz de Investigación y Formación Agraria, Pesquera, Alimentaria y de la Producción Ecológica (IFAPA), centro Alameda del Obispo (Córdoba) y ha sido financiada a través de distintos proyectos:

- Proyecto de investigación complementario al Transforma "Vid y Vino" (PP.AVA.AVA201301.3), otorgado por IFAPA (Investigador Principal: Dra. Zulema Piñeiro Méndez).
- Investigación e innovación tecnológica en vitivinicultura (PP.AVA.AVA201601.3 / PR.AVA.AVA2019.016), otorgado por IFAPA (Investigador Principal: Dr. Enrico Cretazzo).
- Caracterización de alimentos y nuevos productos elaborados: potencial saludable, organoléptico y trazabilidad alimentaria. Estrategias de diversificación y reclamo competitivo (PR.AVA.AVA201601.20), otorgado por IFAPA (Investigador Principal: Dr. José Manuel Moreno Rojas)
- Bodegas Fundador, S.L.U a través del proyecto FEDER-Innterconecta: Factores que influyen en la calidad del Brandy y nuevos sistemas de elaboración del mismo, desde el viñedo al envasado (BESTBRANDY).
- *Accordo di Programma* 2018-2019, unidad de trazabilidad de la Fondazione Edmun Mach (Italia)

El autor de la Tesis Doctoral ha disfrutado de varios contratos laborales en el Centro IFAPA Alameda del Obispo (Córdoba):

- 01/06/2016 a 31/05/2018: Contratado laboral en IFAPA Alameda del Obispo (Córdoba) en el marco de las ayudas para la Promoción de Empleo Joven e Implantación de la Garantía Juvenil en I+D+i del Ministerio de Economía y Competitividad. Contrato núm. 6 de la Resolución 22 de octubre de 2015 (BOJA núm. 211, del 29 de octubre).
- 01/06/2018 a 31/12/2018: Contratado laboral en IFAPA Alameda del Obispo (Córdoba) en el marco de una convocatoria de contratos laborales para proyectos específicos de I+D+F. Contrato núm. 8 de la Resolución 6 de noviembre de 2017 (BOJA núm. 217, pp 48-56).
- 14/01/2019 a 14/07/2019: Contratado laboral en IFAPA Alameda del Obispo (Córdoba) en el marco de una convocatoria de contratos laborales para

proyectos específicos de I+D+F. Contrato núm. 1 de la Resolución 8 de agosto de 2018 (BOJA núm. 158, pp 86-93).

- 15/07/2019 a actualidad: Contratado laboral en IFAPA Alameda del Obispo (Córdoba) en el marco de una convocatoria de contratos laborales para proyectos específicos de I+D+F. Contrato núm. 14 de la Resolución 14 de febrero de 2019 (BOJA núm. 37, pp 20-30).

Agradecimientos

En primer lugar, quiero agradecer el apoyo de mis directores de tesis, el Dr. José Manuel Moreno Rojas y la Dra. Gema Pereira Caro, por haberme acompañado durante todos estos años, y a Isabel López Infante por la tutorización de esta tesis.

Quiero expresar mi especial agradecimiento a José Manuel, por tu paciencia, confianza y dedicación. Por brindarme esta oportunidad y haber sabido acompañarme en los momentos más duros. Por tu capacidad de comprenderme y darme confianza en lo que hago. Por compartir tus conocimientos y guiarme en este proceso de formación que establecerá las bases de lo que soy. Nada de esto hubiera sido posible sin ti.

Gracias a mi familia, a mis padres, a mi hermano y a mi cuñada. Gracias por lo que me habéis enseñado y por apoyarme cuando decidí dedicarme a la investigación. Todo lo que he conseguido y soy es gracias a vosotros.

Al patrón, José Luis, por aguantar mi locura hablando mis idiomas inventados y por los momentos que hemos vivido en el despacho. Gracias también a Raquel, por tu dedicación y ayuda con mi tesis. A José Carlos, por su alegría contagiosa que hace más llevaderos los días duros. A Alicia, Mónica, Elsy y Anna, por los cafés y charlas que nos echamos durante el café y por vuestra disponibilidad.

Gracias a Sacha, por ser siempre generosa y ayudarme con todo lo que te he pedido. Por ser tan paciente conmigo, escucharme y estar siempre a mi lado, y por tantas cosas que soy incapaz de describir con palabras.

Gracias a mis amigos, por haberme acompañado hasta este lugar y por los momentos vividos y que nos quedan por compartir.

Agradecer al Instituto Andaluz de Investigación y Formación Agraria, Pesquera, Alimentaria y de la Producción Ecológica (IFAPA) por los contratos que han hecho posible la realización de esta tesis.

Abreviaturas

º	grado
%	tanto por cien
‰	tanto por mil
α	alfa
γ	gamma
$\delta^{13}C$	delta 13 del carbono
$\delta^{15}N$	delta 15 del nitrógeno
$\delta^{34}S$	delta 34 del azufre
$\delta^{18}O$	delta 18 del oxígeno
$\delta^{2}H$	delta 2 del hidrógeno
µL	microlitro
^{14}N	nitrógeno 14
^{15}N	nitrógeno 15
CAR	carboxen
CE	Comisión Europea
CO2	dióxido de carbono
CV	cross-validation
DA	análisis discriminante
DIABLO	Data Integration Analysis and Biomarker discovery using Latent cOmponents
DOP	Denominación de Origen Protegida
DVB	divinilbenceno
EDTA	ácido etilendiaminotetraacético
ETG	Especialidad Tradicional Garantizada
eV	electrón voltio
FAO	Organización de las Naciones Unidas para la Alimentación y la Agricultura
FAOSTAT	base de datos de la FAO
GC	cromatografía de gases
HCA	análisis de agrupamiento jerárquico
HPLC	cromatografía de líquidos de alta eficacia
HS	espacio de cabeza

Hz	hercio
IFAPA	Instituto Andaluz de Investigación y Formación Agraria, Pesquera, Alimentaria y de la Producción Ecológica
IGP	Indicación Geográfica Protegida
INE	Instituto Nacional de Estadística
Kg	kilogramo
k-NN	k - vecinos más cercanos
LDA	análisis discriminante linear
m	metro
m/z	relación masa-carga
MAPAMA	Ministerio de Agricultura, Pesca, Alimentación y Medio Ambiente de España
Matlab	lenguaje de cálculo técnico desarrollado por MathWorks
METLIN	METLIN Metabolomics Database
min	minuto
mL	mililitro
MS	espectrometría de masas
N	norte
N2	nitrógeno molecular
NaCl	cloruro de sodio
NaOH	hidróxido de sodio
NIR	infrarrojo cercano
NIST	National Institute of Standards and Technology
NMR	resonancia magnética nuclear
nº	número
O	oeste
ºBrix	grados brix
OMS	Organización Mundial de la Salud
p.ej.	por ejemplo
Pa	pascal
PCA	análisis de componentes principales
PDMS	polidimetilsiloxano
PLS	mínimos cuadrados parciales

PX	variedad de uva Pedro Ximénez
ppm	partes por millón
QDA	análisis discriminante cuadrático
R	entorno de programación libre
rCCA	regularized Canonical Correlation Analysis
RD	Real Decreto
RDA	análisis discriminante regularizado
ROC	característica operativa del receptor
s	segundo
SIMCA	análisis de clases por modelado suave independiente
sPLS-DA	análisis discriminante por mínimo cuadrados parciales versión *sparse*
SPME	micro-extracción en fase sólida
SVM	máquinas de soporte vectorial
SY	variedad de uva Syrah
v.	version
v/v	volumen/volumen
V-PDB	Vienna Pee Dee Belemnite

Resumen

La calidad es un tema de actualidad con creciente importancia en la industria alimentaria por sus implicaciones en las preferencias de los consumidores. Por esta razón, las empresas invierten sus recursos en desarrollar nuevos productos o bien modificar ciertas etapas de su proceso de elaboración con el fin de obtener alimentos con una calidad diferenciada. La producción de alimentos de alta calidad viene acompañada de un mayor valor añadido, haciendo atractivo para sus competidores su falsificación y venta fraudulenta, lo cual puede acarrear un impacto económico negativo y daños de imagen.

En las últimas décadas, el desarrollo de técnicas analíticas y quimiométricas ha supuesto un gran avance en el estudio de la calidad y trazabilidad de alimentos, con impactos positivos sobre la industria alimentaria. Por un lado, el estudio de la composición de los alimentos hace posible comprender los complejos mecanismos que modulan las características organolépticas de los alimentos, siendo la calidad aromática uno de los atributos más apreciados por los consumidores por sus implicaciones en la experiencia sensorial.

El aroma es especialmente apreciado en bebidas como el vino y el brandy. Por esta razón, durante años se ha tratado de identificar compuestos aromáticos clave que están detrás de las características sensoriales de este tipo de bebidas. Sin embargo, debido a su complejidad, esta tarea sigue siendo objeto de estudio y aún no están claros todos los mecanismos que producen unas características sensoriales específicas.

En esta Tesis Doctoral, se desarrollaron herramientas analíticas para la determinación del perfil de compuestos volátiles en muestras de vinos espumosos y rosados, y se aplicaron para estudiar el efecto de distintas etapas de elaboración sobre la calidad aromática final de los vinos obtenidos. Mediante el uso de herramientas quimiométricas se logró identificar los compuestos que sufrieron un mayor cambio como consecuencia de estas etapas, postulándose como potenciales marcadores.

Por otro lado, se optimizó y validó un método para la determinación de ésteres en brandies y se aplicó para estudiar la modulación de estos compuestos en Brandy de Jerez elaborado de Solerajes (sistemas de envejecimiento) con distintos tiempos de crianza promedio y tras un proceso de estabilización (por frio y filtración y a temperatura ambiente). Los resultados mostraron el fuerte impacto de ambas etapas de elaboración y permitieron constatar los principales cambios en esta familia de compuestos.

Finalmente, se abordó la trazabilidad alimentaria mediante el desarrollo de una metodología analítica basada en los isotopos estables de 5 bioelementos (C, N, S, O y H), el perfil multi-elemental y técnicas quimiométricas para identificar los mangos y

aguacates producidos en la franja costera de Andalucía, cuyo propósito es acogerse a una Indicación Geográfica Protegida. Los resultados mostraron la capacidad de ambas técnicas analíticas de manera individual y conjuntamente para identificar con altos índices de acierto los mangos y aguacates producidos en Andalucía.

Abstract

Food quality is a current topic with growing importance in the food industry due to its implications on consumer preferences. For this reason, companies destinate resources to develop new products or modifying certain stages of the production process to obtain food stuffs with differentiated quality. The production of high-quality food stuffs is linked to a higher added value, making its counterfeiting and fraudulent sale attractive for competitors. This may have a negative economic impact and image damage.

In recent decades, the development of analytical and chemometric techniques has meant a great advance in the study of food quality and traceability, with a positive impact on the food industry. On the one hand, the study of food composition makes it possible to understand the complex mechanisms that modulate the organoleptic characteristics of foods, aromatic quality being one of the attributes most appreciated by consumers due to its implications in the sensory experience.

The aroma is especially appreciated in beverage such as wine and brandy. Many studies tried to identify key aromatic compounds that are behind the sensory characteristics of these beverages. However, due to its high complexity all the mechanisms that produce specific sensory characteristics are not clear, this task being still under study.

In this Doctoral Thesis, several analytical techniques were developed to determine the profile of volatile compounds in sparkling and rosé wines, and they were applied to study the effect of different stages of production over the final aromatic quality of the wines obtained. The use of chemometric tools made it possible to identify the compounds that underwent greater changes as a consequence of these production stages, being selected as potential markers.

On the other hand, a method for the determination of esters in brandies was optimized and validated, and then applied to study the modulation of these compounds in Brandy de Jerez from *Solerajes* (aging systems) with different average ageing times and after a stabilization process (cold stabilization and stabilization at room temperature). The results showed the main changes in this family of compounds related to these production stages.

Finally, food traceability was addressed through the development of an analytical methodology based on the stable isotopes of 5 bioelements (C, N, S, O and H), the multi-elemental profile and chemometric techniques to identify the mangoes and avocados produced in the coastal strip of Andalusia, whose purpose is to benefit from a Protected Geographical Indication. The results show the high capacity of both analytical techniques individually and in combination to identify the mangoes and avocados produced in Andalusia with high success rates.

Índice

Introducción

La producción de alimentos y bebidas es la principal actividad industrial manufacturera de la Unión Europea. En el año 2018 alcanzó un valor de cifra de negocio de 1,205,000 millones de euros (MAPAMA, 2020), lo cual representó el 15.2 % del total del tejido industrial manufacturero. Dentro de este sector, España ocupó el quinto puesto con un volumen de 125,841.8 millones de euros (9.7 %), por detrás de Francia (17.7 %), Alemania (17,5%), Italia (11,46%) y Reino Unido (9,9%).

En un mercado cada vez más globalizado y especializado, las empresas de este sector se han visto obligadas al desarrollo y evolución continua de sus productos para mantener una posición competitiva. Esto a su vez ha tenido un impacto importante sobre la disponibilidad de productos para los consumidores, que cada vez cuentan con una gama más amplia para elegir. De manera que, conceptos como “calidad” y “seguridad” han adquirido un enorme protagonismo en el proceso de elección de los compradores (Omar, 2013).

La calidad y seguridad alimentaria son un tema de actualidad de creciente importancia tanto en debates públicos, como en política alimentaria, industria y, también en la investigación. Ambos términos se utilizan con frecuencia de manera independiente, aunque la seguridad alimentaria se puede considerar como uno de los aspectos básicos de la calidad.

De acuerdo a la definición que ofrece la Ley 28/2015, de 30 de julio, para la defensa de la calidad alimentaria, ésta se define como el “conjunto de propiedades y características de un producto alimenticio o alimento relativas a las materias primas o ingredientes utilizados en su elaboración, a su naturaleza, composición, pureza, identificación, origen, y trazabilidad, así como a los procesos de elaboración, almacenamiento, envasado y comercialización utilizados y a la presentación del producto final, incluyendo su contenido efectivo y la información al consumidor final especialmente el etiquetado”.

Esta descripción engloba aspectos objetivos y medibles. Una de las principales propiedades que definen la calidad de los alimentos de acuerdo a esta definición son sus características organolépticas, siendo además uno de los mayores atractivos que guía la decisión de comprar de los consumidores. Estas propiedades están íntimamente relacionadas con su composición química, y son resultado de la presencia de distintos compuestos volátiles y no volátiles con diversas estructuras químicas y fisicoquímicas (Longo & Sanromán, 2006). Por esta razón, el estudio de la composición química de los alimentos supone una herramienta de gran valor para entender los mecanismos que

producen propiedades organolépticas positivas, de manera que puedan ser controladas o favorecidas durante el proceso de elaboración.

La calidad alimentaria también puede tener un aspecto subjetivo que engloba términos culturales, sociales y ambientales (Cerri et al., 2019). De manera que un mismo alimento puede ser percibido con distinta calidad en función del consumidor. Algunos ejemplos son la preferencia de ciertos consumidores hacia marcas concretas, hacia productos elaborados en una región geográfica específica, o alimentos obtenidos con un proceso de elaboración particular (ecológicos).

En este sentido, la política de calidad de la Unión Europea tiene entre sus principales objetivos salvaguardar las denominaciones de productos singulares, con el fin de promover sus características únicas, asociadas a una localización geográfica o un método de producción tradicional. Para ello, dispone de sellos de calidad (Figura 1) que reconocen y protegen las denominaciones de ciertos productos alimentarios relacionados con una zona geográfica y un método de producción, como son la Denominación de Origen Protegida (DOP) y la Indicación Geográfica Protegida (IGP). Mientras que la Especialidad Tradicional Garantizada (ETG) hace referencia a métodos de producción tradicional.

Figura 1. Sellos de calidad de la Unión Europea. De izquierda a derecha: DOP, IGP y ETG

El uso de estos sellos asegura a los consumidores la calidad del producto, que verifica la elaboración de acuerdo a las especificaciones de su Consejo Regulador. Los sellos de calidad son además una potente herramienta de *marketing*, repercutiendo en un mayor valor añadido del producto. Esto hace atractiva su imitación y venta fraudulenta por parte de otras empresas competidoras, pudiendo dañar seriamente su reputación. Por esta razón, se necesitan mecanismos de control que verifiquen el origen de estos productos alimentarios.

En los últimos años, el desarrollo de diferentes técnicas analíticas ha supuesto una estrategia con gran potencial para autentificar el origen de los alimentos, siendo algunas de las más utilizadas para este propósito la cromatografía, espectrometría de masas, espectrometría de masas de relaciones isotópicas, espectroscopia, análisis elemental, análisis sensorial y las técnicas moleculares, que son a su vez frecuentemente combinadas con técnicas bioinformáticas (Danezis et al., 2016).

En base a lo expuesto, la investigación de la presente Tesis Doctoral se ha centrado en el desarrollo y aplicación de herramientas analíticas para el estudio de la calidad (vinos y brandies), y la trazabilidad (aguacates y mangos) de diferentes alimentos.

1. Calidad aromática de bebidas

1.1. El vino

La producción de alimentos y bebidas fermentadas tales como el vino, la cerveza o el pan, ha jugado un papel clave en el desarrollo de la sociedad humana. El vino es uno de los productos más diferenciados dentro de la industria alimentaria y ha estado especialmente presente en el mundo occidental a lo largo de los años, con gran relevancia en el plano económico, cultural y social. De acuerdo con el Reglamento UE 1308/2013, esta bebida se define como "el producto obtenido exclusivamente por fermentación alcohólica, total o parcial, de uva fresca, estrujada o no, o de mosto de uva", debiendo tener un grado alcohólico y una acidez dentro del rango establecido en este reglamento, que varía en función de la zona de producción de la uva, adscripción a una denominación o indicación de origen protegida, o excepciones que pueda establecer la Comisión.

En la actualidad es una de las bebidas de mayor consumo en el mundo, alcanzando la cifra de 246 millones de hectolitros en 2019 de acuerdo a la Organización Internacional del Vino (OIV, 2019). En 2020, la producción mundial de vino se estimó en 258 millones de hL, siendo los principales países productores Italia (47.2 millones de hL), Francia (43.9 millones de hL) y España (37.5 millones de hL), que concentraron alrededor del 50 % de la producción mundial (OIV, 2020).

1.1.1. Vinos espumosos

El vino espumoso es un vino que contiene burbujas de dióxido de carbono de forma natural como consecuencia de una segunda fermentación. Hasta finales del siglo XVII, los enólogos franceses trataban de eliminar de sus vinos estas burbujas, ya que provocaban la explosión de las botellas. Sin embargo, un aumento en la preferencia por estos vinos espumosos por parte de los británicos, y en particular de la realeza, llevó a mejorar el proceso de captura deliberada de estas burbujas para producir vinos espumosos de calidad. Este proceso se generalizó principalmente en la región francesa de La Champaña y con el tiempo se extendió a otras áreas como España, Italia, Alemania, Portugal, Sudáfrica, Estados Unidos de América, Reino Unido y Australia (Jones et al., 2014).

Existen principalmente dos métodos de elaboración de vinos espumosos: método Tradicional (también llamado *Champenoise*, pero esta denominación queda restringida a los vinos producidos en la región de la Champaña) y método Charmat, que varía en función de la tecnología de producción utilizada. En el primero, la segunda fermentación se realiza en depósitos de acero inoxidable presurizados, mientras que en el método

Tradicional, la segunda fermentación se lleva a cabo en la botella, seguida de un proceso de crianza sobre lías que produce cambios en la composición de lípidos, carbohidratos, nucleótidos, aminoácidos, péptidos, manoproteínas y compuestos volátiles, como consecuencia de procesos de autólisis (Ubeda et al., 2019). La calidad final de los vinos espumosos depende de varios parámetros, destacando las características de la espuma (tamaño de burbuja, persistencia, espumabilidad o agresividad en boca), color, acidez, y el aroma (Ubeda et al., 2019).

Entre los vinos espumosos más reconocidos y consumidos a nivel mundial se encuentran el Champagne y el Cava, ambos acogidos a una denominación de origen protegida, por lo que su producción está restringida a una zona geográfica (Figura 2).

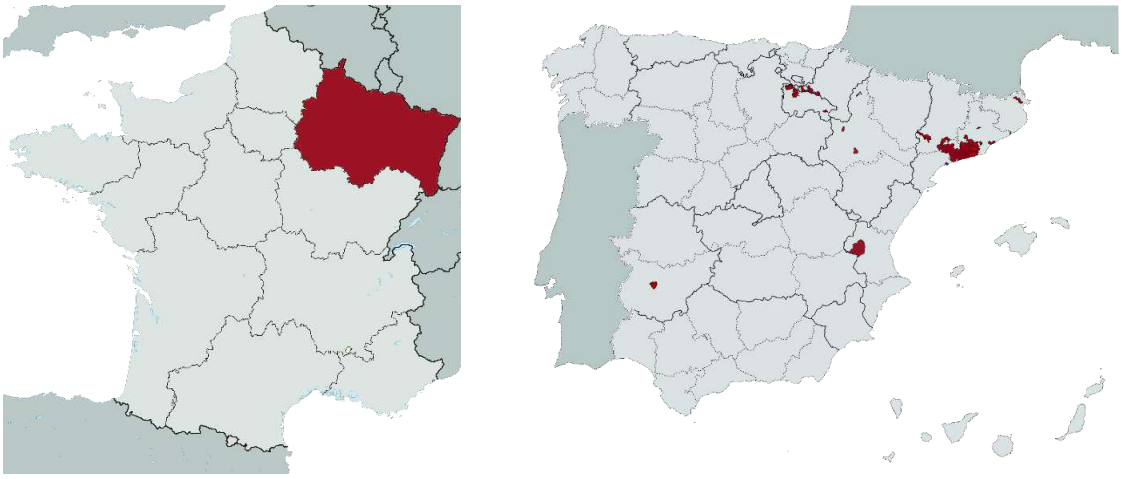

Figura 2. Mapa con las localizaciones (marcadas en rojo) en las que está autorizada la elaboración de Champagne (izquierda) y Cava (derecha) de acuerdo con lo establecido en sus respectivas denominaciones de origen

El consumo de estos vinos ha estado tradicionalmente asociado a fechas especiales, tales como celebraciones o períodos festivos. Sin embargo, esta tendencia ha cambiado en los últimos años hacia un consumo más regular, repercutiendo en una mayor demanda y producción de vinos espumosos. Esto, unido a su alto impacto económico, ha captado la atención de nuevos productores de regiones que no son tradicionalmente productoras de este tipo de vino, entre las cuales se encuentra Andalucía.

1.1.2. Vinos rosados

No existe una definición específica de vino rosado, ya que tanto la Nomenclatura Combinada como la normativa europea sobre el sector vitivinícola solo diferencian un vino blanco de un vino no blanco. Sin embargo, a pesar de que no hay una definición

precisa de vino rosado, existen distintos métodos de elaboración que se pueden dividir en cuatro tipos en función de la práctica enológica utilizada (OIV, 2015):

- **Prensado directo con maceraciones muy cortas**: consiste en el prensado directo de la uva entera o despalillada inmediatamente después de la vendimia y un tiempo corto de maceración con los hollejos (menos de 2 horas) hasta obtener el tono rosado claro. El mosto es separado de los hollejos para el proceso de fermentación (fermentación en virgen), de manera análoga a los vinos blancos.
- **Rosado de maceración de hollejos:** se elabora normalmente a partir de uvas tintas, que se someten a un período de maceración relativamente largo (más de 2 horas) antes de la fermentación alcohólica, con el fin de liberar los componentes del hollejo y la pulpa, permitiendo obtener un tono rosado intenso. El mosto también es separado de los hollejos para el proceso de fermentación.
- **Método *Saignée***: se elabora normalmente a partir de uvas tintas que se someten a un período de maceración relativamente largo (más de 2 horas) antes de la fermentación alcohólica, con el fin de liberar los componentes de la piel y la pulpa hasta el tono rosado deseado. Parte del mosto se separa para la elaboración del vino rosado, mientras que el resto continúa la maceración y fermentación para producir vino tinto.
- **Mezcla de mostos o vinos blancos y tintos**: esta práctica está sujeta a diferentes regulaciones según el país. En la actualidad, la Unión Europea no la autoriza para la elaboración de vinos sin Indicación Geográfica, excepto para la producción de vino espumoso. Sin embargo, se utiliza ampliamente en el resto del mundo.

Mientras el consumo de los vinos blancos y tintos se ha estancado desde comienzos del milenio, el de los vinos rosados no ha parado de aumentar en los últimos años hasta alcanzar un 10 % del consumo mundial de vinos en 2018, con 25.6 millones de hL. Esto ha supuesto un aumento de más del 28 % entre 2002 y 2018, situándose Francia como el país con mayor consumo de este tipo de vinos (35 % del consumo mundial), que ha triplicado su consumo en los últimos 25 años.

Las razones detrás de estas cifras están claramente ligadas a un cambio de paradigma en el consumo de vino. Uno de los aspectos que han tenido un mayor impacto a este respecto es la apariencia visual y la imagen de asociación al placer que se ha conseguido a través de herramientas de *marketing*: “moderno y transgresor, rompe los códigos de un universo reservado sólo a los entendidos”, “su color pálido es agradable

y da la impresión de que contiene menos alcohol que el vino tinto" o "afrutado, seco, bajo en alcohol, un vino fácil de entender (y de beber); en definitiva, un vino sofisticado y de gran calidad" (Peres et al., 2020). A partir de estas observaciones, los millennials que aspiran a un estilo de vida opulento y epicúreo han adoptado este producto, identificándolo como un símbolo accesible de lujo que responde a su deseo de beber algo diferente de sus padres (Business France, 2018).

1.1.3. Origen del aroma en el vino

La calidad del vino es un complejo concepto que envuelve factores extrínsecos como la expectación, y factores intrínsecos como la experiencia sensorial, siendo esta última la dimensión más importante en la percepción de calidad por parte de los consumidores (Charters & Pettigrew, 2007).

El aroma es una de las principales características organolépticas que tienen un mayor impacto sobre la experiencia sensorial. Este atributo está íntimamente ligado a su composición química y es el resultado de complejas interacciones entre compuestos volátiles y no volátiles presentes en esta bebida (Rodríguez-Bencomo et al., 2011). Durante años ha sido objeto de estudio y se ha tratado de identificar y cuantificar compuestos clave responsables de descriptores aromáticos específicos (Campo et al., 2005; Cortés-Diéguez et al., 2015; De-La-Fuente-Blanco et al., 2020; Guth, 1997; Kotseridis & Baumes, 2000; Perestrelo et al., 2019; Pons et al., 2011).

Los compuestos volátiles son los principales responsables del aroma final del vino. Hasta la fecha se han identificado más de 800 (Kuhn et al., 2013), aunque solo unos cuantos contribuyen a la percepción aromática (Polášková et al., 2008). En función de su origen, estos compuestos se pueden clasificar en distintas categorías:

1.1.3.1. Aromas primarios

Provienen de la uva y se forman a través del metabolismo secundario de la vid (Ferrandino & Lovisolo, 2014) jugando un papel clave en la tipicidad del vino (Kuhn et al., 2013; Santos et al., 2004; Visan et al., 2018). Por esta razón, se definen como aromas varietales y pertenecen a un número limitado de familias químicas, incluyendo monoterpenos, sesquiterpenos, C13-norisoprenoides, sulfuros volátiles y metoxipirazinas (Ebeler & Thorngate, 2009). En las uvas, estos compuestos se encuentran normalmente en forma ligada a otras moléculas (no volátiles), aunque también pueden hallarse en forma libre (Styger et al., 2011). Los primeros pueden ser liberados mediante reacciones químicas y enzimáticas durante los procesos de elaboración y envejecimiento del vino, denominándose precursores aromáticos. Se

pueden agrupar a su vez en: precursores glucosídicos, carotenoides, precursores de tioles volátiles y precursores de dimetilsulfurita (Visan et al., 2018).

Debido a su origen, la concentración de los aromas primarios en los vinos está muy ligada a factores como las condiciones climáticas, el suelo del viñedo, las prácticas vitivinícolas o la madurez de la uva, fertilización, localización geográfica o plagas (Carpena et al., 2021; Visan et al., 2018).

1.1.3.2. Aromas secundarios

Se originan durante el tratamiento mecánico de la uva (pre-fermentativos) o durante el proceso de fermentación alcohólica por la actividad metabólica de las levaduras y bacterias (fermentativos) (Carpena et al., 2021). Sus concentraciones finales en el vino dependerán principalmente del tipo de levadura utilizada (*Saccharomyces cerevisiae* o *no Saccharomyces*), tipo de fermentación (espontánea, secuencial o co-inoculación) y el entorno de fermentación (Hirst & Richter, 2016).

Los aromas secundarios del vino obedecen a la presencia de etanol, ácidos grasos volátiles, alcoholes superiores, ésteres, compuestos fenólicos, compuestos carbonílicos o aldehídos (Carpena et al., 2021; Gonzalez & Morales, 2017; Villamor & Ross, 2013). El metabolismo de estos compuestos se muestra en la Figura 3. Su presencia en los vinos está relacionada con características deseables, aunque algunos de ellos pueden otorgar características indeseables cuando se encuentran en concentraciones elevadas, como son el ácido acético, acetato de etilo, acetaldehído, alcoholes superiores o el diacetilo.

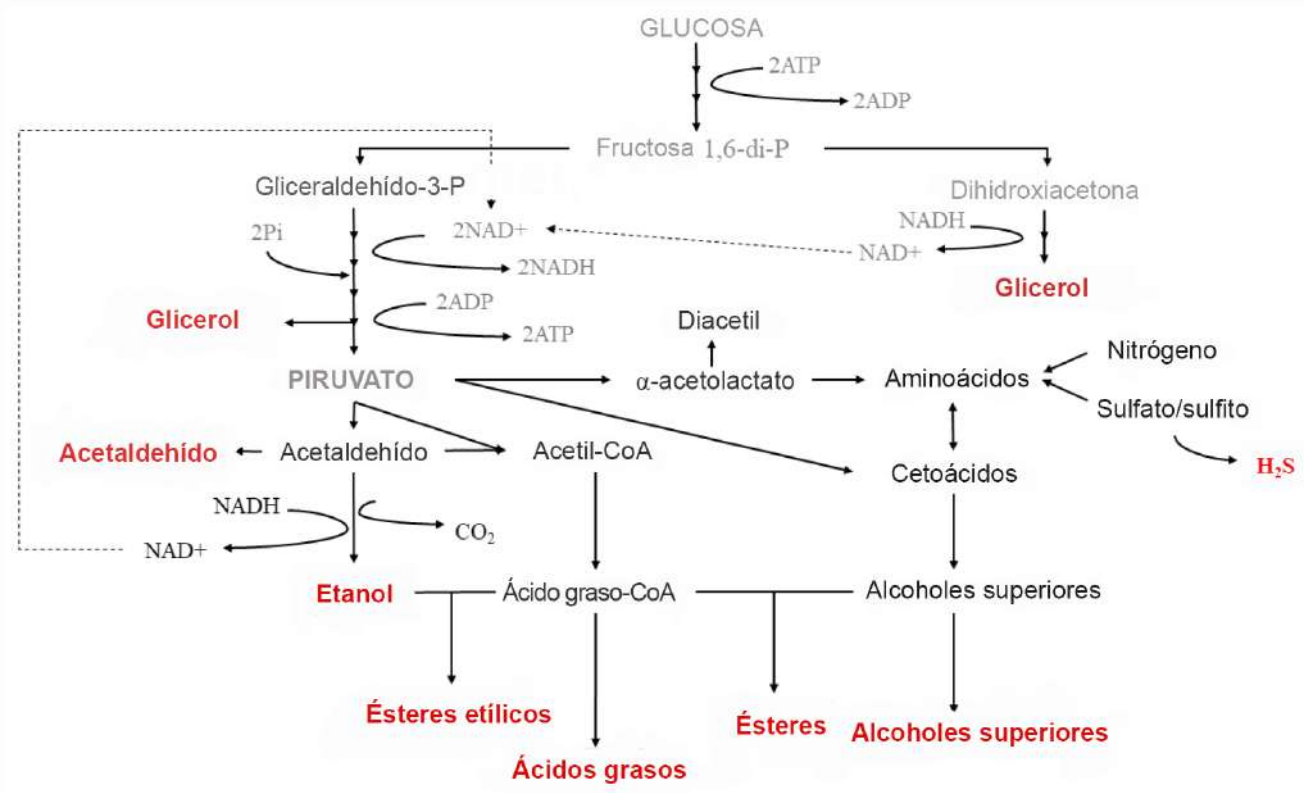

Figura 3. Representación general del metabolismo de los compuestos aromáticos (Carpena et al., 2021)

1.1.3.3. Aromas terciarios

Se forman durante la última etapa de elaboración del vino: el envejecimiento. En esta fase se pierden características derivadas de la uva y la fermentación alcohólica, y se reemplazan por la evolución del aroma primario y secundario, por lo que es una etapa clave para obtener vinos con calidad diferenciada. El aroma del vino adquiere complejidad como resultado de distintos fenómenos, tales como reacciones de esterificación/hidrólisis, reacciones redox, clarificación espontánea, eliminación de CO_2, una lenta y continua difusión del oxígeno a través de los poros de la madera o transferencia de taninos y sustancias aromáticas de la madera al vino (Câmara et al., 2006; Villamor & Ross, 2013). El impacto sobre el perfil aromático final dependerá del tipo de madera utilizada para el envejecimiento, su grado de tostado y edad o la composición inicial del propio vino (Cerdán et al., 2004). Este último aspecto es de especial importancia, ya que no todos los vinos son adecuados para la crianza en madera, debiendo ser de alta calidad, balanceados, con altos contenidos en antocianinas y polifenoles, y un alto grado alcohólico (Ortega-Heras et al., 2004).

1.1.4. Los ésteres en el vino

Los ésteres son una importante familia de compuestos aromáticos que se forman por la unión de ácidos con alcoholes, liberándose una molécula de agua, en un proceso llamado esterificación (Figura 4).

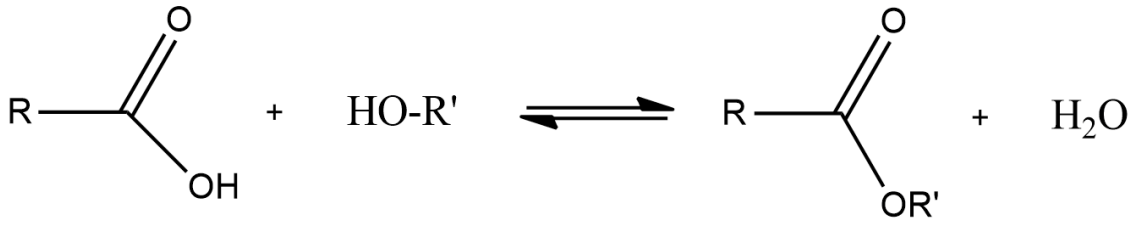

Figura 4. Reacción de esterificación

Esta familia de compuestos aromáticos se encuentra en una gran variedad de productos alimentarios (Gatfield, 1992). En bebidas fermentadas, su concentración es normalmente del orden de trazas, hallándose la mayor parte en niveles inferiores a su umbral de percepción y no superando por lo general los 100 mg/L en su conjunto (Sumby et al., 2010). No obstante, los ésteres son uno de los mayores componentes del vino, constituyendo la segunda familia de compuestos volátiles por detrás de los alcoholes superiores (Figura 5).

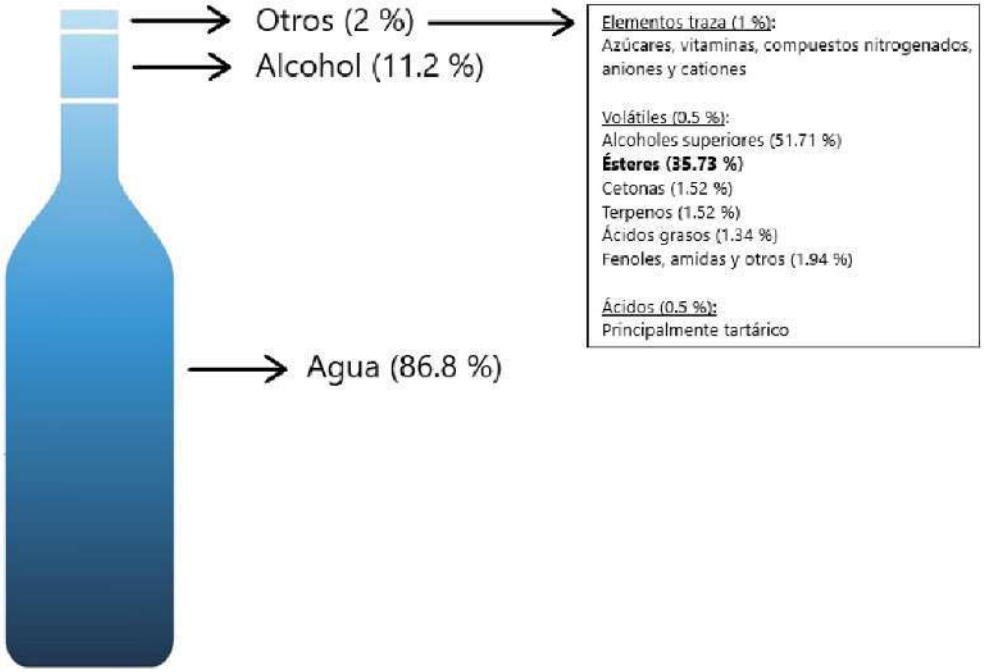

Figura 5. Composición química general del vino y cantidades medias de sus principales componentes. Los valores varían según el tipo de vino. El etanol se representa como peso por volumen (p / v), al igual que todos los demás componentes,

y es equivalente al 14% (v / v). En el vino tinto, los taninos también estarían presentes en concentraciones de hasta 0.4% (p / v). Imagen adaptada de Sumby et al., 2010

En los vinos, los ésteres son principalmente sintetizados enzimáticamente por levaduras durante la fermentación alcohólica, aunque una parte también se forma durante el envejecimiento del vino (Bertrand, 1983; Sumby et al., 2010; Villamor & Ross, 2013). La producción de ésteres está catalizada por esterasas, lipasas y alcohol acetiltransferasas (Sumby et al., 2010) y se ha demostrado que algunos parámetros como el pH, concentración de alcohol, presencia de amino ácidos, temperatura y la composición del vino afectan a la concentración final de estos compuestos en el vino (Guitart et al., 1999; Killian & Ough, 1979; Makhotkina & Kilmartin, 2012; Ribéreau-Gayon et al., 2000).

La contribución de los ésteres en el aroma de los vinos jóvenes, aportando notas frescas y afrutadas, se ha reconocido desde hace varias décadas, habiéndoles asignado un papel menor en los vinos con más de dos o tres años de crianza (Antalick et al., 2014; Ramey & Ough, 1980). Sin embargo, en los últimos años en los que se ha acuñado el concepto de interacción sensorial, se ha aceptado que estos compuestos también son importantes marcadores de las notas afrutadas en vinos con varios años de crianza (Lytra et al., 2013). En este sentido, varios estudios demostraron el impacto de estos compuestos sobre el aroma del vino incluso cuando se encuentran en niveles inferiores a su umbral de percepción, debido a efectos sinérgicos (Escudero et al., 2007; Lytra et al., 2013; Pineau et al., 2009). No obstante, con independencia de estos efectos de interacción, algunos ésteres se encuentran frecuentemente en los vinos en niveles próximos a su umbral de percepción, por lo que pequeños cambios en su concentración pueden conllevar un importante impacto sobre su aroma (Sumby et al., 2010). Por estas y otras razones, entender los mecanismos de síntesis y modulación de esta familia de compuestos resulta una herramienta con gran potencial para lograr vinos de mayor calidad aromática.

Hasta la fecha se han identificado alrededor de 160 ésteres presentes en los vinos (en la Tabla 1 se muestran algunos los principales) (Carpena et al., 2021), aunque la mayoría de estudios se han centrado en dos grandes grupos por su fuerte contribución al aroma del vino: ésteres etílicos y acetatos de alcoholes superiores (Antalick et al., 2014; Sumby et al., 2010). Algunos ésteres que se han encontrado en concentraciones por encima de su umbral de percepción son el 2-hidroxipropanoato de etilo, butanodioato de dietilo, butanoato de etilo, hexanoato de etilo, octanoato de etilo, decanoato de etilo, acetato de etilo, isobutirato de etilo, 2-metilbutanoato de etilo,

isovalerato de etilo, cinamato de etilo, acetato de isoamilo, 2-acetato de feniletilo, acetato de hexilo y 2-hidroxi-4-metilpentanoato (De-La-Fuente-Blanco et al., 2020; Sumby et al., 2010).

Tabla 1. Resumen de los principales ésteres del vino, descripción sensorial y umbrales de percepción. Adaptado de Antalick et al., 2010.

Ester	Descriptor sensorial	Umbral de percepción (μg/L)
propanoato de etilo	Disolvente, fresa madura	2100
isobutirato de etilo	Fresa, kiwi, afrutado, disolvente	15
acetato de propilo	Disolvente, afrutado	
butirato de metilo	Queso, pies sucios, kiwi maduro	
acetato de isobutilo	Disolvente, afrutado	1600
butirato de etilo	Kiwi maduro, fresa madura, queso	20
2-metilbutirato de etilo	Afrutado, kiwi	18
isovalerato de etilo	Queso, afrutado	3
acetato de butilo	Disolvente, afrutado	1800
acetato de isoamilo	Banana	30
valerato de etilo	Fresa, piña, queso	
hexanoato de metilo	Piña, afrutado, manzana	
hexanoato de etilo	Piña, afrutado, manzana	14
butirato de isoamilo	Plátano, manzana, piña, afrutado	
acetato de hexilo	Pera	670
heptanoato de etilo	Piña, afrutado	220
trans-2-hexenoato de etilo	Piña, afrutado	
hexanoato de isobutilo	Afrutado, cera	
octanoato de metilo	Cera, piel de manzana, afrutado	
octanoato de etilo	Cera, piel de manzana, afrutado	580
hexanoato de isoamilo	Plátano, piña, afrutado	
acetato de octilo	Cera, afrutado	800
nonanoato de etilo	Cera, afrutado	
decanoato de metilo	Cera, jabón, afrutado	
decanoato de etilo	Cera, jabón, afrutado	200
octanoato de isoamilo	Cera, jabón, pera	
transgeranato de metilo	Pera	
fenilacetato de etilo	Florido, rosa, vinoso	73
acetato de feniletilo	Florido, mimosa, afrutado, aceituna	250
dodecanoato de etilo	Cera, jabón	
dihidrocinamato de etilo	Afrutado, piña, almendra	1.6
cinamato de etilo	Cereza, afrutado, floral	1.1
2-hidroxiisovalerato de etilo	Afrutado, fresa	
3-hidroxibutirato de etilo	Afrutado, fresa	1800
2-hidroxihexanoato de etilo	Mora	2400
3-hidroxihexanoato de etilo	Cítrico, piña, uva, afrutado	
4-hidroxibutirato de metilo	Afrutado	
4-hidroxibutirato de etilo	Afrutado	
6-hidroxihexanoato de etilo	Afrutado	1200
lactato de etilo	Afrutado, lechoso	154000
succinato de dietilo	Afrutado	200000

1.1.5. Los terpenos en el vino

Los terpenos son compuestos aromáticos constituidos por unidades de isopreno, un hidrocarburo de 5 átomos de carbono (Figura 6).

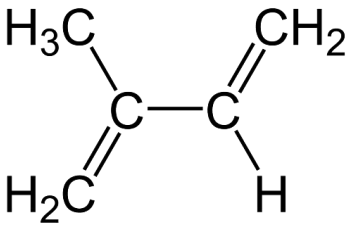

Figura 6. Estructura química del isopreno

Son metabolitos secundarios que ejercen distintas funciones en las plantas, siendo las principales la protección frente a herbívoros y las temperaturas elevadas (Black et al., 2015). Su origen se encuentra en la formación de unidades de isopreno C5 de dimetil alil difosfato e isopentenil difosfato (Figura 7).

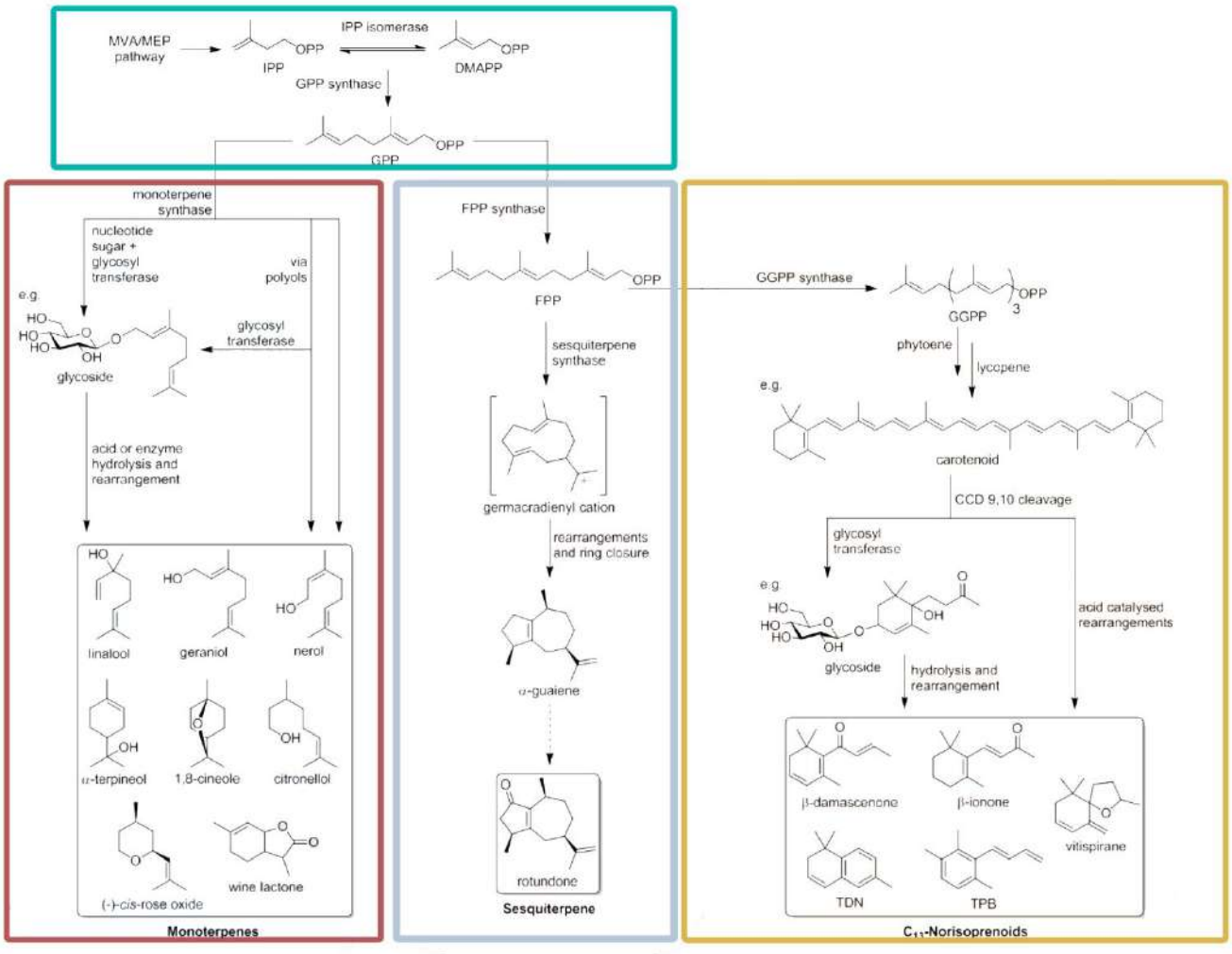

Figura 7. Esquema de producción de los monoterpenos, sesquiterpenos y C_{13}-norisoprenoides. Adaptado de Black et al., 2015

Estos compuestos se encuentran en la uva en forma libre (volátiles), aunque la mayor parte aparecen ligados a azúcares como glucósidos (no volátiles), que pueden ser liberados mediante reacciones de hidrólisis durante el proceso de elaboración del vino. Se trata de los compuestos varietales más estudiados en la uva (*Vitis vinifera),* habiéndose identificado hasta la fecha alrededor de 40, que se agrupan en monoterpenos, sesquiterpenos y C_{13}-norisoprenoides (González-Barreiro et al., 2015). Sin embargo, solo algunos de ellos se han identificado como compuestos con alto poder aromático en los vinos.

Los terpenos contribuyen al carácter afrutado (principalmente cítrico) y floral de los vinos, aunque algunos también aportan aromas a resina (González-Barreiro et al., 2015), semillas y raíces (Câmara et al., 2004). Entre los terpenos con mayor poder aromático destacan los alcoholes monoterpénicos, como el linalool, α-terpineol, nerol, geraniol y citronelol (Gamero et al., 2011; Loscos et al., 2007; Visan et al., 2018).

Debido a su carácter varietal, los terpenos se pueden emplear para identificar la variedad de uva de los vinos. Así, son especialmente abundantes en vinos producidos con las variedades Moscatel (Moscatel de Alejandría, Moscatel de Frontignan, Moscatel Ottonel y Moscatel Blanc), siendo responsables de su aroma típico (Ruiz et al., 2019). La contribución positiva de esta familia de compuestos también ha sido descrita en vinos producidos con variedades de uva como Gewürztraminer, Müller-Thurgau, Riesling, Scheurebe, Sylvaner y Traminer (Ruiz et al., 2019).

1.2. El Brandy de Jerez

El Brandy de Jerez es una bebida espirituosa elaborada por destilación del vino y que cuenta con el sello de calidad de una Indicación Geográfica Protegida (Boletín Oficial la Junta Andalucía, 2018), quedando su producción restringida al llamado Triángulo de Jerez: Jerez de la Frontera, El puerto de Santa María y Sanlúcar de Barrameda. Su particular proceso de elaboración, que se basa en las especificaciones establecidas en el documento técnico de la IGP, le otorga unas características organolépticas que lo distinguen de bebidas similares tales como el Cognac o el Armagnac (Tsakiris et al., 2014).

Un ejemplo es su proceso de destilación, que se realiza en alambiques tradicionales de cobre llamados alquitaras (Figura 8), aunque también puede llevarse a cabo en columnas de fraccionamiento.

Figura 8. Alquitara de cobre tradicional

Una de las características que hacen singular a este producto es su método de envejecimiento, denominado “Criaderas y Solera” (Figura 9). Este consiste en un sistema de diferentes escalas de envejecimiento que va recorriendo el aguardiente (Criaderas) hasta llegar al nivel más bajo (Solera). A lo largo de estas escalas se realiza la extracción periódica de una porción del brandy (conocida como “sacas”) en los niveles más altos de las Criaderas, para la reposición (conocida como “rocíos”) de los niveles más bajos. Así, en la Solera se encuentra la mezcla de brandy de mayor calidad y con mayor tiempo de crianza promedio, que será destinado a su embotellado y comercialización. Este proceso de envejecimiento se realiza en barricas de roble americano (*Quercus alba*) denominadas botas en la zona de Jerez. Generalmente

tienen una capacidad de 500 – 600 L, aunque el Consejo Regulador permite que sean de hasta 1000 L. Además, estas botas deben haber contenido algún tipo de Vino de Jerez en un proceso llamado "envinado".

El Brandy de Jerez se comercializa bajo tres categorías en función de su tiempo de envejecimiento: Brandy Solera (al menos 6 meses), Brandy Solera Reserva (entre 1 y 3 años) y Brandy Solera Gran Reserva (al menos 3 años).

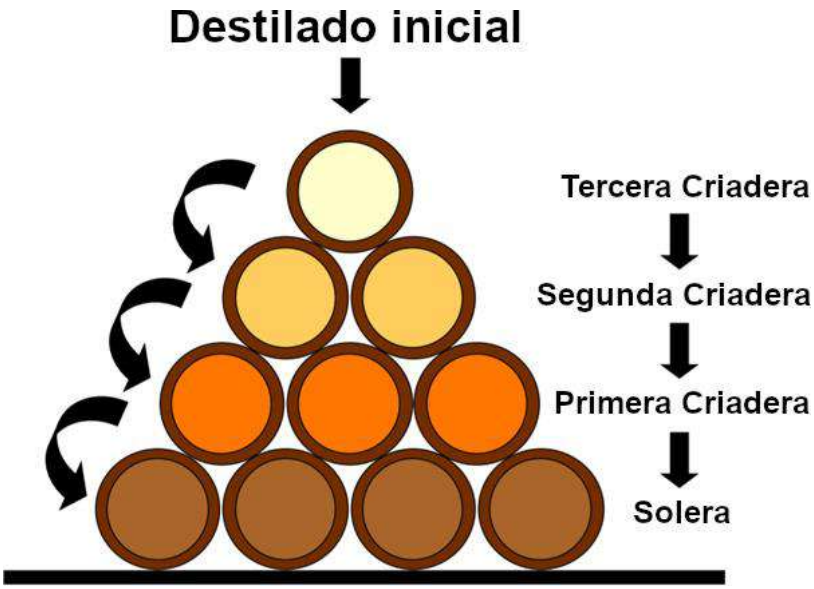

Figura 9. Ilustración del método de "Criaderas y Solera" utilizado para la producción del Brandy de Jerez. Imagen adaptada de Durán-Guerrero et al., 2021.

1.2.1. Aroma del Brandy de Jerez

Al igual que en el vino, el aroma del brandy es uno de los aspectos más importantes relacionado con su calidad y depende de su composición química. El origen de su aroma se encuentra tanto en el vino (descrito en el apartado 1.1) como el proceso de destilación y crianza. Así, se suelen clasificar en aromas primarios (procedentes de la uva), secundarios (formados durante la fermentación alcohólica del vino), terciarios (procedentes de la destilación) y cuaternarios (aparecen durante el proceso de envejecimiento) (Ivanović et al., 2021; Spaho et al., 2013).

La destilación es una etapa determinante en la composición final del Brandy de Jerez, produciéndose un incremento de la concentración de etanol y los constituyentes aromáticos primarios y secundarios (Tsakiris et al., 2014). Durante este proceso tiene lugar la extracción de compuestos volátiles, además de reacciones químicas como

reacciones de esterificación, acetilación, de Maillard y degradaciones de Strecker (Cantagrel et al., 1990; Tsakiris et al., 2014), que determinarán la composición final del destilado. Los principales factores que pueden ser controlados durante este proceso son el vino base utilizado, la temperatura de destilación y el caudal de vino (Tsakiris et al., 2014).

La naturaleza de los destilados obtenidos condicionará la composición aromática del brandy. Estos pueden tratarse de una mezcla de aguardientes de baja graduación alcohólica, inferior al 70 % v/v (*holandas*), aguardientes de media graduación, comprendida entre 70 y 85.9 % v/v, o destilados de alta graduación, con contenidos superiores a 86 % v/v (Durán-Guerrero et al., 2021).

Otro aspecto clave en el aroma del Brandy de Jerez es el origen y acondicionamiento de las botas de roble americano, y su proceso de envinado (tipo de vino que ha contenido y tiempo) o uso previo del barril, es decir, si se ha utilizado anteriormente para producir brandy (Durán-Guerrero et al., 2021).

A pesar de la importancia del perfil de compuestos volátiles sobre el aroma del Brandy de Jerez, la bibliografía disponible hasta la fecha es escasa (Durán-Guerrero et al., 2021). En la Tabla 2 se muestran los principales compuestos volátiles determinados en esta bebida.

Tabla 2. Compuestos volátiles identificados en Brandy de Jerez, descriptores sensoriales y rangos de concentración referenciados en estudios previos. Tabla adaptada de Durán-Guerrero et al., 2021.

Compuestos volátiles	Descriptores sensoriales	Concentración (mg/L)
Alcoholes		
2-butanol	Vinoso / medicinal	1.8
2-metilbutanol	Tostado / afrutado / aceite / alcohólico / vino / whisky	80.9–181.8
2-feniletanol	Rosa / talco / miel	4.99–22.4
Alcohol 2-feniletílico	Rosa / miel	2.16–2.52
3-hexenol (E / Z)	Herbáceo / verde / pasto	0.238–2.245
Butanol	Vinoso / medicinal	7.92–9.36
Hexanol	Hierba cortada / resina / herbáceo / madera	3.99–10.44
Alcoholes isoamílicos	Disolvente / torta / alcohólico / esmalte de uñas / fruta madura	193–678
Isobutanol	Alcohol / solvente / vinoso / esmalte de uñas	119.88–133.92
Metanol	Disolvente / afrutado picante	238.32–245.16
Aldehídos		
Acetaldehído	Manzana guisada / picante	78.84–86.76
Benzaldehído	Tostado / almendra amarga / nuez / ahumado	2.91–35.3
Furanos		
2-Furaldehído	Alcohol / tarta / almendra / pan tostado / incienso / floral	0.19–14.54
5-hidroximetil-2-furaldehído	Rancio / tostado	0.072–87.09
5-metil-2-furaldehído	Tostado / almendra amarga / tarta / quemado / caramelo	0.062–1.94
Ácidos		
Ácido acético	Graso	210.1–307.6
Ácido decanoico	Rancio / queso / cera / plastilina	5.12–15.1
Ácido dodecanoico	Graso / coco / laurel	1.51–7.18
Ácido octanoico	Rancio / queso / graso	0.007–13.4
Ésteres		
Acetato de 2-feniletilo	Afrutado / meloso / floral / rosa	0.013–0.119
Succinato de dietilo	Fruta demasiado madura / lavanda	0.071–5.40
2-metilbutanoato de etilo		0.103–0.241
2-metilpropanoato de etilo		0.064–0.454
Acetato de etilo	Piña / barniz / balsámico / afrutado / disolvente / picante / pegamento	134.28–236.52
Butanoato de etilo	Plátano / piña / fresa	0.327–14.9
Decanoato de etilo	Sintético / rancio	0.64–4.93
Dodecanoato de etilo	Dulce / ceroso / floral / jabonoso / limpio	0.160–1.08
Heptanoato de etilo	Fresa plátano	0.057–0.104
Hexadecanoato de etilo	Ceroso suave	1.44
Hexanoato de etilo	Plátano / manzana verde	0.46–1.79
Isopentanoato de etilo	Afrutado / dulce / manzana / piña / tutti frutti	0.090–0.443
Lactato de etilo	Láctico / yogur / fresa / frambuesa / mantecoso	48.24–50.76
Nonanoato de etilo	Afrutado / rosa / ceroso / ron / vino / tropical	
Octanoato de etilo	Piña / pera / jabonoso / plátano	0.63–5.4
Pentanoato de etilo	Dulce / afrutado / manzana / piña / verde	0.041–0.398
Succinato de etilo	Toffee / café	3.96–7.2
Tetradecanoato de etilo	Suave ceroso / jabonoso	0.36
Acetato de hexilo	Manzana / pera / plátano / floral	0.0004–0.003
Octanoato de isoamilo		0.002–0.018
Acetato de isoamilo	Dulce / afrutado / plátano	0.101–1.098
(E) -Metil-2-octenoato		0.0007–0.0027
Decanoato de metilo		0.001–0.007
Terpenos		
Linalol	Moscatel / rosa / lavanda	0.053–0.590
Nerolidol	Floral / verde / cítrico / amaderado / ceroso	0.002–0.004
α-Terpineno		0.0017
α-Terpineol	Lily / pastel	0.007–0.097
Fenoles volátiles		
4-etilguayacol	Picante / ahumado / tocino / fenólico / clavo	0.046–0.210
Eugenol	Canela / clavo	0.007–0.071
Vanilina	Vainilla	0.13–5.94
Misceláneo		
1,1-dietoxietano	Fruta verde / regaliz / torta / afrutado / fruta demasiado madura	105.84–115.56
β-Damascenona	Afrutado / rosa / ciruela / uva / frambuesa	0.001–0.084

2. Trazabilidad geográfica de alimentos e implicaciones comerciales

2.1. Frutas tropicales en España

El sector de las frutas tropicales ha experimentado un fuerte crecimiento en España durante los últimos años. En 2018, alcanzó la cifra de 325 millones de euros, localizándose el grueso de la producción en Andalucía y destacando los cultivos de mango, aguacate, chirimoya y níspero. Entre ellos, el mango y aguacate se han constituido como unos de los principales cultivos en Málaga y Granada.

2.1.1. Mango

El mango (*Mangifera indica L.*) es la fruta subtropical con mayor volumen de producción en el mundo, con el 52 % del total y el 23 % de la exportación en 2018 (Figura 10). Tiene su origen en la India, donde se cultiva desde hace más de 4000 años y en la actualidad su producción se centra mayoritariamente en zonas con climas tropicales y subtropicales.

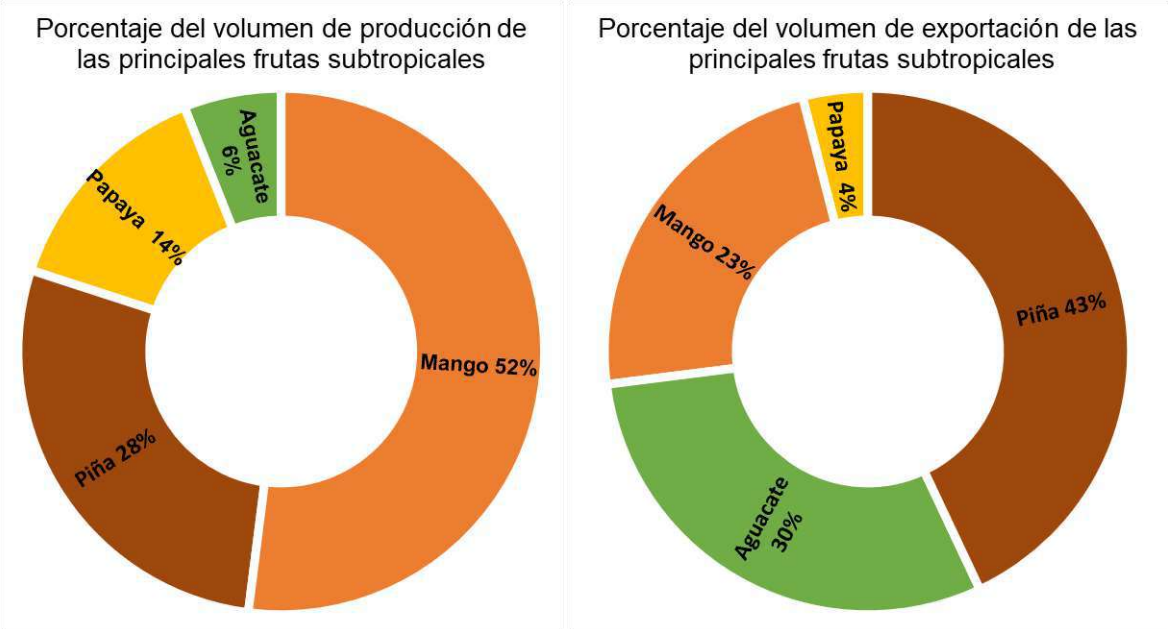

Figura 10. Porcentaje del volumen producción y de exportación mundial de las principales frutas tropicales en 2018 (FAO, 2018)

El mango es apreciado por su valor nutricional y por la presencia de compuestos saludables, siendo particularmente rico en polifenoles y carotenoides (Lauricella et al., 2017). Las principales variedades de mango que se han adaptado al clima y suelo español son *Osteen* (variedad más cultivada en España, con casi el 80 % de la superficie total), *Keitt* (alrededor del 15 % de la superficie total), *Kent*, *Irwin y Tommy Atkins* (AvoGo

Consulting, 2020). En la Figura 11 se muestra una imagen del aspecto visual de cada variedad.

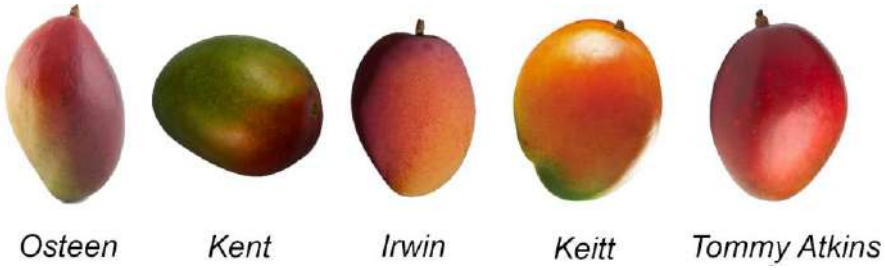

Figura 11. Variedades de mango adaptadas al clima y suelo español

2.1.2. Aguacate

El aguacate (*Persea americana*) es una fruta originaria de México (actualmente el mayor productor mundial). Se trata también de una de las principales frutas tropicales con mayor volumen de producción en el mundo, abarcando un 6 % del total, por detrás del mango, la piña y la papaya (Figura 10). Sin embargo, su importancia en las exportaciones es aún mayor, alcanzando un 30 % del comercio mundial en 2018, que lo situó en segunda posición por detrás de la piña (Figura 10). Las variedades más comercializadas son la *Hass* (la más conocida y producida a nivel mundial), *Fuerte*, *Bacon*, *Cocktail* y *Pinkerton* (Figura 12).

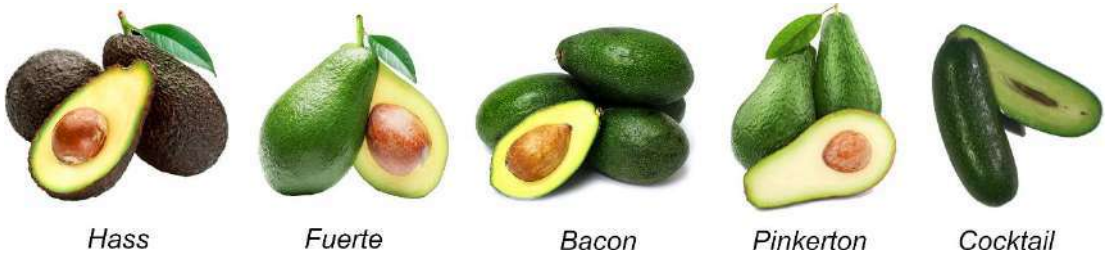

Figura 12. Variedades de aguacate más comercializadas en el mundo y adaptadas al clima y suelo de España

El origen del aguacate en España se remonta a 1955, cuando se realizó la primera plantación comercial en la costa de Granada (Almuñécar). Antes de eso, en las Islas Canarias se habían cultivado árboles de aguacate aislados con semillas sudamericanas. A partir de entonces, las plantaciones de estos árboles aumentaron enormemente y a día de hoy se extienden por las Islas Canarias y la costa de Andalucía (Rodríguez et al., 2019), localizándose en torno al 90 % de la producción de aguacate de España en las zonas de Málaga, Granada y Cádiz.

Las propiedades nutricionales y saludables del aguacate han impulsado de manera importante su consumo en los últimos años. Entre ellas podemos citar su alto contenido en nutrientes esenciales, varios fitoquímicos potenciales para la prevención del cáncer, proteínas, ácidos grasos insaturados, antioxidantes naturales y vitaminas liposolubles menos comunes en otras frutas, y bajo contenido de sodio y grasas (Duarte et al., 2016; Pleguezuelo et al., 2018). Estas propiedades le han hecho ganar la consideración de "superalimento", aunque este término puede ser engañoso e implica declaraciones de propiedades poco realistas (Bhuyan et al., 2019).

2.2. Trazabilidad del mango y el aguacate

España es el único productor y exportador de mango y aguacate de Europa, lo cual le confiere una situación estratégica única por su proximidad y facilidad de incorporación dentro de este mercado (Moreno-Ortega et al., 2019). Esto permite que las frutas se puedan recoger en su punto óptimo de maduración para ser comercializadas rápidamente. Por el contrario, las empresas competidoras, localizadas principalmente en Latinoamérica, Asia y África, requieren de largos períodos de suministro que llega a demorarse hasta varias semanas (barco), afectando de manera importante a la calidad del producto (Bill et al., 2014), ya que en la mayoría de los casos deben recolectarse en estadios inmaduros que conllevan una pérdida de su calidad sensorial. Estos tiempos de suministro se pueden acortar a través del transporte por avión, pero suponen un incremento sustancial del precio que disminuiría su competitividad frente al producto nacional. Así, el mango y aguacate de las regiones costeras andaluzas unas características de calidad diferenciadas en el mercado europeo.

Sin embargo, con la globalización del mercado puede llegar fruta a España desde cualquier país y en cualquier época del año, dejando a las empresas españolas en una situación de vulnerabilidad si no se protegen legalmente. Por esta razón, los productores de mango y aguacate de la costa andaluza han demandado en los últimos años un sello de calidad que los distinga y proteja de los mangos y aguacates producidos en otros países. Esta distinción le otorgaría un valor añadido al producto por su localización geográfica y por los mecanismos de control de la producción que estarían obligados a adoptar los productores bajo las especificaciones y estándares de calidad de la IGP, impactando en la calidad percibida por los consumidores y en sus preferencias de compra.

Actualmente, la asociación Española de Productores de Frutas Tropicales ha iniciado los trámites para lograr una Indicación Geográfica Protegida (IGP) para mangos y aguacates de Málaga y Granada. Un aspecto clave para el establecimiento y

mantenimiento de esta IGP es la disponibilidad de herramientas que permitan identificar y diferenciar los mangos y aguacates producidos bajo ese sello de calidad, de los producidos en otras zonas geográficas. Sin embargo, esta tarea no es trivial y a menudo los métodos tradicionales se han mostrado poco efectivos para ciertos productos.

3. Métodos estadísticos: quimiometría

La quimiometría es un campo interdisciplinar enfocado a la aplicación de métodos matemáticos, estadísticos y de lógica formal para la transformación de señales analíticas y datos químicos en información fácilmente interpretable. En los últimos años, ha adquirido una fuerte relevancia motivada tanto por el desarrollo de las técnicas analíticas, que generan una gran cantidad de información (Brereton et al., 2018), como por la capacidad computacional a bajo coste. La quimiometría abarca una gran variedad de campos, como el diseño de experimentos, procesado de señales analíticas, calibración, resolución de sistemas dinámicos, reconocimiento de patrones y control de procesos.

Los estudios de calidad y trazabilidad alimentaria a menudo requieren de soluciones analíticas que puedan dar respuestas cualitativas. Estas soluciones analíticas generan frecuentemente múltiples medidas para una misma muestra, por lo que el uso de herramientas estadísticas multivariantes resulta altamente eficiente para obtener la mayor cantidad de información de los datos y mejorar su interpretabilidad (Oliveri & Forina, 2012).

En términos generales, las técnicas multivariantes pueden clasificarse en función del método de aprendizaje: supervisado y no supervisado.

3.1. Aprendizaje no supervisado

El objetivo de las técnicas de aprendizaje no supervisado es adquirir la mayor información estructural sobre los datos, ya sea mediante agrupaciones (como el análisis de conglomerados o análisis *cluster*) según su similitud o simplificando su estructura sin perder las características fundamentales (técnicas de reducción de dimensionalidad). A esta última categoría pertenece el análisis de componentes principales (PCA), ampliamente utilizado en investigaciones aplicadas (Grané & Jach, 2014) debido a su facilidad de uso, incorporación en la mayoría de programas estadísticos y alta interpretabilidad.

3.2. Aprendizaje supervisado

Las técnicas de aprendizaje supervisado aprenden a relacionar grupos de variables de entrada y de salida de un modelo, con el objetivo de predecir las salidas para nuevos datos (Cunningham et al., 2008). Estos métodos son a su vez categorizados como modelos de clasificación, cuando las variables de salida son categóricas, y de regresión, cuando las variables de salida son continuas.

Los modelos de clasificación han supuesto un gran avance en el estudio de la calidad y trazabilidad de productos alimentarios con múltiples aplicaciones a lo largo de los años (Cubero-Leon et al., 2014; Jiménez-Carvelo et al., 2019; Oms-Oliu et al., 2013). Se trata de métodos estadísticos que construyen reglas matemáticas o modelos capaces de caracterizar una muestra con respecto a una propiedad cualitativa: pertenencia o no a una población en función de su perfil analítico (Oliveri, 2017). Su funcionamiento se basa en el aprendizaje automático (*machine learning* en inglés) y son referidas como técnicas supervisadas. Existen dos familias de métodos de aprendizaje automático que satisfacen esta necesidad (Oliveri & Forina, 2012):

- **Análisis discriminantes**: asignan las muestras a una de las clases (también referidas como categoría o población) predefinidas en el modelo, por lo que se necesitan dos o más categorías para su construcción (Figura 13a). Por esta razón, es necesario definir perfectamente todas las clases que son introducidas al modelo con un tamaño de muestra representativo de la población, y que en muchas ocasiones es difícil de obtener. La limitación de estas técnicas aparece si se introduce una muestra desconocida que no pertenece a ninguna de las categorías definidas, ya que será forzosamente clasificada como una de ellas (Khan & Madden, 2014). Estas técnicas resultan por lo tanto útiles para encontrar diferencias entre dos o más poblaciones que estén bien definidas. No obstante, también pueden ser modificadas para definir regiones de indecisión (Figura 13a y 1b) y abordar problemas similares al modelaje de clases que se detalla a continuación. Algunos de los modelos más utilizados en el estudio de la calidad y trazabilidad alimentaria son: *linear discriminant analysis* (LDA), *partial least squares discriminant analysis* (PLS-DA), *quadratic discriminant analysis* (QDA), *regularized discriminant analysis* (RDA) o K-nearest neighbor (KNN).

- **Modelaje de clases**: también referidas como “clasificación de una clase”, identifican la compatibilidad de una muestra con las características de una única clase de interés, pudiendo ser construidos para problemas con una o más categorías de muestras. Esta arquitectura solventa el problema de introducir clases desconocidas al modelo, ya que, si la muestra no pertenece a la clase de interés, es clasificada como desconocida (Figura 13c). Son especialmente útiles para problemas en los que la clase objetivo queda perfectamente definida mientras el resto de las clases (que podría ser ilimitado) no necesitan estar necesariamente bien definidas. Es el caso de problemas de verificación del cumplimiento de una especificación determinada, como autentificación de

productos, detección de muestras adulteradas o verificación de pertenencia a un sello de calidad como una DOP o IGP (Khan & Madden, 2014). Algunos de los modelos más utilizados para estos casos son *soft independent modelling of class analogy* (SIMCA), *support vector machines* (SVM), *unequal class models* (UNEQ), *potential function methods* (PFM) o modificaciones de los modelos PLS-DA anteriormente mencionados.

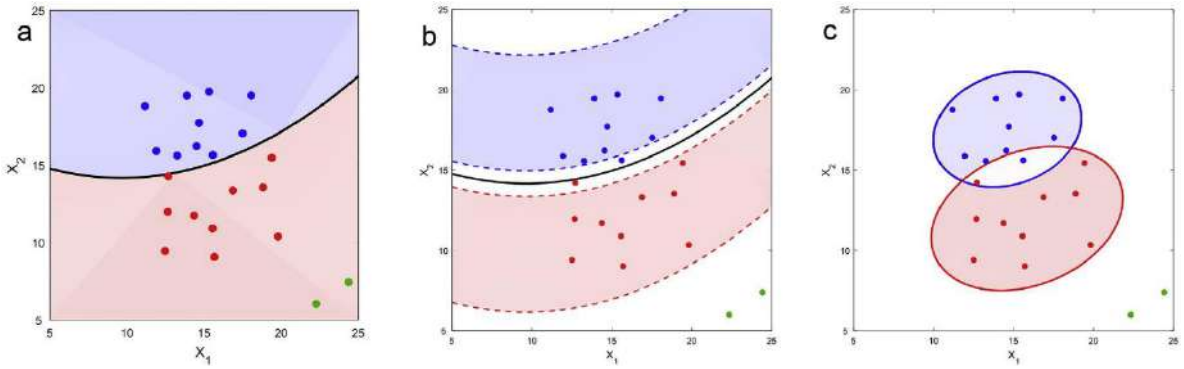

Figura 13. Ejemplo de la estructura para problemas de clasificación de dos clases de (a) análisis discriminante puro, (b) análisis discriminante modificado para definir regiones de indecisión, (c) modelaje de clases. Las muestras que caen en los espacios rojo y azul son clasificadas como pertenecientes a dichas clases, mientras que el color blanco representa regiones de indecisión (la muestra es clasificada como desconocida). Imagen adaptada de Oliveri, 2017.

3.2.1. Optimización y validación de modelos supervisados

La construcción de modelos supervisados implica un proceso de optimización o calibración de sus parámetros, seguida de una validación, cuyo propósito es estimar la capacidad que tiene el modelo de predecir la categoría de nuevas observaciones en base a sus variables de entrada. Esto se conoce como proceso de remuestreo y se basa en optimizar el modelo con un subconjunto de observaciones (llamado *training set*) para ser evaluado o validado con las observaciones restantes (*test set*). Este proceso se puede repetir en múltiples ocasiones para evitar sesgos por la elección de ambos subconjuntos. Algunos de los métodos de remuestreo son los siguientes:

- **Validación simple**: consiste en dividir las observaciones en dos subconjuntos, uno para su entrenamiento y otro para su validación (generalmente en porcentajes como 70 y 30 % respectivamente). La limitación de este tipo de validación es que está fuertemente influenciada por la elección de las

observaciones de cada subconjunto, por lo que no es recomendable su aplicación cuando el número de muestras es pequeño.

- **Validación cruzada simple**: es uno de los métodos de remuestreo más utilizados en la optimización y validación de modelos supervisados. Se basa al igual que el anterior en dividir las muestras en un subconjunto de optimización y otro de validación, con la diferencia de que este proceso se repite en múltiples ocasiones hasta que todas las observaciones han estado en el subconjunto de validación al menos una vez. El error del modelo se calcula como un promedio de todas las repeticiones. Cuando el subconjunto de validación está formado por una sola muestra adopta el nombre de *leave one out cross-validation* (LOOCV). La limitación de este método está en que las muestras de la validación también se utilizan para optimizar los parámetros del modelo, de forma que no son completamente independientes y pueden producir un ligero sobreajuste (Westerhuis et al., 2008).
- **Doble validación cruzada**: es similar al método anterior, con la diferencia de que el subconjunto de optimización es a su vez divido en uno de validación y otro de entrenamiento para optimizar los parámetros del modelo (Westerhuis et al., 2008). Este método permite obtener independencia completa entre la optimización y validación.

Finalmente, y una vez estimada la capacidad del modelo de predecir nuevas muestras, se puede calcular su significancia estadística mediante un test de permutación. El objetivo de este test es calcular la distribución nula (no clasificación) mediante la reorganización de las muestras y compararla con la capacidad real del modelo. Aunque esta etapa no es estrictamente necesaria cuando el proceso de validación se ha realizado correctamente, es recomendable cuando se construyen modelos con un número de variables mucho mayor que el número de muestras para evitar problemas de sobreajuste.

Objetivos

La presente tesis doctoral tiene como objetivo general desarrollar y aplicar herramientas analíticas y quimiométricas para estudiar la calidad y trazabilidad de productos alimentarios. Para ello, se ha dividido la investigación en tres capítulos con varios objetivos específicos:

Capítulo 1: Calidad aromática de vinos espumosos y vinos rosados.

- Objetivo 1.1: Desarrollo de una metodología basada en la microextracción en fase sólida en el espacio de cabeza (HS-SPME), cromatografía de gases (GC) y espectrometría de masas (MS) para determinar terpenos en vinos espumosos. Aplicación de la metodología para caracterizar el perfil de estos compuestos varietales en Champagne y Cava, y comparativa con nuevos vinos espumosos producidos en Andalucía con el mismo método de producción (método Tradicional).
- Objetivo 1.2: Evaluación del impacto sobre el perfil de ésteres de la segunda fermentación en botella llevada a cabo durante el proceso de elaboración de vinos espumosos.
- Objetivo 1.3: Evaluación del impacto sobre el perfil de ésteres de la maceración pre-fermentativa y la crianza sobre lías, llevadas a cabo durante el proceso de elaboración de vinos espumosos producidos con la variedad de uva andaluza Pedro Ximénez.
- Objetivo 1.4: Desarrollo de una metodología estadística integrativa para profundizar en el conocimiento de las interacciones que se producen entre el perfil volátil y no volátil y su relación con las características sensoriales del vino.
- Objetivo 1.5: Impacto sobre el perfil volátil de vinos rosados de la fermentación secuencial con levaduras *no Saccharomyces* en combinación con levaduras *Saccharomyces cerevisiae*.

Capítulo 2: Calidad aromática del Brandy de Jerez.

- Objetivo 2.1: Desarrollo de una metodología basada en la microextracción en fase sólida en el espacio de cabeza (HS-SPME), cromatografía de gases (GC) y espectrometría de masas (MS) para determinar ésteres en brandies. Aplicación en brandies sometidos a un proceso de estabilización frio y filtración para estudiar el comportamiento de los ésteres etílicos de ácidos grasos de cadena larga que están, implicados en la formación de neblina indeseada.
- Objetivo 2.2: Evaluación del proceso de estabilización por frío y filtración que se lleva a cabo antes del embotellado del Brandy de Jerez. Impacto sobre el perfil de ésteres y comparación con la estabilización a temperatura ambiente.

Capítulo 3: Trazabilidad de frutas tropicales producidas en Andalucía.

- Objetivo 3.1: Desarrollo de una metodología basada en isótopos estables, análisis multi-elemental y técnicas quimiométricas para diferenciar los mangos producidos en la zona de la costa andaluza de los producidos en otros países.
- Objetivo 3.2: Desarrollo de una metodología basada en isótopos estables, análisis multi-elemental y técnicas quimiométricas para diferenciar los aguacates producidos en la zona de la costa andaluza de los producidos en otros países.

Aim

The overall aim of this PhD Thesis is the development and application of analytical and chemometric tools to study the food quality and traceability of food products. To do this, the research has been divided into three chapters with several specific objectives:

Chapter 1: Aroma quality of sparkling wines and rosé wines.

- Objective 1.1: Development of a methodology based on headspace solid-phase microextraction (HS-SPME), gas chromatography (GC) and mass spectrometry (MS) to determine terpene compounds in sparkling wines. Application of the methodology to characterize the profile of these varietal compounds in Champagne and Cava, and comparison with new sparkling wines produced in Andalusia with the same production method (Traditional method).
- Objective 1.2: Evaluation of the impact of the second fermentation in bottle on the ester profile of sparkling wines.
- Objective 1.3: Evaluation of the impact of the pre-fermentation maceration and aging on lees carried out during winemaking on the ester profile of sparkling wines from the Pedro Ximénez grape variety.
- Objective 1.4: Development of an integrative statistical methodology to deepen knowledge on the interactions between the volatile and non-volatile profiles, and their relationship with the sensory properties of wine.
- Objective 1.5: Impact of the sequential fermentation with *non-Saccharomyces* in combination with *Saccharomyces cerevisiae* yeasts on the volatile profile of rosé wines.

Chapter 2: Aroma quality of Brandy de Jerez

- Objective 2.1: Development of a methodology based on headspace solid phase microextraction (HS-SPME), gas chromatography (GC) and mass spectrometry (MS) to determine ester compounds in brandies. Application of this methodology to characterize the ester profile of brandies subjected to a cold stabilization process and filtration to study the ethyl esters of long chain fatty acids behaviour, which are involved in the undesirable haze formation.
- Objective 2.2: Evaluation of the cold stabilization and filtration process that takes place before bottling of “Brandy de Jerez”. Impact on the ester profile of these brandies and comparison with the stabilization at room temperature.

Chapter 3: Traceability of tropical fruits produced in Andalusia.

- Objective 3.1: Development of a methodology based on stable isotopes, multi-elemental analysis and chemometric techniques to differentiate mangoes produced in the Andalusian coastal strip from those produced in foreign countries.
- Objective 3.2: Development of a methodology based on stable isotopes, multi-elemental analysis and chemometric techniques to differentiate avocados produced in the Andalusian coastal strip from those produced in foreign countries.

Resultados y discusión

CAPÍTULO 1

CALIDAD AROMÁTICA DE VINOS ESPUMOSOS Y ROSADOS

Resumen

La calidad aromática del vino es uno de los atributos con mayor impacto sobre las preferencias de los consumidores, siendo el resultado de complejas interacciones entre la fracción volátil y no volátil que compone esta bebida. A lo largo de los años se ha tratado de identificar compuestos claves responsables de descriptores aromáticos específicos, así como entender el impacto que tienen distintas etapas del proceso de elaboración sobre los atributos sensoriales de los vinos. Sin embargo, los efectos sinérgicos que aparecen por las interacciones entre distintos compuestos, volátiles y no volátiles, hacen que esta labor no sea trivial, siendo necesario el estudio de grupos de compuestos o incluso de tantos compuestos como sea posible determinar, para entender sus implicaciones.

En este capítulo se desarrollan y aplican metodologías analíticas para determinar el perfil de terpenos en vinos espumosos y el perfil de ésteres en vinos espumosos y rosados, abordando los 5 primeros objetivos específicos.

Primeramente, se optimiza y valida un método basado en HS-SPME-GC-MS para determinar terpenos en vinos espumosos y se caracterizan Cavas, Champagnes y vinos espumosos andaluces. Mediante el uso de técnicas quimiométricas se obtienen las principales diferencias en el perfil de terpenos que tienen las distintas tipologías de vinos, elaborados con distintas variedades de uva y tiempos de crianza.

Por otro lado, se aborda el efecto que tienen distintas etapas del proceso de elaboración de vinos espumosos y rosados sobre el perfil aromático, con especial interés en los ésteres, por su relevancia en las características sensoriales de los vinos. Las etapas estudiadas son la maceración pre-fermentativa, la segunda fermentación en botella y el tiempo de crianza sobre lías en vinos espumosos, y la fermentación secuencial con levaduras *Saccharomyces* y *no Saccharomyces* como alternativa a la convencional en vinos rosados. Finalmente, se utilizan estas muestras de vinos rosados para desarrollar una metodología estadística integrativa que permite evaluar los complejos mecanismos de interacción que existen entre el perfil volátil y no volátil y sus implicaciones en los atributos sensoriales.

ARTÍCULO 1

Multivariate optimization of headspace solid-phase microextraction coupled to gas chromatography-mass spectrometry for the analysis of terpenoids in sparkling wines

José Manuel Muñoz-Redondo, María José Ruiz-Moreno, Belén Puertas, Emma Cantos-Villar, José Manuel Moreno-Rojas

Talanta

208, 120483 (2019)

Q1: 10/81 (Chemistry, Analytical, 2019)

Impact Factor: 5.339

Talanta 208 (2020) 120483

Contents lists available at ScienceDirect

Talanta

journal homepage: www.elsevier.com/locate/talanta

Multivariate optimization of headspace solid-phase microextraction coupled to gas chromatography-mass spectrometry for the analysis of terpenoids in sparkling wines

José Manuel Muñoz-Redondo[a,*], María José Ruiz-Moreno[a], Belén Puertas[b], Emma Cantos-Villar[b], José Manuel Moreno-Rojas[a,**]

[a] Department of Food Science and Health, Andalusian Institute of Agricultural and Fisheries Research and Training (IFAPA), Alameda del Obispo, Avda. Menéndez Pidal, SN, 14004, Córdoba, Spain
[b] Department of Food Science and Health, Andalusian Institute of Agricultural and Fisheries Research and Training (IFAPA), Rancho de la Merced, Ctra. Cañada de la Loba (CA-3102), Km 3, 11471, Jerez de la Frontera, Spain

ARTICLE INFO

Keywords:
GC-MS
Sparkling wine
Terpenes
Response surface methodology
Box-Behnken design
Variable selection

ABSTRACT

A headspace solid-phase microextraction coupled to gas-chromatography and mass spectrometry (HS-SPME-GC-MS) was developed and validated for the determination of 26 terpenes in sparkling wines. The use of a Box-Behnken experimental design, together with the desirability function D, allowed the extraction conditions of the method to be optimized. The optimal extraction conditions were found at a dilution ratio of 2:3, the addition of 3.5 g of NaCl, an extraction temperature of 46 °C and an extraction time of 52 min, using the DVB/CAR/PDMS fibre. Afterwards, the analytical method was successfully validated in terms of linearity, matrix effect, limit of detection and quantification, precision and accuracy. To test the developed method, 35 commercial sparkling wines from different grape varieties, geographical regions and ageing times were analysed and their terpenoid profile was monitored. The use of multivariate statistical tools made it possible to highlight differences in the samples related to the terpene profile. Finally, the most important compounds involved in the discrimination of the samples were identified by means of iterative variable selection procedures.

1. Introduction

Sparkling wine production has shown an important global growth in the last decade. The special winemaking involving two fermentations enables a product to be obtained that results of great interest for consumers, who are increasingly concerned about the quality of wines [1]. In recent years there has been a growing trend towards more regular consumption instead of merely in festive periods, which has driven a steady annual increase in the production of these wines [2]. In addition, the huge economic impact makes it appealing for winemakers to elaborate these wines, and new regions which are not traditionally producers of sparkling wines have increased their production [3].

To challenge the changing market, winemakers look for improvements in wine quality to adapt their production to the preferences of consumers [1]. In this sense, aroma is an important sensory contributor to wine quality. Consumers' perception highly depends on this attribute, which is the result of the interaction of a large number of chemical components (volatile and non-volatile) and sensory receptors [4]. Thus, the characterization of the volatile profile of wines has attracted the attention of researchers, who are developing the tools to better manage their sensory properties. The amount of the volatile compounds in wines depends on several factors including viticultural influences, crop management, grape variety, ripeness and winemaking conditions such as fermentation and ageing [5]. Among the volatile components present in wines, some terpenoids were described as important contributors to wine aroma [6]. They are secondary plant metabolites with a high chemical diversity that are generated from isopentyl pyrophosphate and its isomer dimethylallyl pyrophosphate [6]. Numerous studies have identified these compounds as the axis of sensorial expressions of the typical wine bouquet related to certain grape varieties [7]. Terpenes largely contribute to the fruity and floral aromas of wines but several have resin-like odours [8] as well as odours of seeds and roots [7]. These compounds, which are important aroma precursors, can occur in wine in free forms and bound to a sugar moiety [6].

* Corresponding author.
** Corresponding author.
E-mail addresses: josem.munoz.redondo@juntadeandalucia.es (J.M. Muñoz-Redondo), josem.moreno.rojas@juntadeandalucia.es (J.M. Moreno-Rojas).

https://doi.org/10.1016/j.talanta.2019.120483
Received 17 July 2019; Received in revised form 16 October 2019; Accepted 18 October 2019
Available online 19 October 2019
0039-9140/

Several terpenoids were previously described as key compounds related to the aroma of sparkling wines [9]. However, the role of some terpenes in sparkling wines remains unknown despite their contribution to the aroma. In this sense, megastigmatrienone is a compound related to tobacco aroma, with spicy and peppery notes that has been quantified in white and red wines [10]. Nonetheless, no studies concerning this compound in sparkling wines have been reported to date.

Due to the relatively low concentrations of terpenes in wines and the complexity of wine metabolome, some isolation and pre-concentration step is previously required. Headspace solid-phase microextraction is a simple, solvent-free, quick, effective and cost-saving extraction technique with a great potential for the extraction of volatile compounds in complex matrices [11]. This technique has been widely used in conjunction with gas chromatography-mass spectrometry (GC-MS). Studies can be found in the literature dealing with volatile compounds in sparkling wines [3,9,12–15]. However, to the authors' knowledge, no HS-SPME methods have been developed to optimize the extraction of terpenes in sparkling wines. The optimization of this technique may be achieved through response surface methodology (RSM). This multivariate optimization allows the study of all explanatory variables at one time, avoiding the misleading results often obtained when the levels of one variable are changed while the others remain invariable (classic one-variable-at-a-time). Afterwards, multiple response optimization can be addressed to obtain the operating conditions that yield the best compromise signals for multiple target metabolites. It aims at ensuring compliance of all the involved responses, being of particular interest for metabolites with low signals.

Considering the importance of terpene compounds in the aroma of wines, and that no analytical method exists to quantify these metabolites in sparkling wines, this study aimed at optimize and validate an HS-SPME-GC-MS methodology for the simultaneous quantification of different classes of terpenoids present in sparkling wines. Subsequently, 20 Cavas, 8 Champagnes and 7 Andalusian sparkling wines were analysed. Moreover, advanced chemometric tools were employed to study the changes occurring in the terpene profile of the samples based on the ageing time, grape variety and origin of the sparkling wine.

2. Material and methods

2.1. Wine samples

A total of 35 commercial sparkling wines were collected for this study, including different varieties, ageing time, vintage and geographical origin. All the wine samples were frozen at −80 °C until analysis to assure its stability. The experimental design included 20 Cavas and 8 Champagnes which are produced according to the regulation of their respective protected designations of origin (PDO) and 7 sparkling wines produced in Andalusia (southern Spain) with a similar elaboration procedure but without an established PDO. All the Champagnes had had over 24 months of ageing due to the specification of this PDO. Meanwhile, the ageing period of Cava and Andalusian sparkling wines ranged from 9 months to over 30.

2.2. Reagents and materials

HPLC-grade ethanol was supplied by J.T. Baker Chemicals B. V. (Deventer, Holland). Milli-Q water was obtained from a Milli-Q Plus water system (Millipore, Spain). EDTA (ethylenediaminetetraacetic acid) was supplied by Panreac Applichem (Barcelona, Spain). Sigma Aldrich (Madrid, Spain) supplied the sodium chloride, ACS reagent grade (purity 99.8%) and standard compounds; 1-hexan-d_{13}-ol (98%) used as internal standard, cis-citral (56.2%) in a mix of isomers, trans-ocimene (74.8%), linalyl acetate (97.2%), trans-linalyl oxide (68.4%) in a mix of isomers, 1,4-cineole (99.2%), eucalytol (99.5%), (±)-camphor (97%), (−)-terpinen-4-ol (95.9%), *p*-cymene (99.8%), terpinolene (94.6%), γ-terpinene (98.5%), (−)-β-citronellol (99.4%), neryl acetate (98.6%), geranyl acetate (99.3%), cis-geraniol (98.6%), α-terpineol (98.6%), β-cyclocitral (96.2%), a mix of cis-nerolidol (52.3%) and trans-nerolidol isomers (47.2%), (±)-citronellal (95.0%) and β-damascenone (99.0%). 1,1,6-Trimethyl-1,2-dihydronaphthalene (TDN, 80%) was purchased from ChemCruz Biochemicals (Texas, USA). Megastigmatrienone as mix of isomers: megastigmatrienone 6Z8E (3.78%), megastigmatrienone 6Z8Z (13.72%), megastigmatrienone 6E8E (1.10%) and megastigmatrienone 6E8Z (10.77%) was supplied by Symrise (Holzminden, Germany).

2.3. Automated HS-SPME-GC–MS analysis

A total of 25 mL of the sparkling wine samples were spiked with 20 µL of a stock solution of 1-hexan-d_{13}-ol in ethanol at 200 mg/L. Then, the samples were diluted 2:3 with EDTA solution (200 mM and pH 7.0 adjusted with NaOH 1.0 M) and 10 mL of this dilution were placed in a 20 mL SPME vial filled with 3.5 g of NaCl. Next, the mixture was homogenized with a vortex shaker for 30 s and placed in a Combipal autosampler tray (CTC Analytics, Zwingen, Switzerland). The volatiles were sampled by HS-SPME with a previously conditioned 50/30 µm DVB/CAR/PDMS fibre (StableFlex/SS) supplied by Supelco (Bellefonte, PA, USA). The vials were incubated at 500 rpm for 2 min at 40 °C and the extraction of the volatiles was carried out at 46 °C for 52 min under continuous stirring at 500 rpm. The desorption time and temperature were fixed at 15 min and 250 °C respectively. This process was performed in a Trace GC ultragas chromatograph (Thermo Fisher Scientific S. p.A., Rodano, Milan, Italy). Afterwards, the desorbed samples passed to an ISQ Single MS spectrometer (Thermo Fisher Scientific, Austin, Texas, USA). The injection was performed in splitless mode for 0.75 min and a BP21 column of 50 m × 0.32 mm and 0.25 µm film thickness (SGE Analytical Science, UK) was used for the separation. The carrier gas was helium at a column-head pressure of 8.2 psi. The oven temperature program was set at 40 °C for 5 min, raised to 220 °C at 3 °C/min and held for 30 min. The MS operated in electron ionization mode at 70 eV using selected-ion-monitoring (SIM) mode. The transfer line and source temperature of the MS were set at 230 °C and 200 °C respectively. The identification procedure was performed by comparing the retention times and mass spectra with those of the pure standards. For the quantification of the compounds, calibration curves were built using two commercial Cavas and one Champagne with naturally low concentrations of target analytes spiked with a mixture of the analytes at seven levels of concentration. A pooled quality control (QC) sample was repeatedly analysed along all the experimentation to avoid misleading results due to metabolite degradation processes, changes on the equipment settings and sample preparation. Only metabolites with stable responses (RSD ≤ 20 in the QCs), were considered in the method.

2.4. Method development

2.4.1. Fibre selection

Three fibres with different coated stationary phases and film thicknesses were compared to examine the extraction efficiency of all terpenoids (50/30 µm DVB/CAR/PDMS, 85 µm CAR/PDMS and 100 µm PDMS, Supelco, Bellefonte, PA, USA). Each fibre was conditioned following the manufacturer's instructions. After the vials were stirred at 500 rpm for 2 min at 40 °C, the extraction of the volatile fraction of the samples was carried out for 45 min at 50 °C under continuous stirring at 500 rpm. Then, the fibre was introduced into the injector inlet for 15 min at 250 °C under splitless mode.

2.4.2. Optimization of HS-SPME conditions

The extraction conditions of the method were optimized to achieve the best chromatographic signals. Response surface methodology was used to model the peak response. Four three-level parameters were used to build a second order Box-Behnken design using the Matlab R2016a program. The levels of the model were as follows: temperature (30, 40,

50 °C), time (30, 45, 60 min), ionic strength (2, 3, 4 g of NaCl) and dilution (1:9, 3:7 and 1:1). The optimization of the models was performed using the desirability function D, a multiple response approach [16] using the program R v. 3.5.0.

2.5. Method validation

The validation of the method was assessed by considering several parameters: linearity of the calibration curves, precision (RSD %), accuracy (recovery at different spiked levels), limit of detection (LOD) and limit of quantification (LOQ). For linearity, three replicates of calibration solutions built in different wine matrices were analysed. LOD and LOQ were assessed using the signal-to-noise ratio for which the lowest injected concentration signal was still measurable for each analyte. Ratios of 3:1 and 10:1 were used for the LOD and LOQ respectively. Intra-day (repeatability) was assessed using identical samples (n = 7) of spiked Cava at two levels of concentration. Inter-day (reproducibility) was evaluated using an identical non-spiked sample of Cava monitored for a month (n = 10). Five replicates at two levels of concentration were used to evaluate the recovery of the method. The matrix effect was assessed by comparing the slope of three calibration curves built on different wine matrices, as previously described in Ref. [17].

2.6. Statistical analysis

The data acquired from the sparkling wines with the developed methodology were submitted to statistical analyses. A univariate approach was carried out using the R v. 3.5.0 program. The variance of the data was analysed by means of Levene's and Kolmogorov-Smirnov tests for homoscedasticity and normality requirements. Statistically meaningful differences were considered for $p < 0.05$. Fisher's Least Significant Difference (LSD) test was used for comparison of means followed by a multivariate statistical approach to unravel the structure of the data. A Principal Component Analysis (PCA) was carried out for data exploration. Partial Least Squares Discriminant Analysis (PLS-DA) was used for classification tasks and selection of the most discriminative compounds. Models were optimized on the basis of a double cross-validation scheme previously described in Szymanska et al. [18], using M-fold cross-validation in the outer loop (a total of 30 submodels were built) and leave-one-out cross validation in the inner loop. Balanced Error Rate (BER) measured at the Mahalanobis distance was used as the diagnostic statistic to assess the prediction ability of each model. The statistical significance of the PLS-DA models was calculated as follows:

$$P - value = 1 + (BER_P \leq BER)/N$$

where ($BER_P \leq BER$) is the number of elements in the H_0 distribution that are smaller or equal to BER of the original data. H_0 distribution was generated by permuting randomly the labels of the samples, in our case N = 1000 permutations since it was large enough to sample the tails of the distribution and to attain a p-value up to 0.001. The BER of the original data was calculated averaging the 30 values obtained from the 30 submodels generated during the cross-validation. Selection of the most discriminative compounds was performed following a similar iterative procedure described in Khakimov et al. [19]. The raw data set was randomly divided in a test and calibration set at a ratio 1:3 (outer loop), keeping the same proportion of samples belonging to each class in both sets. The calibration set was further used for the optimization of each sub-model using a leave-one-out re-sampling procedure (inner loop). At this step, Variable Importance in Projection (VIP) scores were obtained and only compounds that exceeded an initial threshold, set to 0.7, were used to build a new model with the optimized components on the full calibration set. The VIP value threshold was increased 0.05, the test set was predicted with the optimized model and the BER value was kept. This process was repeated as long as the BER of each new model with a reduced number of variables decreased or remained unchanged. A total of 100 models were built using this iterative procedure, and variables which were selected in at least 70% of the calibration and validation set pairs were further used to build a final model, which was validated using the previously mentioned double cross-validation scheme described in Szymanska et al. [18]. The quality of the final models after variable reduction and PLS-DA built with all the variables was compared. All the multivariate data analyses were performed using in-house routines based on the *mixOmics* package [20] from the R v. 3.5.0.

3. Results and discussion

A preliminary GC-MS scan of several sparkling wines (Cava, Champagne and Andalusian sparkling wines) was performed. The chromatographic profile showed a large number of volatile compounds present in these wines. Thus we decided to develop a precise, accurate and robust method for the simultaneous determination of the main volatile terpenoids found in sparkling wines.

3.1. Optimization of HS-SPME fibre

Terpenoids display vast chemical diversity, meaning different polarities and boiling points. Thus, variations in the optimal extraction conditions of each terpenic compound were expected. To select the best extraction conditions, three fibres were tested covering important extraction properties: 100 µm PDMS fibre is appropriate for volatile non-polar and low molecular weight compounds; 85 µm CAR/PDMS fibre has been widely used for polar volatile analytes, allowing higher adsorption and desorption yielding; while 50/30 µm DVB/CAR/PDMS fibre ensures the extraction of compounds with an extensive range of molecular masses (40–275) [21,22]. The peak signal of the target compounds grouped by sub-families was measured for each fibre (Supplementary Fig. 1). The PDMS fibre displayed the lowest extraction yield for terpenoids. This fibre only showed a good extraction capacity compared with the rest in the case of sesquiterpenes. CAR/PDMS and DVB/CAR/PDMS fibres were the best in terms of peak signal responses. Both fibres presented similar behaviour in the lower boiling point monoterpenes and C13-norisorprenoids, with non-significant differences in their responses. However, the CAR/PDMS fibre was less effective at extracting the higher boiling point monoterpenes and sesquiterpenes (Supplementary Fig. 1). In light of these results, the DVB/CAR/PDMS fibre was selected as optimal for developing the method.

3.2. Optimization of the HS-SPME conditions

The HS-SPME yield can be affected by changes in the experimental conditions. Four parameters (extraction temperature, extraction time, ionic strength and dilution of the sample) were chosen to optimize the extraction conditions because of their influence in the instrumental response [17,22–25]. Several variables such as desorption time and sample agitation were not included in the optimization procedure since they do not strongly impact on the sensitivity of HS-SPME [23].

3.2.1. Extraction temperature and time

The temperature influences the extraction process of the HS-SPME procedure because the partition coefficients strongly depend on this parameter. Higher temperatures allow volatile compounds to overcome energy barriers, facilitating the release of the volatile profile into the headspace [26]. However, an increase in the temperature does not always provide higher extraction rates, depending on the nature of the analytes [27]. The extraction temperature displayed a critical point at 50 °C, since the Millard reaction and Stecker degradation could appear for terpenes exceeding this temperature [10,27]. For this reason, temperatures between 30 and 50 °C were used to avoid misleading results. Meanwhile, the extraction time determines when the analyte reaches the distribution equilibrium between the sample solution phase and the

SPME stationary phase. The extraction time ranged between 30 and 60 min.

3.2.2. Salt addition and dilution of the sample

The addition of salts increases the ionic strength of the samples. This decreases the solubility of the organic compounds and affects the partition coefficient, improving the extraction of the analytes. However it can lead to a loss of fibre selectivity [28]. The amount of salt chosen (NaCl, in our case) ranged between 2 and 4 g. Moreover, the selection of an appropriate dilution ratio may reduce matrix interferences [29] and is useful to control the ethanol content. This parameter ranged from 1:9 to 1:1 (X_{sample}:X_{AEDT}).

3.2.3. Response surface methodology for the optimization of the HS-SPME conditions

A Box-Behnken design (BBD) was applied to optimize the analytical method. BBD is a class of rotatable or nearly rotatable second-order design based on three levels at −1, 0 and + 1 combinations in terms of coded factors [16]. A second order model was fitted for each compound, considering the interaction among the factors involved. A total of 24 experiments by duplicate and 6 centre points were run. To avoid misleading results caused by the effects of systematic errors, all the experiments were carried out randomly. Terpenes were grouped in 4 subfamilies (Table 1) and a response surface model was fitted for each one using the stepwise regression approach (forward and backward selection) that minimized the Bayesian Information Criterion (BIC). The following mathematical model was fitted to each subfamily of terpenes to relate the variation of the response area with the changes in the 4 factors:

$$Y_i = \alpha_0 + \beta_1 {*} X_1 + \beta_2 {*} X_2 + \beta_3 {*} X_3 + \beta_4 {*} X_4 + \beta_{12} {*} X_1 {*} X_2 + \beta_{13} {*} X_1 {*} X_3 + \beta_{14} {*} X_1 {*} X_4 + \beta_{23} {*} X_2 {*} X_3 + \beta_{24} {*} X_2 {*} X_4 + \beta_{34} {*} X_3 {*} X_4 + \beta_{11} {*} X_1^2 + \beta_{22} {*} X_2^2 + \beta_{33} {*} X_3^2 + \beta_{44} {*} X_4^2$$

where, Y_i is the response (peak area of the compound i), α_0 is the intercept, β_j and β_{jk} are the coefficients indicating the effect on the responses and X_i are the factors. The response surface models were obtained considering only the coefficients with a p-value ≤ 0.05. An analysis of variance (ANOVA) was performed to evaluate the suitability of the fitted models and identify their statistical significance (Table 1). The lack of fit was not significant at 95% in any case and the determination coefficients were adequate (Table 1). Next, the signal optimization of the different subfamilies of terpenes was addressed by means of the desirability function D. This function, advocated by Derringer and Suich [30], is an increasingly popular approach suitable for simultaneous optimization of multiple responses. Each individual response is transformed from the experimental domain to a desirability function d, ranging from d = 0 (when the response value is unacceptable) to d = 1 (for fully desirable responses). Afterwards, the global desirability function D is calculated as the geometric mean of the individual desirability values. This fitness function is assessed as an individual output response. To solve the optimization, a simulation approach with a genetic algorithm was used [31] with the D function as the objective to maximize. The crossover and mutation probabilities were set at 0.8 and 0.1 respectively with 5% elitism. The results showed the highest D function value for the following conditions: extraction temperature of 46 °C, extraction time of 52 min, a dilution ratio of 2:3 and 3.5 g of salt addition.

Table 1
Analysis of variance (ANOVA) for the fitted models obtained from the second order Box-Behnken design.

Group of terpenes	R^{2a}	R^{2b}_{Λ}	LoF[c]	p-value (model)
Σ Sesquiterpenes	0.947	0.913	0.183	< 0.001
Σ C_{13}-Norisoprenoids	0.891	0.867	0.283	< 0.001
Σ Less Volatile Monoterpenes	0.897	0.857	0.614	< 0.001
Σ More Volatile Monoterpenes	0.906	0.856	0.131	< 0.001

[a] Coefficient of determination.
[b] Coefficient of determination adjusted.
[c] Lack of fit test. Values higher than 0.05 indicate insignificant lack of fit.

3.3. Testing method performance

Once the parameters of the extraction conditions were optimized, the GC-MS methodology was validated. An isotopically labelled internal standard 1-hexan-d_{13}-ol was used to normalize the peak areas of each compound to improve the precision of the analytical method. The analytical conditions used for the experiments were the following: 50/30 µm DVB/CAR/PDMS fibre, 52 min of extraction at 46 °C, 10 mL of sample diluted 2:3 in EDTA solution and 3.5 g of NaCl. The analytes were desorbed at 250 °C for 15 min.

3.3.1. Linearity and limits of detection

Three calibration curves were built in three different wine matrices: a young multi-varietal Cava, an old mono-varietal Cava and an old multi-varietal Champagne. The calibration curves were fitted by means of least-squares linear regression and a weighting factor was tested for each compound to prevent domination at the top levels of the curve (Table 2). The least amount of weighting that minimized the sum of the relative errors in the regression was selected and the determination coefficient (R^2) was obtained. All the compounds displayed adequate linearity, with $R^2 \geq 0.99$ (Table 2). The limits of detection (LODs) and quantification (LOQs) were calculated as the lowest injected concentration for which validation was achieved, with a signal-to-noise ratio of 3 and 10 respectively.

3.3.2. Precision and accuracy

The repeatability and reproducibility of the method was evaluated by the relative standard deviation (RSD %). The RSD values ranged from 2 to 20% for the repeatability at two levels and from 7 to 19% for the reproducibility (Table 2). The accuracy was calculated in terms of recovery. For the two levels of concentration, the recovery yields varied between 81 and 119% (Table 2). The matrix effect was assessed by comparing the slope of three calibration curves built in different wine matrices (from different varieties, ageing, geographical origin and vintage) and calculating the RSD. This value ranged between 2 and 20% in the studied compounds (Table 2).

3.4. Application to wine analysis

The developed and validated methodology was applied to characterize 35 commercial sparkling wines (20 Cavas, 8 Champagnes and 7 Andalusian sparkling wines) from different grape varieties (Chardonnay and multivarietal sparkling wines) and with different ageing times (from 9 up to more than 30 months) and origins (Champagne, Cava and Andalusian sparkling wine). The analyses were carried out in duplicate. The mean concentrations with the standard deviation are shown in Supplementary Table 1. The terpene concentration ranges were in accordance to those found in previous studies with similar matrices [6,10,15,32–41]. The components found in the highest levels were cis-citral (8.1–28.4 µg/L), trans-linalyl oxide (12–112 µg/L) and α-terpineol (0.90–21.2 µg/L).

3.4.1. Univariate approach

Analyses of variance (ANOVA) were carried out (Table 3) in order to highlight differences in the samples related to the following factors: ageing time, grape variety and origin of the sparkling wines. Differences were found among samples due to the ageing time. The sparkling wines with longer ageing periods displayed higher concentrations of trans-linalyl oxide, eucalyptol, (−)-terpinen-4-ol, neryl acetate, (±)-citronellal and β-damascenone. Meanwhile, (−)-β-citronellol and α-

Table 2
Retention indexes, ions, linearity, precision, accuracy, detection and quantification limits of each terpene compound in the sparkling wines analysed.

Analyte	LRI[a]	Ions (*m/z*)[b]	Linearity[c]						LOD[e] (µg/L)	LOQ[f] (µg/L)	Precision (RSD %)			Accuracy[i]		
			Slope	Intercept	Range	R^2	RSD	Relative Error	n[d]		Intra-day[g]		Inter-day[h]	Added (µg/L)	Recovery at low level (%)	Added (µg/L)	Recovery at high level (%)
											Level A	Level B					
Monoterpenes																	
cis-citral	1674	69/109/123	0.0040	0.0088	0.26–51.9	0.998	12	0.14	0	0.08	0.26	7	19	16	5.19	112	26.0	95
trans-ocimene	1245	93/121/136	0.2034	0.0003	0.013–1.38	0.997	16	0.11	0.5	0.004	0.013	4	12	11	0.14	85	0.69	81
trans-linalyl oxide	1462	94/68/112	0.0024	0.0029	0.75–150.5	0.999	14	0.14	0	0.23	0.75	15	8	16	15.0	115	75.2	101
Eucalyptol	1189	108/111/139	0.0370	−0.0009	0.10–10.5	0.998	17	0.19	1	0.03	0.10	13	6	16	1.0	113	5.2	99
(±)-camphor	1497	108/95/152	0.0130	0.0032	0.44–44.2	0.998	8	0.09	1	0.13	0.44	8	4	13	4.4	104	22.1	98
(−)-terpinen-4-ol	1590	111/136/154	0.0491	0.0049	0.047–9.6	0.997	19	0.12	0	0.014	0.047	4	2	15	0.96	108	4.8	107
1, 4-cineole	1191	111/125/154	0.0280	0.0015	0.079–8.0	0.999	11	0.09	0	0.024	0.079	8	4	17	0.80	110	4.0	97
p-cymene	1255	119/91/134	0.4609	0.0042	0.088–8.9	0.994	13	0.09	2	0.026	0.088	6	6	7	0.89	108	4.4	101
Terpinolene	1271	121/105/119	0.1483	−0.0003	0.048–4.9	0.995	16	0.12	2	0.014	0.048	6	5	9	0.48	100	2.4	99
γ-terpinene	1235	121/119/136	0.0643	0.0008	0.081–8.2	0.996	18	0.12	0	0.024	0.081	14	5	14	0.82	104	4.1	103
(−)-β-citronellol	1764	123/109/138	0.0343	−0.0007	0.050–10.2	0.993	2	0.30	0	0.015	0.050	7	10	15	1.0	93	5.1	103
cis-geraniol	1798	69/93/136	0.1364	0.0257	0.089–8.9	0.999	9	0.09	0	0.027	0.089	7	4	14	0.89	106	4.5	94
α-terpineol	1689	139/121/136	0.0050	0.0008	0.21–42.6	0.998	9	0.23	0	0.06	0.21	8	8	19	4.3	116	21.3	114
β-cyclocitral	1609	152/109/137	0.0808	0.0068	0.043–8.7	0.999	14	0.10	0	0.013	0.043	14	9	11	0.87	101	4.4	102
Linalyl acetate	1553	93/121/136	0.0526	0.0088	0.094–9.5	0.991	15	0.19	2	0.028	0.094	17	20	17	0.94	118	4.7	89
Neryl acetate	1723	136/93/121	0.0745	−0.0014	0.098–9.9	0.997	11	0.07	1	0.029	0.098	14	6	17	0.99	98	4.9	94
Geranyl acetate	1753	136/93/121	0.1194	−0.0003	0.020–2.1	0.998	10	0.12	1	0.006	0.020	14	18	16	0.21	98	1.0	102
(±)-citronellal	1475	69/121/154	0.0050	−0.0009	0.24–48.21	0.998	15	0.28	0	0.161	0.482	17	13	14	4.82	113	24.1	117
Sesquiterpenes																		
cis-nerolidol	1995	161/93/107	0.0589	0.0020	0.025–5.0	0.996	9	0.10	0	0.008	0.025	12	8	12	0.50	87	2.5	98
trans-nerolidol	2037	161/93/107	0.1103	0.0020	0.022–4.5	0.993	4	0.32	0	0.007	0.022	8	6	16	0.45	117	2.3	89
C_{13}-*Norisoprenoids*																		
TDN	1729	172/142/157	0.3528	0.0313	0.25–50.4	0.991	5	0.07	0.5	0.08	0.25	11	9	14	5.0	86	25.2	94
β-damascenone	1813	190/121/175	0.0685	0.0488	0.72–144.6	0.992	16	0.16	2	0.22	0.72	10	7	12	14.5	114	72.3	117
Megastigma 6Z8E	2141	190/119/161	0.0329	0.0009	0.061–6.1	0.993	7	0.19	0.5	0.018	0.061	11	8	18	0.61	84	3.1	94
Megastigma 6Z8Z	2188	190/119/162	0.0200	0.0028	0.11–22.2	0.998	6	0.10	0	0.03	0.11	8	7	14	2.2	119	11.1	118
Megastigma 6E8E	2255	190/119/163	0.0353	0.0011	0.017–1.8	0.999	7	0.13	1	0.005	0.017	10	13	16	0.18	103	0.89	100
Megastigma 6E8Z	2288	190/119/164	0.0102	0.0025	0.087–17.5	0.997	11	0.11	0	0.026	0.087	5	12	15	1.7	107	8.7	100

[a] Experimental linear retention indexes in a BP21 chromatographic column.
[b] Ions used for identification; in bold ions used for quantification in SIM mode.
[c] For linearity, each terpene concentration was tested in 5 calibration curves.
[d] Weighting factor ($1/x^n$) selected for built the calibration curve. n = 0, 0.5, 1 and 2 were tested.
[e] LOD: limit of detection in sparkling wine (signal/noise concentration = 3) and.
[f] LOQ: limit of quantification in sparkling wine (signal/noise concentration = 10).
[g] Intra-day (repeatability) was evaluated using identical samples of spiked wine (n = 7).
[h] Inter-day (reproducibility) was evaluated using an identical non-spiked sparkling wine monitored during one month (n = 8).
[i] Average (n = 7) recoveries (%) of ester compounds in sparkling wine samples at two different level of concentrations.

Table 3
One-way Analysis of variance (ANOVA) for the origin, grape variety and ageing time factors carried out in the sparkling wines analysed.

Compound	Ageing time[a]				Grape variety[b]			Origin[c]			
	A1	A2	A3	p-value[(d)]	CH	MV	p-value[(d)]	AN	C	CHA	p-value[(d)]
Monoterpenes											
cis-citral	18	17	16	ns	16b	18a	*	23a	17b	16b	***
trans-ocimene	< LOQ	0.015	0.013	ns	0.014	0.013	ns	0.015	0.013	0.014	ns
trans-linalyl oxide	24b	35a	42a	***	42a	34b	*	52a	39b	35b	*
Eucalyptol	0.12b	0.12b	0.20a	*	0.17	0.17	ns	0.29a	0.17b	0.17b	**
(±)-Camphor	0.53	0.59	0.78	ns	0.68	0.71	ns	2.06a	0.70b	0.69b	***
(−)-terpinen-4-ol	0.53b	0.63a	0.61a	*	0.59	0.62	ns	0.82a	0.61b	0.58b	***
1,4-cineole	0.26	0.26	0.37	ns	0.23b	0.42a	***	0.35	0.32	0.34	ns
p-cymene	< LOQ	< LOQ	< LOQ	–	< LOQ	< LOQ	–	< LOQ	< LOQ	< LOQ	–
Terpinolene	< LOQ	< LOQ	< LOQ	–	< LOQ	< LOQ	–	< LOQ	< LOQ	< LOQ	–
γ-terpinene	0.092	0.121	0.168	ns	0.14	0.15	ns	0.965a	0.175b	< LOQ	***
(−)-β-citronellol	0.34a	0.37a	0.17b	***	0.26	0.23	ns	0.39a	0.28a	0.15b	**
cis-geraniol	0.50	0.55	0.39	ns	0.34b	0.55a	***	0.30b	0.47a	0.39 ab	*
α-terpineol	6.7a	4.5b	2.5c	***	2.9b	4.3a	*	11.1a	4.0b	2.5b	***
β-cyclocitral	0.28 ab	0.28a	0.23b	*	0.23	0.26	ns	0.35a	0.28b	0.17c	***
Linalyl acetate	< LOD	< LOD	< LOD	–	< LOD	< LOD	–	< LOQ	< LOD	< LOD	–
Neryl acetate	0.14b	0.21a	0.21a	*	0.22a	0.18b	*	0.30a	0.20b	0.19b	***
Geranyl acetate	0.021	0.021	< LOQ	ns	< LOQ	0.023a	***	0.029a	0.021b	< LOQ	***
(±)-citronellal	3.8b	6.0a	5.7a	**	5.6	5.4	ns	8.6a	5.6b	5.3b	***
Sesquiterpenes											
cis-nerolidol	0.14b	0.29a	0.22 ab	*	0.26a	0.19b	*	0.31a	0.25a	0.17b	*
trans-nerolidol	0.332 ab	0.772a	0.082b	*	0.44	0.14	ns	0.139	0.369	0.093	ns
C_{13}-Norisoprenoids											
TDN	2.21	3.5	1.93	ns	1.02b	3.70a	***	4.57a	3.19a	0.28b	***
β-damascenone	1.53b	3.62a	3.23a	***	3.5a	2.7b	*	3.0	3.0	3.2	ns
Megastigma 6Z8E	0.091	0.156	0.126	ns	0.13	0.12	ns	0.154a	0.151a	0.072b	**
Megastigma 6Z8Z	0.30	0.59	0.55	ns	0.62a	0.43b	*	0.79a	0.60 ab	0.34b	*
Megastigma 6E8E	0.019	0.049	0.047	ns	0.055a	0.032b	*	0.068a	0.051 ab	0.026b	*
Megastigma 6E8Z	0.28	0.71	0.62	ns	0.72a	0.46b	*	0.95a	0.69 ab	0.35b	*

(d) p-value of the One-Way ANOVA; ns: p-value > 0.05, *: 0.05 < p-value < 0.01, **: 0.01 < p-value < 0.001, ***: p-value < 0.001. LOD: limit of detection. LOQ: limit of quantification.

[a] Wines from different ageing times. A1: 9–15 months of ageing; A2: 15–24 months of ageing; A3: over 24 months of ageing. Only cava and champagne wines are included.

[b] Grape variety of the sparkling wines. CH: Chardonnay; MV: Multivarietal. Only Cavas and Champagnes are included.

[c] Classification of wines according to the origin. AN: Andalusian sparkling wines; CA: Cavas; CHA: Champagnes.

terpineol were found in higher contents in younger sparkling wines. In the case of the sesquiterpenes cis-nerolidol and trans-nerolidol, the highest concentrations were observed in wines with an intermediate ageing time, A2, that ranged from 15 to 24 months (Table 3). Regarding the grape variety factor, some differences in the terpenic profile were highlighted. Only Chardonnay and multivarietal Champagnes and Cavas were included to obtain a factorial design. The Chardonnay grape variety showed a slightly higher content of megastigma isomers, β-damascenone, cis-nerolidol, neryl acetate and trans-linalyl oxide. The contrary behaviour was observed for cis-citral, 1,4-cineole, cis-geraniol, α-terpineol, geranyl acetate and TDN, displaying higher concentrations in multivarietal sparkling wines. On the other hand, several compounds showed significant variations according to the origin of sparkling wines factor. Andalusian sparkling wines showed the highest concentrations of many terpenes (Table 3). Meanwhile, the Cavas and Champagnes showed a more similar terpene composition, but the contents of (−)-β-citronellol, β-cyclocitral, cis-nerolidol, geranyl acetate, TDN and megastigmatrienone 6Z8E were significantly higher in Cavas.

3.4.2. Multivariate approach

In order to search for differences in the samples related to the effect of the studied factors and to detect systematic errors and trends, a multivariate approach was followed. The data was first autoscaled and a Principal Component Analysis (PCA) was constructed. PCA [42] is a variable reduction technique that allows highly correlated variables to be transported to a lower-dimensional domain containing the uncorrelated information (built by the Principal Components; PCs). Scores and loadings were plotted in the subspace spanned by the first two PCs (Supplementary Fig. 2), since the remaining PCs contained irrelevant information for our study (figures not shown). The first two PCs accounted for the 48% of the accumulative variance found in samples. The complexity and variability of the sparkling wines analysed did not allow a clear differentiation to be observed among them. However, a higher scattering effect was observed for the Andalusian sparkling wines, while Champagnes and Cavas were allocated in a lower scattering area. The limited geographic region, as well as the controlled quality rules permitted in the PDO specifications of Cava and Champagne sparkling wines could explain these results. Subsequently, classification models were built for each factor maintaining a factorial design structure. Partial Least Squares Discriminant Analysis (PLS-DA), a linear model commonly used for classification tasks that is able to predict the class of new samples [20] was performed. First, a PLS-DA model with all the variables (compounds) was optimized and validated on the basis of a double cross validation scheme. Afterwards, an iterative procedure based on VIP scores was followed to select the most discriminative compounds, which were further used to optimize and validate a new model. This routine was used to highlight the effect of the ageing time factor on the sparkling wines. Only the samples grouped in A1 (9–15 months of ageing) and A3 (more than 24 months of ageing) were included in the final model. A2 (15–24 months of ageing) were kept out of the model due to the ageing closeness to A1 and A3 sparkling wines. The final discriminant analysis, obtained after selection of the most discriminative compounds, displayed an overall mean BER of 0.24 with a statistical significance of 0.025 (Table 4). This

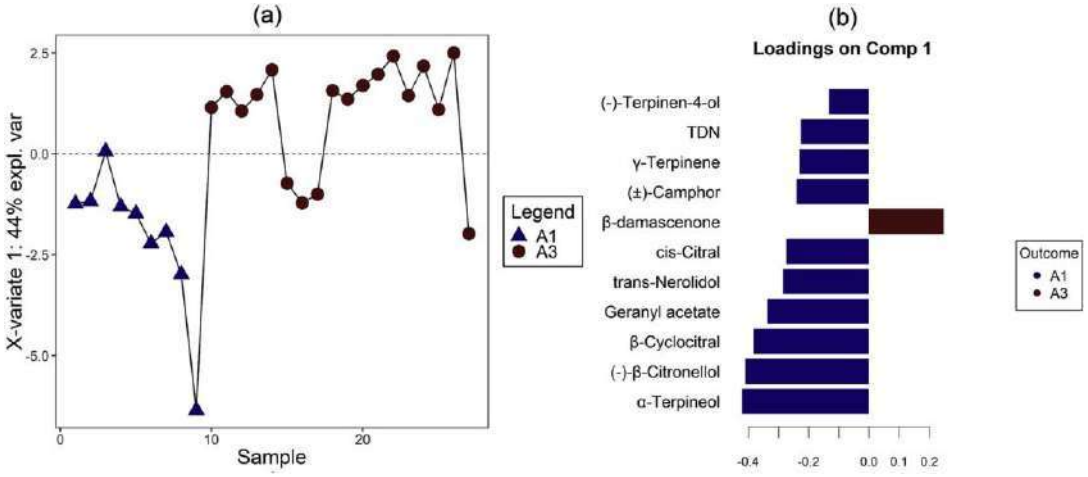

Fig. 1. Graphical outputs of the Partial Least Squares Discriminant Analysis (PLS-DA) performed on the ageing time factor after variable reduction. (a) Scores plot for the component 1 (X-variate 1) and (b) loading contribution barplots on component 1 for compounds selected in the iteration procedure. Colour indicates the class for which the compound has a maximal mean value. Bar length represents the multivariate regression coefficient with either a positive or negative sign for that particular feature on each component, i.e., the importance of each variable in the model. A1: sparkling wines with 9–15 months of ageing; A3: sparkling wines with more than 24 months of ageing. (For interpretation of the references to colour in this figure legend, the reader is referred to the Web version of this article.)

Table 4
Performance of the PLS-DA models carried out for the ageing time, grape variety and wine style factors. A comparison of performances before and after the iterative variable selection process based on VIP scores was included.

Classification	Model[a]	Mean overall BER[b]	p-value[c]	Class	Mean class BER[d]
A1 vs A3	All variables	0.34 ± 0.08	0.105	A1	0.47 ± 0.13
				A3	0.21 ± 0.06
	Variable reduction	0.24 ± 0.07	**0.025**	A1	0.28 ± 0.11
				A3	0.20 ± 0.05
CH vs PL	All variables	0.26 ± 0.06	**0.020**	CH	0.27 ± 0.06
				PL	0.25 ± 0.06
	Variable reduction	0.17 ± 0.05	< **0.001**	CH	0.22 ± 0.07
				PL	0.12 ± 0.07
AN vs C vs CH	All variables	0.18 ± 0.07	< **0.001**	AN	0.08 ± 0.10
				C	0.25 ± 0.10
				CH	0.21 ± 0.13
	Variable reduction	0.10 ± 0.04	< **0.001**	AN	0.05 ± 0.07
				C	0.18 ± 0.07
				CH	0.08 ± 0.06

[a] PLS-DA models constructed with either all variables and variables selected in an iterative procedure based on Variable Importance in Projection (VIP).
[b] Mean overall BER values with the standard deviation calculated on the basis of 30 PLS-DA submodels in a double-cross validation scheme.
[c] Model statistical significance was calculated on the basis of a permutation test (N = 1000) using the mean overall BER as diagnostic statistic. Statistically significant models (p-value ≤ 0.05) were highlighted in bold.
[d] Mean class BER values with the standard deviation calculated on the basis of 30 PLS-DA submodels in a double-cross validation scheme.

was a substantial improvement on the model built with all the variables (BER = 0.34 and p-value > 0.05, and thus, non-significant model). Most of the 30 submodels were optimized for 1 component, that is plotted in Fig. 1. Some terpenoids such as α-terpineol, (−)-β-citronellol, β-cyclocitral, geranyl acetate, trans-nerolidol, cis-citral, (±)-camphor, γ-terpinene, TDN and (−)-terpinen-4-ol, showed higher mean concentrations in the A1 sparkling wines, as well as β-damascenone in A3 sparkling wines. The key role played by some of these terpenoids during the ageing of sparkling wines has already been described. Norisoprenoids, such as TDN, have already been described as ageing markers of Cavas [43]. Perez-Magariño et al. [41] reported a decrease in some terpenes that was particularly pronounced for (−)-β-citronellol, while a slight decrease in nerolidol was observed in Champagnes during ageing in bottles [44]. α-Terpineol, which is related to the characteristic fruitiness and floral notes of young wines [45], was selected as the most discriminative compound in A1 sparkling wines.

According to the grape variety, the samples were grouped into Chardonnay and multivarietal wines, removing the Andalusian sparkling wines with other grape varieties to achieve a factorial design. The variable selection process improved again the quality of the PLS-DA model from an initial BER of 0.26 (model built with all variables) to a final BER of 0.17 (Table 4). The most repeated optimized number of components in the 30 submodels during the cross validation was 2. The compounds selected after the variable reduction iteration were considered as potential volatile markers and are shown in Fig. 2. Among them, geranyl acetate, 1,4-cineole, TDN and cis-geraniol were highlighted as the most important contributors to differentiate multivarietal sparkling wines and displayed higher mean levels in this labelled class of wines. Meanwhile, the Chardonnay sparkling wines were richer in some C_{13}-norisoprenoids such megastigmatrienone 6E8E, β-damascenone, megastigmatrienone 6E8Z and megastigmatrienone 6Z8Z, as well as the sesquiterpene cis-nerolidol, all of them selected as potential volatile markers of sparkling wines elaborated with Chardonnay grapes. It is of note that β-damascenone was previously found in high concentrations in Chardonnay wines [46] and it was suggested that this compound was involved in the typicality of wines elaborated from this grape [47]. In addition, a previous study reported an increase in this compound during the second fermentation in sparkling wines [39], emphasizing the potential importance of β-damascenone in the typicality of sparkling wines elaborated from Chardonnay grapes. Moreover, C_{13}-norisoprenoids have gained research attention due to their wide range of sensory descriptors, reported as floral, fruity, petrol and fly spray [6]. More recently, high concentrations of these compounds were shown to be positively correlated with the quality of wines [48]. In this sense, cis-geraniol and 1,4-cineole (Fig. 2) were found as important discriminative compounds for multivarietal sparkling wines.

The same procedure was followed to classify the wines according to the origin factor. The samples were grouped into Cava, Champagne and Andalusian sparkling wines. A satisfactory classification performance was obtained for the PLS-DA model after the variable selection process, with a mean overall BER of 0.10, which improved the initial 0.18

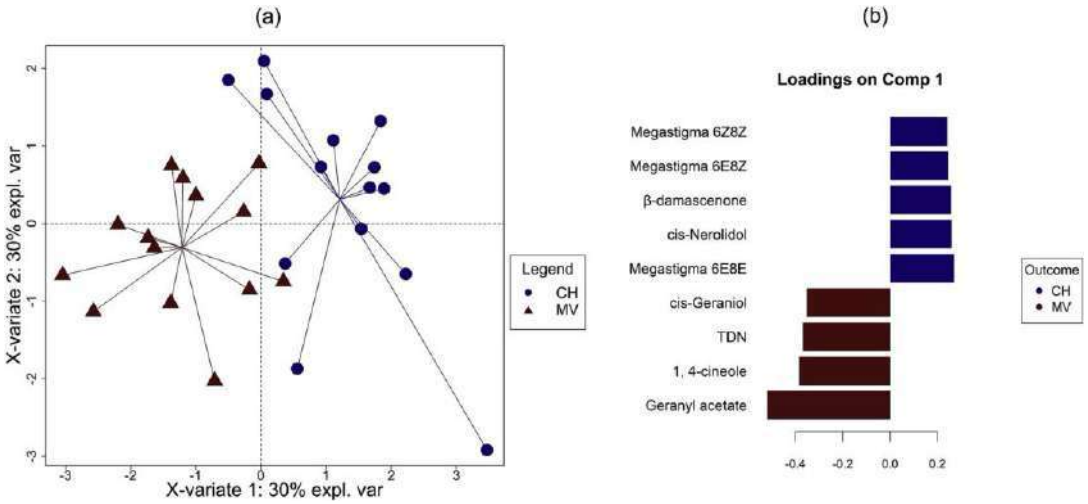

Fig. 2. Graphical outputs of the Partial Least Squares Discriminant Analysis (PLS-DA) performed on the grape variety factor after variable reduction. (a) Scores scatter plot for the subspace spanned by the component 1 (X-variate 1) and component 2 (X variate 2). (b) loading contribution barplots on component 1 for compounds selected in the iteration procedure. Colour indicates the class for which the compound has a maximal mean value. Bar length represents the multivariate regression coefficient with either a positive or negative sign for that particular feature on each component, i.e., the importance of each variable in the model. CH: Chardonnay sparkling wines, MV: multivarietal sparkling wines. (For interpretation of the references to colour in this figure legend, the reader is referred to the Web version of this article.)

balanced error rate of the PLS-DA constructed with all the variables (Table 4). The most repeated number of components in the 30 fitted submodels during the cross validation was 3. From this model, a clear differentiation can be observed between the Andalusian sparkling wines and the others in the X-variate 1 (component 1), which accounted for the 42% of the total variance found in the samples (Fig. 3). A total of 10 monoterpenes were selected on this component as important discriminators of the Andalusian sparkling wines, including 8 monoterpenes: (±)-camphor, (−)-terpinen-4-ol, cis-citral, α-terpineol, (±)-citronellal, β-cyclocitral, geranyl acetate and (−)-β-citronellol and 2 C_{13}-norisoprenoids: TDN and Megastigma 6Z8E. Meanwhile, cis-geraniol was selected as a potential marker for Cavas. The higher concentrations of terpenoids found in Andalusian sparkling wines could be associated with viticultural influences such as vine water deficit, crop thinning, soil type, sunlight exposure, UV-B radiation and basal leaf removal [49], linked to the use of grape varieties adapted to the special climatic conditions of this region. These findings open new avenues in the research into the elaboration of Andalusian sparkling wines, recently introduced onto the market and with their own typicality.

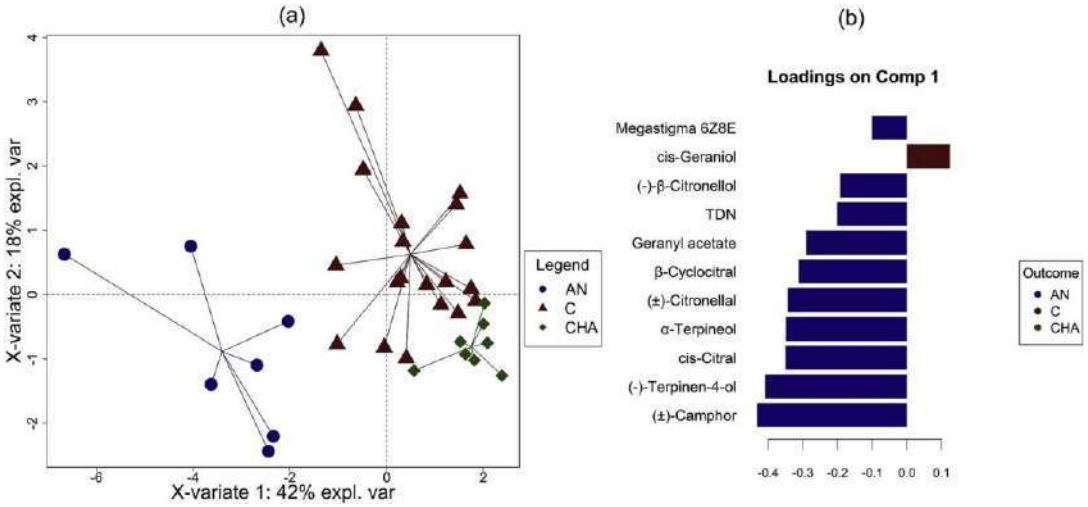

Fig. 3. Graphical outputs of the Partial Least Squares Discriminant Analysis (PLS-DA) performed on the sparkling wine style factor after variable reduction. (a) Scores scatter plot for the subspace spanned by the component 1 (X-variate 1) and component 2 (X variate 2). (b) loading contribution barplots on component 1 for compounds selected in the iteration procedure. Colour indicates the class for which the compound has a maximal mean value. Bar length represents the multivariate regression coefficient with either a positive or negative sign for that particular feature on each component, i.e., the importance of each variable in the model. AN: Andalusian sparkling wines; C: Cavas; CHA: Champagnes. (For interpretation of the references to colour in this figure legend, the reader is referred to the Web version of this article.)

4. Conclusions

A multivariate approach was performed to optimize the HS-SPME conditions for the quantification of terpene compounds in sparkling wines through GC-MS. Four factors affecting the HS-SPME were optimized by means of a second order Box-Behnken design. All the factors significantly affected the peak response of the chromatographic compounds. The linearity of the method was satisfactory in the range evaluated for each compound, with determination coefficients higher than 0.99. Good precision, accuracy, LOD and LOQ were attained for all the terpenoids included in the method. The optimized methodology was then applied to commercial sparkling wines from different geographical regions, ageing times and grape varieties. Differences in the terpene profile were observed regarding the ageing factor, grape variety and origin of the sparkling wines analysed. The potential of β-damascenone to modulate the typicality of sparkling wines produced from Chardonnay grapes was highlighted. Finally, Andalusian sparkling wines showed a different terpene profile to Cavas and Champagnes, mainly driven by higher contents of these compounds.

Notes

The authors declare no competing financial interest.

Fundings

This study has been funded by the Andalusian Institute of Agricultural and Fisheries Research and Training (IFAPA) through the Project PP.AVA.AVA201601.3.

Acknowledgments

This study was financed by the Andalusian Institute of Agricultural and Fisheries Research and Training (IFAPA) and the European Commission funds (European Rural Development Funds, ERDF) through the project 'Investigación e innovación tecnológica en vitivinicultura' (PR.AVA.AVA201601.3). José Manuel Muñoz-Redondo was awarded a research contract (2015–2017) from the Andalusian Institute of Agricultural and Fisheries Research and Training (IFAPA), the European Social Fund (ESF) and the Youth Employment Initiative (YEI). Maria José Ruiz-Moreno was awarded a postdoctoral research contract (2013–2017) from the Andalusian Institute of Agricultural and Fisheries Research and Training (IFAPA) and the European Social Fund (ESF).

Appendix A. Supplementary data

Supplementary data to this article can be found online at https://doi.org/10.1016/j.talanta.2019.120483.

References

[1] S. Torresi, M.T. Frangipane, G. Anelli, Biotechnologies in sparkling wine production. Interesting approaches for quality improvement: a review, Food Chem. 129 (2011) 1232–1241.
[2] The International Organisation of Vine and Wine, (2014).http://www.oiv.int/en/the-international-organisation-of-vine-and-wine (accessed July 22, 2018)..
[3] M.J. Ruiz-Moreno, J.M. Muñoz-Redondo, F.J. Cuevas, A. Marrufo-Curtido, J.M. León, P. Ramírez, J.M. Moreno-Rojas, The influence of pre-fermentative maceration and ageing factors on ester profile and marker determination of Pedro Ximenez sparkling wines, Food Chem. 230 (2017) 697–704.
[4] G. Styger, B. Prior, F.F. Bauer, Wine flavor and aroma, J. Ind. Microbiol. Biotechnol. 38 (2011) 1145–1159.
[5] R.F. Alves, A.M.D. Nascimento, J.M.F. Nogueira, Characterization of the aroma profile of Madeira wine by sorptive extraction techniques, Anal. Chim. Acta 546 (2005) 11–21.
[6] C.A. Black, M. Parker, T.E. Siebert, D.L. Capone, I.L. Francis, Terpenoids and their role in wine flavour: recent advances, Aust. J. Grape Wine Res. 21 (2015) 582–600.
[7] J. de S. Câmara, P. Herbert, J.C. Marques, M.A. Alves, Varietal flavour compounds of four grape varieties producing Madeira wines, Anal. Chim. Acta 513 (2004) 203–207.
[8] C. González-Barreiro, R. Rial-Otero, B. Cancho-Grande, J. Simal-Gándara, Wine aroma compounds in grapes: a critical review, Crit. Rev. Food Sci. Nutr. 55 (2015) 202–218.
[9] C. Ubeda, R.M. Callejón, A.M. Troncoso, A. Peña-Neira, M.L. Morales, Volatile profile characterisation of Chilean sparkling wines produced by traditional and Charmat methods via sequential stir bar sorptive extraction, Food Chem. 207 (2016) 261–271.
[10] D. Slaghenaufi, M.-C. Perello, S. Marchand-Marion, S. Tempere, G. de Revel, Quantitative solid phase microextraction–Gas chromatography mass spectrometry analysis of five megastigmatrienone isomers in aged wine, Anal. Chim. Acta 813 (2014) 63–69.
[11] C.-H. Xu, G.-S. Chen, Z.-H. Xiong, Y.-X. Fan, X.-C. Wang, Y. Liu, Applications of solid-phase microextraction in food analysis, TrAC Trends Anal. Chem. (Reference Ed.) 80 (2016) 12–29.
[12] J. Bosch-Fusté, M. Riu-Aumatell, J.M. Guadayol, J. Caixach, E. López-Tamames, S. Buxaderas, Volatile profiles of sparkling wines obtained by three extraction methods and gas chromatography–mass spectrometry (GC–MS) analysis, Food Chem. 105 (2007) 428–435.
[13] J.M. Muñoz-Redondo, F.J. Cuevas, J.M. León, P. Ramírez, J.M. Moreno-Rojas, M.J. Ruiz-Moreno, Quantitative profiling of ester compounds using HS-SPME-GC-MS and chemometrics for assessing volatile markers of the second fermentation in bottle, J. Agric. Food Chem. 65 (2017) 2768–2775.
[14] R.D. Soares, J.E. Welke, K.P. Nicolli, M. Zanus, E.B. Caramão, V. Manfroi, C.A. Zini, Monitoring the evolution of volatile compounds using gas chromatography during the stages of production of Moscatel sparkling wine, Food Chem. 183 (2015) 291–304.
[15] J. Torrens, M. Riu-Aumatell, S. Vichi, E. López-Tamames, S. Buxaderas, Assessment of volatile and sensory profiles between base and sparkling wines, J. Agric. Food Chem. 58 (2010) 2455–2461.
[16] S.C. Ferreira, R.E. Bruns, H.S. Ferreira, G.D. Matos, J.M. David, G.C. Brandao, E.P. da Silva, L.A. Portugal, P.S. Dos Reis, A.S. Souza, others, Box-Behnken design: an alternative for the optimization of analytical methods, Anal. Chim. Acta 597 (2007) 179–186.
[17] G. Antalick, M.-C. Perello, G. de Revel, Development, validation and application of a specific method for the quantitative determination of wine esters by headspace-solid-phase microextraction-gas chromatography–mass spectrometry, Food Chem. 121 (2010) 1236–1245.
[18] E. Szymańska, E. Saccenti, A.K. Smilde, J.A. Westerhuis, Double-check: validation of diagnostic statistics for PLS-DA models in metabolomics studies, Metabolomics 8 (2012) 3–16.
[19] B. Khakimov, S.K. Poulsen, F. Savorani, E. Acar, G. Gürdeniz, T.M. Larsen, A. Astrup, L.O. Dragsted, S.B. Engelsen, New nordic diet versus average Danish diet: a randomized controlled trial revealed healthy long-term effects of the New Nordic Diet by GC–MS blood plasma metabolomics, J. Proteome Res. 15 (2016) 1939–1954.
[20] F. Rohart, B. Gautier, A. Singh, K.-A. Le Cao, MixOmics: an R package for 'omics feature selection and multiple data integration, PLoS Comput. Biol. 13 (2017) e1005752.
[21] J.S. Aulakh, A.K. Malik, V. Kaur, P. Schmitt-Kopplin, A Review on solid phase micro extraction—high performance liquid chromatography (SPME-HPLC) analysis of pesticides, Crit. Rev. Anal. Chem. 35 (2005) 71–85.
[22] L. Rebière, A.C. Clark, L.M. Schmidtke, P.D. Prenzler, G.R. Scollary, A robust method for quantification of volatile compounds within and between vintages using headspace-solid-phase micro-extraction coupled with GC–MS–Application on Semillon wines, Anal. Chim. Acta 660 (2010) 149–157.
[23] M. Di Carro, F. Ardini, E. Magi, Multivariate optimization of headspace solid-phase microextraction followed by gas chromatography–mass spectrometry for the determination of methylpyrazines in cocoa liquors, Microchem. J. 121 (2015) 172–177.
[24] F. Gandolfi, L. Malleret, M. Sergent, P. Doumenq, Parameters optimization using experimental design for headspace solid phase micro-extraction analysis of short-chain chlorinated paraffins in waters under the European water framework directive, J. Chromatogr., A 1406 (2015) 59–67.
[25] E.T. Sousa, F. de M. Rodrigues, C.C. Martins, F.S. de Oliveira, P.A. de P. Pereira, J.B. de Andrade, Multivariate optimization and HS-SPME/GC-MS analysis of VOCs in red, yellow and purple varieties of Capsicum chinense sp. peppers, Microchem. J. 82 (2006) 142–149.
[26] Z. Zhang, J. Pawliszyn, Headspace solid-phase microextraction, Anal. Chem. 65 (1993) 1843–1852.
[27] T. Chmiel, M. Kupska, W. Wardencki, J. Namieśnik, Application of response surface methodology to optimize solid-phase microextraction procedure for chromatographic determination of aroma-active monoterpenes in berries, Food Chem. 221 (2017) 1041–1056.
[28] H. Prosen, L. Zupančič-Kralj, Solid-phase microextraction, TrAC Trends Anal. Chem. (Reference Ed.) 18 (1999) 272–282.
[29] L.B. Abdulra'uf, G.H. Tan, Chemometric approach to the optimization of HS-SPME/GC–MS for the determination of multiclass pesticide residues in fruits and vegetables, Food Chem. 177 (2015) 267–273.
[30] G. Derringer, Simultaneous optimization of several response variables, J. Qual. Technol. 12 (1980) 214–219.
[31] S.H.R. Pasandideh, S.T.A. Niaki, Multi-response simulation optimization using genetic algorithm within desirability function framework, Appl. Math. Comput. 175 (2006) 366–382.
[32] G. Antalick, S. Tempère, K. Šuklje, J.W. Blackman, A. Deloire, G. de Revel, L.M. Schmidtke, Investigation and sensory characterization of 1, 4-Cineole: a

potential aromatic marker of Australian Cabernet Sauvignon wine, J. Agric. Food Chem. 63 (2015) 9103–9111.
[33] E.P. Barros, N. Moreira, G.E. Pereira, S.G.F. Leite, C.M. Rezende, P.G. de Pinho, Development and validation of automatic HS-SPME with a gas chromatography-ion trap/mass spectrometry method for analysis of volatiles in wines, Talanta 101 (2012) 177–186.
[34] V. Caliari, V.M. Burin, J.P. Rosier, M.T. BordignonLuiz, Aromatic profile of Brazilian sparkling wines produced with classical and innovative grape varieties, Food Res. Int. 62 (2014) 965–973.
[35] E. Campo, J. Cacho, V. Ferreira, The chemical characterization of the aroma of dessert and sparkling white wines (Pedro Ximenez, Fino, Sauternes, and Cava) by gas chromatography- olfactometry and chemical quantitative analysis, J. Agric. Food Chem. 56 (2008) 2477–2484.
[36] D.L. Capone, K. Van Leeuwen, D.K. Taylor, D.W. Jeffery, K.H. Pardon, G.M. Elsey, M.A. Sefton, Evolution and occurrence of 1, 8-cineole (eucalyptol) in Australian wine, J. Agric. Food Chem. 59 (2011) 953–959.
[37] E. Coelho, M.A. Coimbra, J.M.F. Nogueira, S.M. Rocha, Quantification approach for assessment of sparkling wine volatiles from different soils, ripening stages, and varieties by stir bar sorptive extraction with liquid desorption, Anal. Chim. Acta 635 (2009) 214–221.
[38] A.S. Ferreira, P.U. Pinho, Analytical method for determination of some aroma compounds on white wines by solid phase microextraction and gas chromatography, J. Food Sci. 68 (2003) 2817–2820.
[39] S. Ganss, F. Kirsch, P. Winterhalter, U. Fischer, H.-G. Schmarr, Aroma changes due to second fermentation and glycosylated precursors in Chardonnay and Riesling sparkling wines, J. Agric. Food Chem. 59 (2011) 2524–2533.
[40] R. Lopez, M. Aznar, J. Cacho, V. Ferreira, Determination of minor and trace volatile compounds in wine by solid-phase extraction and gas chromatography with mass spectrometric detection, J. Chromatogr., A 966 (2002) 167–177.
[41] S. Pérez-Magariño, M. Ortega-Heras, L. Martínez-Lapuente, Z. Guadalupe, B. Ayestarán, Multivariate analysis for the differentiation of sparkling wines elaborated from autochthonous Spanish grape varieties: volatile compounds, amino acids and biogenic amines, Eur. Food Res. Technol. 236 (2013) 827–841.
[42] H. Martens, T. Naes, Multivariate Calibration, John Wiley & Sons, 1992.
[43] F. Torchio, S.R. Segade, V. Gerbi, E. Cagnasso, M. Giordano, S. Giacosa, L. Rolle, Changes in varietal volatile composition during shelf-life of two types of aromatic red sweet Brachetto sparkling wines, Food Res. Int. 48 (2012) 491–498.
[44] D. Loyaux, S. Roger, J. Adda, The evolution of champagne volatiles during ageing, J. Sci. Food Agric. 32 (1981) 1254–1258.
[45] S.-J. Lee, A.C. Noble, Characterization of odor-active compounds in Californian Chardonnay wines using GC-olfactometry and GC-mass spectrometry, J. Agric. Food Chem. 51 (2003) 8036–8044.
[46] N. Loscos, P. Hernández-Orte, J. Cacho, V. Ferreira, Evolution of the aroma composition of wines supplemented with grape flavour precursors from different varietals during accelerated wine ageing, Food Chem. 120 (2010) 205–216.
[47] J. Jaffré, D. Valentin, J.-M. Meunier, A. Siliani, M. Bertuccioli, Y. Le Fur, The Chardonnay wine olfactory concept revisited: a stable core of volatile compounds, and fuzzy boundaries, Food Res. Int. 44 (2011) 456–464.
[48] M.-P. Sáenz-Navajas, J.-M. Avizcuri, J. Ballester, P. Fernández-Zurbano, V. Ferreira, D. Peyron, D. Valentin, Sensory-active compounds influencing wine experts' and consumers' perception of red wine intrinsic quality, LWT - Food Sci. Technol. (Lebensmittel-Wissenschaft -Technol.) 60 (2015) 400–411.
[49] C.A. Black, M. Parker, T.E. Siebert, D.L. Capone, I.L. Francis, Terpenoids and their role in wine flavour: recent advances, Aust. J. Grape Wine Res. 21 (2015) 582–600.

ARTÍCULO 2

Quantitative Profiling of Ester Compounds Using HS-SPME-GC-MS and Chemometrics for Assessing Volatile Markers of the Second Fermentation in Bottle

José Manuel Muñoz-Redondo, Francisco Julián Cuevas, Juan Manuel León, Pilar Ramírez, José Manuel Moreno-Rojas and María José Ruiz-Moreno

Journal of Agricultural and Food Chemistry

65(13), 2768-2775 (2017)

Q1: 2/57 (Agriculture, Multidisciplinary, 2019)

Impact Factor: 3.412

JOURNAL OF AGRICULTURAL AND FOOD CHEMISTRY

Article

pubs.acs.org/JAFC

Quantitative Profiling of Ester Compounds Using HS-SPME-GC-MS and Chemometrics for Assessing Volatile Markers of the Second Fermentation in Bottle

José Manuel Muñoz-Redondo,[†] Francisco Julián Cuevas,[†] Juan Manuel León,[‡] Pilar Ramírez,[‡] José Manuel Moreno-Rojas,*[,†] and María José Ruiz-Moreno*[,†]

[†]Postharvest technology and food industry department, Andalusian Institute of Agricultural and Fisheries Research and Training (IFAPA), Centro Alameda del Obispo, Avda Menéndez Pidal, 14004 Córdoba, Spain

[‡]Crop production department, Andalusian Institute of Agricultural and Fisheries Research and Training (IFAPA), Centro Cabra-Priego, Ctra Cabra-Doña Mencía, km 2.5, 11940 Cabra, Spain

Supporting Information

ABSTRACT: A quantitative approach using HS-SPME-GC-MS was performed to investigate the ester changes related to the second fermentation in bottle. The contribution of the type of base wine to the final wine style is detailed. Furthermore, a discriminant model was developed based on ester changes according to the second fermentation (with 100% sensitivity and specificity values). The application of a double-check criteria according to univariate and multivariate analyses allowed the identification of potential volatile markers related to the second fermentation. Some of them presented a synthesis-ratio around 3-fold higher after this period and they are known to play a key role in wine aroma. Up to date, this is the first study reporting the role of esters as markers of the second fermentation. The methodology described in this study confirmed its suitability for the wine aroma field. The results contribute to enhance our understanding of this fermentative step.

KEYWORDS: *second fermentation, sparkling wines, SPME, volatile compounds, esters, chemometrics*

INTRODUCTION

The wine industry needs constantly to integrate alternative winemaking strategies to meet emerging consumer preferences. This challenge concerns the researchers and winemakers, especially in the historical wine regions where there is a broad recognition in the international marketplaces. A short-term strategy for wineries is the sparkling wine production due to its high added value and its valuable economic impact as was suggested by Caliari et al.[1]

The sparkling wines from traditional method are currently elaborated by means of a second fermentation of a base wine followed by aging in contact with lees in sealed bottles. This special winemaking allows a final product to be obtained with distinctive features. Cacho and Ferreira[2] described the aroma as one of the main attributes used to classify the high quality of wines. Compared to other wine types, limited literature can be found for sparkling wines. The majority of studies[3,4] involving volatile compounds and sparkling wines have been mainly focused on the aging stage. Nonetheless, there is a lack of studies explaining the changes during the second fermentation despite their important contribution through yeasts during the alcoholic fermentation. Some studies[5,6] established differences between aged sparkling wines and their respective base wines. Meanwhile, others authors[7,8] reported changes in volatile profiles related to second fermentation. However, the analytical methodology used did not allow quantitation of the minor compounds with a recently demonstrated sensory impact. In this sense, increasing our knowledge of this winemaking process can result in a greater control for winemakers over the final product obtained. Esters are mainly produced during alcoholic fermentation by yeasts. New insights on wine aroma research related to the role of esters for monitoring winemaking processes and linked to the sensory contribution have been recently reported.[9−11]

Frequently, ester compounds occur in complex matrices at very different concentration levels. In this sense, headspace solid phase microextraction (HS-SPME) has demonstrated a great potential for the quantitation of ester compounds in different wine matrices as was shown before.[12] The quantitation of components is necessary to establish their odorant contribution. After, the study of interactions is another actual challenge where multivariate analyses could help to elucidate perceptual interaction phenomena among volatile compounds. Chemometrics have proven to be a useful tool with regard to food and beverage quality, as has been reviewed.[13] Particularly, partial least squares discriminant analysis (PLS-DA) has been successfully employed[14,15] as a classification and prediction technique in volatile composition approaches. In addition, the use and interpretation of the VIP (variable importance in projection) values obtained from this model makes it possible to determine potential volatile markers in the classes selected as previous studies showed.[16,17] This methodology can enhance our understanding related to a winemaking process and no references concerning volatile markers of the second fermentation have been reported.

Received: November 23, 2016
Revised: March 5, 2017
Accepted: March 11, 2017
Published: March 11, 2017

DOI: 10.1021/acs.jafc.6b05265
J. Agric. Food Chem. 2017, 65, 2768−2775

Journal of Agricultural and Food Chemistry Article

In this study a quantitative approach using HS-SPME-GC-MS was performed to investigate the aromatic impact of the second fermentation in bottle. Changes in ester profiles are discussed and new potential volatile markers linked to this winemaking step have been proposed using chemometrics.

MATERIALS AND METHODS

Chemicals. HPLC-grade ethanol was obtained from J.T. Baker Chemicals B.V. (Denventer, Holland). Milli-Q water was obtained from a Milli-Q Plus water system (Millipore, Spain) with 0.04 μS/cm. Sodium chloride, ACS reagent grade (purity ≥99.8%) and standard compounds; ethyl butyrate (≥99%), ethyl hexanoate (≥99%), ethyl octanoate (≥99%), propyl acetate (≥99%), 2-methypropyl acetate (≥99%), 3-methylbutyl acetate (≥99%), hexyl acetate (≥99%), phenylethyl acetate (≥99%), ethyl 2-methylpropanoate (98%), ethyl 2-methylbutyrate (≥99%), ethyl 3-methylbutyrate (≥99%), ethyl phenylacetate (98%), ethyl dihydrocinnamate (98%), ethyl cinnamate (98%), methyl hexanoate (≥99%), methyl octanoate (≥99%), methyl decanoate (≥99%), 3-methylbutyl butyrate (98%), 3-methylbutyl hexanoate (98%), 3-methylbutyl octanoate (98%), ethyl valerate (>99%), ethyl heptanoate (98%), ethyl nonanoate (98%), ethyl propanoate (≥99%), and 2-methylpropyl hexanoate (≥99%) were purchased from Sigma-Aldrich (Madrid, Spain).

Wine Samples. The grapes used for this study were grown under strictly controlled conditions in the experimental vineyards (37° 29′ 53″ N; 04° 25′ 51″ W). The winemaking process was carried out at the experimental winery "Cabra-Priego Research Center" (Instituto de Investigación y Formación Agraria y Pesquera, IFAPA) in Córdoba (Spain). Pedro Ximénez grapes (600 kg) from 2014 campaign were harvested at 175−181 g/L of sugar content. The grapes were divided into different batches to obtain white wines without maceration (hereinafter called as PX), white wines from prefermentative cryomaceration (PX-C), and rosé wines (PX-SY).

In the first batch, the grapes were destemmed (Beta 5000, Beta, Spain), crushed in a stainless-steel crusher provided with rubber rollers (Coinme S.L. Spain), and soft pressed using a vertical press (Alfa, Coinme S.L. Spain) at pressures less than 1 bar. The grape juice was divided into three stainless steel tanks with a 50 L capacity corrected using tartaric acid (Panreac, Spain) to pH 3.2−3.3 and sulphited at 70 mg/L (Solfosol, Sepsa-Enartis, Spain). Alcoholic fermentation was performed at a controlled temperature (18 °C ± 1 °C) using *Saccharomyces cerevisae* yeast (Passion Viniferm yeasts, 20 g/hL, Agrovin, Spain) and nutrients (Actimax-Bio, 10 g/hL, Agrovin, Spain). After fermentation, the wines were clarified with Ictioclar (Agrovin, Spain) at 2 g/hL and bentonite (Microcol FT, 20 g/hL, Laffort, France), stabilized (at −4 °C during 7 days), and filtered (BECO depth filter sheets, KD 2, 32 × 32 cm; Agrovin, Spain) to obtain the Pedro Ximénez base wines without maceration. In the second batch, Pedro Ximénez grapes were destemmed, (Beta 5000, Beta, Spain), crushed in a stainless-steel crusher with rubber rollers (Coinme S.L. Spain), and sulphited at 50 mg/kg (Solfosol, Sepsa-Enartis, Spain). Enzymes (Enozym AROME, Agrovin, Spain) at 30 mg/kg were added and a prefermentative cryomaceration of 6 h at 10 °C was carried out before pressing. Afterward, the resulting grape juices were fermented following the same conditions described above, to obtain the base wines from musts macerated with skins. For rosé wines, Syrah grapes (300 kg) were harvested at 210−215 g/L of sugar content, destemmed (Beta 5000, Beta, Spain), crushed in a stainless-steel crusher (Coinme S.L. Spain), and placed in 100 L stainless steel tanks. They were corrected using tartaric acid (Panreac, Spain) to pH 3.4−3.5 and sulphited at 50 mg/kg (Solfosol, Sepsa-Enartis, Spain). Alcoholic fermentation was started after yeast addition (Caracterviniferm, 20 g/hL, Agrovin, Spain), and nutrients (Actimax-Bio, 10 g/hL Agrovin Spain) which proceeded for 8 days at controlled temperature (24 °C ± 1 °C) in 100 L stainless steel tanks. Malolactic fermentation was induced with *Oenococcus oeni* (Viniferm OE104, 1.0 L/100 hL, Agrovin, Spain) and nutrients Actimax OENI, 10 g/hL Agrovin, Spain). Ferments were pressed to 2 bar pressure using a vertical press (MOD.40, InVIA, Spain) when the residual sugars decreased to <2 g/L. Afterward, wines were clarified with Ictioclar (Agrovin, Spain) at 2.0 g/hL and bentonite (Microcol FT, Laffort, France) at 50 g/hL, cold-stabilized in a cold chamber at −4 °C during 7 days, and filtered (BECO depth filter sheets, KD 2, 32 × 32 cm; Agrovin, Spain). Finally, Syrah wines were blended with the Pedro Ximénez wines without maceration (PX) in a proportion (20:80) to obtain the rosé base wines (PX-SY). The base wines complied with the legal and quality standards dictated by the European regulation.[18]

The second fermentation was performed following the traditional or *champenoise* method in bottle. A total of 144 bottles (48 bottles/tank) for each condition were submitted to second fermentation. The base wines were adjusted to 20 mg/L of free SO_2 before *tirage*. The *tirage liquor* consisted of 24 g/L of sucrose, 15 g/hL of Actimax-Bio nutrients (Agrovin, Spain), and 20 g/hL bentonite (Laffort, France). The yeast used was Viniferm PDM (var. bayanus) at 20 g/hL (Agrovin, Spain). The second fermentation took place at 15 °C in closed bottles of 0.75 cL (Vidrierías Pérez Campos, S.L, Spain). The residual sugars and pressure control were periodically monitored by using afrometers (Agrovin) for bottles with crown caps from 0 to 10 bar. This fermentation was completed after 11−12 weeks. Wines were hand disgorged by expert personnel specialized using a "neck freezer" (R-56 model, Roger Cuñat Torres, Spain) containing a freezing solution at −30 °C during 7 min. Bottles were closed with a cork cap, which was secured to the neck with a wire cap before being analyzed in the laboratory.

Enological Parameters. Ethanol (% Vol.), residual sugars, pH, total, and volatile acidity were obtained by following the official analytical methods dictated by the International Organization of Vine and Wine.[19] Total phenolic content was calculated with a photometric procedure (Folin-Ciocalteu) using a previously published method.[20] Results were expressed as equivalents of gallic acid (mg/L).

Automated HS-SPME-GC-MS Analysis. Concentration of esters was determined using a headspace solid-phase microextraction (HS-SPME) followed by gas chromatography−mass spectrometry (GC-MS) as described by Antalick et al.[12] Wine samples of 25 mL were spiked with 20 μL of internal standard mix ethanol solution at 200 mg/L of isotopically labeled esters; [$^2H_3$]-ethyl butyrate, [$^2H_{11}$]-ethyl hexanoate, [$^2H_{15}$]-ethyl octanoate, and [$^2H_5$]-ethyl cinnamate, supplied by CDN isotopes (Pointe-Claire, Canada). Ten milliliters of the spiked samples was diluted 1:3 with Milli-Q (0.04 μS/cm) water, and the samples were placed into a 20 mL SPME vial filled with 3.5 g of NaCl. The capped vials were homogenized for 30 s in a vortex shaker, placed in a Combipal autosampler tray (CTC Analytics), and analyzed using HS-SPME-GC-MS. A 100 μm of previously conditioned PDMS fiber (Supelco, Bellefont, PA, USA) was used. The vials were stirred at 500 r.p.m for 2 min at 40 °C. Extraction was set at 40 °C for 30 min and desorption was performed at 250 °C for 15 min. The fiber was desorbed into a Trace GC ultragas chromatograph (Thermo Fisher Scientific S.p.A., Rodano, Milan, Italy) coupled to a ISQ Single Quadrupole MS spectrometer (Thermo Fisher Scientific, Austin, Texas, USA). The injection mode was splitless for 0.75 min. The column was a BP21 of 50 m × 0.32 mm, 0.25 μm film thickness (SGE Analytical Science, UK). The carrier gas was helium at a column-head pressure of 8.0 psi. The oven temperature was programmed at 40 °C for 5 min, raised to 220 °C at 3 °C/min, and then held for 30 min. The MS transfer line and source temperature were 230 and 200 °C, respectively. The mass spectrometer operated in electron ionization mode at 70 eV using selected-ion-monitoring (SIM) mode. Identification of all esters was carried out by comparing retention times and mass spectra with those of pure standards. Quantitation procedure and isotopic labeled standards were also followed according to Antalick et al.[12] A commercial wine spiked with a mixture of target compounds (at nine different levels of concentration) was used for the construction of calibration curves. For the quantitation of ethyl dihydrocinnamate, ethyl cinnamate, ethyl phenylacetate, and isoamyl octanoate a more appropriated linearity range was used (0.08−51 μg/L). Each calibration point was analyzed in triplicate and calibration ranges regression were higher than 0.990 for all compounds unless for ethyl octanoate (0.977) and isoamyl octanoate (0.978).

DOI: 10.1021/acs.jafc.6b05265
J. Agric. Food Chem. 2017, 65, 2768−2775

Journal of Agricultural and Food Chemistry Article

Table 1. Enological Parameters of Wines; Two-Way ANOVA for Base Wine Type, Second Fermentation Factors, and Their Interactions

	base wine type[a]				second fermentation			interaction
enological parameters[g]	PX	PX-C	PX-SY	*p*-value[b]	before[c]	after[d]	*p*-value[b]	*p*-value[b]
ethanol (% Vol.)	11.96ab	11.78b	12.12a	*	11.25b	12.66a	***	ns
residual sugars (g/L)	1.70	1.81	1.25	ns	1.22	1.96	ns	ns
pH (20 °C)	3.14b	3.17ab	3.19a	*	3.14b	3.20a	***	**
total acidity[e] (g/L)	5.57	5.71	5.79	ns	5.61b	5.78a	*	ns
volatile acidity[f] (g/L)	0.32	0.35	0.31	ns	0.29b	0.36a	***	ns
total phenolic compounds[g] (mg/L)	115c	166b	288a	***	192	187	ns	ns

[a]PX: Pedro Ximénez wines without cryomaceration; PX-C: Pedro Ximénez wines from cryomaceration; PX-SY: Rosé wines from blending Pedro Ximénez and Syrah wines (80:20). [b]Significance level: ns = nonsignificant; *= $p < 0.05$; **= $p < 0.01$; ***= $p < 0.001$. [c]Wines before the second fermentation. [d]Wines after the second fermentation. [e]Calculated as tartaric acid. [f]Calculated as acetic acid. [g]Calculated as gallic acid equivalents. [h]Values shown are the results of two bottles from each tank (three tanks) for each condition.

Table 2. Concentrations of Ester Compounds (μg/L) in Wines; Two-Way ANOVA for Base Wine Type, Second Fermentation Factors, and Their Interactions

		base wine type[c]				second fermentation				interaction
group[a]	compound[bi]	PX	PX-C	PX-SY	*p*-value[d]	before[e]	after[f]	*p*-value[d]	VIP[g]	*p*-value[d]
EEFAs	ethyl butyrate	144b	82c	163a	***	110b	150a	***	1.1	ns
	ethyl hexanoate	525a	253b	504a	***	357b	498a	***	1.3	ns
	ethyl octanoate	607a	296c	494b	***	341b	590a	***	1.3	***
	ΣEEFAs	1276a	632c	1161b	***	807b	1238a	***		ns
HAAs	propyl acetate	4.1b	3.1c	10.2a	***	5.7	5.9	ns	0.0	ns
	2-methylpropyl acetate	20b	10c	24a	***	17b	19a	***	0.5	ns
	3-methylbutyl acetate	663b	335c	775a	***	591	591	ns	0.0	ns
	hexyl acetate	34a	14b	32a	***	32a	21b	***	1.2	ns
	phenylethyl acetate	79a	58b	80a	***	65b	80a	***	1.2	ns
	ΣHAAs	799b	420c	921a	***	710	717	ns		ns
EEBAs	ethyl 2-methylpropanoate	46c	59a	50b	***	27b	**76a**	***	**1.5**	***
	ethyl 2-methylbutyrate	7b	16a	7b	***	5b	15a	***	1.1	***
	ethyl 3-methylbutyrate	12b	17a	11b	***	6b	20a	***	1.4	***
	ethyl phenylacetate	0.9b	1.8a	0.7c	***	0.5b	1.7a	***	1.1	***
	ΣEEBAs	65b	95a	68b	***	39b	113a	***		***
cinnamates	ethyl dihydrocinnamate	0.28b	0.41a	0.24c	***	0.42a	0.20b	***	1.3	***
	ethyl cinnamate[h]	0.028	0.030	0.027	ns	0.030	0.027	ns	0.2	ns
	Σcinnamates	0.31b	0.45a	0.27c	***	0.45a	0.23b	***		***
MEFAs	methyl hexanoate	0.40c	0.62a	0.52b	***	0.48b	0.54a	**	0.3	*
	methyl octanoate	0.48c	0.54b	0.59a	**	0.38b	0.69a	***	1.3	***
	methyl decanoate	0.14a	0.07b	0.08b	**	0.06b	0.14a	***	0.8	*
	ΣMEFAs	1.02b	1.23a	1.19a	**	0.92b	1.37a	***		ns
IEFAs	3-methylbutyl butyrate	0.27a	0.12b	0.26a	***	0.17b	0.26a	***	1.3	ns
	3-methylbutyl hexanoate	0.88a	0.65c	0.78b	***	0.41b	**1.14a**	***	**1.5**	ns
	3-methylbutyl octanoate	0.92a	0.37c	0.56b	***	0.36b	0.87a	***	0.9	***
	ΣIEFAs	2.06a	1.15c	1.60b	***	0.93b	2.27a	***		**
EEOCNFAs	ethyl valerate	0.28b	0.34a	0.30b	*	0.20b	0.41a	***	1.4	*
	ethyl heptanoate	0.32b	1.52a	0.37b	***	0.36b	1.12a	***	0.8	***
	ethyl nonanoate	0.84a	0.50c	0.69b	***	0.38b	0.97a	***	1.2	***
	ΣEEOCNFA	1.44b	2.36a	1.36b	***	0.94b	2.49a	***		***
miscellaneous	ethyl propanoate	81c	160a	111b	***	91b	143a	***	1.1	ns
	2-methylpropyl hexanoate	0.18a	0.08c	0.15b	***	0.08b	0.19a	***	1.4	*
	Σmiscellaneous	81c	160a	111b	***	91b	143a	***		ns
	total esters	2225a	1312b	2266a	***	1650b	2218a	***		ns

[a]EEFAs: ethyl esters of fatty acids; HAAs: higher alcohol acetates; EEBAs: ethyl esters of branched acids; MEFAs: methyl esters of fatty acids; IEFAs: isoamyl esters of fatty acids; EEOCNFAs: ethyl esters of odd carbon number fatty acids. [b]Identification confirmed by comparing mass spectra and retention time with those of authentic standard. [c]PX: Pedro Ximénez wines without cryomaceration; PX-C: Pedro Ximénez wines from cryomaceration; PX-SY: Rosé wines from blending Pedro Ximénez and Syrah wines (80:20). [d]Significance level: ns = nonsignificant; * = $p < 0.05$; ** = $p < 0.01$; *** = $p < 0.001$. [e]Wines before the second fermentation. [f]Wines after the second fermentation. [g]Variable importance in projection. [h]Concentration values comprised between the limit of detection (LOD = 0.023 μg/L) and the limit of quantitation (LOQ = 0.080 μg/L). [i]Values shown are the results (μg/L) of two bottles from each tank (three tanks) for each condition. Concentrations and VIP values considered for potential markers are highlighted in bold type letter. VIP: variable importance in projection.

DOI: 10.1021/acs.jafc.6b05265
J. Agric. Food Chem. 2017, 65, 2768−2775

Journal of Agricultural and Food Chemistry Article

Statistical Software. The univariate analysis was performed using Statistix (v. 9.0, Analytical Software, FL, USA). The data were subjected to the analysis of variance using Shapiro Wilk's and Levene's tests for normality and homoscedasticity requirements. Differences at $p < 0.05$ were considered to be statistically significant. A comparison of means based on least significant differences (LSD, Fisher's test) was performed. The multivariate analysis was performed using PLS toolbox (v. 5.5.1, eigenvector, USA) under MATLAB 2008R (v. 7.6.0, Mathworks, USA) workspace.

RESULTS AND DISCUSSION

Enological Parameters. Regarding the influence of the type of base wine (Table 1), ethanol and pH were slightly higher in the PX-SY wines while the highest levels of total phenolic compounds were found in PX-SY wines (288 mg/L), followed by PX-C (166 mg/L) and PX ones (115 mg/L). This behavior was expected due to the extraction of phenolic compounds from the skins to the juices during the respective winemaking steps as was shown before.[21] Concerning the second fermentation, an increase in ethanol, pH, total acidity and volatile acidity was observed. Meanwhile, nonsignificant differences were observed in residual sugars and total phenolic compounds. Interactions were only found in the pH parameter. This was due to a slightly higher increase found in the PX wines than in the PX-C and PX-SY ones after the second fermentation. Enological parameters confirmed that wines after second fermentation were within legal, quality, and usual ranges.

Volatile Composition. The ester compounds were classified into different groups (Table 2) according to their chemical structure and origin as follows: ethyl esters of fatty acids (EEFAs); higher alcohol acetates (HAAs); ethyl esters of branched acids (EEBAs); cinnamates; methyl esters of fatty acids (MEFAs); isoamyl esters of fatty acids (IEFAs); ethyl esters of odd carbon number fatty acids (EEOCNFA); and miscellaneous esters (MEs).

The influence of the base wine type and the second fermentation was studied (Table 2). Both factors impacted the total ester concentrations. A higher total ester content was found in the PX-SY and PX wines (around 1.7 fold) than in the PX-C ones, while the second fermentation produced an average increase in the total ester content, from 1650 μg/L in base wines to 2218 μg/L in wines after the second fermentation (Table 2).

Ethyl Esters of Fatty Acids. Regarding the impact of the type of base wine, EEFA contents differentiated wines into three groups (Table 2). Levels in the PX and PX-SY wines were found to be around 1.9 fold higher than in the PX-C ones (Table 2). These findings are in agreement with other studies described in literature.[10,22,23] Regarding these compounds, ethyl octanoate showed the highest values in the PX wines (607 μg/L) compared to the PX-SY (494 μg/L) and PX-C ones (296 μg/L). Meanwhile, the highest contents of ethyl butyrate were obtained in the PX-SY wines.

After the second fermentation, a synthesis of EEFA compounds was observed. EEFAs increased around 1.5 fold compared to the base ones (Table 2). A lower genesis was found for the shortest carbon chain ester compounds (ethyl butyrate, 1.3 fold higher) in comparison with the longest one (ethyl octanoate, 1.7 fold higher). Furthermore, this compound was subjected to interaction effects (Table 2). Thus, the type of base wine had a different effect on the final contents of ethyl octanoate after the second fermentation. Medium-chain EEFAs have been reported to be less influenced during aging.[10] Thus, our results emphasize the importance of the second fermentation and the base wine on the final EEFA contents and therefore, on their well-known sensory contribution to wine aroma.[10,24]

Higher Alcohol Acetates. In literature, several factors have been reported to affect HAA concentrations: grape variety and grape maturity,[25] prefermentative treatments,[26−28] vinification conditions,[29] and aging[3,4,10] among others. The HAA contents in our samples classified the wines into three groups (Table 2). The lower HAA contents in the PX-C wines compared to the PX wines could be related to polyphenol bulk in the first fermentation. In fact, HAA synthesis has been reported to be less effective in the presence of higher levels of phenolic compounds.[30] On the other hand, the higher contents in propyl, 2-methylpropyl and 3-methylbutyl acetates found in PX-SY wines (Table 2) compared to PX, might be related with the varietal character of Syrah cultivar used for the blending as has been suggested by Antalick et al.[25] However, this speculation will need to be studied in the future using appropriate investigations.

Regarding the second fermentation, different trends were observed among HAA compounds. 2-Methylpropyl and phenylethyl acetates increased during this stage, while a decrease was observed for hexyl acetate (Table 2). A faster hydrolysis phenomena for the longer-carbon chain of HAAs (hexyl acetate) could be suggested, as reported by Antalick et al.[10] However, the current study does not support the previous findings observed for phenylethyl acetate. In our samples, we observed a higher synthesis/hydrolysis ratio for this compound during the second fermentation. This finding is novel and we suggest that the differences reported could be related with the yeast strain used, which strongly influences the phenylethyl acetate contents, as has been reported in literature.[31] No interaction effects were found for the above-mentioned compounds (Table 2). Hence, they showed similar responses regardless of the type of base wine during this stage.

Ethyl Esters of Branched Acids. Regarding the influence of the base wine type, the PX-C wines stood out for having higher EEBA contents than the rest (around 1.4 fold; Table 2). In this group, ethyl 2-methylbutyrate and ethyl phenylacetate presented the highest concentrations, reaching levels close to 2.0−2.5 fold higher in PX-C wines (Table 2). We suggest that the differences could be related with a more complete extraction of amino acids during the skin maceration step performed in the PX-C base wines, as has been shown in literature.[10] Concerning the second fermentation, an important synthesis of EEBAs (around 2.0 fold higher) was found (Table 2). The synthesis of EEBAs during alcoholic fermentation through the Ehrlich pathway is widely known.[10,25,32]

Furthermore, an interaction effect was found for EEBAs (Table 2). This allowed us to observe different synthesis ratios during the second fermentation according to the base wine type used. In addition to this, the PX-C and PX-SY showed higher contents of EEBAs than the PX after the second fermentation. It has been hypothesized that a specific EEBAs profile in wines might originate from the redox balance regulation of yeast metabolism.[10,25] However, such hypothesis requires further investigation.

To the authors' knowledge, it is the first time that EEBAs have been described as relevant compounds related to the second fermentation in bottles, supporting the importance of the base wine at the starting point on the final contents of this group. Given their low detection threshold[43,44] and potential

DOI: 10.1021/acs.jafc.6b05265
J. Agric. Food Chem. 2017, 65, 2768−2775

Journal of Agricultural and Food Chemistry Article

role through perceptual interaction phenomena[11] we emphasize the importance of studying these compounds in depth.

Cinnamates. Cinnamates grouped the wines into three different classes according to their contents (Table 2). The highest levels were found in the PX-C wines (0.41 μg/L), followed by the PX (0.28 μg/L) and PX-SY ones (0.24 μg/L) (Table 2). A varietal origin of cinnamates has been yet reported.[33] However, the precursor compounds of cinnamates still remain unknown. In this sense, a more complete extraction of odorless precursors in the PX-C base wines might explain the different contents found. Thus, our results contribute to support the presence of odorless precursors of ethyl dihydrocinnamate in Pedro Ximénez grapes. To the authors' knowledge, the present study is the first to report varietal differences in the ester profiles of Pedro Ximénez base wines made from different prefermentative strategies.

The second fermentation affected in a different way the cinnamate contents compared to the other groups. A decrease in cinnamate compounds was observed once this step was finished (Table 2). This decrease could be linked to different interactions by yeasts to release volatile compounds derived from precursors or to absorb them, as it was previously found for cinnamate compounds during aging with lees.[33] Thus, the higher values found in the base wines seemed to be affected in the wines produced after the second fermentation.

Methyl Esters of Fatty Acids. Changes in MEFAs were found according to the type of base wine. The PX-C and PX-SY wines presented higher contents (Table 2) than the PX ones. Methyl hexanoate and octanoate followed this same trend, while methyl decanoate presented levels around 2.0 fold higher in PX wines (Table 2). Thus, the winemaking steps affected these compounds in different ways.

Concerning the second fermentation, an increase in all MEFA compounds (0.92 to 1.37 μg/L) was found (Table 2). Methyl hexanoate reached the highest levels in the PX-C wines, while different ratio increases were found for methyl octanoate (2.0 fold higher in the PX-C and PX-SY wines and 1.5 fold higher in the PX ones). In this sense, a source of variability and modulated responses were displayed for these compounds according to the interaction effects shown.

Isoamyl Esters of Fatty Acids. Lower concentrations of IEFAs were found in the PX-C wines cryomacerated with skins (Table 2). 3-Methylbutyl hexanoate and octanoate displayed significantly higher levels in the PX (0.88 μg/L and 0.92 μg/L, respectively) than in PX-SY wines (0.78 μg/L and 0.56 μg/L).

Regarding the second fermentation, 3-methylbutyl esters of fatty acids increased after this step (2.0 fold higher approx.). 3-Methylbutyl hexanoate showed the highest increase. Indeed a different trend was also observed for 3-methylbutyl octanoate according to the type of base wine used. Increases around 2.0-fold higher were found for this compound in the PX-C and PX-SY wines after the second fermentation compared to the base ones, while ratios around 4.0-fold higher were found in the PX wines. Thus, the synthesis of this compound during this period seems to be modulated by the base wine composition. The mechanisms involved will require further investigation to be assessed.

Ethyl Esters of Odd Carbon Number of Fatty Acids. The PX-C wines showed the highest values of EEOCNFAs compared to the others, while the second fermentation produced an increase in this group (Table 2). The significant interaction found (Table 2) allowed us to observe different synthesis ratios according to the type of base wine used. In addition to this, ethyl valerate was around 1.2-fold higher in the PX and PX-C wines, while the PX-SY wines showed a 0.6-fold increase. The highest levels of ethyl heptanoate were found in the PX-C wines (increases around 2.3-fold higher were found after second fermentation). Meanwhile, ethyl nonanoate displayed the highest values in the PX wines (increases were around 2.2-fold higher in the wines after the second fermentation compared to the base ones).

Miscellaneous Esters. The base wine type used and the second fermentation affected the contents of MEs (Table 2). In this regard, the PX-C (160 μg/L) wines showed the highest values followed far behind by the PX-SY (111 μg/L) and PX ones (81 μg/L). Regarding the second fermentation, ethyl propanoate showed a similar increase during this period regardless the type of base wine used (no interaction effect), while higher levels of 2-methylpropyl hexanoate (MEs) were found in the PX wines. Changes in these compounds after second fermentation are novel findings and further studies may be necessary to enhance our knowledge of these compounds. The MEFAs, IEFAs, EEOCNFAs, and miscellaneous esters have not been studied in depth.

Study of the Potential Volatile Markers of the Second Fermentation. A multivariate approach was performed to establish the impact of the second fermentation on the ester profiles. A matrix of 18 (samples) × 25 (ester concentrations) was used to build the mode (X matrix). A supervised technique is able to account the variability according to the classes that have been selected by the enologist or analytical chemistries compared to other exploratory tools (PCA, HCA,...). In this sense, it was able to account the importance of each variable in the final model obtaining real potential markers in accordance with Gromski. et al.[34] The partial least squares discriminant analysis (PLS-DA) is a supervised technique and was chosen because of its referenced suitability in volatile studies.[14,35,36] The wines before and after second fermentation were labeled as class 1 (value = 0) and class 2 (value = 1), respectively (Y matrix). Several preprocessing transformations previously referenced[14,37] were evaluated and the selection was based on the lowest root mean squares error in cross validation (RMSECV). 'Autoscaling' (a mean-centering followed by the division of each column by the standard deviation of that column) was selected by reaching the lowest RMSECV values.

Orthogonalization transformation ensures that all linear modeling will produce model components that are related only in the variation that is informative for the response matrix, improving the model fitting and predictability as was shown before.[38,39] Hotelling T^2 versus Q^2 residuals plot was employed to detect outlier samples because its referenced suitability.[40] In this sense, no outliers were detected in our samples. Leave-one-out cross validation (LOOCV) was used as the resampling validation methodology.

Two latent variables (LVs) were selected as the optimal number of latent variables using the criteria of the lowest prediction error in RMSECV and the percentage of covariance captured in X matrix. Sensitivity (samples of interest correctly assigned) and specificity (nonclass samples correctly non-assigned) rates were 100% (Table 3).

Scores and loadings for the two first LVs are illustrated in Figure 1. In the score plot, the two latent variables of the model explained around 80.4% of total variance in the X matrix. LV1 explained 65.81% of data variability and clearly differentiated the wines before and after second fermentation. In the loading plot, the compounds situated at the highest positive coefficients

DOI: 10.1021/acs.jafc.6b05265
J. Agric. Food Chem. 2017, 65, 2768−2775

Journal of Agricultural and Food Chemistry Article

Table 3. Statistics Results of the OPLS-DA Model Performed According to the Second Fermentation

statistics of the model[a]	second fermentation model
sensitivity (Cal)	100
specificity (Cal)	100
RMSEC	0.034
R^2 Cal	0.995
sensitivity (CV)	100
specificity (CV)	100
RMSECV	0.058
R^2 CV	0.987

[a]Sensitivity: proportion of positives that are correctly identified. Specificity: proportion of negatives that are correctly identified. RMSEC: root mean squares error at the calibration step. RMSECV: root mean squares error at the cross validation step. R^2 Cal: regression coefficient for the calibration set. R^2CV: regression coefficient for the internal validation set.

of LV1 were the most important contributors differentiating wines after the second fermentation (Table 2). On the other hand, the compounds with the highest negative values of LV1 were the main contributors differentiating the wines before second fermentation (Table 2). Meanwhile, LV2 explained around 14.59% of data variability in the X matrix (Figure 1) and separated the rosé wines from the rest before second fermentation, and the wines without maceration from the rest after second fermentation. A recent approach to detect potential volatile markers was applied.[35,41] Briefly, a double-check criteria to identify these compounds were considered based on the multivariate analysis (holistic view) and univariate analysis. Thus, compounds with variable importance in projection (VIP) ≥ 1.5 and the category "a" in the LSD test analysis (at significance level = 0.01) were selected as potential volatile markers (Table 2).

Accordingly, the compounds identified as candidate markers of the second fermentation were ethyl 2-methylpropanoate and 3-methylbutyl hexanoate (Table 2). However, other compounds, including ethyl 3-methylbutyrate, 2-methylpropyl hexanoate, and ethyl valerate, displayed VIP values close to 1.5 and they were in concordance with the univariate analysis criteria. Thus, the above-mentioned compounds could play an important role in the differences related to this fermentative step. Although no compound could be selected as a potential marker of the base wines, ethyl dihydrocinnamate was in concordance with our univariate analysis criteria and presented VIP values close to 1.5. Therefore, this compound might also be a key contributor in base wines.

Ethyl esters of branched acids seem to play a key role in wine aroma through perceptual interaction phenomena among aromatic compounds.[11,42,44] In this sense, the second fermentation and the type of base wine used could affect the sensorial profile of wines, these being important contributors. Hence, our results emphasize that these compounds could be useful for controlling the aroma quality of these wines. However, further approaches concerning sensory, odor thresholds, and perceptual interaction phenomena for sparkling wines are necessary; since these still remain to be challenges for the scientific community in which the supervised chemometric methods could be a promising tool.

This research highlights the effect of the second fermentation in wine ester composition. This study states that wine base composition could be a potential factor in assessing the distinctive styles of sparkling wines responding to different alternatives for diversification by wineries. The novel approach

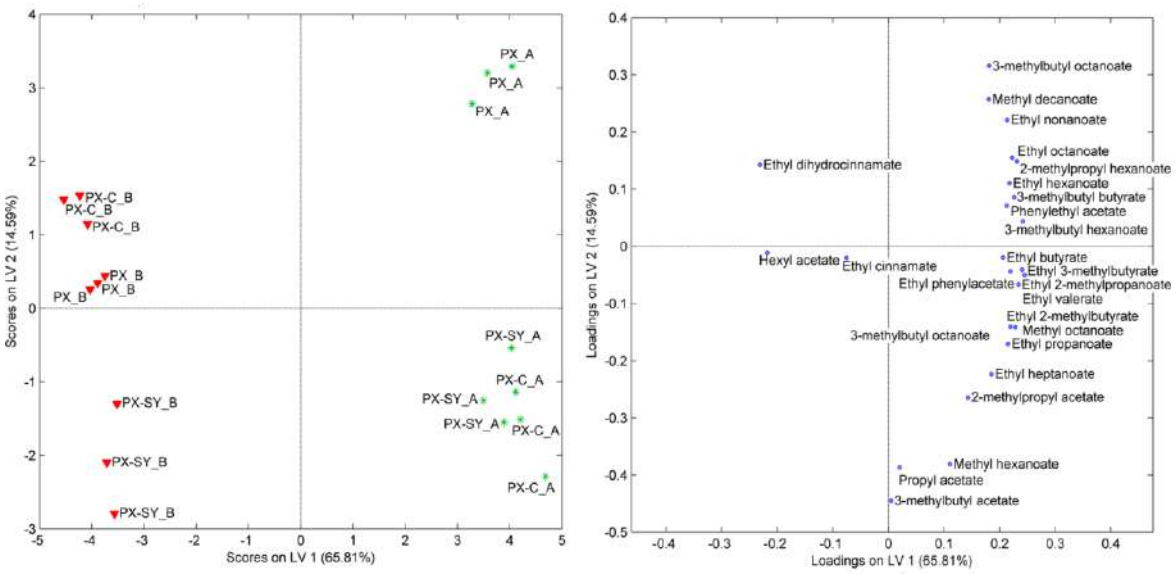

Figure 1. Score and loading plots from the orthogonal partial least squares discriminant analysis (OPLS-DA) based on the second fermentation. The inverse red triangle for samples before the second fermentation and green asterisk for samples after the second fermentation. Each score represents the mean value of two bottles from each tank. PX_B: Pedro Ximénez before second fermentation PX_A: Pedro Ximénez after second fermentation; PX-C_B: Pedro Ximénez wines from cryomaceration before the second fermentation; PX-C_A: Pedro Ximénez wines from cryomaceration after the second fermentation; PX-SY_B: Rosé wines from blending Pedro Ximénez and Syrah wines (80:20) before the second fermentation; PX-SY_A: Rosé wines from blending Pedro Ximénez and Syrah wines (80:20) after the second fermentation.

DOI: 10.1021/acs.jafc.6b05265
J. Agric. Food Chem. 2017, 65, 2768−2775

using HS-SPME-GC-MS, supervised chemometric tools, and variable selection algorithm allowed us to identify volatile markers related to the second fermentation. Several of these markers could play a key role in aroma of sparkling wines highlighting the importance of being monitored during the aging of lees. To our knowledge, this is the first article reporting volatile markers related to this fermentative step. The methodology described confirmed its suitability to the field of wine aroma and new perspectives into sensory and ester composition of sparkling wines are proposed.

■ ASSOCIATED CONTENT

Supporting Information

The Supporting Information is available free of charge on the ACS Publications website at DOI: 10.1021/acs.jafc.6b05265.

Interaction effects of wine-type strategy and second fermentation factors on ester compounds; ester compounds, monitored ions, odor descriptors, and detection thresholds; mean concentrations with standard deviation of ester compounds for PX, PX-C, and PX-SY wines, before and after the second fermentation (PDF)

■ AUTHOR INFORMATION

Corresponding Authors

*Phone: +34 671 53 27 16. Fax: +34 957 01 60 43. E-mail: josem.moreno.rojas@juntadeandalucia.es.

*Phone: +34 671 53 27 16. Fax: +34 957 01 60 43. E-mail: mariaj.ruiz.moreno@juntadeandalucia.es.

ORCID

José Manuel Muñoz-Redondo: 0000-0002-8912-4354

María José Ruiz-Moreno: 0000-0002-0688-3014

Funding

This work was funded by the Andalusian Institute of Agricultural and Fisheries Research and Training (IFAPA) through the project 'Proyecto de investigación complementario al Transforma Vid y Vino' (PR.AVA.AVA201301.3), the European Social Fund (ESF), the European Rural Development Fund (ERDF). José Manuel Muñoz-Redondo was granted a research contract at Andalusian IFAPA inside the National Youth Guarantee System funded through the ESF, and the Youth Employment Initiative (YEI). María José Ruiz-Moreno was granted a postdoctoral research contract funded by the Andalusian IFAPA and the ESF. Juan Manuel León was granted a technical contract funded by the Andalusian IFAPA and the ESF.

Notes

The authors declare no competing financial interest.

■ REFERENCES

(1) Caliari, V.; Burin, V. M.; Rosier, J. P.; BordignonLuiz, M. T. Aromatic profile of Brazilian sparkling wines produced with classical and innovative grape varieties. *Food Res. Int.* **2014**, *62*, 965−973.

(2) Cacho, J.; Ferreira, V. *The aroma of wine. Handb. fruit Veg. flavors 2010*; Wiley: New Jersey, USA, 2010; pp 303−317.

(3) Pérez-Magariño, S.; Ortega-Heras, M.; Bueno-Herrera, M.; Martínez-Lapuente, L.; Guadalupe, Z.; Ayestarán, B. Grape variety, aging on lees and aging in bottle after disgorging influence on volatile composition and foamability of sparkling wines. *LWT-Food Sci. Technol.* **2015**, *61*, 47−55.

(4) Riu-Aumatell, M.; Bosch-Fusté, J.; López-Tamames, E.; Buxaderas, S. Development of volatile compounds of cava (Spanish sparkling wine) during long ageing time in contact with lees. *Food Chem.* **2006**, *95*, 237−242.

(5) Welke, J. E.; Zanus, M.; Lazzarotto, M.; Pulgati, F. H.; Zini, C. A. Main differences between volatiles of sparkling and base wines accessed through comprehensive two dimensional gas chromatography with time-of-flight mass spectrometric detection and chemometric tools. *Food Chem.* **2014**, *164*, 427−437.

(6) Torrens, J.; Riu-Aumatell, M.; Vichi, S.; López-Tamames, E.; Buxaderas, S. Assessment of volatile and sensory profiles between base and sparkling wines. *J. Agric. Food Chem.* **2010**, *58*, 2455−2461.

(7) Hidalgo, P.; Pueyo, E.; Pozo-Bayón, M. A.; Martínez-Rodríguez, A. J.; Martín-Álvarez, P.; Polo, M. C. Sensory and analytical study of rosé sparkling wines manufactured by second fermentation in the bottle. *J. Agric. Food Chem.* **2004**, *52*, 6640−6645.

(8) Pozo-Bayón, M. A.; Pueyo, E.; Martín-Álvarez, P. J.; Martínez-Rodríguez, A. J.; Polo, M. C. Influence of yeast strain, bentonite addition, and aging time on volatile compounds of sparkling wines. *Am. J. Enol. Vitic.* **2003**, *54*, 273−278.

(9) Renault, P.; Coulon, J.; de Revel, G.; Barbe, J.-C.; Bely, M. Increase of fruity aroma during mixed T. delbrueckii/S. cerevisiae wine fermentation is linked to specific esters enhancement. *Int. J. Food Microbiol.* **2015**, *207*, 40−48.

(10) Antalick, G.; Perello, M.-C.; de Revel, G. Esters in wines: New Insight through the Establishment of a Database of French Wines. *Am. J. Enol. Vitic.* **2014**, *65*, 293−304.

(11) Lytra, G.; Tempere, S.; Le Floch, A.; de Revel, G.; Barbe, J.-C. Study of sensory interactions among red wine fruity esters in a model solution. *J. Agric. Food Chem.* **2013**, *61*, 8504−8513.

(12) Antalick, G.; Perello, M.-C.; de Revel, G. Development, validation and application of a specific method for the quantitative determination of wine esters by headspace-solid-phase micro-extraction-gas chromatography−mass spectrometry. *Food Chem.* **2010**, *121*, 1236−1245.

(13) Efenberger-Szmechtyk, M.; Nowak, A.; Kregiel, D. Implementation of chemometrics in quality evaluation of food and beverages. *Crit. Rev. Food Sci. Nutr.* **2017**, In press. 10.1080/10408398.2016.1276883.

(14) Cynkar, W.; Dambergs, R.; Smith, P.; Cozzolino, D. Classification of Tempranillo wines according to geographic origin: Combination of mass spectrometry based electronic nose and chemometrics. *Anal. Chim. Acta* **2010**, *660*, 227−231.

(15) Perestrelo, R.; Barros, A. S.; Rocha, S. M.; Câmara, J. S. Establishment of the varietal profile of *Vitis vinifera* L. grape varieties from different geographical regions based on HS-SPME/GC−qMS combined with chemometric tools. *Microchem. J.* **2014**, *116*, 107−117.

(16) Farrés, M.; Platikanov, S.; Tsakovski, S.; Tauler, R. Comparison of the variable importance in projection (VIP) and of the selectivity ratio (SR) methods for variable selection and interpretation. *J. Chemom.* **2015**, *29*, 528−536.

(17) Mehmood, T.; Liland, K. H.; Snipen, L.; Sæbø, S. A review of variable selection methods in partial least squares regression. *Chemom. Intell. Lab. Syst.* **2012**, *118*, 62−69.

(18) European Union. European Commission Decision 2009/606/EC of 10 July 2009 implementing Council Regulation (EC) No 479/2008 concerning the categories of grapevine products, oenological practices and the applicable restrictions. *Off. J. Eur. Communities: Legis.* **2009**, *193*, 1−59.

(19) OIV *Compendium of International Methods of Analysis of Wines and Musts*; Office International de la Vigne et du Vin. Recueil des méthodes internationales d'analyse des vins et des moûts: París, 1990.

(20) Ganss, S.; Kirsch, F.; Winterhalter, P.; Fischer, U.; Schmarr, H.-G. Aroma changes due to second fermentation and glycosylated precursors in Chardonnay and Riesling sparkling wines. *J. Agric. Food Chem.* **2011**, *59*, 2524−2533.

(21) Gómez-Plaza, E.; Gil-Muñoz, R.; López-Roca, J. M.; Martínez-Cutillas, A.; Fernández-Fernández, J. I. Phenolic compounds and color stability of red wines: Effect of skin maceration time. *Am. J. Enol. Vitic.* **2001**, *52*, 266−270.

(22) Herraiz, T.; Martin-Alvarez, P. J.; Reglero, G.; Herraiz, M.; Cabezudo, M. D. Effects of the presence of skins during alcoholic

DOI: 10.1021/acs.jafc.6b05265
J. Agric. Food Chem. 2017, 65, 2768−2775

fermentation on the composition of wine volatiles. *VITIS-Journal Grapevine Res.* **1990**, *29*, 239−249.
(23) Piñeiro, Z.; Natera, R.; Castro, R.; Palma, M.; Puertas, B.; Barroso, C. G. Characterisation of volatile fraction of monovarietal wines: Influence of winemaking practices. *Anal. Chim. Acta* **2006**, *563*, 165−172.
(24) Herrero, P.; Sáenz-Navajas, P.; Culleré, L.; Ferreira, V.; Chatin, A.; Chaperon, V.; Litoux-Desrues, F.; Escudero, A. Chemosensory characterization of Chardonnay and Pinot Noir base wines of Champagne. Two very different varieties for a common product. *Food Chem.* **2016**, *207*, 239−250.
(25) Antalick, G.; Šuklje, K.; Blackman, J. W.; Meeks, C.; Deloire, A.; Schmidtke, L. M. Influence of grape composition on red wine ester profile: comparison between Cabernet Sauvignon and Shiraz cultivars from Australian warm climate. *J. Agric. Food Chem.* **2015**, *63*, 4664−4672.
(26) Cejudo-Bastante, M. J.; Castro-Vázquez, L.; Hermosín-Gutiérrez, I.; Pérez-Coello, M. S. Combined effects of prefermentative skin maceration and oxygen addition of must on color-related phenolics, volatile composition, and sensory characteristics of Airén white wine. *J. Agric. Food Chem.* **2011**, *59*, 12171−12182.
(27) Petropulos, V. I.; Bogeva, E.; Stafilov, T.; Stefova, M.; Siegmund, B.; Pabi, N.; Lankmayr, E. Study of the influence of maceration time and oenological practices on the aroma profile of Vranec wines. *Food Chem.* **2014**, *165*, 506−514.
(28) Selli, S.; Canbas, A.; Cabaroglu, T.; Erten, H.; Lepoutre, J.-P.; Gunata, Z. Effect of skin contact on the free and bound aroma compounds of the white wine of *Vitis vinifera* L. cv Narince. *Food Control* **2006**, *17*, 75−82.
(29) Rojas, V.; Gil, J. V.; Piñaga, F.; Manzanares, P. Acetate ester formation in wine by mixed cultures in laboratory fermentations. *Int. J. Food Microbiol.* **2003**, *86*, 181−188.
(30) Ribéreau-Gayon, P.; Glories, Y.; Maujean, A.; Dubourdieu, D. *Handbook of Enology. The chemistry of wine stabilization and treatments*; Wiley: Chichester, UK, 2000; Vol. 2.
(31) Álvarez-Pérez, J. M.; Campo, E.; San-Juan, F.; Coque, J. J. R.; Ferreira, V.; Hernández-Orte, P. Sensory and chemical characterisation of the aroma of Prieto Picudo rosé wines: The differential role of autochthonous yeast strains on aroma profiles. *Food Chem.* **2012**, *133*, 284−292.
(32) Hazelwood, L. A.; Daran, J.-M.; van Maris, A. J.; Pronk, J. T.; Dickinson, J. R. The Ehrlich pathway for fusel alcohol production: a century of research on Saccharomyces cerevisiae metabolism. *Appl. Environ. Microbiol.* **2008**, *74*, 2259−2266.
(33) Loscos, N.; Hernández-Orte, P.; Cacho, J.; Ferreira, V. Fate of grape flavor precursors during storage on yeast lees. *J. Agric. Food Chem.* **2009**, *57*, 5468−5479.
(34) Gromski, P. S.; Muhamadali, H.; Ellis, D. I.; Xu, Y.; Correa, E.; Turner, M. L.; Goodacre, R. A tutorial review: Metabolomics and partial least squares-discriminant analysis - a marriage of convenience or a shotgun wedding. *Anal. Chim. Acta* **2015**, *879*, 10−23.
(35) Cuevas, F. J.; Moreno-Rojas, J. M.; Arroyo, F.; Daza, A.; Ruiz-Moreno, M. J. Effect of management (organic vs conventional) on volatile profiles of six plum cultivars (*Prunus salicina* Lindl.). A chemometric approach for varietal classification and determination of potential markers. *Food Chem.* **2016**, *199*, 479−484.
(36) Perestrelo, R.; Silva, C.; Câmara, J. S. A useful approach for the differentiation of wines according to geographical origin based on global volatile patterns. *J. Sep. Sci.* **2014**, *37*, 1974−1981.
(37) Berrueta, L. A.; Alonso-Salces, R. M.; Héberger, K. Supervised pattern recognition in food analysis. *J. Chromatogr. A* **2007**, *1158*, 196−214.
(38) Jumtee, K.; Komura, H.; Bamba, T.; Fukusaki, E. Predication of Japanese green tea (Sen-cha) ranking by volatile profiling using gas chromatography mass spectrometry and multivariate analysis. *J. Biosci. Bioeng.* **2011**, *112*, 252−255.
(39) Wehrens, R. *Chemometrics with R: Multivariate Data Analysis in the Natural Sciences and Life Sciences*; Springer Science & Business Media, 2011.
(40) Lindon, J. C.; Nicholson, J. K.; Holmes, E. *The handbook of metabonomics and metabolomics*; Elsevier, 2011.
(41) Wang, C.; Dong, R.; Wang, X.; Lian, A.; Chi, C.; Ke, C.; Guo, L.; Liu, S.; Zhao, W.; Xu, G.; Li, E.; et al. Exhaled volatile organic compounds as lung cancer biomarkers during one-lung ventilation. *Sci. Rep.* **2014**, *4*, 7312.
(42) Ferreira, V.; Sáenz-Navajas, M. P.; Campo, E.; Herrero, P.; de la Fuente, A.; Fernández-Zurbano, P. Sensory interactions between six common aroma vectors explain four main red wine aroma nuances. *Food Chem.* **2016**, *199*, 447−456.
(43) Ferreira, V.; Lopez, R.; Cacho, J. F. Quantitative determination of the odorants of young red wines from different grape varieties. *J. Sci. Food Agric.* **2000**, *80*, 1659−1667.
(44) Herrero, P.; Sáenz-Navajas, P.; Culleré, L.; Ferreira, V.; Chatin, A.; Chaperon, V.; Escudero, A.; Litoux-Desrues, F. Chemosensory characterization of Chardonnay and Pinot Noir base wines of Champagne. Two very different varieties for a common product. *Food Chem.* **2016**, *207*, 239−250.

DOI: 10.1021/acs.jafc.6b05265
J. Agric. Food Chem. 2017, 65, 2768−2775

ARTÍCULO 3

The influence of pre-fermentative maceration and ageing factors on ester profile and marker determination of Pedro Ximenez sparkling wines

María José Ruiz-Moreno, José Manuel Muñoz-Redondo, Francisco Julián Cuevas, Almudena Marrufo-Curtido, Juan Manuel León, Pilar Ramírez, José Manuel Moreno-Rojas

Food Chemistry

230, 697-704 (2017)

Q1: 7/133 (Food Science & Technology, 2017)

Impact Factor: 4.946

Food Chemistry 230 (2017) 697–704

Contents lists available at ScienceDirect

Food Chemistry

journal homepage: www.elsevier.com/locate/foodchem

The influence of pre-fermentative maceration and ageing factors on ester profile and marker determination of Pedro Ximenez sparkling wines

María José Ruiz-Moreno [a,*], José Manuel Muñoz-Redondo [a], Francisco Julián Cuevas [a], Almudena Marrufo-Curtido [a,b,1], Juan Manuel León [c], Pilar Ramírez [c], José Manuel Moreno-Rojas [a,*]

[a] Postharvest Technology and Food Industry Department, Andalusian Institute of Agricultural and Fisheries Research and Training (IFAPA), Centro Alameda del Obispo, Avda Menéndez Pidal, 14004 Córdoba, Spain
[b] Postharvest Technology and Food Industry Department, Andalusian Institute of Agricultural and Fisheries Research and Training (IFAPA), Centro Rancho de la Merced, Ctra Trebujena Km 2.1, 11471, Jerez de la Frontera, Spain
[c] Crop Production Department, Andalusian Institute of Agricultural and Fisheries Research and Training (IFAPA), Centro de Cabra, Ctra Cabra-Doña Mencía, km 2.5, 11940 Cabra, Spain

ARTICLE INFO

Article history:
Received 17 October 2016
Received in revised form 3 March 2017
Accepted 9 March 2017
Available online 10 March 2017

Keywords:
Aroma
Ester
Volatile
Chemometrics
Multivariate analyses
Sparkling wines
OPLS-DA
Markers

ABSTRACT

The influence of pre-fermentative maceration and ageing factors on the ester profiles of Pedro Ximenez sparkling wines was evaluated. The pre-fermentative maceration consisted of the skin-maceration of musts at 10 °C for 6 h. The sparkling wines were produced following the Champenoise method. Samples were monitored at 3, 6 and 9 months of ageing on lees. Sparkling wines with pre-fermentative maceration displayed higher contents of ethyl esters of branched acids and cinnamates. Meanwhile, those without maceration showed higher levels of ethyl esters of fatty acids and higher alcohol acetates. The study of statistical interactions elucidated different hydrolytic kinetics and developments in higher alcohol acetates and ethyl esters of branched acids during ageing. The application of a dual criterion based on univariate (ANOVA) and multivariate analyses (OPLS–DA) allowed us to identify new potential volatile markers related to pre-fermentative maceration and ageing time, reported for the first time in sparkling wines.

1. Introduction

Recently, a new wine market paradigm based on product diversification has emerged for winemakers (Pozo-Bayón, Martínez-Rodríguez, Pueyo, & Moreno-Arribas, 2009). This has given consumers a large choice of typologies of wines, different qualities and prices. A good example of the diversification of wine types is sparkling wines. While the worldwide production of still wines has increased by 7% over the 10 last years, that of sparkling wines increased by more than 40% over the same period (OIV. The International Organisation of Vine, 2014). In addition, although the production of sparkling wine is lower than other wines in terms of quantity, the economic impact of this product is very important, due to its high added value and increased production on a global scale (Caliari, Burin, Rosier, & BordignonLuiz, 2014; Torresi, Frangipane, & Anelli, 2011). This increasing interest in sparkling wines is bound to new market segments for sparkling wines, resulting in changes in the global market for this product. Thereby, cava exceeded the exports of champagne in volume terms during 2015 (Institut del Cava., 2015; Le Comité Champagne., 2015) and the production of sparkling wines from Russia, USA, Ukraine, Australia, Hungary or Brazil has rapidly increased in the last few years (OIV, 2014).

Winemakers and the scientific community are searching for new collaborative platforms to enhance the peculiarities and distinctive characteristics of their wines (Caliari et al., 2014; Pozo-Bayón et al., 2009). These distinctive characteristics of the wines are usually given by local or regional grape varieties. In this context, Pedro Ximenez is an autochthonous white grape variety traditionally used for the production of Sherry-type wines in the Montilla–Moriles designation of origin (Andalusia, Spain). The versatility and attitude of this variety have been well proven (comprising the organic production, sun-drying and oxidative and biological ageing) producing many different styles of wines. The grape variety and other factors, such as crop management, ripe-

* Corresponding authors.
E-mail addresses: mariaj.ruiz.moreno@juntadeandalucia.es (M.J. Ruiz-Moreno), josem.moreno.rojas@juntadeandalucia.es (J.M. Moreno-Rojas).
[1] Current address: Laboratory for Aroma Analysis and Enology, Instituto Alimentario de Aragón (IA2), Associate unit to Instituto de las Ciencias de la Vid y el Vino (ICVV) (UR-CSIC-GR), Department of Analytical Chemistry, Faculty of Sciences, University of Zaragoza, 50009 Zaragoza, Spain.

http://dx.doi.org/10.1016/j.foodchem.2017.03.048
0308-8146/

ness, and base wine composition, have been well reported to impact on the quality of sparkling wine (Pozo-Bayón et al., 2009; Riu-Aumatell, Bosch-Fusté, López-Tamames, & Buxaderas, 2006). Skin maceration induces compositional modifications as well as the extraction of grape-derived components in grape juices. Furthermore, the traditional or Champenoise method, involving a second fermentation and ageing in contact with lees, also produces compositional changes impacting on the final quality of the product (Pozo-Bayón et al., 2009; Riu-Aumatell et al., 2006).

Skin maceration is usually performed in the production of rosé sparkling wines. Several authors concur with the use of this operation as an oenological practice to improve the quality of sparkling wines from red grape varieties (Martínez-Lapuente, Guadalupe, Ayestarán, & Pérez-Magariño, 2015; Pozo-Bayón et al., 2009). However, to our knowledge, comparative studies have not explored the influence of pre-fermentative strategies on the distinctive aroma styles of sparkling wines, and this requires investigation. In this sense, deepening our understanding of the aromatic impact of this pre-fermentative operation may offer a promising strategy for obtaining sparkling wines with differential aromatic characteristics.

Aroma is considered one of the most decisive quality attributes in wines and a key factor impacting on consumers' preferences and tasting experience (Antalick et al., 2015; Lockshin & Corsi, 2012; Sáenz-Navajas, Ballester, Pêcher, Peyron, & Valentin, 2013). In this sense, the role of ester compounds in wine aroma is a current topic of research. The growing interest in the characterization of wine esters is not only due to their direct sensory contribution but also to complex synergistic interactions affecting aroma perception (Escudero, Campo, Fariña, Cacho, & Ferreira, 2007; Lytra, Tempere, Le Floch, de Revel, & Barbe, 2013). Esters are formed as a result of the reaction of an alcohol with a carboxylic acid functional group. These molecules are mainly synthesized by two mechanisms in wines: during alcoholic fermentation through enzymatic reactions produced by yeasts and during wine ageing by chemical esterification between alcohol and acid functional groups at low pH (Sumby, Grbin, & Jiranek, 2010). Besides the mechanisms of genesis, ester hydrolysis and ester oxidation by hydroxyl radical-related processes could modulate their contents over the winemaking process (Ramey & Ough, 1980). Recent studies have reported that the maturity of grapes, fermentation strategy and ageing factors greatly affect the ester profile of wine and consequently impact on its aroma. In the case of the Pedro Ximenez grapes, the impact of pre-fermentative maceration on cinnamates has not been reported. Moreover, studies focused on the role of ester compounds in sparkling wines modified by skin maceration and ageing are scarce.

Given the importance of ester compounds and their sensory impact, numerous approaches have been developed to characterize ester compounds in wines (Marquez, Serratosa, Merida, Zea, & Moyano, 2014; Ubeda, Callejón, Troncoso, Peña-Neira, & Morales, 2016). In this sense, headspace solid-phase microextraction (HS-SPME) is a suitable, quick, simple and solvent-free technique. HS-SPME coupled to gas chromatography with mass spectrometry detection (GC–MS) has been widely used for this purpose (Antalick, Perello, & de Revel, 2010; Perestrelo, Barros, Rocha, & Câmara, 2014). This technique can produce a large amount of data for each sample. Therefore, multivariate approaches are used to handle tangled data since the univariate analysis may ignore other interactions found in complex models (Cozzolino, Cynkar, Shah, Dambergs, & Smith, 2009).

The aim of this study was to examine the impact of pre-fermentative maceration and ageing factors on the ester composition of Pedro Ximenez sparkling wines. For that purpose, a novel methodology based on HS-SPME-GC–MS and chemometrics was developed to highlight the potential volatile markers of both factors.

2. Materials and methods

2.1. Wine samples

Sparkling wines were elaborated at IFAPA, Cabra-Priego (37° - 29′ 53″N; 04° 25′ 51″ W) following the traditional or Champenoise method (consisting of a second fermentation of base wines in closed bottles and ageing on lees before disgorging). A 600-kg batch of Pedro Ximenez grapes from the 2014 campaign were harvested at 18.5 19.0 °Brix and divided into two. The first 300-kg batch of grapes (NM samples) was destemmed, crushed and pressed. The grape juices were divided into stainless steel tanks of 50 L. They were corrected, sulfited (at 70 mg L^{-1}) and then alcoholic fermentation was carried out at a controlled temperature of 18 °C, obtaining the NM base wines. The yeast and nutrients used were Pasionviniferm (Agrovin, Spain) at 20 g h L^{-1} and Actimax Bio at 10 g h L^{-1} (Agrovin, Spain), respectively. Next, the base wines were clarified, stabilized and filtered. In the second batch (M), 300 kg of grapes were destemmed, crushed and sulfited (at 50 mg kg^{-1}). Enozym AROME enzyme at a dose of 30 mg kg^{-1} (Agrovin, Spain) was added. Afterwards, a pre-fermentative maceration of the must in contact with the skins was performed for 6 h at 10 °C before pressing. Then, the grape juices were corrected and fermented following the same conditions described for the NM base wines. The tirage liquor consisted of 24 g L^{-1} of sucrose, yeast Viniferm PDM at 20 g hL^{-1} (Agrovin. Spain), Actimax Bio at 15 g h L^{-1} (Agrovin, Spain) and bentonite at 20 g h L^{-1} (Laffort, France). A second fermentation was performed at 15 °C in closed bottles of 0.75 L. The pressure and residual sugars were measured periodically. This fermentation was completed after 11 12 weeks. Then, the sparkling wines were kept at 12 °C and collected at 0, 3, 6 and 9 months of ageing on lees, riddled, disgorged, corked and submitted to analysis. A total of 48 bottles were analyzed. The two treatments (N and NM) were sampled in duplicate at each time (beginning of ageing, 3, 6 and 9 months) for each of the three fermentative tanks.

2.2. Oenological parameters

Ethanol (% vol.), residual sugars, pH, total and volatile acidity were determined following the official analytical methods (OIV, 2014). Optical density at $\lambda = 420$ nm was determined using a spectrophotometer (Lambda 25; Perkin-Elmer, Waltham, MA). Total phenolic content was determined by photometric procedure (Folin-Ciocalteu). The results were expressed as mg L^{-1} of gallic acid.

2.3. Chemicals and reagents

HPLC-grade ethanol was obtained from J.T. Baker Chemicals B. V. (Deventer, Holland). Milli-Q water was obtained from a Milli-Q Plus water system (Millipore, Spain). Sigma Aldrich (Madrid, Spain) supplied the sodium chloride, ACS reagent grade (purity ≥99.8%) and standard compounds; ethyl butyrate (≥99%), ethyl hexanoate (≥99%), ethyl octanoate (≥99%), propyl acetate (≥99%), isobutyl acetate (≥99%), isoamyl acetate (≥99%), hexyl acetate (≥99%), phenylethyl acetate (≥99%), ethyl isobutyrate (98%), ethyl 2-methylbutyrate (≥99%), ethyl isovalerate (≥99%), ethyl phenylacetate (98%), ethyl dihydrocinnamate (98%), ethyl cinnamate (98%), methyl hexanoate (≥99%), methyl octanoate

(≥99%), methyl decanoate (≥99%), isoamyl butyrate (98%), isoamyl hexanoate (98%), isoamyl octanoate (98%), ethyl heptanoate (98%), ethyl nonanoate (98%), ethyl propanoate (≥99%), isobutyl hexanoate (≥99%).

2.4. Automated HS-SPME-GC–MS analysis

The sparkling wine samples (25 mL) were spiked with 20 μL of internal standard mix solution at 200 μg L^{-1} of isotopically labelled esters: [$^2H_3$]-ethyl butyrate, [$^2H_{11}$]–ethyl hexanoate, [$^2H_{15}$]-ethyl octanoate, and [$^2H_5$]-ethyl cinnamate, supplied by CDN isotopes (Pointe-Claire, Canada). Spiked samples (10 mL) diluted 1:3 with Mili–Q water were placed into a 20-mL SPME vial filled with 3.5 g of NaCl. The capped vials were homogenized for 30 s in a vortex shaker, placed in a Combipal autosampler tray (CTC Analytics, Zwingen, Switzerland) and analyzed by HS-SPME-GC–MS. A previously conditioned 100 μm PDMS fibre (Supelco, Bellefonte, PA) was used. The vials were stirred at 500 rpm for 2 min at 40 °C. Extraction was set at 40 °C for 30 min and desorption was performed at 250 °C for 15 min. The fibre was desorbed into a Trace GC Ultra gas chromatograph (Thermo Fisher Scientific S.p.A., Rodano, Milan, Italy) coupled to an ISQ Single Quadrupole MS spectrometer (Thermo Fisher Scientific, Austin, TX). The injection mode was splitless for 0.75 min. The column was a BP21 of 50 m × 0.32 mm, 0.25 μm film thickness (SGE Analytical Science, UK). The carrier gas was helium at a column head pressure of 8.0 psi. The oven temperature was programmed at 40 °C for 5 min, raised to 220 °C at 3 °C min^{-1}, and then held for 30 min. The MS transfer line and source temperature were 230 °C and 200 °C, respectively. The mass spectrometer operated in electron ionization mode at 70 eV using selected ion monitoring (SIM) mode. Identification was carried out by comparing retention times and mass spectra with those of pure standards. Calibration curves were built using a commercial sparkling wine spiked with a mixture of the target compounds at nine concentrations levels and analyzed following the procedure described above. The method performance was evaluated in a sparkling wine matrix (Supplementary Table 1).

2.5. Statistical analysis

Univariate analysis was performed using Statistix (v 9.0, Analytical Software, Tallahassee, FL). The data were subjected to analysis of variance using Shapiro Wilk's and Lenève's tests for normality and homoscedasticity requirements. Differences at $p < 0.05$ were considered to be statistically significant. A comparison of means based on least significant differences (LSD, Fisher's test) was performed. Multivariate analysis (OPLS–DA, orthogonal-partial least squares discriminant analysis) was performed using PLS toolbox (v. 5.5.1, Eigenvector Research Inc., Manson, WA) under MATLAB 2008R (v. 7.6.0; Mathworks, Natick, MA) workspace.

3. Results and discussion

3.1. Oenological parameters

The oenological parameters of the sparkling wines are shown in Table 1. Regarding the pre-fermentative strategy, higher values for pH, volatile acidity, absorbance at λ = 420 nm and total phenolic content were found in the M sparkling wines. Meanwhile, ageing factor only affected the pH of the sparkling wines, a slight decrease being observed at 3 months of ageing. Despite the differences found, the oenological parameters confirmed that the sparkling wines fulfilled the legal and quality standards.

3.2. Aroma composition

The volatile compounds were classified into different groups according to their chemical structure and origin (Table 2). The chemical groups included: ethyl esters of fatty acids (EEFAs), higher alcohol acetates (HAAs), ethyl esters of branched acids (EEBAs), cinnamates, methyl esters of fatty acids (MEFAs), isoamyl esters of fatty acids (IEFAs), ethyl esters of odd carbon number fatty acids (EEOCNFA) and compounds grouped in a miscellaneous group (MEs). Concerning their relative composition (Supplementary Table 2 and Supplementary Table 3), EEFAs were the major group (with concentration ranges between 855 1537 μg L^{-1}), followed by HAAs (239 771 μg L^{-1}), EEBAs (96 284 μg L^{-1}) and miscellaneous compounds (98 209 μg L^{-1}). Meanwhile, IEFAs (1.7 3.7 μg L^{-1}), EEOCNFA (1.6 3.0 μg L^{-1}), MEFAs (0.9 1.5 μg L^{-1}) and cinnamates (0.19 0.3 μg L^{-1}) showed the lowest quantitative contribution. A two-way analysis of variance (ANOVA) was carried out. The factors studied were pre-fermentative strategy and ageing. The results are shown in Table 2.

3.3. Univariate analysis

3.3.1. Pre-fermentative maceration factor

Regarding the pre-fermentative maceration, significant differences between the aroma profiles were observed. The sparkling wines from pre-fermentative maceration (M) showed a lower content of total esters (Table 2). This behaviour is mainly due to a decrease in the EEFA and HAA groups in the M sparkling wines. These results are in agreement with the literature (Herraiz, Martin-Alvarez, Reglero, Herraiz, & Cabezudo, 1990). Piñeiro et al. (2006) also found a similar behaviour in EEFA contents in wines produced under pre-fermentative maceration, due to a decrease in ethyl hexanoate and octanoate compounds. However, the mechanisms involved in the reduction of EEFAs in wines from pre-fermentative maceration still remain unclear. EEFAs are generally produced during alcoholic fermentation by yeasts (Antalick, Perello, & de Revel, 2014). Winemaking conditions such as temperature, aeration, skin contact and yeast strain have been described as the main factors affecting their EEFA concentrations (Antalick et al., 2014; Sumby et al., 2010). Moreover, the differential composition of the fermentative medium (lipids, amino acids, phenolic compounds) has been reported to modulate the ester profile of wines (Antalick et al., 2014; Antalick et al., 2015).

Higher levels of phenolic compounds limit lipoxygenase activity (Yu et al., 2013). The repression of the lipoxygenases limits the degradation of unsaturated fatty acids that are related to the production of EEFAs. Moreover, the substrate of this reaction has been described as the major factor limiting the production of EEFAs (Robinson et al., 2014). Thus, higher levels of phenolic compounds (Table 1) could be related to the lower EEFA contents. Meanwhile, HAAs are formed from an alcohol and acetyl-CoA during alcoholic fermentation (Saerens, Delvaux, Verstrepen, & Thevelein, 2010) and are catalysed by alcohol acetyltransferases I and II (ATF1, ATF2). The increasing amount of unsaturated fatty acids in the medium (derived from a lower lipoxygenase activity) repress the enzymatic activity and, subsequently, the production of HAAs during fermentation (Robinson et al., 2014). In this sense, the lower HAA concentration found in the M sparkling wines could also be due to higher phenolic content (Table 1), as suggested in the literature (Antalick et al., 2014; Ribéreau-Gayon, 2000). Therefore, the higher levels of phenolic compounds obtained in the M sparkling wines could be involved in the reduction of HAAs and EEFAs in a different manner, limiting the substrate of the reaction (EEFAs) or limiting the kinetics of the reaction (HAAs).

On the other hand, the M sparkling wines presented higher levels of EEBAs, cinnamates, MEFAs, EEOCNFAs and miscellaneous

Table 1
Sparkling wine oenological parameters. Two-way ANOVA for pre-fermentative maceration and ageing factors and interaction (pre-fermentative maceration × ageing) effect.

	Pre-fermentative maceration			Ageing (months)					Interaction
	NM[a]	M[b]	*p*-value[c]	0	3	6	9	*p*-value[c]	*p*-Value[c]
Ethanol (vol%)	12.6	12.4	ns	12.6	12.4	12.5	12.6	ns	ns
Residual sugars (g L^{-1})	2.3	2.4	ns	2.3	2.2	2.5	2.4	ns	ns
pH (20 °C)	3.18b	3.24a	***	3.20ab	3.17b	3.24a	3.22a	**	ns
Total acidity[d] (g L^{-1})	5.58	5.67	ns	5.74	5.65	5.51	5.59	ns	ns
Volatile acidity[e] (g L^{-1})	0.33b	0.39a	***	0.37	0.39	0.37	0.35	ns	ns
Absorbance at 420 nm	0.04b	0.06a	***	0.05	0.05	0.05	0.05	ns	ns
Total phenolic content[f] (mg L^{-1})	116b	162a	***	139	141	138	137	ns	ns

[a] NM: Sparkling wines elaborated without skin maceration.
[b] M: Sparkling wines elaborated from skin maceration.
[c] Significance level: ns = non-significant. * = $p < 0.05$. ** = $p < 0.01$. *** = $p < 0.001$.
[d] Calculated as tartaric acid.
[e] Calculated as acetic acid.
[f] Gallic acid equivalents.

Table 2
Concentrations of ester compounds (μg L^{-1}) in sparkling wines. Two-way ANOVA for pre-fermentative maceration and ageing factors and interaction (pre-fermentative maceration × ageing) effect.

Group[d]	Compound	Pre-fermentative maceration				Ageing (months)						Interaction
		NM[a]	M[b]	p-Value[c]	VIP	0	3	6	9	p-Value[c]	VIP	p-Value[c]
EEFAs	Ethyl butyrate	144a	102b	***	0.9	130	118	112	131	ns	0.2	ns
	Ethyl hexanoate	571a	312b	***	1.4	449	451	407	459	ns	0.1	ns
	Ethyl octanoate	**769a**	459b	***	**1.5**	606	626	628	594	ns	0.2	ns
	ΣEEFAs	1484a	872b	***	–	1186	1196	1147	1185	ns	–	ns
HAAs	Propyl acetate	3.2	3.0	ns	0.1	**3.9a**	2.8b	3.0b	2.6b	***	**2.2**	ns
	Isobutyl acetate	16a	12b	***	1.0	16a	13c	13c	14b	***	1.3	***
	Isoamyl acetate	407a	251b	***	1.0	**502a**	290b	275bc	249c	***	**2.8**	***
	Hexyl acetate	16a	7b	***	1.1	**18a**	10b	10b	8b	***	**2.2**	**
	Phenylethylacetate	52a	37b	***	0.4	**76a**	40b	33c	30c	***	**2.9**	*
	ΣHAAs	495a	310b	***	–	617a	355b	333bc	304c	***	–	***
EEBAs	Ethyl isobutyrate	97b	135a	***	0.7	78c	119b	118b	**149a**	***	**2.1**	**
	Ethyl 2-methylbutyrate	15b	39a	***	1.2	17c	27b	29b	**36a**	***	**1.6**	***
	Ethyl isovalerate	27b	40a	***	0.9	22c	35b	34b	**43a**	***	**2.2**	*
	Ethyl phenylacetate	1.3b	2.8a	***	1.4	2.0ab	2.2a	1.8b	2.1a	*	0.0	ns
	ΣEEBAs	140b	217a	***	–	119c	183b	183b	230a	***	–	***
Cinnamates	Ethyl dihydrocinnamate	0.18b	0.22a	***	0.7	0.2	0.2	0.2	0.2	ns	0.9	ns
	Ethyl cinnamate	0.027	0.028	ns	0.0	0.027	0.026	0.027	0.031	ns	0.0	ns
	Σcinnamates	0.21b	0.25a	**	–	0.25	0.23	0.22	0.22	ns	–	ns
MEFAs	Methyl hexanoate	0.36b	0.66a	***	1.3	0.52	0.48	0.52	0.51	ns	0.1	ns
	Methyl octanoate	0.51b	0.64a	***	0.9	0.65a	0.56b	0.53b	0.57b	**	1.4	ns
	Methyl decanoate	0.14a	0.07b	***	0.7	0.16a	0.12b	0.09bc	0.08c	**	1.2	ns
	ΣMEFAs	1.0b	1.4a	***	–	1.3a	1.1b	1.1b	1.2b	*	–	ns
IEFAs	Isoamyl butanoate	0.32a	0.19b	***	1.2	0.24	0.25	0.24	0.28	ns	0.4	ns
	Isoamyl hexanoate	1.32a	1.03b	***	0.8	1.13	1.24	1.17	1.16	ns	0.2	ns
	Isoamyl octanoate	1.66a	0.57b	***	1.4	0.95b	1.19a	1.10ab	1.23a	*	0.7	ns
	ΣIEFAs	3.3a	1.8b	***	–	2.3	2.7	2.5	2.7	ns	–	*
EEOCNFAs	Ethyl heptanoate	0.4b	**2.2a**	***	**1.5**	1.4	1.3	1.3	1.3	ns	0.2	ns
	Ethyl nonanoate	1.42a	0.78b	***	1.2	0.98	1.12	1.09	1.22	ns	0.4	ns
	ΣEEOCNFAs	1.9b	3.0a	***	–	2.4	2.4	2.3	2.5	ns	–	ns
Miscellaneous	Ethyl propanoate	103b	189a	***	1.3	144	137	146	158	ns	0.0	ns
	Isobutyl hexanoate	0.22a	0.12b	***	1.3	0.19a	0.18a	0.16b	0.17ab	*	0.4	ns
	Σmiscellaneous	103b	189a	***	–	144	137	146	158	ns	–	ns
	Total esters	2229a	1595b	***	–	2072a	1877b	1815b	1883b	***	–	*

[a] NM: Sparkling wines elaborated without skin maceration.
[b] M: Sparkling wines elaborated from skin maceration.
[c] Significance level: ns = non-significant. * = $p < 0.05$. ** = $p < 0.01$. *** = $p < 0.001$.
[d] EEFAs: Ethyl esters of fatty acids; HAAs: Higher alcohol acetates; EEBAs: Ethyl esters of branched acids; MEFAs: Methyl esters of fatty acids; IEFAs: Isoamyl esters of fatty acids; EEOCNFAs: Ethyl esters of odd carbon number fatty acids. Concentrations and VIP values considered for potential markers are highlighted in bold type letter.

compounds, compared to the NM sparkling wines. EEBAs derive from the metabolism of amino acids. Recently, variations in EEBAs related to grape maturity have been reported (Antalick et al., 2015). However, our samples did not present significant differences in their degree of ripeness, emphasizing, therefore, the impact of the pre-fermentative maceration. Increases in this group have been postulated in rosé and red wines to be related to a higher extraction of the corresponding amino acids during the winemaking stages in the presence of skins (Antalick et al., 2014). Nonetheless, to our knowledge, no data concerning the impact of pre-fermentative strategies on EEBAs have been described in sparkling wines. In this sense, our results advocate the modulation of EEBA contents by pre-fermentative maceration, as has been suggested in the literature for rosé and red wines.

Concerning cinnamates, the M sparkling wines presented higher concentrations of ethyl dihydrocinnamate (20% approx.) than the NM sparkling wines. The varietal contribution to concentrations of ethyl dihydrocinnamate is well known. It could also be

modulated during the winemaking process. Noble rot or sun-drying dehydration processes have been correlated with increases in this compound by still unknown mechanism(s) (Antalick et al., 2014; Campo, Cacho, & Ferreira, 2008).

Regarding MEFAs, higher levels of methyl hexanoate and octanoate were found in the M sparkling wines and lower levels of methyl decanoate. The EEOCNFA group was also affected by the maceration process, its concentration increasing (1.9 μg L^{-1} in NM sparkling wines compared to 3.0 μg L^{-1} in M ones), ethyl heptanoate standing out as the main contributor to this group. Concerning the miscellaneous compounds, ethyl propanoate was affected by the maceration procedure, its concentration increasing in M sparkling wines. The higher concentrations of ethyl propanoate in the M sparkling wines may derive from enriched macerated juices in amino acids, as suggested in the literature (Antalick et al., 2014).

3.3.2. Ageing factor

The ester profile was significantly influenced by the ageing on lees (Table 2). The highest value for the total esters parameter was found at the beginning of the ageing (0 months of ageing, 2072 μg L^{-1}) while, afterwards, it decreased (at 3 months) maintaining those values until the end of the ageing period (9 months of ageing). Nonetheless, not all the ester groups were influenced in the same way. The EEFA, cinnamate, IEFA, EEOCNFA and the miscellaneous groups were not affected by the ageing factor, as was demonstrated in previous research (Antalick et al., 2014). Concerning the EEFA group, the explanation was related to the equilibrium between the corresponding acids and ethanol for the medium-chain ethyl fatty acids (Antalick et al., 2014).

The ageing process significantly affected the concentrations of the HAA, EEBA and MEFA groups. However, the impact of ageing on those groups was different. HAAs decreased by more than 50% during the ageing, reaching the lowest concentrations in the sparkling wines at the end of this period (after 9 months). This trend was in accordance with the literature (Francioli, Torrens, Riu-Aumatell, López-Tamames, & Buxaderas, 2003; Riu-Aumatell et al., 2006), phenylethyl, hexyl and isoamyl acetates being the main contributors to this decrease (around 60%, 55% and 50% respectively). The results were in agreement with another study (Antalick et al., 2014) in which it was hypothesised that longer carbon chain acetates suffered faster hydrolysis compared to the shorter ones (propyl acetate and isobutyl acetate).

The EEBA group presented increased concentrations with ageing (from 119 μg L^{-1} to 230 μg L^{-1}), according to results reported in the literature (Antalick et al., 2014; Díaz-Maroto, Schneider, & Baumes, 2005; Rodríguez-Bencomo, Ortega-Heras, & Pérez-Magariño, 2010). The main EEBA compounds contributing to this trend were ethyl isobutyrate, ethyl 2-methylbutyrate and ethyl isovalerate, which showed a 1.9-fold increase between sparkling wines from 0 to 9 months of ageing. Meanwhile, ethyl phenylacetate was the least affected compound during this period. A lower synthesis ratio has also been described in the literature for this compound (Antalick et al., 2014), supporting our results. The MEFA group showed the highest concentrations at 0 months of ageing, decreasing by about 15% in sparkling wines at 3 months and remaining constant during the remaining ageing period. MEFAs have not been studied in depth in the literature. Only a few studies reported lower contents of this group in aged red wines than in young ones (Antalick et al., 2014; Gammacurta, Marchand, Albertin, Moine, & de Revel, 2014) and no references concerning ageing on lees have been found to date.

3.3.3. Interaction effects

The total content of esters displayed significant interactions (Table 2). It meant that ageing factor affected the aroma profile of the M and NM sparkling wines in a different way. Total esters decreased during ageing in the NM (from 2480 to 2150 μg L^{-1}) but they remained constant in the M wines (around 1600 μg L^{-1}, Supplementary Table 4). The HAA and EEBA groups also showed significant interactions. Decreases in HAA in both types of sparkling wines were observed once 3 months in contact with lees was reached. After this period, different trends were found between the NM and M sparkling wines (Supplementary Table 4). In the NM sparkling wines, HAAs decreased by around 16%, from 3 to 9 months of ageing. Meanwhile, the M wines displayed non-significant differences. Moreover, the hydrolysis phenomena described for the HAA group in the last paragraph was significantly less marked in the M sparkling wines. Lower variations in hexyl and isobutyl acetates were found in the M sparkling wines (decreases of 2.0 and 1.0-fold for hexyl and isobutyl acetates after 9 months of ageing in M sparkling wines, compared to the 2.5-fold and 1.3-fold decreases in the NM ones), supporting the less important hydrolysis phenomena in M sparkling wines. The impact of different chemical compositions of wines on ester hydrolysis has been suggested (Makhotkina & Kilmartin, 2012; Ribéreau-Gayon, 2000), which might help to understand the different trends observed.

EEBAs increased during the first 3 months of ageing, remained at constant levels until 6 months and increased again in the last period. However, the interaction effect revealed that the behaviour of the NM and M sparkling wines differed, ethyl 2-methylbutyrate standing out as the most affected compound. A higher synthesis of this compound was found in the M sparkling wines compared to the NM ones. The synthesis of EEBAs during ageing has been widely demonstrated. However, to the authors' knowledge this is the first study to report that the use of pre-fermentative maceration in sparkling wines seems to induce a higher genesis of EEBAs over ageing. EEBA volatilization was less altered by the non-volatile matrix, as reported in the literature (Lorrain et al., 2013). This fact might help to explain the higher synthesis of EEBAs observed in the M sparkling wines. Further studies to elucidate the mechanisms involved in this issue should be conducted.

3.4. Multivariate analysis

A multivariate analysis approach was performed to establish how the factors under study affected the ester profiles. The supervised chemometric techniques are able to match the analytical data obtained to a label or class. The most widely used of the supervised techniques is the partial least squares discriminant analysis (PLS-DA). PLS-DA is a multivariate method that has been referenced in the analysis of volatile compounds in wine for this purpose (Cynkar, Dambergs, Smith, & Cozzolino, 2010; Perestrelo et al., 2014). This technique combines principal component analysis with multiple regression features. It is based on a co-variance algorithm mixing two matrices, the explanatory matrix (X) that represents the rows dataset and the explicative matrix (Y) as a vector in accordance with the different classes studied. In addition, orthogonal signal correction can be used alongside the PLS-DA model as a way to remove variation in the irrelevant dataset to predict the dependent variable, and this resultant model (OPLS-DA) can be easier to interpret.

Two OPLS-DA models were performed (Fig. 1). The matrix used was built with 24 rows × 24 columns. The rows represented the samples and the columns the volatile compounds. The first model was based on the pre-fermentative strategy, labelling the NM sparkling wines as class 1 and the M ones as class 2. The second OPLS-DA model was built based on ageing effect, labelling sparkling wines without ageing (0 months) as class 1 and aged sparkling wines (3, 6 and 9 months of ageing) as class 2. In both statistical methods, only two latent variables were selected due to the per-

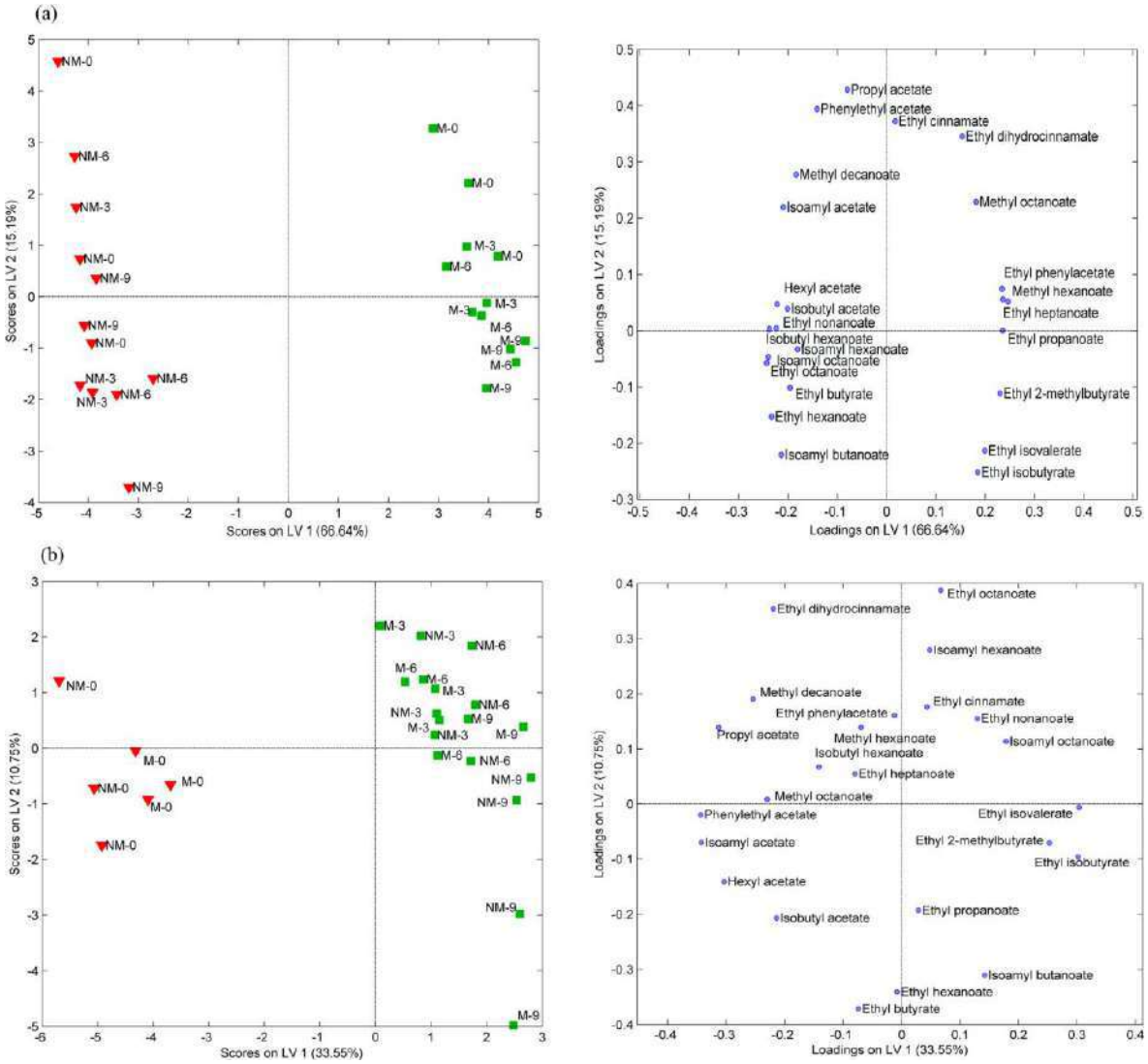

Fig. 1. Orthogonal partial least squares discriminant analysis (OPLS-DA) performed on (a) pre-fermentative maceration and (b) ageing classes of sparkling wines. Scores and loadings are shown in the two first latent variables.

centage of covariance captured in the *X*-matrix and the lowest root mean squares error in cross validation (RMSECV). The scores and loadings were plotted in a plane defined by these two latent variables (LV1 and LV2) in each case. The models achieved high sensitivity and specificity rates (100%, Table 3). Hotelling-s T^2 *versus* Q^2 residuals plot was selected as the outlier detection technique and it has been referenced in multivariate studies (Lindon, Nicholson, & Holmes, 2011). Therefore, each volatile compound was weighted according to their value, to improve the model prediction (Berrueta, Alonso-Salces, & Héberger, 2007). Several pre-processing techniques were evaluated (log transformation, mean centring, pareto scaling and autoscaling), 'auto-scaling' achieving the highest prediction ability. The re-sampling methodology used in this study was leave-one-out cross validation (LOOCV). Moreover, two data subsets were randomly obtained, the training set (66% of the samples) and the test set (33% of the samples for the external validation).

The first OPLS-DA model (Fig. 1a) established the impact of the pre-fermentation strategy on the ester composition of the sparkling wines. LV1 and LV2 explained 81.83% of the total variance in the *X*-matrix and 99.10% of the variance found in *Y*-matrix. LV1 held up to 66.64% of the data variability and separated the M sparkling wines from the NM ones. The main characteristic compounds of the M sparkling wines were those with the highest positive coefficients of LV1 and separated them from NM ones. Likewise, compounds distributed on the highest negative values of LV1 were the most characteristic of NM sparkling wines. Additionally, the second multivariate analysis performed allowed us to establish the impact of ageing on the volatile profiles of the sparkling wines (Fig. 1b). The results obtained explained 44.30% of the total variance in the *X*-matrix, responding to 95.70% of the

Table 3
Statistics results of the OPLS-DA models performed according to the pre-fermentative maceration and ageing factors.

Classes[a]	Pre-fermentative maceration[b]		Ageing	
	NM	M	Young wines	Aged wines
Calibration step				
Sensitivity (Cal)	100	100	100	100
Specificity (Cal)	100	100	100	100
RMSEC:	0.056	0.056	0.090	0.090
R^2	0.987	0.987	0.947	0.947
Cross-validation step				
Sensitivity (CV)	100	100	100	100
Specificity (CV)	100	100	100	100
RMSECV	0.089	0.089	0.179	0.179
R^2	0.969	0.969	0.835	0.835
External validation				
Sensitivity (CV)	100	100	100	100
Specificity (CV)	100	100	100	100
RMSEP	0.09	0.09	0.136	0.136
R^2	0.975	0.975	0.921	0.921

[a] Sensitivity: Proportion of positives that are correctly identified. Specificity: Proportion of negatives that are correctly identified. RMSEC: Root mean squares error at the calibration step. RMSECV: Root mean squares error at the cross validation step. RMSEP: Root mean squares error at the external validation R^2: Regression coefficient.
[b] NM: Sparkling wines elaborated without skin maceration; M: Sparkling wines elaborated from skin maceration.

variance found in the *Y*-matrix. LV1 explained 33.55% of the data variability and separated young sparkling wines (0 months of ageing) from the rest (sparkling wines with 3, 6 and 9 ageing period). Compounds distributed on the highest positive coefficients of LV1 separated aged sparkling wines from the young ones. Meanwhile, compounds situated on the highest negative values differentiated the young sparkling wines. Both models were internally and externally validated and successful results were achieved (Table 3).

3.5. Potential volatile markers

A novel approach was followed to detect volatile marker compounds (Cuevas, Moreno-Rojas, Arroyo, Daza, & Ruiz-Moreno, 2016). The methodology was based on two criteria: variable importance projection (VIP) values (calculated from the OPLS-DA models in the multivariate analysis) and the category of the factorial analysis of variance (univariate analysis) used under low dimensional datasets. Potential volatile markers were selected in compounds with a VIP $\geq$ 1.5 and category ***a*** (non-shared with other compounds) in the univariate analysis with a Fisher's least significance level of 0.01 (Table 2). This methodology allowed us to identify potential markers linked to the pre-fermentative strategy and ageing factors.

Regarding the pre-fermentative maceration, ethyl heptanoate was the only compound selected as a candidate marker of the M sparkling wines (Table 2). Likewise, ethyl octanoate was selected as candidate marker of the NM sparkling wines. Nonetheless, other compounds such as ethyl phenylacetate, methyl hexanoate and ethyl propanoate for the M sparkling wines, and ethyl hexanoate, isoamyl octanoate and isobutyl hexanoate for the NM sparkling wines displayed VIP coefficients close to 1.5 and the non-shared category ***a*** in the univariate analysis. Thus, the above compounds may also be considered as potential contributors linked to each named factor.

With regard to ageing marker compounds, three EEBAs (ethyl isovalerate, ethyl isobutyrate and ethyl 2-methylbutyrate) were obtained as candidate markers of aged sparkling wines (Table 2). However, in the literature we can find that ethyl isobutyrate was reported as a marker of aged Fino wines (Moreno, Zea, Moyano, & Medina, 2005). On the other hand, the HAAs (phenylethyl acetate, isoamyl acetate, propyl acetate and hexyl acetate) were the potential volatile markers of young sparkling wines. These results are in agreement with the literature, where it was found that isoamyl acetate, phenylethyl acetate and hexyl acetate were characteristic compounds of young sparkling wines (Francioli et al., 2003). Additionally, as described above for the pre-fermentative maceration factor, methyl octanoate displayed a VIP value close to 1.5 and it may also be considered as a potential aromatic contributor linked to young sparkling wines.

Among the volatile markers identified above, only a few may be considered as the main contributors to the sensory differences of the different sparkling wines. To identify them, the potential markers were related with their odour activity (Supplementary Table 1). Thus, ethyl octanoate (odour threshold 580 $\mu g\,L^{-1}$) presented concentrations above the threshold in all the NM sparkling wines. Meanwhile, ethyl hexanoate (odour threshold 14 $\mu g\,L^{-1}$) and isoamyl acetate (threshold 30 $\mu g\,L^{-1}$) were odorants, regardless of the pre-fermentative strategy. However, their concentrations were significantly higher in the NM sparkling wines than in the M ones. Ethyl isobutyrate (odour threshold 15 $\mu g\,L^{-1}$) and ethyl isovalerate (odour threshold 3 $\mu g\,L^{-1}$) presented concentrations above the threshold. However, the levels were significantly higher in the M sparkling wines. Ethyl 2-methylbutyrate (threshold 18 $\mu g\,L^{-1}$) showed a remarkably different behaviour. In the NM sparkling wines, it displayed levels above the threshold only at 9 months of ageing, while it was an odorant compound in all the M sparkling wines regardless of the ageing period.

4. Conclusions

The results highlighted the impact of pre-fermentative maceration and ageing on the aroma profile of sparkling wines. The pre-fermentative maceration significantly affected the ester profile of sparkling wines. Higher levels of EEBAs, cinnamates, MEFAs, EEOCNFAs and miscellaneous compounds were found in the sparkling wines obtained from a pre-fermentative maceration and higher levels of ethyl esters of fatty acids (EEFAs) and higher alcohol acetates (HAAs) were found in those without pre-fermentative maceration. Ethyl heptanoate, ethyl phenylacetate, methyl hexanoate and ethyl propanoate stood out as potential volatile markers of the pre-fermentative maceration, while ethyl isovalerate, ethyl isobutyrate and ethyl 2-methylbutyrate were identified as ageing markers. The ageing factor affected the ester profile of the wines with and without maceration in different ways, highlighting the importance of additional research focused on the contribution

of EEBAs to wine aroma during ageing. Further studies focusing on monitoring the sensory impact of the reported markers should also be performed to verify the impact of this differential ester profile resulting from the pre-fermentative maceration and ageing in sparkling wines.

Acknowledgments

This work was funded by the internal funds of the Andalusian Institute of Agricultural and Fisheries Research and Training (IFAPA) through the Project 'Proyecto complementario al Transforma "Vid y Vino" (PP.AVA.AVA201301.3), the European Social Fund (ESF), the European Rural Development Fund (ERDF).

José Manuel Muñoz Redondo was granted a research contract funded at Andalusian Institute of Agricultural and Fisheries Research and Training (IFAPA), inside the National Youth Guarantee System funded through the European Social Fund (ESF) and the Youth Employment Initiative (YEI). Maria José Ruiz Moreno was granted a postdoctoral research contract funded by the Andalusian Institute of Agricultural and Fisheries Research and Training (IFAPA) and the European Social Fund (ESF). Almudena Marrufo Curtido was granted a research contract funded by the Andalusian Institute of Agricultural and Fisheries Research and Training (IFAPA) and the European Social Fund (ESF). Juan Manuel León was granted a technical contract funded by Andalusian Institute of Agricultural and Fisheries Research and Training (IFAPA) and the European Social Fund (ESF).

Appendix A. Supplementary data

Supplementary data associated with this article can be found, in the online version, at http://dx.doi.org/10.1016/j.foodchem.2017.03.048.

References

Antalick, G., Perello, M.-C., & de Revel, G. (2010). Development, validation and application of a specific method for the quantitative determination of wine esters by headspace-solid-phase microextraction-gas chromatography–mass spectrometry. *Food Chemistry, 121*(4), 1236–1245.

Antalick, G., Perello, M.-C., & de Revel, G. (2014). Esters in wines: New Insight through the Establishment of a Database of French Wines. *American Journal of Enology and Viticulture, 65*(3), 293–304.

Antalick, G., Šuklje, K., Blackman, J. W., Meeks, C., Deloire, A., & Schmidtke, L. M. (2015). Influence of grape composition on red wine ester profile: comparison between Cabernet Sauvignon and Shiraz cultivars from Australian warm climate. *Journal of Agricultural and Food Chemistry, 63*(18), 4664–4672.

Berrueta, L. A., Alonso-Salces, R. M., & Héberger, K. (2007). Supervised pattern recognition in food analysis. *Journal of Chromatography A, 1158*(1), 196–214.

Caliari, V., Burin, V. M., Rosier, J. P., & BordignonLuiz, M. T. (2014). Aromatic profile of Brazilian sparkling wines produced with classical and innovative grape varieties. *Food Research International, 62*, 965–973.

Campo, E., Cacho, J., & Ferreira, V. (2008). The chemical characterization of the aroma of dessert and sparkling white wines (Pedro Ximenez, Fino, Sauternes, and Cava) by gas chromatography- olfactometry and chemical quantitative analysis. *Journal of Agricultural and Food Chemistry, 56*(7), 2477–2484.

Cozzolino, D., Cynkar, W. U., Shah, N., Dambergs, R. G., & Smith, P. A. (2009). A brief introduction to multivariate methods in grape and wine analysis. *International Journal of Wine Research, 1*(1), 123–130.

Cuevas, F. J., Moreno-Rojas, J. M., Arroyo, F., Daza, A., & Ruiz-Moreno, M. J. (2016). Effect of management (organic vs conventional) on volatile profiles of six plum cultivars (Prunus salicina Lindl.). A chemometric approach for varietal classification and determination of potential markers. *Food Chemistry, 199*, 479–484.

Cynkar, W., Dambergs, R., Smith, P., & Cozzolino, D. (2010). Classification of Tempranillo wines according to geographic origin: Combination of mass spectrometry based electronic nose and chemometrics. *Analytica Chimica Acta, 660*(1), 227–231.

Díaz-Maroto, M. C., Schneider, R., & Baumes, R. (2005). Formation pathways of ethyl esters of branched short-chain fatty acids during wine aging. *Journal of Agricultural and Food Chemistry, 53*(9), 3503–3509.

Escudero, A., Campo, E., Fariña, L., Cacho, J., & Ferreira, V. (2007). Analytical characterization of the aroma of five premium red wines. Insights into the role of odor families and the concept of fruitiness of wines. *Journal of Agricultural and Food Chemistry, 55*(11), 4501–4510.

Francioli, S., Torrens, J., Riu-Aumatell, M., López-Tamames, E., & Buxaderas, S. (2003). Volatile compounds by SPME-GC as age markers of sparkling wines. *American Journal of Enology and Viticulture, 54*(3), 158–162.

Gammacurta, M., Marchand, S., Albertin, W., Moine, V., & de Revel, G. (2014). Impact of yeast strain on ester levels and fruity aroma persistence during aging of bordeaux red wines. *Journal of Agricultural and Food Chemistry, 62*(23), 5378–5389.

Herraiz, T., Martin-Alvarez, P. J., Reglero, G., Herraiz, M., & Cabezudo, M. D. (1990). Effects of the presence of skins during alcoholic fermentation on the composition of wine volatiles. *VITIS-Journal of Grapevine Research, 29*(4), 239–249.

Institut del Cava. (2015). <http://www.institutdelcava.com/identidad/estadisticas-del-cava> Accessed October 10, 2016.

Le Comité Champagne. (2015). <http://www.champagne.fr/fr/economie/expeditions-de-vins-de-champagne> Accessed October 10, 2016.

Lindon, J. C., Nicholson, J. K., & Holmes, E. (2011). *The handbook of metabonomics and metabolomics*. Elsevier.

Lockshin, L., & Corsi, A. M. (2012). Consumer behaviour for wine 2.0: A review since 2003 and future directions. *Wine Economics and Policy, 1*(1), 2–23.

Lorrain, B., Tempere, S., Iturmendi, N., Moine, V., de Revel, G., & Teissedre, P.-L. (2013). Influence of phenolic compounds on the sensorial perception and volatility of red wine esters in model solution: An insight at the molecular level. *Food Chemistry, 140*(1), 76–82.

Lytra, G., Tempere, S., Le Floch, A., de Revel, G., & Barbe, J.-C. (2013). Study of sensory interactions among red wine fruity esters in a model solution. *Journal of Agricultural and Food Chemistry, 61*(36), 8504–8513.

Makhotkina, O., & Kilmartin, P. A. (2012). Hydrolysis and formation of volatile esters in New Zealand Sauvignon blanc wine. *Food Chemistry, 135*(2), 486–493.

Marquez, A., Serratosa, M. P., Merida, J., Zea, L., & Moyano, L. (2014). Optimization and validation of an automated DHS–TD–GC–MS method for the determination of aromatic esters in sweet wines. *Talanta, 123*, 32–38.

Martínez-Lapuente, L., Guadalupe, Z., Ayestarán, B., & Pérez-Magariño, S. (2015). Role of major wine constituents in the foam properties of white and rosé sparkling wines. *Food Chemistry, 174*, 330–338.

Moreno, J. A., Zea, L., Moyano, L., & Medina, M. (2005). Aroma compounds as markers of the changes in sherry wines subjected to biological ageing. *Food Control, 16*(4), 333–338.

Perestrelo, R., Barros, A. S., Rocha, S. M., & Câmara, J. S. (2014). Establishment of the varietal profile of Vitis vinifera L. grape varieties from different geographical regions based on HS-SPME/GC–qMS combined with chemometric tools. *Microchemical Journal, 116*, 107–117.

Piñeiro, Z., Natera, R., Castro, R., Palma, M., Puertas, B., & Barroso, C. G. (2006). Characterisation of volatile fraction of monovarietal wines: Influence of winemaking practices. *Analytica Chimica Acta, 563*(1), 165–172.

Pozo-Bayón, M. Á., Martínez-Rodríguez, A., Pueyo, E., & Moreno-Arribas, M. V. (2009). Chemical and biochemical features involved in sparkling wine production: from a traditional to an improved winemaking technology. *Trends in Food Science & Technology, 20*(6), 289–299.

Ramey, D. D., & Ough, C. S. (1980). Volatile ester hydrolysis or formation during storage of model solutions and wines. *Journal of Agricultural and Food Chemistry, 28*(5), 928–934.

Ribéreau-Gayon, P. (2000). *The chemistry of wine stabilization and treatments*. Wiley.

Riu-Aumatell, M., Bosch-Fusté, J., López-Tamames, E., & Buxaderas, S. (2006). Development of volatile compounds of cava (Spanish sparkling wine) during long ageing time in contact with lees. *Food Chemistry, 95*(2), 237–242.

Robinson, A. L., Boss, P. K., Solomon, P. S., Trengove, R. D., Heymann, H., & Ebeler, S. E. (2014). Origins of grape and wine aroma. Part 1. Chemical components and viticultural impacts. *American Journal of Enology and Viticulture, 65*(1), 1–24.

Rodríguez-Bencomo, J. J., Ortega-Heras, M., & Pérez-Magariño, S. (2010). Effect of alternative techniques to ageing on lees and use of non-toasted oak chips in alcoholic fermentation on the aromatic composition of red wine. *European Food Research and Technology, 230*(3), 485–496.

Sáenz-Navajas, M.-P., Ballester, J., Pêcher, C., Peyron, D., & Valentin, D. (2013). Sensory drivers of intrinsic quality of red wines: effect of culture and level of expertise. *Food Research International, 54*(2), 1506–1518.

Saerens, S. M., Delvaux, F. R., Verstrepen, K. J., & Thevelein, J. M. (2010). Production and biological function of volatile esters in Saccharomyces cerevisiae. *Microbial Biotechnology, 3*(2), 165–177.

Sumby, K. M., Grbin, P. R., & Jiranek, V. (2010). Microbial modulation of aromatic esters in wine: current knowledge and future prospects. *Food Chemistry, 121*(1), 1–16.

OIV. The International Organisation of Vine and Wine. (2014). <http://www.oiv.int/en/the-international-organisation-of-vine-and-wine> Accessed October 10, 2016.

Torresi, S., Frangipane, M. T., & Anelli, G. (2011). Biotechnologies in sparkling wine production. Interesting approaches for quality improvement: A review. *Food Chemistry, 129*(3), 1232–1241.

Ubeda, C., Callejón, R. M., Troncoso, A. M., Peña-Neira, A., & Morales, M. L. (2016). Volatile profile characterisation of Chilean sparkling wines produced by traditional and Charmat methods via sequential stir bar sorptive extraction. *Food Chemistry, 207*, 261–271.

Yu, S.-H., Hsieh, H.-Y., Pang, J.-C., Tang, D.-W., Shih, C.-M., Tsai, M.-L., & Ellipsis Mi, F.-L. (2013). Active films from water-soluble chitosan/cellulose composites incorporating releasable caffeic acid for inhibition of lipid oxidation in fish oil emulsions. *Food Hydrocolloids, 32*(1), 9–19.

ARTÍCULO 4

A Statistical Workflow to Evaluate the Modulation of Wine Metabolome and Its Contribution to the Sensory Attributes

José Manuel Muñoz-Redondo, Belén Puertas, Gema Pereira-Caro, José Luis Ordóñez-Díaz, María José Ruiz-Moreno, Emma Cantos-Villar and José Manuel Moreno-Rojas

Fermentation

7(2), 72 (2021)

Q1 (Plant Science, 2020)

CiteScore Scopus: 6.0

fermentation

MDPI

Article

A Statistical Workflow to Evaluate the Modulation of Wine Metabolome and Its Contribution to the Sensory Attributes

José Manuel Muñoz-Redondo [1,*], Belén Puertas [2], Gema Pereira-Caro [1], José Luis Ordóñez-Díaz [1], María José Ruiz-Moreno [1], Emma Cantos-Villar [2] and José Manuel Moreno-Rojas [1,*]

[1] Department of food Science and Health, Andalusian Institute of Agricultural and Fisheries Research and Training (IFAPA), Alameda del Obispo Avda, Menéndez Pidal, s/n, 14004 Córdoba, Spain; mariag.pereira@juntadeandalucia.es (G.P.-C.); josel.ordonez@juntadeandalucia.es (J.L.O.-D.); mariaj.ruiz.moreno@juntadeandalucia.es (M.J.R.-M.)

[2] Department of Food Science and Health, Andalusian Institute of Agricultural and Fisheries Research and Training (IFAPA), Cañada de la Loba, 11471 Jerez de la Frontera, Spain; mariab.puertas@juntadeandalucia.es (B.P.); emma.cantos@juntadeandalucia.es (E.C.-V.)

* Correspondence: josem.munoz.redondo@juntadeandalucia.es (J.M.M.-R.); josem.moreno.rojas@juntadeandalucia.es (J.M.M.-R.); Tel.: +34-666-306-651 (J.M.M.-R.); +34-671-532-758 (J.M.M.-R.)

Abstract: A data-processing and statistical analysis workflow was proposed to evaluate the metabolic changes and its contribution to the sensory characteristics of different wines. This workflow was applied to rosé wines from different fermentation strategies. The metabolome was acquired by means of two high-throughput techniques: gas chromatography–mass spectrometry (GC-MS) and liquid chromatography–mass spectrometry (LC-MS) for volatile and non-volatile metabolites, respectively, in an untargeted approach, while the sensory evaluation of the wines was performed by a trained panel. Wine volatile and non-volatile metabolites modulation was independently evaluated by means of partial least squares discriminant analysis (PLS-DA), obtaining potential markers of the fermentation strategies. Then, the complete metabolome was integrated by means of sparse generalised canonical correlation analysis discriminant analysis (sGCC-DA). This integrative approach revealed a high link between the volatile and non-volatile data, and additional potential metabolite markers of the fermentation strategies were found. Subsequently, the evaluation of the contribution of metabolome to the sensory characteristics of wines was carried out. First, the all-relevant metabolites affected by the different fermentation processes were selected using PLS-DA and random forest (RF). Each set of volatile and non-volatile metabolites selected was then related to the sensory attributes of the wines by means of partial least squares regression (PLSR). Finally, the relationships among the three datasets were complementary evaluated using regularised generalised canonical correlation analysis (RGCCA), revealing new correlations among metabolites and sensory data.

Keywords: data-integration; untargeted; multivariate analysis; metabolomics; chemometrics; rosé wines; yeasts; sequential inoculation

Citation: Muñoz-Redondo, J.M.; Puertas, B.; Pereira-Caro, G.; Ordóñez-Díaz, J.L.; Ruiz-Moreno, M.J.; Cantos-Villar, E.; Moreno-Rojas, J.M. A Statistical Workflow to Evaluate the Modulation of Wine Metabolome and Its Contribution to the Sensory Attributes. *Fermentation* **2021**, *7*, 72. https://doi.org/10.3390/fermentation7020072

Academic Editor: Sergi Maicas

Received: 23 March 2021
Accepted: 30 April 2021
Published: 5 May 2021

1. Introduction

Wine quality perception by consumers is a complex concept involving a sensory experience and consumers' expectation [1]. The sensory experience in wine tasting is related to its organoleptic attributes, such as aroma, taste and mouthfeel, which are further linked to its chemical composition [1,2]. In recent years, the advent of robust and high-throughput analytical techniques such as gas chromatography–mass spectrometry (GC-MS) and liquid chromatography–mass spectrometry (LC-MS) has prompted the study of the metabolic profile of foods and beverages. In this sense, untargeted strategies, that aim to simultaneously measure as many compounds as possible present in samples [3], have been successfully used to untangling the wine metabolome in the last few years [4–9]. However,

the data generated by these analytical platforms are complex, with multi-scale (different orders of magnitude) and multivariate (different chemical substances) properties [10], requiring the use of proper statistical methodologies to correctly process and extract the relevant information.

The complete workflow in metabolomics studies to extract the biological information from the raw files generated by the high-throughput analytical techniques generally includes a pre-processing (convert the raw instrumental files into organised and tabulated file formats), pre-treatment (refinement of the pre-processed data for posterior data analysis) and statistical analysis of the data (application of appropriate algorithms to find the relevant biological information) [11].

Pre-processing of GC-MS and LC-MS chromatograms must fulfil the correct identification of the mass spectrum of individual metabolites and the accurate determination of metabolites abundance in each sample, being challenging due to coelution of analytes within single chromatographic peaks and retention time shifts between samples [12]. For this reason, several bioinformatics tools such as PARAFAC2, AMDIS, ChromaTOF, eRah, XCMS, MS-Dial, MZmine 2, MarkerView, or Compound Discoverer among others have been developed to automatically pre-process chromatographic data. For GC-MS data, the so-called PARAllel FACtor analysis2 (PARAFAC2) algorithm [13] demonstrated to successfully handle complex situations with coelutions, low signal-to-noise (S/N) ratio and retention time shifted chromatographic peaks, with the advantage that only the number of components of the model in a selected region of the chromatogram is required to be set, diminishing the risk of modelling problems [12]. Meanwhile, for pre-processing of LC-MS data, the XCMS framework implementing the feature detection algorithm *centWave*, the time alignment algorithm *OBI-warp,* and the grouping of features across samples algorithm *group.density* [14], has yielded better metabolite identification abilities than other widely-used similar methods, while keeping a high quantification performance [3].

During the pre-treatment step, the pre-processed data are filtered, cleaned, drift corrected, missing value imputed, normalized, transformed and/or scaled [15] with the aim to make it adequate for the subsequent statistical analysis.

Finally, statistical analyses are performed on the data to discover the relevant biological information. Different computational and statistical methods have been developed for this task, comprising unsupervised and supervised analysis [11]. In metabolomics studies, unsupervised analyses are fundamentally used to explore and unravel the structure of the data, aiming at detecting sample clusters or systematic trends and errors. One of the most popular and powerful unsupervised statistics used in metabolomics studies is principal component analysis (PCA), based on dimensionality reduction [16]. Meanwhile, supervised learning methods are used for classification, prediction and biomarker discovering, dealing with datasets that have response variables either continuous (regression problems) or discrete (classification problems) [16]. Partial least squares (PLS) and its discriminant extension PLS-DA are one of the most popular methods used for regression and classification problems, respectively, in metabolomics studies due to its high performance and easy interpretation [17]. These models are useful when the data are acquired from the same omics platform (i.e., LC-MS or GC-MS or nuclear magnetic resonance (NMR), etc.), since simple concatenation of different omics data ignores their heterogeneity and a single type of omics is mainly highlighted [18]. However, metabolomics studies usually involve measurements from different omics platforms that may contain latent biological relationships and the independent assessment of each biological domain may not reveal that information. To overcome this, several frameworks implementing multi-omics data integration have emerged [19], including the unsupervised regularised generalised canonical analysis (RGCCA) and its sparse discriminant version sGCC-DA (DIABLO), which are useful multiblock methods to study the relationships between blocks of data measured in different platforms and to identify the main subsets of variables involved in those relationships [18].

The aim of this study was to establish a data processing and statistical analysis pipeline to (1) evaluate the impact of different elaboration processes on the metabolome of wines, acquired by means of two high throughput analytical platforms in an untargeted approach: GC-MS (volatile metabolites) and LC-MS (non-volatile metabolites), and to (2) relate those changes with their sensory descriptors. An optimal pre-treatment and pre-processing of the data generated from both analytical platforms was proposed to ensure its quality. Variable selection procedures were used to reveal the metabolites more impacted by the different wine elaboration processes. Each single omics data set and the sensory data were independently assessed by means of univariate and multivariate statistical analyses to study the impact of the wine elaboration process. The relationships between each single analytical platform and the sensory descriptors were evaluated by means of partial least squares regression (PLSR) models. Finally, the data obtained from the three sources were treated as a whole by means of data integration models to reveal hidden correlations.

2. Materials and Methods

2.1. Wine Samples

The red grape varieties *Vitis vinifera* L. cv. Garnacha and L. cv. Cabernet Sauvignon were used to elaborate rosé wines with three fermentation strategies (classes of the factorial design). Both grapes were picked at optimum ripeness, destemmed, and crushed. The maceration process was performed for 24 h with the addition of 40 mg/L of sulphur dioxide (SO_2) (Enartis, La Rioja, Spain). During the maceration tank filling the enzymes (Enartiszym Arom MP, Enartis, La Rioja, Spain) were added according to the supplier's recommendations (3 g/100 kg). The resulting musts were softly pressed homogenized and dejuiced at 4 °C for 24 h with the addition of 2.5 mL/hL of pectolytic enzymes (EnartisZym Blanco L, Enartis, La Rioja, Spain). At the beginning of the monoculture fermentation the *Saccharomyces cerevisiae* yeasts (Red Fruit, Enartis, La Rioja, Spain) were added at 25 g/hL, while in the sequential inoculations the *non-Sc* yeasts (*Torulaspora delbrueckii* TD291 Biodiva™ and *Metschnikowia pulcherrima* MP346 Flavia®) at 25 g/hL were used as starters of the fermentation, and 1 day later *Sc* yeasts were also added at 25 g/hL. The *non-Sc* yeasts were supplied by Lallemand as activated dried yeasts (ADY). The alcoholic fermentation was carried out at 17–18 °C. To control the kinetics of the alcoholic fermentation, density and temperature were daily monitored. The alcoholic fermentation finished when residual sugar concentrations were under 2 g/L. The wines we <re racked 15 days after the final alcoholic fermentation by cold settling using 60 g/hL of bentonite (Enartis, La Rioja, Spain) and 15 mL/hL of liquid gelatin at 30% (Enartis, La Rioja, Spain). After two months of cold stabilization at 0 °C, the wines were filtered, first using CKPV 16 plates (Cordenons, Milan, Italy) and then using a membrane cartridge of 1.0, 2.0 and 0.45 µm (Millipore), and then bottled using agglomerated cork caps (Selecork model, Tapones del Sur, Jerez de la Frontera, Spain).

2.2. Analysis, Data Acquisition and Processing of Headspace Solid-Phase Microextraction Coupled with Gas Chromatography-Mass Spectrometry (HS-SPME-GC-MS) Data

The volatile metabolome of the wines was determined using headspace solid-phase microextraction coupled with gas chromatography-mass spectrometry (HS-SPME-GC-MS). Samples of 15 mL were diluted 1:1 with EDTA solution (200 mM and pH 7.0 adjusted with NaOH 1.0 M) and 10 mL of this dilution were transferred to a 20 mL SPME vial closed with a 18mm magnetic PTFE/Sil headspace cap after the addition of 3.5 mg of NaCl. The samples processed were then homogenized in a vortex shaker for 30 s and placed in the autosampler tray (CTC Analytics, Zwingen, Switzerland). The fibre used for the HS-SPME was DVB/CAR/PDMS (1 cm, StableFlex/SS) supplied by Supelco (Bellefonte, PA, USA). The vials were incubated at 500 r.p.m for 2 min at 40 °C. The volatile fraction was extracted at 40 °C for 38 min followed by the desorption at 250 °C for 15 min into a Trace GC ultragas chromatograph (Thermo Fisher Scientific S.p.A., Rodano, Milan, Italy) coupled to an ISQ Single Quadrupole MS spectrometer (Thermo Fisher Scientific, Austin, TX, USA). Injection

was set to splitless mode for 0.75 min. GC separation was performed on a BP21 column (50 m × 0.32 mm × 0.25 µm) (SGE Analytical Science, Milton Keynes, United Kingdom). The carrier gas used was helium at a flow rate of 1.7 mL/min. The oven temperature started at 40 °C for 5 min, then raised to 220 °C at 3 °C/min and maintained for 30 min. The MS transfer line and ion source temperatures were 230 °C and 200 °C, respectively. The mass spectrometer operated in electron ionization mode at 70 eV. Mass spectra were recorded in the 50–400 m/z value range and the scanning frequency was 5 scans/s. The Thermo Xcalibur v. 2.2 software was used to control both the Combipal autosampler and GC-MS.

Raw untargeted GC-MS data from rosé wines were acquired in Xcalibur file format (.raw) and converted to the international ANDI file format (.cdf) by means of the file converter tool implemented in Xcalibur. They were then pre-processed (Figure 1) to convert the chromatograms into extracted data (tables of metabolite chromatographic areas). The raw .cdf files with a three-way array structure (elution time × mass spectra × samples) were deconvoluted by means of the PARAFAC2 algorithm. The chromatograms were first divided into 335 intervals in the elution time dimension in order to reduce the complexity and a single model was built for each interval. For each model, one to eight components were fitted and the selection of the optimal number of components was based on model fit (%), core consistency, distribution of the residuals, comparison of the resolved mass spectral profiles against the raw profiles, and retention times of the weighted elution profiles. The freely-available platform PARADISe v. 3.88 was used to implement this framework [12]. To verify the quality of the data, pooled quality control (QC) samples were repeatedly injected throughout the whole sequence. Different levels of metabolite identification confidence were categorized in accordance with the proposed minimum reporting criteria defined by the metabolomic standard initiative [20]. Two orthogonal properties: linear retention index (LRI) calculated with the equation of Van den Dool and Kratz, and fragmentation mass spectrum, were used for metabolite identification. Three levels of identification were considered. The resolved PARAFAC2 mass spectrums and linear retention index were compared against an authentic chemical standard analysed under the same experimental conditions for definitive identification (level 1). Level 2 was considered for metabolites showing a match factor (MF) > 850 and LRI ± 30 compared to the NIST database. Level 3 was considered for metabolites with 650 ≤ MF ≤ 85 a and LRI ± 30 compared to the NIST database. Since close values of MF and reverse match factor (RMF) are related to low levels of background, RMF was used to control the quality of each metabolite background subtraction.

2.3. *Analysis, Data Acquisition and Processing of Using Ultra-High-Performance Liquid Chromatography High-Resolution Mass Spectrometry (UHPLC-HRMS) Data*

The relative non-volatile metabolome of rosé wines was determined using ultra-high-performance liquid chromatography coupled to an Exactive Orbitrap mass spectrometer (UHPLC-HRMS) controlled by the Thermo Xcalibur v. 2.2 software. A total of 1 mL of each rosé wine sample was centrifuged at 15,000 rpm for 10 min at 20 °C (Eppendorf™ 5424 Microcentrifuges, Hamburg, Germany) and 200 µL of the supernatant were transferred into a 1.5 mL amber glass vial, mixed with 380 µL of acetonitrile and placed in the autosampler refrigerated at 10 °C of a Dionex Ultimate 3000 RS UHPLC system coupled to an Exactive Orbitrap mass spectrometer detector (Thermo Fisher Scientific, San Jose, CA, USA). Hydrophilic interaction separation was carried out on a 2.1 mm × 150 mm ACQUITY UPLC 1.7 µm BEH amide column, equipped with an ACQUITY UPLC BEH amide 1.7 µm van-guard pre-column (Waters, Barcelona, Spain). The temperature of the column was maintained at 40 °C and two mobile phases were used: A: acetonitrile and B: acetonitrile-water (2:98) + 1 mM ammonium formate. The injection volume was 5 µL and the separation was obtained at a flow rate of 0.4 mL/min with a 40 min gradient. The gradient started at 5% B for 4 min, raised to 28% B in 25 min, raised to 60% B in 30 min, maintained for 0.5 min before rising to 80% B in 33 min. After that, the column was equilibrated to the previous conditions within 10 min. Full scans were recorded in the *m/z* range from 100 to 1000 with a resolution of 50,000 Hz and with a full AGC target of

100,000 charges, using 2 microscans. Analyses were also based on scans with in-source collision-induced dissociation (CID) at 25.0 eV. MS experiment condition with HESI in positive ionization (separately analysed) mode was: (i) capillary temperature was 325 °C, the heater temperature was 300 °C, the sheath gas was 25 units, the auxiliary gas was 4 units, and the spray voltage was 4.0 kV. While the MS experiment condition with HESI in negative ionization (separately analysed) mode was: (i) capillary temperature was 325 °C, the heater temperature was 300 °C, the sheath gas was 20 units, the auxiliary gas was 2 units, and the spray voltage was 4.0 kV.

Raw untargeted UHPLC-ESI-MS data from rosé wines were acquired in the Xcalibur file format (.raw) and converted to the international ANDI file format (.cdf) by means of the file converter tool implemented in the Xcalibur software. Then, the data were pre-processed (Figure 1) using the R package XCMS v. 3.4.4 [21]. Peak picking, retention time correction and grouping parameters from XCMS were optimised by means of a Box-Behnken design using the R package IPO v. 1.8.1 [22]. The centWave algorithm was selected for peak picking, while the OBI-warp and density methods were used for retention time corrections and grouping, respectively. Then, the features derived from the same metabolite and annotation of the ion species were grouped with the R package CAMERA v. 1.38.1 [23]. Scripts including XCMS optimised parameter settings and CAMERA are given in the Supplementary material R scripts. Metabolite annotation was performed on the basis of the minimum reporting criteria of the four identification levels defined by the metabolomic standard initiative [20] and described in [24]. The mass-based searching tool MetaboQuest was used to find putative metabolite identities from the HMDB and METLIN databases. The results shown in Supplementary Tables S1 and S2 were compared against the feature list from the WinMet database [9] by using an automated R routine (available in the Supplementary material R scripts) that matches neutral masses of WinMet with the putative metabolites obtained in MetaboQuest and selects the candidates present in both lists. Finally, the metabolites were manually inspected and annotated for up to 5 ppm error.

2.4. Sensory Analysis

The sensory analysis of the wines was performed at IFAPA Rancho de la Merced (Jerez) by means of a tasting panel composed of 10 trained panellists between 35 and 55 years. The panellists were trained following the AENOR (UNE-EN ISO 8586:2014 and UNE 87022:1992) standards and the procedure was the same than that described in [25]. The wine description terminology agreed by consensus included 5 attributes scored in an olfactory phase (scent intensity, red fruit, black fruit, citrus fruit and tree fruit) and 6 attributes scored in a taste phase (taste intensity, acidity, alcohol, complexity, balance and persistence).

2.5. Statistical Analysis

The data from the different sources were pre-treated in different ways (Figure 1). The sensorial scores were only autoscaled before the integration approach. Meanwhile, the data from both analytical platforms were first cleaned, replacing features with non-detected single classes but detected in other classes by the minimum peak area reported in the data matrix divided by 2. Next, the data were peak filtered by removing rows (samples) or columns (features) with missing values $\geq$30% across all classes. To reduce the contribution of the experimental and analytical variability, the data were drift corrected by fitting a smoothed cubic spline onto the QC samples as described by [26]. The R function smooth.spline was used, and the smoothing parameter was set to 1 after its optimization using leave-one-out cross validation at different values of this hyperparameter. The drift correction was performed as followed (Equation (1)):

$$X_{corrected}\,(i) = X_{original}\,(i) + mean(X_{QC}) - f_{drift}(i) \quad (1)$$

where i is the injection order of each sample, $X_{corrected}$ is the corrected value of a feature, $mean(X_{QC})$ is the mean value of all the QC samples used to fit the smoothed cubic function

and f_{drift} is the smoothed cubic function. Subsequently, features with an RSD > 20 and RSD > 30 in QC samples for LC-MS and GC-MS data respectively were removed. Random forest imputation was applied to impute missing values using the R package missForest [27]. QC samples were not included in the data to ensure a proper imputation based on patterns of the real wine data. Next, data were probabilistic quotient normalised (PQN) using the median of the QC samples, since it is less sensitive to outliers than the mean [28]. Finally, GC-MS and LC-MS data were autoscaled. Throughout this pre-treatment, principal component analyses (PCA) including QCs were conducted to unravel the structure of the data and to detect systematic trends and errors.

Univariate analyses were performed on the data without autoscaling. Normality and heteroscedasticity were checked with the Shapiro–Wilk's and Levene's tests respectively, and the variables that failed the parametric assumptions were box-cox transformed. Two-way analysis of variance (ANOVA) and Tukey's honestly significant difference (HSD) post-hoc tests were then applied to identify differences in the metabolites and sensory descriptors due to the factors studied.

Partial least squares discriminant analysis (PLS-DA) was used for the selection of the most discriminative features (potential markers) and for classification tasks, which were further used for the biological interpretation. The optimization and validation of the PLS-DA models were based on a double cross-validation described by [29]. Briefly, the cross-validation consisted of two nested loops, referred to as inner and outer loops. In the former, the model was optimised using leave-one-out exhaustive cross-validation. In the latter, a 4-fold cross-validation made it possible to assess the performance of the final discriminant model. The optimization and validation of the models were based on the balanced error rate (BER) measured at the Mahalanobis distance. The significance of the PLS-DA models was obtained through the following equation (Equation (2)):

$$p\text{-}value = 1 + (HP_P \leq HP)/N \quad (2)$$

where HP is a hyperparameter: BER, number of misclassification (NMC) or the area under receiver operating characteristic curve (AUROC), and ($HP_P \leq HP$) is the number of elements in the H_0 distribution which are smaller or equal to the hyperparameter of the original data. H_0 distribution was generated by random permutation of sample labels. N = 1000 permutations were simulated, since this number was large enough to sample the distribution tails and attain a p-value up to 0.001. The BER, NMC and AUROC of the original data were calculated by averaging the values of each hyperparameter obtained from the sub-models fitted during the cross-validation. The selection of the most discriminative metabolites (potential markers) followed an iterative workflow based on variable importance in projection (VIP) described in [30]. Alternatively, the data from the three different sources was integrated using the framework DIABLO, which is the supervised extension of sparse generalized canonical correlation analysis (sGCC-DA) [18].

Partial least squares regression (PLSR) was used to predict the sensory attributes scores from the volatile and the non-volatile profile separately. Afterwards, the simultaneous integration of the three datasets was carried out by means of RGCCA implemented in the R package mixOmics [18]. To this end, the R package MUVR [31] was first used to extract the all-relevant variables from the LC-MS and GC-MS platforms, i.e., all features influenced by the studied factor (in this case the fermentation strategy) once the non-informative features were removed. A PLS-DA and random forest (RF) models were independently fitted in each single dataset using a double cross-validation scheme. The all-relevant variables from both discriminant analyses were merged to perform the PLSR and RGCCA models.

Fermentation **2021**, *7*, 72

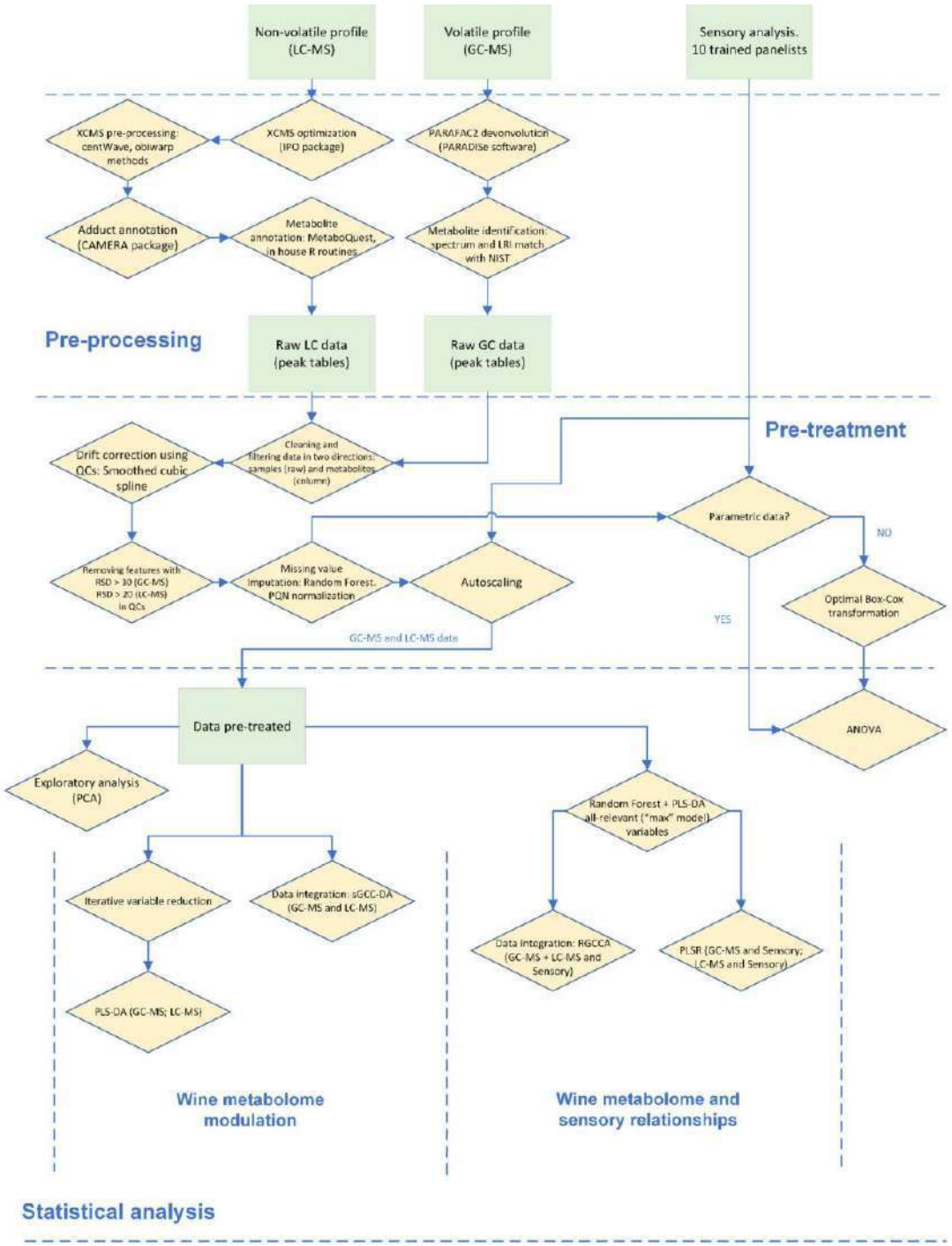

Figure 1. Flowchart illustrating the step-by-step processes followed to convert raw data into processed data to extract biological interpretations.

Fermentation **2021**, *7*, 72

3. Results

3.1. Volatile Profile

Prior to GC-MS injection of the real samples, pooled QCs were used to optimize the dilution factor and the extraction fibre employed. Dilution ratios of 1:1, 1:2, 1:4 and non-dilution were tested in three different fibres, which covered a vast range of polarities, such as PDMS, CAR/PDMS and DVB/CAR/PDMS. The combination of the DVB/CAR/PDMS fibre and non-dilution yielded the best results in terms of total chromatographic peak signal (sensitivity). However, the DVB/CAR/PDMS fibre and 1:1 dilution ratio were selected, since 10% more features could be detected with low deviation coefficients (20% RSD), improving stability. Subsequently, the real rosé wine samples were analysed with the optimised methodology. PARAllel FACtor analysis2 (PARAFAC2) deconvolution algorithm [13] was used to pre-process the converted data, with a total of 505 molecular features assigned to detected peaks. After the pre-treatment step, 429 features remained in the data set, among which 126 were definitive—or putatively identified (Supplementary Table S3). PCAs including QC samples were used during data pre-treatment to check the quality of the data (Figure 2). The quality of the raw data (before pre-treatment) was quite satisfactory, since QCs were allocated in a narrow region and samples were grouped according to the fermentation strategy. However, the pre-treatment workflow proposed in this study led to a slight improvement of the final data, with QCs and samples belonging to the same fermentation strategy being allocated in closer areas.

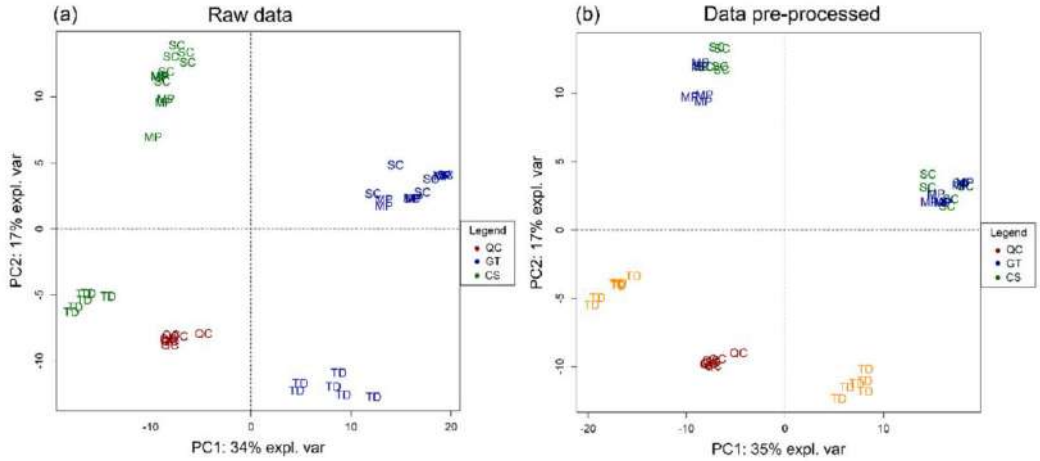

Figure 2. Principal component analysis (PCA) performed for the gas chromatography (GC) data during pre-treatment. (**a**) Raw data and (**b**) pre-treated data. Quality control samples (QCs) are included to verify the quality of the data. *TD*: wines fermented with sequential inoculation of *Torulaspora delbrueckii* and *Saccharomyces cerevisiae*. *MP*: wines fermented with sequential inoculation of *Metchnikovia pulcherrima* and *Saccharomyces cerevisiae*. *SC*: wines fermented with monoculture of *Saccharomyces cerevisiae*.

Afterwards, a two-way ANOVA (Supplementary Table S3) was performed to study the effect of the fermentation strategy, that impacted to different chemical groups, especially esters, alcohols and terpenes, independently of the grape variety of the wine (Supplementary Table S3). Rosé wines that followed a sequential inoculation with the Flavia *Metschnikowia pulcherrima* yeasts (*Sc-Mp*) showed statistically significant differences compared with those fermented with the monoculture Red Fruit *Saccharomyces cerevisiae* yeasts (*Sc*). However, the sequential inoculation with Biodiva *Torulaspora delbrueckii* yeasts (*Sc-Td*) produced rosé wines with the most distinct volatile profile, with overall lower contents of esters and aldehydes, but an increase in several alcohols and terpenes (Supplementary Table S3). Subsequently, the main wine volatile metabolites linked to the fermentation strategy were

Fermentation **2021**, *7*, 72

selected by means of a variable reduction procedure based on variable importance in projection (VIP) from the PLS-DA model. These metabolites were considered as potential markers of the fermentation strategy and a new model was fitted using the reduced data. The performance of the PLS-DA including the potential volatile markers displayed a mean overall BER of 0.08 ± 0.06 and *p*-values from the permutation test below 0.05 in the three diagnostic statistics (Table 1). This resulted in a slight improvement compared to the model fitted with all the variables (BER of 0.11 ± 0.08), and the complexity of the model was reduced from 3 to 2 components. The X-variate 1 explained a high 65% of the total variance found in the rosé wine samples, that separated the *Sc-Td* wines from the rest (Figure 3). This result supported the more distinct volatile profile of *Sc-Td* wines previously observed in the ANOVA. Considering the annotated compounds, 3-ethoxy-1-propanol, ethyl decanoate, 1-dodecanol, methyl 4-decenoate, (E)-nerolidol and ethyl 2-methylpropanoate (ethyl isobutyrate) were selected as the most discriminative metabolites of this fermentation strategy by displaying higher overall content. Meanwhile, *Sc* and *Sc-Mp* wines were separated in X-variate 2, that explained the 20% of the total variance of the samples (Figure 3). The volatile metabolites involved in such differentiation were pentyl-cyclopropane, isopentyl hexanoate and ethyl heptanoate, found in overall higher concentrations in *Sc-Mp* wines, and 3-isopropyl-1-pentanol (3-ethyl-4-methylpentanol), ethyl trans-3-hexenoate, (E,E)-farnesol and 3-furaldehyde, that were found in higher contents in *Sc* wines.

Table 1. Model performance of the partial least squares discriminant analysis (PLS-DA) models built to discriminate yeast fermentation strategy and grape variety used to elaborate the rosé wine samples.

Analytical Platform	Model	Mean Overall BER [1]	Ncomp	Class	Mean Class Error [2]	*p*-Value [3]
GC-MS	Allvariables	0.11 ± 0.08	3	*Sc-Td*	0.01 ± 0.03	BER: <0.001
				Sc-Mp	0.15 ± 0.16	NMC: 0.024
				Sc	0.18 ± 0.17	AUROC: 0.020
GC-MS	Variable reduction	0.08 ± 0.06	2	*Sc-Td*	0.00 ± 0.00	BER: <0.001
				Sc-Mp	0.12 ± 0.11	NMC: 0.007
				Sc	0.14 ± 0.11	AUROC: 0.003
LC-MS	Allvariables	0.17 ± 0.10	4	*Sc-Td*	0.14 ± 0.09	BER: <0.001
				Sc-Mp	0.07 ± 0.13	NMC: 0.120
				Sc	0.29 ± 0.21	AUROC: 0.035
LC-MS	Variable reduction	0.02 ± 0.04	2	*Sc-Td*	0.00 ± 0.00	BER: <0.001
				Sc-Mp	0.05 ± 0.11	NMC: 0.027
				Sc	0.00 ± 0.02	AUROC: 0.002

[1] Mean overall balanced error rate (BER) values with the standard deviation calculated on the basis of 200 PLS-DA sub-models in a double-cross validation scheme. [2] Mean class error values with the standard deviation calculated on the basis of 200 PLS-DA sub-models in a double-cross validation scheme. [3] Model statistical significance was calculated on the basis of a permutation test (N = 1000) using the mean overall BER, number of misclassifications (NMC) and the area under receiver operating characteristic curve (AUROC) as diagnostic statistics. Statistically significant models (p-value ≤ 0.05) were highlighted in bold. *Sc-Td*: wines fermented with sequential inoculation of *Torulaspora delbrueckii* and *Saccharomyces cerevisiae*. *Sc-Mp*: wines fermented with sequential inoculation of *Metchnikovia pulcherrima* and *Saccharomyces cerevisiae*. *Sc*: wines fermented with monoculture of *Saccharomyces cerevisiae*.

Fermentation **2021**, *7*, 72

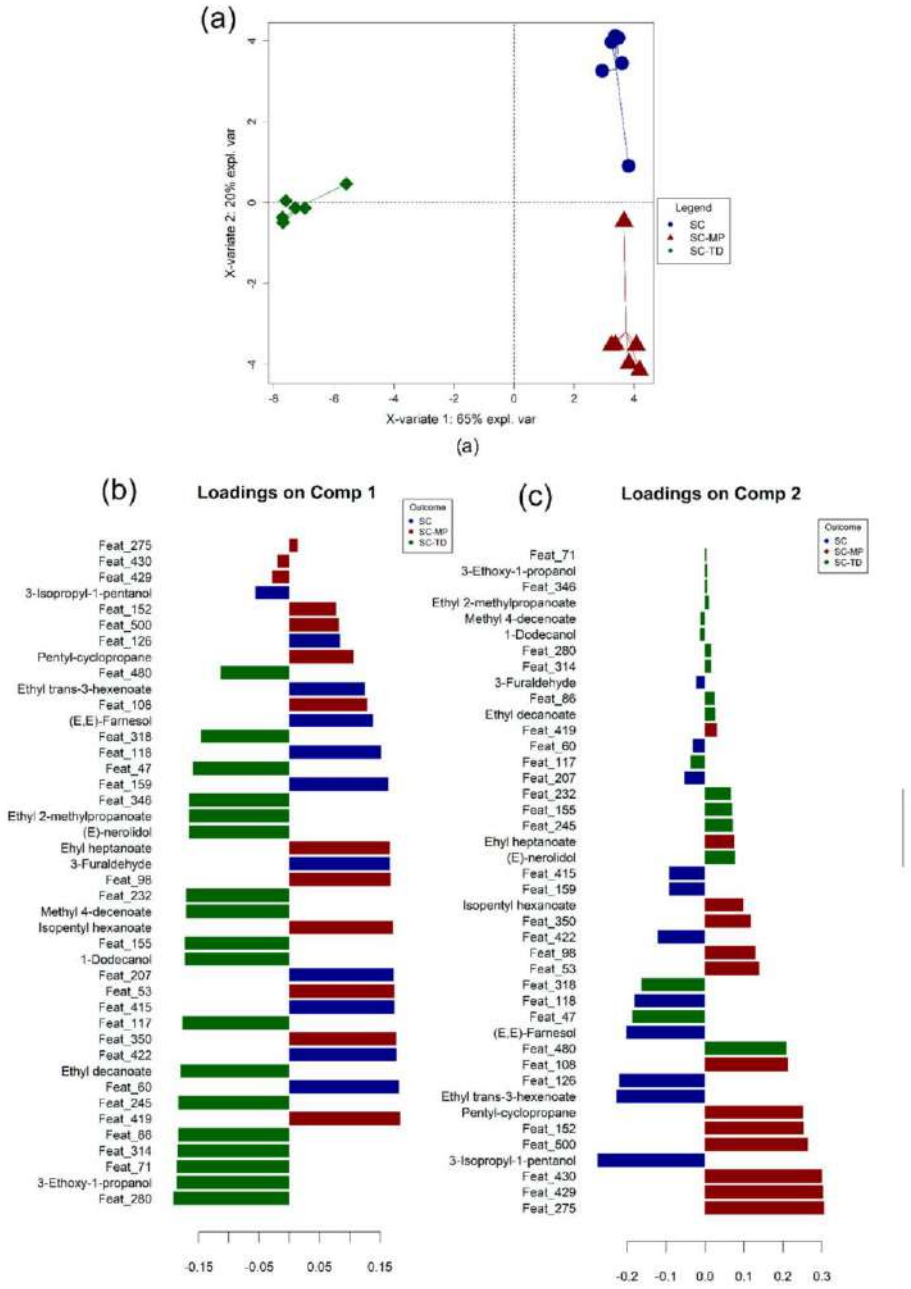

Figure 3. Graphical outputs of the partial least squares discriminant analysis (PLS-DA) performed to classify rosé wines according to the fermentation strategy on the basis of their volatile profile. (**a**) Scores plot for the components 1 and 2; (**b**) and (**c**) loading contribution barplot on components 1 and 2. Colour indicates the class for which the compound has a maximal mean value. Bar length represents the multivariate regression coefficient with either a positive or negative sign for that particular feature of each component, i.e., the importance of each variable in the model. *Sc-Td*: wines fermented with sequential inoculation of *Torulaspora delbrueckii* and *Saccharomyces cerevisiae*. *Sc-Mp*: wines fermented with sequential inoculation of *Metchnikovia pulcherrima* and *Saccharomyces cerevisiae*. *Sc*: wines fermented with monoculture of *Saccharomyces cerevisiae*.

3.2. Non-Volatile Profile

The optimization of the dilution procedure for the wine samples was achieved using pooled QC samples. Direct injection and dilution ratios of 1:1, 1:2 and 1:5 were tested. Samples were analysed and processed to extract the features, and two parameters were considered to select the best dilution conditions: total sum area (response) and number of features with RSD <30 (stability). The dilution of the samples yielded a reduction in the response but increased the stability of the features. In positive ionization mode, the compounds were most stable at a dilution ratio of 1:2, which captured close to 2-fold more compounds with RSD <30 than direct injection. Meanwhile, in negative ionization mode, the dilution ratio of 1:5 displayed slightly better results than 1:2 in terms of response. However, this dilution ratio was discarded due to loss of sensitivity (around 50% compared to 1:2). Therefore, the best consensus in terms of sensitivity and stability was obtained for a dilution ratio of 1:2, which was used for the analysis of the real samples. Respective totals of 1801 and 4275 features for positive and negative ionization modes were obtained after XCMS pre-processing, and 1167 and 1701 features remained respectively after data pre-treatment step. PCAs including QC samples were again used during the pre-treatment process to verify the quality of the data (Figures 4 and 5 for negative and positive ESI modes, respectively). Data acquired in negative ESI mode displayed an important batch effect which was highlighted by the QC samples, and after data pre-treatment this effect was successfully eliminated (Figure 4). Although a batch effect was not observed in positive ionization mode, an improvement in the final quality of the data was also achieved after the pre-treatment process, since QCs and samples were grouped closer and better separated (Figure 5).

As for the volatile data, ANOVA and PLS-DA models were used to disclose the relevant biological information contained in the data. The ANOVA showed clear differences in the non-volatile profile of the rosé wines due to the fermentation strategy regardless of the grape variety, with amino acids and organic acids being the most impacted compound families (Supplementary Table S4). The variable reduction procedure allowed us to obtain a PLS-DA with improved classification performance compared to the model fitted with all the metabolites, displaying a BER of 0.02 $\pm$ 0.04 and p-values from the permutation test below 0.05 using the three diagnostic statistics (Table 1). A total of 38 metabolites were selected as markers and the model was optimized for two components accounting for 88% of the total variance found in the samples, which were clearly grouped according to the fermentation strategy (Figure 6). As found for the volatile profile, *Sc-Td* wines displayed the most distinct non-volatile profile, since these wines were separated from the rest on component 1 (X-variate 1), that explained the 71% of the total variance of samples. Among the annotated compounds, glutamic acid and D-mannitol/dulcitol were selected as potential markers of the fermentation strategy, displaying higher overall concentrations in *Sc-Td* wines (Figure 6). Meanwhile the variance explained in component 2 made it possible to differentiate *Sc-Mp* from *Sc* wines, being the non-volatile metabolites quinic acid and imidazole acetic acid selected as potential markers of *Sc-Mp* wines (Figure 6).

Fermentation **2021**, *7*, 72

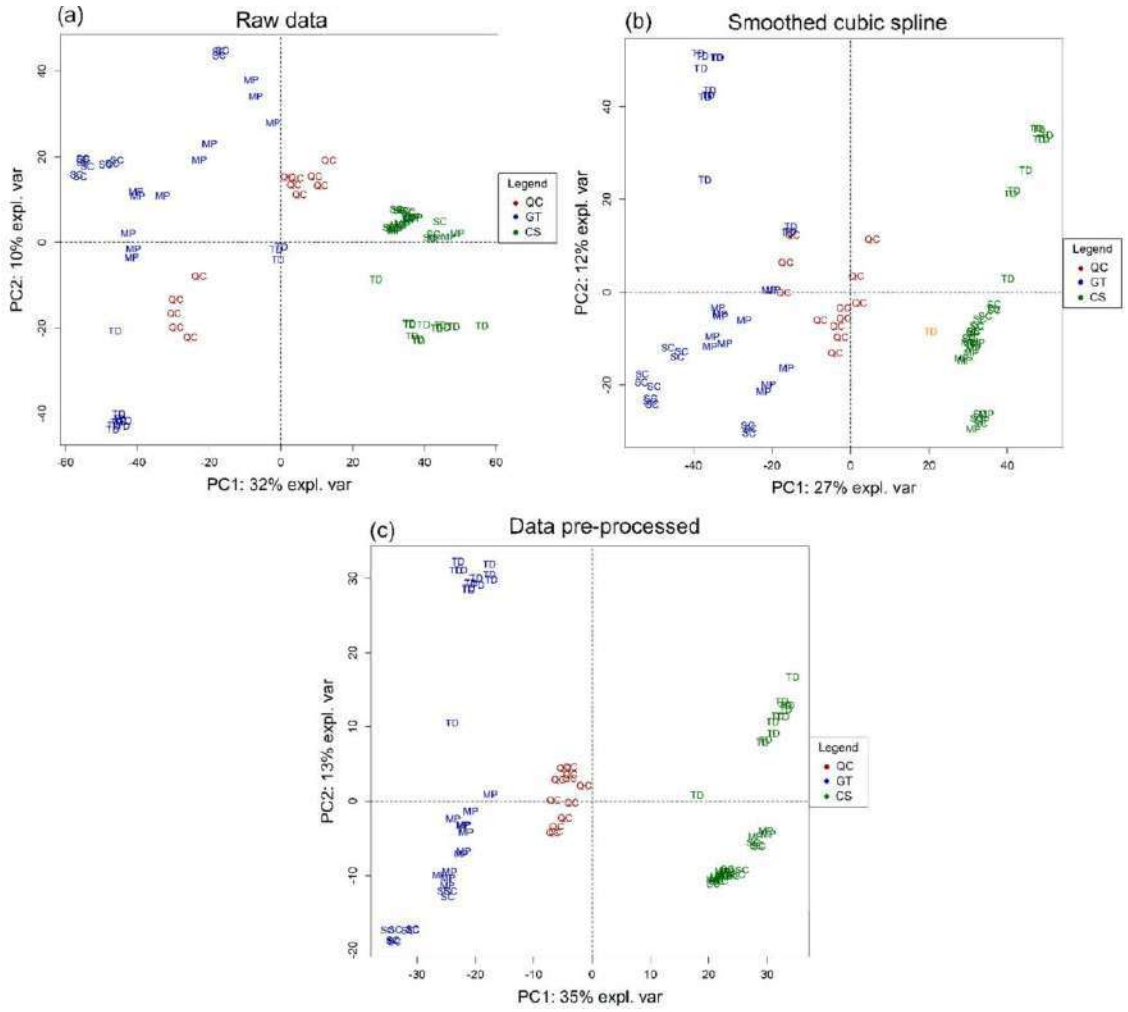

Figure 4. Principal component analysis (PCA) performed for the liquid chromatography (LC) negative ESI mode data during pre-treatment. (**a**) Raw data, (**b**) after smoothed cubic spline and (**c**) pre-treated data. Quality control samples (QCs) are included to verify the quality of the data. *TD*: wines fermented with sequential inoculation of *Torulaspora delbrueckii* and *Saccharomyces cerevisiae*. *MP*: wines fermented with sequential inoculation of *Metchnikovia pulcherrima* and *Saccharomyces cerevisiae*. *SC*: wines fermented with monoculture of *Saccharomyces cerevisiae*.

Fermentation **2021**, *7*, 72

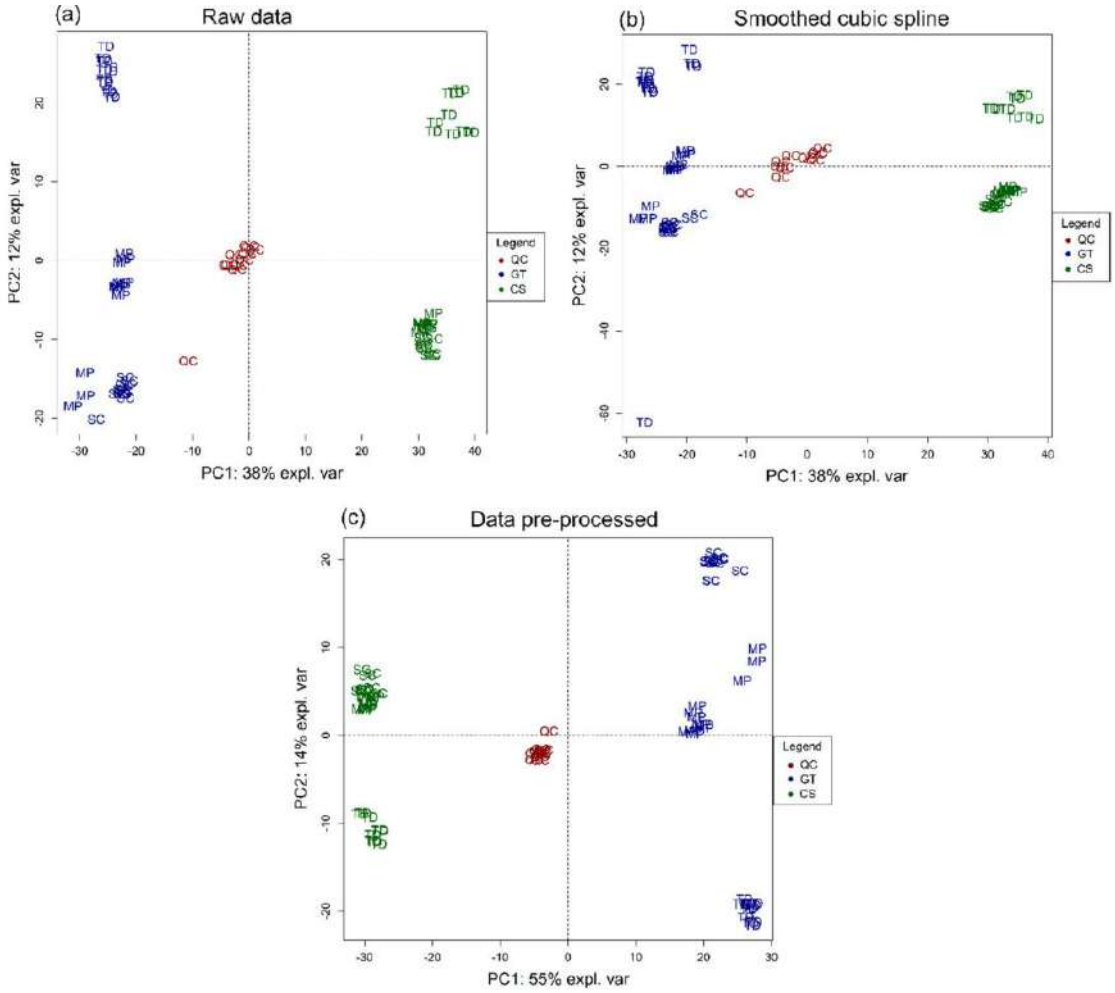

Figure 5. Principal component analysis (PCA) performed for the LC positive ESI mode data during pre-treatment. (**a**) Raw data, (**b**) after smoothed cubic spline and (**c**) pre-treated data. Quality control samples (QCs) are included to verify the quality of the data. *TD*: wines fermented with sequential inoculation of *Torulaspora delbrueckii* and *Saccharomyces cerevisiae*. *MP*: wines fermented with sequential inoculation of *Metchnikovia pulcherrima* and *Saccharomyces cerevisiae*. *SC*: wines fermented with monoculture of *Saccharomyces cerevisiae*.

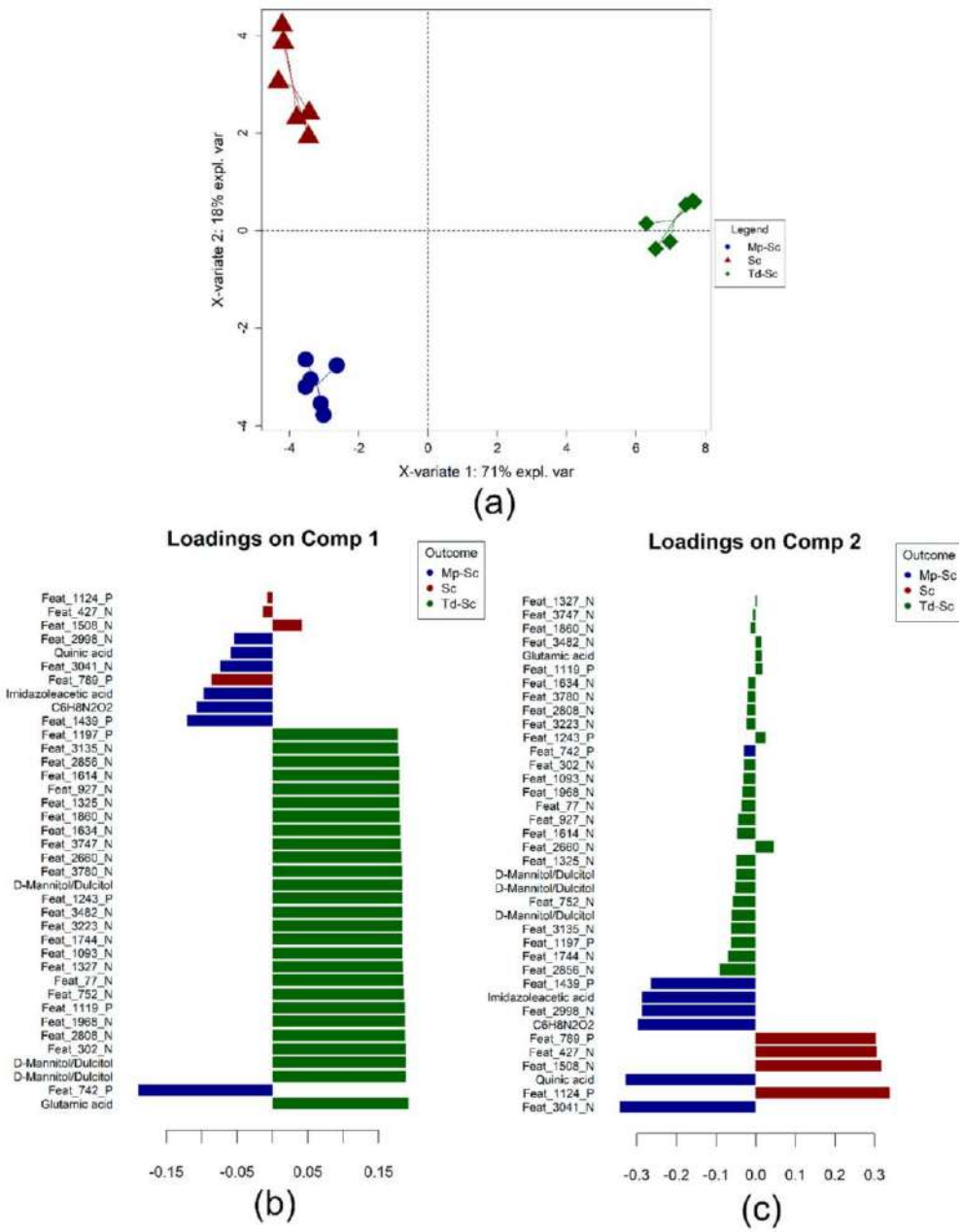

Figure 6. Graphical outputs of the partial least squares discriminant analysis (PLS-DA) performed to classify rosé wines according to the fermentation strategy on the basis of their non-volatile profile. (**a**) Scores plot for the components 1 and 2; (**b**,**c**) loading contribution barplot on components 1 and 2. Colour indicates the class for which the compound has a maximal mean value. Bar length represents the multivariate regression coefficient with either a positive or negative sign for that particular feature of each component, i.e., the importance of each variable in the model. *Sc-Td*: wines fermented with sequential inoculation of *Torulaspora delbrueckii* and *Saccharomyces cerevisiae*. *Sc-Mp*: wines fermented with sequential inoculation of *Metchnikovia pulcherrima* and *Saccharomyces cerevisiae*. *Sc*: wines fermented with monoculture of *Saccharomyces cerevisiae*.

3.3. Sensory Attributes

The impact of the fermentation strategy on the sensory attributes of wines was assessed by means of a two-way ANOVA. All the sensory attributes except taste intensity were affected by the fermentation strategy (Table 2). Overall higher scores were assigned to *Sc* and *Sc-Mp* wines regarding scent intensity, red fruit, black fruit, citrus fruit, tree fruit, acidity, alcohol and complexity. In addition, *Sc* wines displayed the highest scores in balance, followed by *Sc-Mp* wines. Persistence was the only sensory descriptor with the highest score in *Sc-Td* wines (Table 2).

Table 2. Two-way analysis of variance (ANOVA) performed on the sensory scores of the rosé wines from different fermentation strategies and grape varieties.

Sensory Descriptor	*Sc-Td* [1]	*Sc-Mp* [2]	*Sc* [3]	*p*-Value [4]	CS [5]	GT [6]	*p*-Value	Interactions (*p*-Value)
Scent intensity	6.0b	6.2ab	6.6a	*	6.4	6.1	ns	***
Red fruit	1.35b	1.97a	2.01a	***	1.90	1.66	ns	ns
Black fruit	1.47b	1.99a	2.03a	*	2.95a	0.71b	***	***
Citrus fruit	0.86b	1.65a	1.84a	***	1.00b	1.90a	***	***
Tree fruit	1.10b	1.78a	2.12a	***	1.58	1.75	ns	**
Taste intensity	5.8	5.5	5.6	ns	5.9a	5.4b	**	ns
Acidity	4.5b	4.9a	5.0a	**	4.6b	5.0a	*	ns
Alcohol	4.7b	5.0a	4.9a	**	4.8	4.9	ns	ns
Complexity	4.1b	4.6a	4.7a	***	4.6a	4.3b	*	ns
Balance	4.1c	5.0b	5.7a	***	4.5b	5.3a	***	**
Persistence	5.1a	4.2b	4.3b	***	4.7	4.4	ns	*

[1] Sc-Td: wines fermented with sequential inoculation of *Torulaspora delbrueckii* and *Saccharomyces cerevisiae*. [2] Sc-Mp: wines fermented with sequential inoculation of *Metchnikovia pulcherrima* and *Saccharomyces cerevisiae*. [3] Sc: wines fermented with monoculture of *Saccharomyces cerevisiae*. [4] *p*-value from the two-way ANOVA. ns: not significant, * : 0.05 > *p*-value > 0.01, ** : 0.01 > *p*-value > 0.001, and *** : *p*-value < 0.001. Mean values with different letters differ significantly. [5] CS: Cabernet sauvignon. [6] GT: Garnacha Tinta.

3.4. Data Integration: Sparse Generalised Canonical Correlation Analysis Discriminant Analysis (sGCC-DA) Approach

To look for the most important metabolites and sensory descriptors linked to the wine fermentation strategy, sparse generalized canonical correlation discriminant analysis (DIABLO) was also performed integrating the three datasets. This multi-block data analysis framework maximises the covariance between the data from the different analytical platforms and identifies the multi-omics signature that better discriminates the target outputs [18]. A consensus between maximising the correlation of datasets and the discrimination was adopted by setting the connection of blocks to a link of 0.7 [18]. The sGCC-DA model was optimized for three components, displaying a satisfactory error rate of 0 for both LC and GC analytical platforms and 0.222 for the sensory data. The Pearson's correlation coefficient revealed a good connection between the different blocks, with values above 0.85, being observed the highest correlations for the volatile and non-volatile metabolites blocks (Figure 7).

This approach made it possible to identify additional markers of the fermentation strategy which were not previously selected during the independent assessment of each analytical platform (Figure 8). The new potential markers selected were 1-undecanol and shikimic acid for Sc-Mp wines, which were respectively in around 9-fold and 6-fold higher concentrations compared to the Sc-Td wines, and duplicated in both cases the concentrations of Sc wines (Supplementary Tables S3 and S4). Meanwhile, linalyl anthranilate, ethyl 5-hexenoate, hexyl acetate and proline betaine for were selected as potential markers for Sc wines, found in around 1.5 to 4-fold higher concentrations in comparison to Sc-Td and Sc-Mp wines (Supplementary Tables S3 and S4).

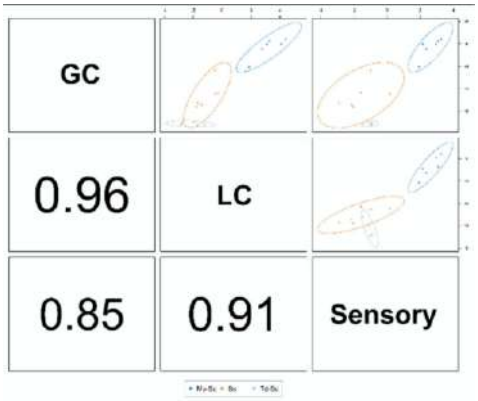

Figure 7. Pearson correlation plot obtained from the sparse generalised canonical correlation analysis discriminant analysis (sGCC-DA) model.

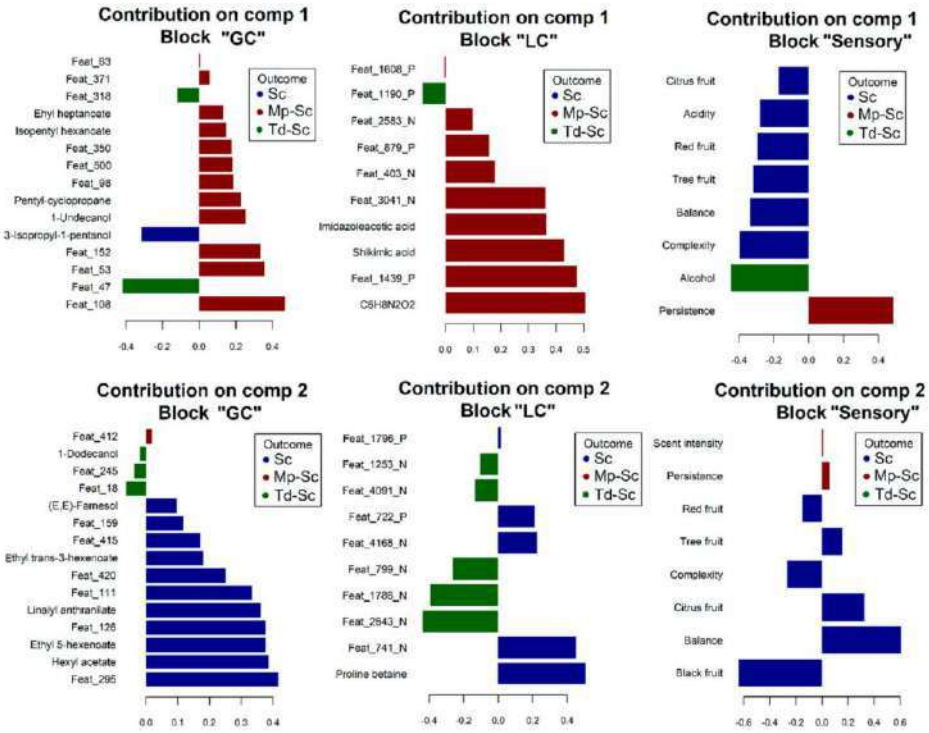

Figure 8. Loading contribution barplot on components 1 and 2 for the different blocks of the sGCC-DA. Colour indicates the class for which the compound has a maximal mean value. Bar length represents the multivariate regression coefficient with either a positive or negative sign for that particular feature of each component, i.e., the importance of each variable in the model.

3.5. Partial Least Squares (PLS) Regression

The relationships between the sensory attributes and the metabolite composition of wines was studied by means of partial least squares (PLS) regression. To that end, PLS1 and PLS2 regression was computed for each analytical platform (LC-MS and GC-MS), which were used as independent variables to predict the response of each sensory attribute

(dependent variables). The models were fitted using the all-relevant variables previously selected by means of the MUVR package implemented in R (Supplementary Figure S1). A total of 74 and 247 metabolites for GC and LC platforms were, respectively, selected as relevant, which were obtained by combining the results from a PLS-DA and random forest (RF) models. For both platforms, a better performance was observed for PLS-DA over RF to discriminate and select a major number of relevant compounds.

The root mean squares error (RMSE) and R^2 were used to optimise the number of component of the PLS models. Using PLS1 regression, the sensory descriptors balance, black fruit and citrus fruit were satisfactory predicted by the volatile and non-volatile profiles with R^2 in cross validation higher than 0.72, while good predictions of the descriptors complexity and tree fruit were also obtained using the non-volatile data (Supplementary Figures S2 and S3).

To study the correlation between the sensory data and the volatile profile, PLS2 regression was subsequently performed. The model fitted with the volatile and sensory data was optimised for two components, which explained a 66% of the total variance found in the X matrix. In Supplementary Figure S4, the correlation loadings plot from the PLS2 highlights the contribution of each variable to each component. Greater distances from the origin implies stronger correlations. Thus, variables falling within the inner circumference displayed light associations. In addition, if variables are represented as vectors sourcing from the origin, acute angles between vectors of two variables indicate positive correlations, while obtuse angles indicate negative correlations. The sensory attributes balance, citrus fruit, acidity, tree fruit and alcohol were highly correlated with 3-isopropyl-1-pentanol. Meanwhile, red fruit, complexity and black fruit were positively correlated with 3-methylpentanol, methyl 4-decenoate, 3-ethoxy-1-propanol, (E)-nerolidol, ethyl decanoate, ethyl 2-methylpropanoate, trans-3-hexen-1-ol and 1-dodecanol. Finally, positive correlations were observed between the sensory descriptor persistence and isopentyl hexanoate, ethyl heptanoate and pentyl cyclopropane. Only two sensory descriptors were poorly correlated with the volatile profile data (taste intensity and scent intensity). Only scent intensity fell within the inner circumference, meaning weak correlations of this descriptor with the volatile data. For the LC-MS data, a PLS regression was optimized for 2 components, which explained 80% of the total variance in the X matrix. The sensory attributes balance, citrus fruit, acidity and alcohol were slightly and positively correlated with several amino acids (alanine, glutamic acid, 2-Phenylglycine, L-Alanine, N-propyl-/L-Alloisoleucine/L-Isoleucine/L-norleucine, L-leucyl-L-proline, N-acetyl-L-ornithine, N-acetylproline, phenylalanine, proline betaine and suberylglycine). Meanwhile, persistence, taste intensity and to a lower extent black fruit displayed light positive correlation with cycloleucine, uracil and two organic acids (imidazole acetic acid and shikimic acid). The remaining sensory descriptors were placed within the inner circumference, being again the scent intensity descriptor in this area.

3.6. Data Integration: Regularised Generalised Canonical Correlation Analysis (RGCCA) Approach

Once the relationships between the sensory attributes and the metabolite composition of wines were independently assessed (GC-sensory and LC-sensory), regularized generalized canonical correlation analysis (RGCCA) was performed to integrate the three datasets. The connection of the three blocks was set to a link of 1 to maximise their correlations. As stated in the previous section, a total of 74 and 247 metabolites for GC and LC platforms were, respectively, selected as relevant and were used to built the RGCCA model. Using this approach, all the sensory attributes fell between the two circumferences of the correlation circle plot, showing important correlations with several metabolites (Figure 9). As stated in the PLSR models, citrus fruit, balance, acidity, tree fruit and alcohol descriptors were highly correlated with 3-isopropyl-1-pentanol (A5). In addition, other compounds such as ethyl 5-hexenoate (E3), hexyl acetate (E7), linalyl anthranilate (T3), proline betaine (AA11) and alanine (AA2) were found to be also related with these sensory descriptors. In this approach, scent intensity was allocated between the two circumferences,

showing correlations with 2-pyrimidine acetic acid (OA1), 2-phenylglycine (AA4) and trans-3-hexen-1-ol (A7), as well as with complexity, black fruit, red fruit and taste intensity. Meanwhile, the sensory descriptor persistence was negatively correlated with most of the sensory descriptors and positively correlated with imidazole acetic acid (OA4), L-alanine, N-propyl-/L-alloisoleucine/L-isoleucine/L-norleucine (OA6), uracil (M2), 1-undecanol (A3), isopentyl hexanoate (E8), ethyl heptanoate (E1), pentyl-cyclopropane (M1), 1-nonanol (A2) and ethyl hexanoate (E5). The rest of volatile and non-volatile metabolites were allocated within the inner circumference and therefore, no correlations were established.

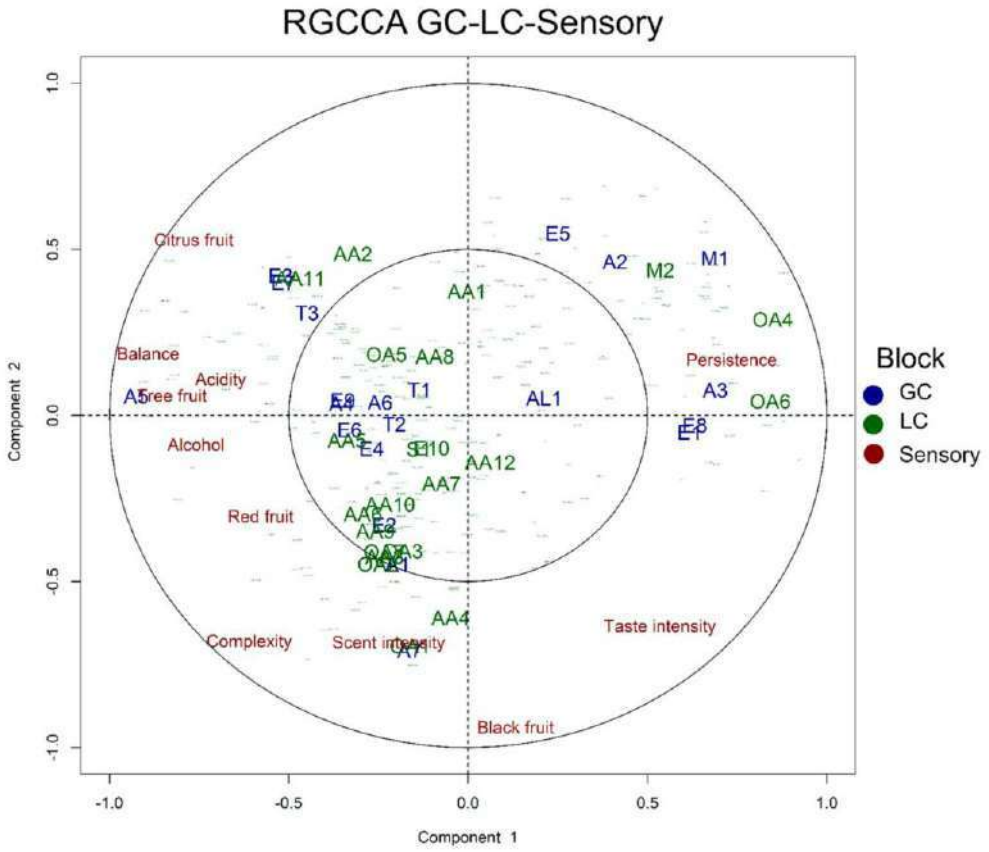

Figure 9. Circle correlation plot from the regularised generalised canonical correlation analysis (RGCCA) performed on the volatile, non-volatile and sensory data. A: alcohol, E: ester, M: miscellaneous, AA: amino acid, OA: organic acid.

4. Discussion

The pre-processing and data pre-treatment workflow proposed in this study for the volatile and non-volatile profile made it possible to extract the signal of a large number of metabolites with low deviation coefficients. The use of automatic pre-processing softwares (IPO-XCMS-CAMERA for LC-MS data and PARAFADISe implementing PARAFAC2 for GC-MS data) with low number of parameters required to be set, diminished the risk of modelling problems. The pre-treatment step included cleaning and filtering of the data (samples and metabolites), drift corrections based on QCs, removing molecular features with high RSD, missing value imputation, PQN normalization and autoscaling, and the quality of the data was checked by means of different PCAs (Figures 2, 4 and 5). The proposed workflow allowed us to adequate the data for the subsequent statistical analyses. The use of quality control samples (QCs) analysed along the analytical sequences, combined

with PCA was demonstrated to be a strong tool to verify the quality of the final data. In our case, this methodology was especially useful for the non-volatile data since higher variability in those data was observed (Figures 4 and 5). In particular, LC-MS data acquired in negative ionization mode suffered of an important drift that was revealed by two well separated clusters of QCs in the PCA (Figure 4). On this basis, we recommend the systematic use of QCs for metabolomics studies to both verify the quality of the data and to correct for drifts or batch effects.

The independent (PLS-DA and PLSR) and integrative (sGCCA-DA and RGCCA) statistical analysis led to complementary results of modulation of the wine metabolome and the relationships with their sensory descriptors, obtaining robust potential markers of the fermentation strategy which had important contribution on the sensory characteristics of the wines. To study the link between wine metabolome and sensory descriptors, a previous selection of the all-relevant metabolites involved in the fermentation strategy was performed by means of PLS-DA and RF. This methodology reduced the complexity of the final PLSR and RGCCA models by focusing on the compounds that were modulated by yeasts, making it easier the interpretation.

Interestingly, the markers selected from the sGCCA-DA approach were highly correlated with the sensory descriptors. Several metabolites such as 3-isopropyl-1-pentanol, isopentyl hexanoate, ethyl heptanoate, pentyl-cyclopropane, ethyl trans-3-hexenoate, (E,E)-farnesol, 1-dodecanol and imidazole acetic acid were selected as markers in both the independent and integrative assessments (Figures 3, 6 and 8). However, others such as 1-undecanol (A3) and shikimic acid (OA6), which were very positively correlated with persistence of the wines and to a lower extent with taste intensity, and linalyl anthranilate (T3), ethyl 5-hexenoate (E3), hexyl acetate (E7) and proline betaine (A11), highly correlated with citrus fruit, balance, acidity, tree fruit and alcohol descriptors (Figure 9), were not selected during the independent assessment. Therefore, the integration of both data sets revealed hidden biological information, supporting this approach to complement the classical independent assessment.

Several sensory descriptors displayed high correlation between predicted and observed sensory attribute scores in the PLSR1 assessment (Supplementary Figures S2 and S3), highlighting the quality of the metabolic data to make sensory predictions. The RGCCA also led to additional information hidden during the independent assessments with PLSR. While scent intensity fell within the inner circumference in the PLSR model, intermediate correlations were established with 2-pyrimidine acetic acid (OA1), 2-phenylglycine (AA4) and trans-3-hexen-1-ol (A7), complexity, black fruit, red fruit and taste intensity (Figure 9). These results highlight the potential of using PLSR in combination with RGCCA to extract subtle information that could be ignored in an independent assessment.

The results obtained in this work were in accordance with literature regarding the lower contents of isoamyl acetate, hexyl acetate and medium chain ethyl fatty acids as well as the higher contents of diethyl succinate found in *Sc-Td* wines [32,33]. *Sc-Td* also favoured the production of some terpenes such as linalool and geraniol, in agreement with previous findings [34]. The selected potential marker of *Sc-Td* wines 3-ethoxy-1-propanol, has been described as a compound highly dependent on yeast strain and species, and it was also found in higher concentrations in the wines elaborated with *Td* yeasts [35]. Three of the selected potential markers of *Sc-Td* were esters (ethyl decanoate, methyl 4-decenoate and ethyl 2-methylpropanoate). The formation of esters during fermentation and their concentration relationships with the predominant yeast strains have been widely described in the literature [36]. These compounds are present at low concentrations in wine, often below the aroma threshold concentration, but make a strong contribution to the aroma of wine through synergistic interaction effects. In agreement with our findings, previous studies have reported increases in ethyl decanoate and ethyl 2-methylpropanoate in wines fermented with *Td* yeasts and its contribution was related to the fruity character of wines [37,38]. In addition, we found positive correlations between these esters and the sensory descriptors red fruit, complexity and black fruit in the PLSR model (Supplementary

Figure S4). Several esters not selected as potential markers of the fermentation strategy, such as ethyl 2-methylbutyrate and ethyl phenylacetate, were also found in significantly higher concentrations in rosé wines fermented with *Sc-Td* (Supplementary Table S3). The larger production capacity of *Td* yeasts, a synergistic effect between *Td* and *Sc* [39] or modifications in the nitrogen available for *Sc* species due to *non-Sc* yeasts activity could explain these results. Another volatile compound selected as a potential marker of the fermentation strategy was (E)-nerolidol, a sesquiterpene derived from farnesyl pyrophosphate, which can be produced by *Td* yeasts [40] and was found in significantly higher concentrations in the *Sc-Td* fermented rosé wines (Supplementary Table S3). In addition, several terpenes such as geranyl ethyl ether, (Z)-β-farnesene, nerolidyl acetate, linalool and citronellol were found in higher contents in these wines (Supplementary Table S3). The impact of terpenoids on the grape aroma typicity highlights the importance of the fermentation strategy and the yeasts selected for winemaking to obtain wines with specific sensory characteristics. The selected potential marker 1-dodecanol has pleasant flowery descriptors at low concentrations, but it may give unpleasant aromas to the wine at high concentrations [41]. In our study this compound displayed slightly positive correlations with red fruit, complexity and black fruit. (E,E)-farnesol, which was selected as a potential marker of *Sc* wines is a isoprenoid alcohol with lemon descriptors [42]. This compound was found to be slightly related to the citrus fruit descriptor in the PLSR, although in the integrative approach fell within the inner circumference. The selected potential marker mannitol is a polyol mainly present in high-quality full bodied wines [43], although no important correlations of this metabolite and sensory descriptors were observed. Interactions between grapes and yeasts were found, and in general, the wines fermented with *Sc-Td* had lower fruity descriptors in agreement with literature [26,44]. This reduced fruitiness could be explained by the lack of ageing in the wines analysed, since *Td* tend to enhance fruitiness with time (aged wines) [37].

5. Conclusions

A data processing and statistical analysis pipeline was proposed to study the metabolome modulation of wines with different characteristics and to relate it to their sensory descriptors. This methodology was then applied to study the effect of different fermentation strategies in the elaboration of rosé wines with two grape varieties. A classical independent assessment of the volatile, non-volatile and sensory data made it possible to identify the most relevant metabolites and wine descriptors influenced by the fermentation strategy. Afterwards, this approach was complemented with the statistical integration of the entire metabolome and the sensory descriptors, revealing new potential markers that were highly correlated with the sensory attributes of the wines. A parallel workflow was followed to study the relationships among the metabolome and the sensory attributes of the wines, first by assessing the independent volatile and non-volatile profiles and finally by statistical integration of the three data sets. Strong correlations among sensory descriptors and metabolites were found by means of partial least squares regression and data integration strategies, demonstrating the suitability of combining both methodologies for making robust interpretations of the interrelationships in these complex biological systems.

Supplementary Materials: The following are available online at https://www.mdpi.com/article/10.3390/fermentation7020072/s1, Figure S1: Balanced error rates (BER) obtained for the partial least squares discriminant analysis (PLS-DA) and random forest (RF) double-cross validated models used to select for the maximum number of relevant variables in GC data (a and b) and LC data (c and d), Figure S2: Partial least squares regression (PLSR) performed to predict the sensory descriptors from the volatile profile, Figure S3: Partial least squares regression (PLSR) performed to predict the sensory descriptors from the non-volatile profile, Figure S4: Correlation loadings plot from the partial least squares regression (PLS2) performed on the GC-sensory and LC-sensory data sets, Table S1: non-volatile metabolites identification results from MetaboQuest using the Metlin database. Positive ionization ESI mode, Table S2: Non-volatile metabolites identification results from MetaboQuest using the Metlin database. Negative ionization ESI mode, Table S3: Two-way analysis of variance (ANOVA) for the inoculation strategy and variety using both the identified and non-identified

volatile metabolites, Table S4: Two-way analysis of variance (ANOVA) for the inoculation strategy and variety using both the identified and non-identified non-volatile metabolites.

Author Contributions: Conceptualization, J.M.M.-R. (José Manuel Muñoz-Redondo), B.P., E.C.-V. and J.M.M.-R. (José Manuel Moreno-Rojas); methodology, J.M.M.-R. (José Manuel Muñoz-Redondo), J.L.O.-D., G.P.-C.; software, J.M.M.-R. (José Manuel Muñoz-Redondo); validation, J.M.M.-R. (José Manuel Muñoz-Redondo); formal analysis, J.M.M.-R. (José Manuel Muñoz-Redondo); investigation, B.P., E.C.-V., G.P.-C., J.M.M.-R. (José Manuel Muñoz-Redondo) and J.L.O.-D.; resources, G.P.-C.; data curation, J.M.M.-R. (José Manuel Muñoz-Redondo); writing—original draft preparation, J.M.M.-R. (José Manuel Muñoz-Redondo); writing—review and editing, B.P., E.C.-V., and J.M.M.-R. (José Manuel Moreno-Rojas); visualization, J.M.M.-R. (José Manuel Muñoz-Redondo) and J.M.M.-R. (José Manuel Moreno-Rojas); supervision, J.M.M.-R. (José Manuel Moreno-Rojas); project administration, J.M.M.-R. (José Manuel Moreno-Rojas), G.P.-C., B.P. and E.C.-V.; funding acquisition, B.P. All authors have read and agreed to the published version of the manuscript.

Funding: This research was funded by the Andalusian Institute of Agricultural and Fisheries Research and Training (IFAPA) through the Project "Investigacioón e Innovación Tecnoloógica en Vitivinicultura" (PR.AVA.AVA2019.016) and the European Rural Development Fund (ERDF, EU). J. M. Muñoz-Redondo and J. L. Ordoñez-Diaz were awarded a research contract funded by the Andalusian Institute of Agricultural and Fisheries Research and Training (IFAPA), within the National Youth Guarantee System funded through the European Social Fund (ESF) and the Youth Employment Initiative (YEI). G. Pereira-Caro was supported by a postdoctoral research contract funded by IFAPA and the ESF (03/2014 to 03/2017) and by a postdoctoral "Juan de la Cierva-Incorporación" research contract funded by the Spanish Ministry of Economy, Industry and Competitiveness (FJCI-2015-26433; 04/2017 to 03/2019). M. J. Ruiz-Moreno was supported by a research contract funded by IFAPA and the ESF (09/2012 to 08/2017).

Institutional Review Board Statement: Not applicable.

Informed Consent Statement: Not applicable.

Data Availability Statement: Not applicable.

Conflicts of Interest: The authors declare no conflict of interest. The funders had no role in the design of the study; in the collection, analyses, or interpretation of data; in the writing of the manuscript; or in the decision to publish the results.

References

1. Siegrist, M.; Cousin, M.-E. Expectations Influence Sensory Experience in a Wine Tasting. *Appetite* **2009**, *52*, 762–765. [CrossRef] [PubMed]
2. Sherman, E.; Coe, M.; Grose, C.; Martin, D.; Greenwood, D.R. Metabolomics Approach to Assess the Relative Contributions of the Volatile and Non-Volatile Composition to Expert Quality Ratings of Pinot Noir Wine Quality. *J. Agric. Food Chem.* **2020**, *68*, 13380–13396. [CrossRef] [PubMed]
3. Li, Z.; Lu, Y.; Guo, Y.; Cao, H.; Wang, Q.; Shui, W. Comprehensive Evaluation of Untargeted Metabolomics Data Processing Software in Feature Detection, Quantification and Discriminating Marker Selection. *Anal. Chim. Acta* **2018**, *1029*, 50–57. [CrossRef]
4. Arapitsas, P.; Ugliano, M.; Marangon, M.; Piombino, P.; Rolle, L.; Gerbi, V.; Versari, A.; Mattivi, F. Use of Untargeted Liquid Chromatography–Mass Spectrometry Metabolome to Discriminate Italian Monovarietal Red Wines, Produced in Their Different Terroirs. *J. Agric. Food Chem.* **2020**, *68*, 13353–13366. [CrossRef]
5. Šuklje, K.; Carlin, S.; Stanstrup, J.; Antalick, G.; Blackman, J.W.; Meeks, C.; Deloire, A.; Schmidtke, L.M.; Vrhovsek, U. Unravelling Wine Volatile Evolution during Shiraz Grape Ripening by Untargeted HS-SPME-GC × GC-TOFMS. *Food Chem.* **2019**, *277*, 753–765. [CrossRef] [PubMed]
6. Pinu, F.R. Grape and Wine Metabolomics to Develop New Insights Using Untargeted and Targeted Approaches. *Fermentation* **2018**, *4*, 92. [CrossRef]
7. Rocchetti, G.; Gatti, M.; Bavaresco, L.; Lucini, L. Untargeted Metabolomics to Investigate the Phenolic Composition of Chardonnay Wines from Different Origins. *J. Food Compos. Anal.* **2018**, *71*, 87–93. [CrossRef]
8. Whitener, M.E.B.; Stanstrup, J.; Panzeri, V.; Carlin, S.; Divol, B.; Du Toit, M.; Vrhovsek, U. Untangling the Wine Metabolome by Combining Untargeted SPME–GCxGC-TOF-MS and Sensory Analysis to Profile Sauvignon Blanc Co-Fermented with Seven Different Yeasts. *Metabolomics* **2016**, *12*, 53. [CrossRef]
9. Arbulu, M.; Sampedro, M.C.; Gómez-Caballero, A.; Goicolea, M.A.; Barrio, R.J. Untargeted Metabolomic Analysis Using Liquid Chromatography Quadrupole Time-of-Flight Mass Spectrometry for Non-Volatile Profiling of Wines. *Anal. Chim. Acta* **2015**, *858*, 32–41. [CrossRef]

10. Castro, C.C.; Martins, R.C.; Teixeira, J.A.; Ferreira, A.C.S. Application of a High-Throughput Process Analytical Technology Metabolomics Pipeline to Port Wine Forced Ageing Process. *Food Chem.* **2014**, *143*, 384–391. [CrossRef]
11. Goodacre, R.; Broadhurst, D.; Smilde, A.K.; Kristal, B.S.; Baker, J.D.; Beger, R.; Bessant, C.; Connor, S.; Capuani, G.; Craig, A. Proposed Minimum Reporting Standards for Data Analysis in Metabolomics. *Metabolomics* **2007**, *3*, 231–241. [CrossRef]
12. Johnsen, L.G.; Skou, P.B.; Khakimov, B.; Bro, R. Gas Chromatography–Mass Spectrometry Data Processing Made Easy. *J. Chromatogr. A* **2017**, *1503*, 57–64. [CrossRef]
13. Amigo, J.M.; Skov, T.; Bro, R.; Coello, J.; Maspoch, S. Solving GC-MS Problems with Parafac2. *TrAC Trends Anal. Chem.* **2008**, *27*, 714–725. [CrossRef]
14. Mahieu, N.G.; Genenbacher, J.L.; Patti, G.J. A Roadmap for the XCMS Family of Software Solutions in Metabolomics. *Curr. Opin. Chem. Biol.* **2016**, *30*, 87–93. [CrossRef] [PubMed]
15. Considine, E.C.; Salek, R.M. A Tool to Encourage Minimum Reporting Guideline Uptake for Data Analysis in Metabolomics. *Metabolites* **2019**, *9*, 43. [CrossRef]
16. Ren, S.; Hinzman, A.A.; Kang, E.L.; Szczesniak, R.D.; Lu, L.J. Computational and Statistical Analysis of Metabolomics Data. *Metabolomics* **2015**, *11*, 1492–1513. [CrossRef]
17. Worley, B.; Powers, R. Multivariate Analysis in Metabolomics. *Curr. Metab.* **2013**, *1*, 92–107.
18. Rohart, F.; Gautier, B.; Singh, A.; Le Cao, K.-A. MixOmics: An R Package for 'omics Feature Selection and Multiple Data Integration. *PLoS Comput. Biol.* **2017**, *13*, e1005752. [CrossRef] [PubMed]
19. Wanichthanarak, K.; Fahrmann, J.F.; Grapov, D. Genomic, Proteomic, and Metabolomic Data Integration Strategies. *Biomark. Insights* **2015**, *10*, BMI–S29511. [CrossRef]
20. Sumner, L.W.; Amberg, A.; Barrett, D.; Beale, M.H.; Beger, R.; Daykin, C.A.; Fan, T.W.-M.; Fiehn, O.; Goodacre, R.; Griffin, J.L.; et al. Proposed Minimum Reporting Standards for Chemical Analysis. *Metabolomics* **2007**, *3*, 211–221. [CrossRef] [PubMed]
21. Smith, C.A.; Want, E.J.; O'Maille, G.; Abagyan, R.; Siuzdak, G. XCMS: Processing Mass Spectrometry Data for Metabolite Profiling Using Nonlinear Peak Alignment, Matching, and Identification. *Anal. Chem.* **2006**, *78*, 779–787. [CrossRef] [PubMed]
22. Libiseller, G.; Dvorzak, M.; Kleb, U.; Gander, E.; Eisenberg, T.; Madeo, F.; Neumann, S.; Trausinger, G.; Sinner, F.; Pieber, T.; et al. IPO: A Tool for Automated Optimization of XCMS Parameters. *BMC Bioinform.* **2015**, *16*. [CrossRef] [PubMed]
23. Kuhl, C.; Tautenhahn, R.; Böttcher, C.; Larson, T.R.; Neumann, S. CAMERA: An Integrated Strategy for Compound Spectra Extraction and Annotation of LC/MS Data Sets. *Anal. Chem.* **2012**, *84*, 283–289. [CrossRef]
24. Arapitsas, P.; Della Corte, A.; Gika, H.; Narduzzi, L.; Mattivi, F.; Theodoridis, G. Studying the Effect of Storage Conditions on the Metabolite Content of Red Wine Using HILIC LC–MS Based Metabolomics. *Food Chem.* **2016**, *197*, 1331–1340. [CrossRef] [PubMed]
25. Puertas, B.; Jimenez-Hierro, M.J.; Cantos-Villar, E.; Marrufo-Curtido, A.; Carbú, M.; Cuevas, F.J.; Moreno-Rojas, J.M.; González-Rodríguez, V.E.; Cantoral, J.M.; Ruiz-Moreno, M.J. The Influence of Yeast on Chemical Composition and Sensory Properties of Dry White Wines. *Food Chem.* **2018**, *253*, 227–235. [CrossRef]
26. Kokla, M.; Klåvus, A.; Noerman, S.; Koistinen, V.M.; Tuomainen, M.; Zarei, I.; Meuronen, T.; Häkkinen, M.R.; Rummukainen, S.; Babu, A.F. "NoTaMe": Workflow for Non-Targeted LC-MS Metabolic Profiling. *Metabolites* **2020**, *10*, 135.
27. Kokla, M.; Virtanen, J.; Kolehmainen, M.; Paananen, J.; Hanhineva, K. Random Forest-Based Imputation Outperforms Other Methods for Imputing LC-MS Metabolomics Data: A Comparative Study. *BMC Bioinform.* **2019**, *20*, 492. [CrossRef] [PubMed]
28. Noonan, M.J.; Tinnesand, H.V.; Buesching, C.D. Normalizing Gas-Chromatography–Mass Spectrometry Data: Method Choice Can Alter Biological Inference. *BioEssays* **2018**, *40*, 1700210. [CrossRef]
29. Szymańska, E.; Saccenti, E.; Smilde, A.K.; Westerhuis, J.A. Double-Check: Validation of Diagnostic Statistics for PLS-DA Models in Metabolomics Studies. *Metabolomics* **2012**, *8*, 3–16. [CrossRef]
30. Muñoz-Redondo, J.M.; Ruiz-Moreno, M.J.; Puertas, B.; Cantos-Villar, E.; Moreno-Rojas, J.M. Multivariate Optimization of Headspace Solid-Phase Microextraction Coupled to Gas Chromatography-Mass Spectrometry for the Analysis of Terpenoids in Sparkling Wines. *Talanta* **2020**, *208*, 120483. [CrossRef]
31. Shi, L.; Westerhuis, J.A.; Rosén, J.; Landberg, R.; Brunius, C. Variable Selection and Validation in Multivariate Modelling. *Bioinformatics* **2019**, *35*, 972–980. [CrossRef] [PubMed]
32. Sadoudi, M.; Tourdot-Maréchal, R.; Rousseaux, S.; Steyer, D.; Gallardo-Chacón, J.-J.; Ballester, J.; Vichi, S.; Guérin-Schneider, R.; Caixach, J.; Alexandre, H. Yeast–Yeast Interactions Revealed by Aromatic Profile Analysis of Sauvignon Blanc Wine Fermented by Single or Co-Culture of Non-Saccharomyces and Saccharomyces Yeasts. *Food Microbiol.* **2012**, *32*, 243–253. [CrossRef]
33. Renault, P.; Miot-Sertier, C.; Marullo, P.; Hernández-Orte, P.; Lagarrigue, L.; Lonvaud-Funel, A.; Bely, M. Genetic Characterization and Phenotypic Variability in Torulaspora Delbrueckii Species: Potential Applications in the Wine Industry. *Int. J. Food Microbiol.* **2009**, *134*, 201–210. [CrossRef]
34. Benito, S. The Impact of Torulaspora Delbrueckii Yeast in Winemaking. *Appl. Microbiol. Biotechnol.* **2018**, *102*, 3081–3094. [CrossRef] [PubMed]
35. Velázquez, R.; Zamora, E.; Álvarez, M.L.; Ramírez, M. Using Torulaspora Delbrueckii Killer Yeasts in the Elaboration of Base Wine and Traditional Sparkling Wine. *Int. J. Food Microbiol.* **2019**, *289*, 134–144. [CrossRef] [PubMed]
36. Sumby, K.M.; Grbin, P.R.; Jiranek, V. Microbial Modulation of Aromatic Esters in Wine: Current Knowledge and Future Prospects. *Food Chem.* **2010**, *121*, 1–16. [CrossRef]

37. Oliveira, I.; Ferreira, V. Modulating Fermentative, Varietal and Aging Aromas of Wine Using Non-Saccharomyces Yeasts in a Sequential Inoculation Approach. *Microorganisms* **2019**, *7*, 164. [CrossRef] [PubMed]
38. Renault, P.; Coulon, J.; de Revel, G.; Barbe, J.-C.; Bely, M. Increase of Fruity Aroma during Mixed T. Delbrueckii/S. Cerevisiae Wine Fermentation Is Linked to Specific Esters Enhancement. *Int. J. Food Microbiol.* **2015**, *207*, 40–48. [CrossRef] [PubMed]
39. Gobert, A.; Tourdot-Maréchal, R.; Morge, C.; Sparrow, C.; Liu, Y.; Quintanilla-Casas, B.; Vichi, S.; Alexandre, H. Non-Saccharomyces Yeasts Nitrogen Source Preferences: Impact on Sequential Fermentation and Wine Volatile Compounds Profile. *Front. Microbiol.* **2017**, *8*, 2175. [CrossRef]
40. King, A.; Richard Dickinson, J. Biotransformation of Monoterpene Alcohols by Saccharomyces Cerevisiae, Torulaspora Delbrueckii and Kluyveromyces Lactis. *Yeast* **2000**, *16*, 499–506. [CrossRef]
41. Jiang, B.; Zhang, Z. Volatile Compounds of Young Wines from Cabernet Sauvignon, Cabernet Gernischet and Chardonnay Varieties Grown in the Loess Plateau Region of China. *Molecules* **2010**, *15*, 9184–9196. [CrossRef] [PubMed]
42. Coelho, E.; Coimbra, M.A.; Nogueira, J.M.F.; Rocha, S.M. Quantification Approach for Assessment of Sparkling Wine Volatiles from Different Soils, Ripening Stages, and Varieties by Stir Bar Sorptive Extraction with Liquid Desorption. *Anal. Chim. Acta* **2009**, *635*, 214–221. [CrossRef] [PubMed]
43. Soetaert, W.; Vanhooren, P.T.; Vandamme, E.J. The production of mannitol by fermentation. In *Carbohydrate Biotechnology Protocols*; Springer: Berlin/Heidelberg, Germany, 1999; pp. 261–275.
44. Azzolini, M.; Tosi, E.; Lorenzini, M.; Finato, F.; Zapparoli, G. Contribution to the Aroma of White Wines by Controlled Torulaspora Delbrueckii Cultures in Association with Saccharomyces Cerevisiae. *World J. Microbiol. Biotechnol.* **2015**, *31*, 277–293. [CrossRef] [PubMed]

ARTÍCULO 5

Impact of Sequential Inoculation with the Non-*Saccharomyces T. delbrueckii* and *M. pulcherrima* Combined with *Saccharomyces cerevisiae* Strains on Chemicals and Sensory Profile of Rosé Wines

José Manuel Muñoz-Redondo, Belén Puertas, Emma Cantos-Villar, María Jesús Jiménez-Hierro, María Carbú, Carlos Garrido, María José Ruiz-Moreno, and José Manuel Moreno-Rojas

Journal of Agricultural and Food Chemistry

65(13), 2768-2775 (2017)

Q1: 4/58 (Agriculture, Multidisciplinary, 2019)

Impact Factor: 4.192

JOURNAL OF AGRICULTURAL AND FOOD CHEMISTRY

pubs.acs.org/JAFC Article

Impact of Sequential Inoculation with the Non-*Saccharomyces T. delbrueckii* and *M. pulcherrima* Combined with *Saccharomyces cerevisiae* Strains on Chemicals and Sensory Profile of Rosé Wines

José Manuel Muñoz-Redondo,* Belén Puertas, Emma Cantos-Villar, María Jesús Jiménez-Hierro, María Carbú, Carlos Garrido, María José Ruiz-Moreno, and José Manuel Moreno-Rojas*

Cite This: *J. Agric. Food Chem.* 2021, 69, 1598−1609 Read Online

ACCESS | Metrics & More | Article Recommendations | Supporting Information

ABSTRACT: Controlled inoculations of non-*Saccharomyces* yeasts are becoming increasingly used to produce high-quality wines due to their enological potential. In this study, we evaluated the impact of sequential inoculation with the commercial non-*Saccharomyces* yeasts (*Torulaspora delbrueckii* and *Metschnikowia pulcherrima*) in combination with *Saccharomyces cerevisiae* on the chemical and sensory profile of rosé wines. Sequential inoculation with *T. delbrueckii* produced wines with an overall reduction in esters, mainly explained by the lower concentrations of ethyl esters of medium-chain fatty acids and isoamyl acetate. The lower ester concentrations of these wines were related to a reduction in fruity descriptors. An increase was observed, however, in other minor esters such as cinnamates and ethyl esters of branched acids. Zinc, ethyl isobutyrate, and ethyl dihydrocinnamate were selected as potential markers for this fermentation strategy. Sequential inoculation with *M. pulcherrima* resulted in rosé wines with an enhanced ester profile, reduced acetaldehyde, and increased anthocyans and tannins. Compared to the control wines fermented with *S. cerevisiae*, the changes observed in these wines were far subtler, especially for the volatile profile, sensory characteristics, and color parameters, with isobutyl hexanoate and isoamyl butyrate being selected as potential markers.

KEYWORDS: *yeasts, sequential inoculation, rosé wines, multivariate analysis, esters, sensory, data fusion, non-Saccharomyces*

INTRODUCTION

In the environment, many microorganisms coexist across different ecosystems, competing for resources and interacting with each other. To date, the role of yeasts, bacteria, and filamentous fungi under enological conditions still remains a central question. Among these microbial organisms, yeasts are considered to have the greatest influence on wines due to their important role in conducting alcoholic fermentation.[1] The simultaneous growth and complex ecological interactions of different yeast strains during wine fermentation produce physicochemical changes in the enological environment with important consequences on the organoleptic quality of the final wines.[2] Consequently, *Saccharomyces cerevisiae* (Sc) strains have been widely used in winemaking due to their ability to induce reliable, rapid, and consistent fermentation.[3] However, in recent years, the role of non-*Saccharomyces* strains have been re-evaluated. *Torulaspora delbrueckii* (Td) has been commonly used for the production of red and rosé wines and has been reported to increase the concentration of several volatile esters due to its high β-glucosidase activity.[4] Other non-*Saccharomyces* strains such as *Metschnikowia pulcherrima* (Mp) have also attracted attention from winemakers due to their high β-glucosidase activity and their capacity to decrease volatile acidity and increase the production of esters, terpenols, medium-chain fatty acids, higher alcohols, and glycerol.[4] However, both non-*Saccharomyces* (non-Sc) strains have been reported to show lower resistance to SO_2, lower biomass yields from batch cultures, and slower growth rate compared to Sc strains, as well as a moderate to low fermentative power and generation of biogenic amine precursors.[5−7] Consequently, these yeasts are usually combined with more powerful fermenters such as Sc strains for large-scale wine production. In recent years, research has focused its attention on sequential fermentations of non-Sc in association with Sc strains to improve the quality of wines due to synergistic interaction effects of both yeast species.[4,8−12] Sequential inoculation (SI) strategies are used to ensure the dominance and persistence of non-Sc in the first stages of the fermentation[8] and, therefore, to favor the specific markers of these strains.[13] Afterward, due to the lower ethanol tolerance of non-Sc strains, the high fermenter Sc yeasts are sequentially inoculated to ensure a proper final fermentation ending without residual sugars or colorizations of undesirable microorganisms.[14] To date, studies evaluating the impact of sequential fermentation on the quality of wines have been focused on white and red wines, and to the best of our knowledge, there are no studies concerning rosé wines.

Several studies have addressed the impact of *T. delbrueckii*[4,9,11,13,15−17] and *M. pulcherrima*[4,18] strains in sequential

Received: November 4, 2020
Revised: January 13, 2021
Accepted: January 16, 2021
Published: January 28, 2021

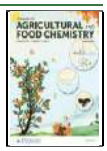

https://dx.doi.org/10.1021/acs.jafc.0c06970
J. Agric. Food Chem. 2021, 69, 1598−1609

Journal of Agricultural and Food Chemistry pubs.acs.org/JAFC Article

fermentations, revealing positive effects on taste, aroma, and enological characteristics. However, the mechanisms involved in such positive effects remain unclear.[13] Given the complexity of wine matrices, the assessment of the results through classical univariate statistical procedures may result in loss of useful information or interpretation difficulties. Therefore, multivariate approaches are commonly used to provide a more comprehensive study of the contribution of different variables to the factor under study. In this sense, partial least squares discriminant analysis (PLS-DA) is a prediction technique commonly employed to assess food samples based on their chemical profile[15] due to its versatility and ability to detect the most discriminative variables.[19]

The aim of this study was to assess for the first time the impact of sequential fermentation with the commercial non-*Saccharomyces* yeasts *T. delbrueckii* and *M. pulcherrima* in combination with *S. cerevisiae* strains on the chemicals and sensory profile of rosé wines through a multivariate approach.

MATERIAL AND METHODS

Chemicals. High-performance liquid chromatography (HPLC)-grade ethanol was obtained from J.T. Baker Chemicals B.V. (Denventer, Holland). Milli-Q water was produced by a Milli-Q Plus water system (Millipore, Spain). Sigma-Aldrich (Madrid, Spain) supplied the following: sodium chloride, ACS reagent grade (purity ≥99.8%), and the standard compounds ethyl butyrate (≥99%), ethyl hexanoate (≥99%), ethyl octanoate (≥99%), ethyl decanoate (≥99%), ethyl dodecanoate (≥99%), ethyl myristate (≥99%), ethyl palmitate (≥99%), ethyl stearate (≥99%), propyl acetate (≥99%), isobutyl acetate (≥99%), phenylethyl acetate (≥99%), isoamyl acetate (≥99%), hexyl acetate (≥99%), ethyl isobutyrate (98%), ethyl 2-methylbutyrate (≥99%), ethyl isovalerate (≥99%), ethyl phenylacetate (98%), ethyl cinnamate (98%), ethyl dihydrocinnamate (98%), methyl hexanoate (≥99%), methyl octanoate (≥99%), methyl decanoate (≥99%), ethyl valerate (≥99.7%), ethyl heptanoate (98%), ethyl nonanoate (98%), isoamyl butyrate (98%), isobutyl hexanoate (≥99%), acetaldehyde (≥99.5%), ethyl acetate (≥99%), methanol (≥99.8%), *N*-propanol (≥99%) isobutanol (≥99%), 2-methyl-1-butanol (≥99%), and 3-methyl-1-butanol (≥99%).

Rosé Wine Fermentation. Semi-industrial winemaking processes (Figure 1) were carried out during the 2017 harvest at the "Rancho de la Merced" experimental winery (latitude 36°41′11.22″; longitude N 6°8′9.815″W) located in Jerez de la Frontera (Cádiz, Spain). The red grape varieties *Vitis vinifera* L. cv. Garnacha tinta (810 kg) and L. cv. Cabernet Sauvignon (700 kg) were used to produce the wines. Both varieties were picked up at optimum ripeness, destemmed, and crushed. Maceration was carried out at 8 °C for 24 h with the addition of 40 mg/L of sulfur dioxide (SO_2) (Solfosol, 150 g/L, Enartis, Spain). The enzymes (Enartiszym Arom MP, Enartis, Spain) were added during the maceration tank filling according to the supplier's recommendations at 3 g/100 kg. Afterward, the musts were soft pressed with a pneumatic press, homogenized, and the juice was extracted at 4 °C, for 24 h, with the addition of 2.5 mL/hL of pectolytic enzymes (Blanco "L", Enartis, Spain). The resulting juices from each grape variety were divided into nine stainless steel tanks of 50 L capacity, filled with 38 and 45 L of Cabernet Sauvignon and Garnacha tinta juices, respectively, to assay three different fermentative strategies by triplicate. In the control fermentation (CT), the *S. cerevisiae* (Sc) yeasts (Red Fruit, Enartis, Spain) were added at the beginning of the fermentation at 25 g/hL. In the sequential inoculations (SI), the non-Sc yeasts (*T. delbrueckii* TD291 Biodiva or *M. pulcherrima* MP346 Flavia) were used to start fermentations at 25 g/hL, and 1 day later, Sc yeasts were also added at 25 g/hL. The non-Sc yeasts were supplied by Lallemand as active dried yeasts (ADY), and both the rehydration and inoculation procedures were carried out according to the supplier's recommendations. The alcoholic fermentation took place at a controlled

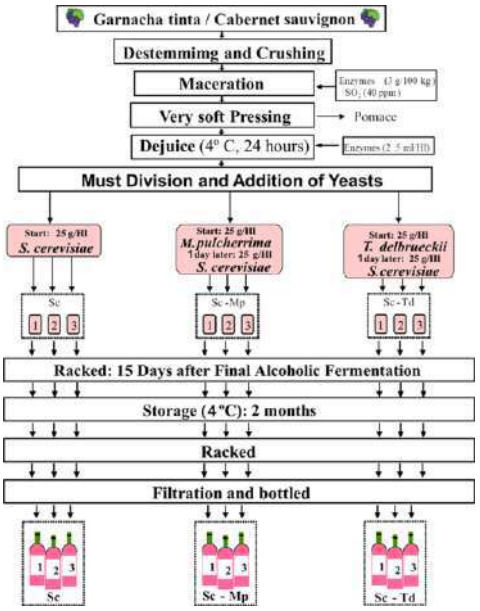

Figure 1. Flowchart illustrating the step-by-step processes followed to elaborate rosé wines with three different fermentation strategies.

temperature of 17−18 °C. Daily density and temperature were monitored to control the kinetics of the alcoholic fermentation. The alcoholic fermentation finished when residual sugar concentrations were under 2 g/L. The wines were racked 15 days after the final alcoholic fermentation. After 2 months of cold stabilization at 4 °C, the wines were filtered using Opticap XL 4 Capsule, 2.0/1.2 μm Nominal (Millipore).

Percentage of Yeast Implantation. The monitoring of the yeast strains for the three assays (CT, SI-Td, and SI-Mp) was carried out at the end of alcoholic fermentation. Thirty isolated yeasts were randomly selected for every assay and were inoculated into a yeast extract−peptone−dextrose (YPD) medium (bacteriological peptone, 20 g/L; yeast extract, 10 g/L; glucose, 20 g/L) and incubated for 24 h at 30 °C. The total DNA was extracted following the procedure of Ottaviani et al.[20] The microsatellite multiplex polymerase chain reaction (PCR) technique described by Vaudano et al.[21] was used to screen the *S. cerevisiae* red fruit strain. The *T. delbrueckii* and *M. pulcherrima* strains were identified by the randomly amplified polymorphic DNA (RAPD)-PCR technique using primer M14 (5′-GAG GGT GGG GCC GTT-3′).[22] The amplified PCR products were separated by electrophoresis on 2.5% agarose gels in 1× Tris/borate/ethylenediaminetetraacetic acid (EDTA) (TBE) buffer and Roti GelStain (5 μL/100 mL, Carl Roth GmbH). The image of the gel was digitalized in a Molecular Imager apparatus (Gel-Doc XR, Bio-Rad) and analyzed using Quantity One 1-D software (Bio-Rad).

Enological Parameters. Ethanol, reducing sugars, total acidity, volatile acidity, pH, dry extract, glycerol, anthocyans, tannins, organic acids (acetic, citric, succinic, tartaric, malic, and lactic), and metals (Fe, Cu, Zn, Ca, Na, and K) were determined according to the official analytical methods established by the International Organization of Vine and Wine.[23] The major volatile compounds (acetaldehyde, ethyl acetate, methanol, *n*-propanol, isobutanol, and isoamyl alcohols) were determined in the same way as described by Puertas et al.,[11] using gas chromatography coupled to a flame ionization detector (PerkinElmer XL AutoSystem) and the software Turbochrom v.4.1 (PerkinElmer, Madrid, Spain).

Ester Analysis by Headspace Solid-Phase Microextraction Coupled to Gas Chromatography-Mass Spectrometry (HS-SPME-GC-MS). The concentration of the volatile esters was determined by means of headspace solid-phase microextraction

https://dx.doi.org/10.1021/acs.jafc.0c06970
J. Agric. Food Chem. 2021, 69, 1598−1609

Journal of Agricultural and Food Chemistry pubs.acs.org/JAFC Article

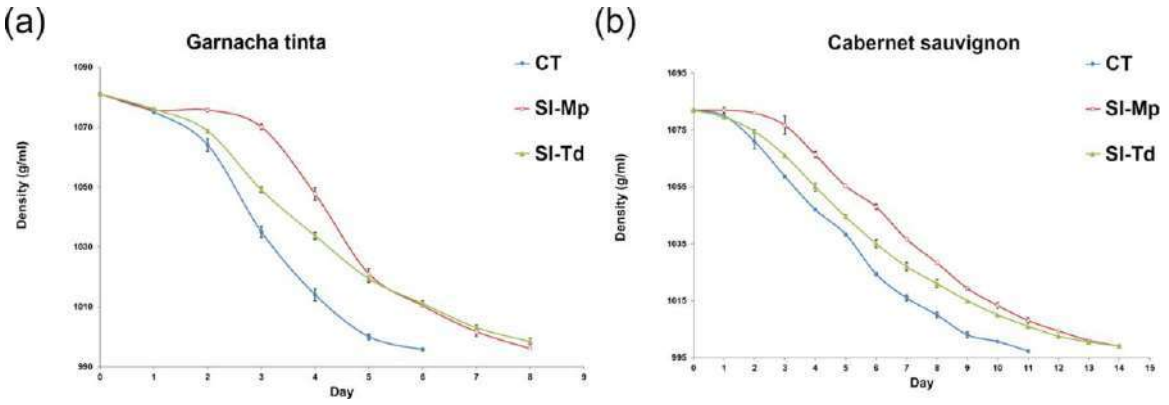

Figure 2. Progression of the alcoholic fermentation process by measured density for (a) Garnacha tinta and (b) Cabernet Sauvignon wines. CT: wines fermented with *S. cerevisiae* strains; SI-Td: wines fermented with sequential inoculation of *T. delbrueckii* and *S. cerevisiae* strains; and SI-Mp: wines fermented with sequential inoculation of *M. pulcherrima* and *S. cerevisiae* strains.

coupled to gas chromatography-mass spectrometry (HS-SPME-GC-MS). A total of 25 mL of each sample was spiked with 20 μL of an internal standard (IS) mix solution at 200 mg/L of deuterated esters [$^2H_3$]-ethyl butyrate, [$^2H_{11}$]-ethyl hexanoate, [$^2H_{15}$]-ethyl octanoate, [$^2H_5$]-ethyl trans-cinnamate, [$^2H_{23}$]-ethyl dodecanoate, [$^2H_{27}$]-ethyl myristate, [$^2H_{31}$]-ethyl palmitate, and [$^2H_{35}$]-ethyl stearate supplied by CDN isotopes (Pointe-Claire, Canada). Then, 15 mL of the spiked samples were diluted 1:1 with EDTA solution (200 mM and pH 7.0 adjusted with NaOH 1.0 M) and 10 mL of this dilution was placed into a 20 mL solid-phase microextraction (SPME) vial containing 3.5 g of NaCl and it was closed with an 18 mm magnetic poly(tetrafluoroethylene)/silicone (PTFE/Sil) headspace cap. The samples were then homogenized in a vortex shaker for 30 s and placed in the tray of an autosampler (CTC Analytics, Zwingen, Switzerland). The fiber used for the HS-SPME methodology was a poly-(dimethylsiloxane) (PDMS) of 100 μm supplied by Supelco (Bellefonte, PA). The vials were incubated at 500 rpm for 2 min at 40 °C. The ester fraction extraction was carried out at 40 °C for 38 min, followed by the desorption at 250 °C for 15 min into a Trace GC Ultra gas chromatograph (Thermo Fisher Scientific S.p.A., Rodano, Milan, Italy) coupled to an ISQ Single Quadrupole MS spectrometer (Thermo Fisher Scientific, Austin, TX). The GC-MS conditions described by Antalick et al.[24] were used. Chromatograms were acquired in the Xcalibur file format (.raw), and the preprocessing was performed manually in the Thermo Xcalibur software v.2.2. The deuterated internal standards were used to normalize the responses of the target esters analyzed. Next, the relative concentration of esters was drift-corrected in all of the samples, including those used for calibration curves, to reduce the contributions of experimental and analytical errors. This was accomplished by fitting a smoothed cubic spline onto a set of pooled quality control (QC) samples repeatedly injected along the experimental sequences as previously described.[25] Subsequently, two calibration curves were fitted with the corrected data using an optimized weighting factor to prevent domination at the top levels of the curves (Table S1, Supporting Information) as described by Muñoz-Redondo et al.[19] and the ester concentration was calculated. The results of this procedure were compared against those without the drift correction. Ester identification was carried out on the basis of the proposed minimum reporting criteria defined by the metabolomics standard initiative.[26] Only definitive identified compounds (level 1) were considered. For this, two orthogonal properties, the linear retention index and fragmentation mass spectrum of the target esters, were compared against their authentic chemical standard analyzed under the same experimental conditions.

Sensory Analysis. The sensory analysis of the wines was performed at IFAPA Rancho de la Merced (Jerez) by a tasting panel composed of 10 expert (six women and four men) panelists between 35 and 55 years old with a considerable tasting experience. The panelists were trained following the AENOR (UNE-EN ISO 8586:2014 and UNE 87022:1992) standards, and the procedure was similar to that described by Puertas et al.[15] The wine description terminology agreed by consensus included five aromas and six taste attributes. The sensory attributes scored in the olfactory phase were scent intensity, red fruit, black fruit, citrus fruit, and tree fruit. The attributes scored in the taste phase were taste intensity, acidity, alcohol, complexity, balance, and persistence.

Statistical Analysis. A smoothed cubic spline was fitted to the QC samples to correct GC-MS data using the R smooth.spline function. The smoothing parameter was optimized to 0.5 by means of leave-one-out cross-validation. Principal component analyses (PCA) were performed to check the structure and quality of the drift-corrected data.

Univariate analyses were carried out to disclose differences in the samples. First, the Levene's and Shapiro–Wilk's tests were used to check the heteroscedasticity and normality of the data and the variables that failed the parametric assumptions were Box–Cox transformed. A two-way analysis of variance (ANOVA) and the post hoc Tukey's honestly significant difference (HSD) tests were used to identify differences in the data due to the grape variety and fermentation strategy, which were considered statistically significant at a p-value $\leq$0.05. Subsequently, all of the data acquired from the different analytical platforms (conventional parameters, organic acids, metals, major volatile compounds, parameters related to color and esters) and the sensory data were merged to extract the most relevant information in a low-level data fusion strategy as described by Puertas et al.[15] For this purpose, the data was first autoscaled, concatenated sample-wise, and the new dataset containing all of the measures was used to carry out a partial least squares discriminant analysis (PLS-DA). The model was double cross-validated as described by Szymańska et al.[27] M-fold and leave-one-out cross-validations were used in the outer and inner loops, respectively, and a total of 50 submodels were built. The optimization and validation of the PLS-DA models were based on the hyperparameter balanced error rate (BER). The statistical significance of the model was calculated from a permutation test (N = 1000) as described in a previous study.[19] Finally, an iterative variable selection procedure based on variable importance in projection (VIP) scores outlined by Muñoz-Redondo et al.[19] was carried out to select the most discriminative variables.

All of the statistical analyses were performed using statistical R v.4.0.0 software. The multivariate analyses were carried out by applying in-house routines based on the R package mixOmics.[28]

RESULT AND DISCUSSION

Kinetics of the Alcoholic Fermentation. The kinetic curves recorded during alcoholic fermentation were affected by

https://dx.doi.org/10.1021/acs.jafc.0c06970
J. Agric. Food Chem. 2021, 69, 1598−1609

Journal of Agricultural and Food Chemistry pubs.acs.org/JAFC Article

Table 1. ANOVA Performed on the Relative Abundances of the Yeast Strains Present in Rosé Wines at the End of the Alcoholic Fermentation[a]

	grape variety			fermentation strategy				interaction
yeast	GT	CS	*p*-value	CT	SI-Td	SI-Mp	*p*-value	*p*-value
Sc (%)	46	51	ns	94a	23b	28b	***	ns
Td (%)	1.2b	8.1a	***	0.0b	14.0a	0.0b	***	***
Mp (%)	0	0	ns	0	0	0	ns	ns
other yeast (%)	52.9	41.0	ns	5.8b	63.4a	71.7a	***	**

[a]*p*-value of the two-way ANOVA; ns: not significant, *: 0.05 > *p*-value > 0.01, **: 0.01 > *p*-value > 0.001, and ***: *p*-value < 0.001. Mean values with different letters differ significantly. GT: Garnacha tinta; CS: Cabernet Sauvignon; CT: wines fermented with *S. cerevisiae* strains; SI-Td: wines fermented with sequential inoculation of *T. delbrueckii* and *S. cerevisiae* strains; and SI-Mp: wines fermented with sequential inoculation of *M. pulcherrima* and *S. cerevisiae* strains.

the fermentation strategy and the grape variety assayed (Figure 2). Alcoholic fermentation performed with juices from Cabernet Sauvignon was significantly slower, ranging from 11 to 14 days, than fermentation with Garnacha juices, which took from 6 to 8 days. Fermentations conducted by the *S. cerevisiae* yeasts were the fastest, while both sequential inoculation strategies took 2−3 days longer. A similar behavior has been reported previously in sequential fermentations using *S. cerevisiae* in association with *T. delbrueckii* (SI-Td).[15,16,29] In the case of sequential fermentations involving *T. delbrueckii*, the density started to decrease faster than those involving *M. pulcherrima*, although the final fermentation time was the same (Figure 2). The higher fermentative character of *T. delbrueckii* (moderate fermenter) than *M. pulcherrima* (low fermenter) may explain this phenomenon.

Implantation of Yeasts. To study the implantation of yeast strains, we analyzed the relative abundances of the strains present at the end of the fermentation of the rosé wines and compared the results by means of a two-way ANOVA (Table 1). We observed higher abundances of Td strains in the wines fermented with Cabernet Sauvignon (8.1% as opposed to 1.2% in Garnacha tinta wines). As expected, the Sc strains inoculated during fermentation were present at the end of the three fermentative assays, with a predominant 94% of abundance in the control wines (Table 1). In the SI-Td wines, a slight mean presence (14%) of Td was detected at the end of the fermentation, which depended highly on the grape used to elaborate the wines. In Cabernet Sauvignon, the presence of these yeasts was 24.3% compared to a low 3.6% in Garnacha tinta wines (Table S2, Supporting Information). Although Td is a moderate ethanol producer, it is able to survive at high ethanol concentrations, as previously confirmed.[4] Besides, the absence of Mp in the last stage of the fermentation agreed with the literature, which confirmed that Mp cannot survive at high ethanol concentrations.[4,30]

Enological Parameters. Different enological parameters were considered to evaluate the quality of the rosé wines produced with different fermentation strategies and grape varieties, including several conventional parameters, organic acids, metals, major volatile compounds, and parameters related to color (Table 2). The fermentation strategy and grape variety affected the enological parameters of the rosé wines (Table 2). In agreement with previous studies,[10,15,29] a lower ethanol contents of about 0.5% (v/v) (Table 2) was observed in the wines sequentially fermented with Td yeasts, although other authors[16,31] did not find statistically significant differences in ethanol in similar works. Meanwhile, SI-Mp showed no statistical differences in ethanol contents compared to the control wines (Table 2), which is in contrast with the decreases observed by other authors in ethanol production for sequential fermentations with *M. pulcherima*,[32−34] that vary from 0.2 to 1% (v/v). The SI-Td wines presented about 1.3 g/L higher contents of glycerol, which is an active contributor to the in-mouth sensory properties of wines, especially sweetness.[13] The current results agree with previous studies reporting similar increases of glycerol,[4,11,35] while other authors have reported no differences in glycerol production by *T. delbrueckii*.[7] Meanwhile, SI-Mp wines did not show statistical differences in glycerol contents compared to the control wines (Table 2). This contrasts with previous studies reporting increases for up to 75% in wines fermented with *M. pulcherrima*.[33] The amount of this compound depends on several factors such as yeast strain, fermentation temperature, grape variety, and its degree of ripeness,[36] with a threshold taste concentration of 5.2 g/L.[37] The contents of glycerol found in all of the samples exceeded this threshold concentration, highlighting the potential impact on the rosé wines produced with the sequential fermentation of Sc and Td yeasts. The sequential inoculation with Td yeasts produced rosé wines with about 3 g/L more dry extract (Table 2), which could be related to the higher polysaccharide contents reported for Td compared to Sc previously.[38] Sequential inoculations with *T. delbrueckii* yeasts also produced rosé wines with about 0.1 (g/L AcH) increased volatile acidity due to higher levels of acetic acid (Table 2). This result is in agreement with a previous study reporting increases in acetic acid, varying from 0.2 to 0.4 g/L, in sequential fermentation with *T. delbrueckii* compared to *S. cerevisiae* controls.[9] However, this behavior contrasts with the previous results describing a reduction in the volatile acidity or acetic acid in sparkling wines and white wines sequentially fermented with Td yeasts that ranged between 0.06 and 0.25 g/L,[4,13] although the values for volatile acidity expressed in acetic acid were within acceptable ranges, varying from 0.18 to 0.50 g/L in all of the samples. A slight increase of about 0.06 (g/L AcH) was also observed in rosé wines sequentially fermented with *M. pulcherrima* yeasts (Table 2). Previous studies have also reported similar increases in acetic acid in sequential fermentation with *M. pulcherrima*,[4,31] while other works reported no statistical differences[39,40] or even the opposite effect.[5,33] A previous study reported up to 40% of variability between several strains of *T. delbrueckii* and *M. pulcherrima*[41] that may explain the discrepancies between the different studies for the volatile acidity. The fermentation strategy also impacted the total acidity of the rosé wines, which displayed the lowest levels in the SI-Mp wines due to low overall contents of succinic, tartaric, malic, and lactic acid (Table 2). The higher lactic acid and low malic acid contents observed in the SI-Td wines were an indicator of malolactic

https://dx.doi.org/10.1021/acs.jafc.0c06970
J. Agric. Food Chem. 2021, 69, 1598−1609

Journal of Agricultural and Food Chemistry pubs.acs.org/JAFC Article

Table 2. Two-Way ANOVA for the Grape and Fermentation Strategy Used for Rosé Wine Elaboration[a,b]

	grape			fermentation strategy				interaction
enological parameter	GT	CS	*p*-value	CT	SI-Td	SI-Mp	*p*-value	*p*-value
conventional parameters								
ethanol (% v/v)	11.3	11.4	ns	11.6a	11.1b	11.5a	***	ns
reducing sugars (g/L)	1.43	1.32	ns	1.10b	1.92a	1.11b	***	ns
total acidity (g/L de TH2)	4.6b	5.4a	***	5.1a	5.0a	4.8b	***	***
volatile acidity (g/L AcH)	0.25b	0.43a	***	0.29c	0.39a	0.35b	***	***
pH	3.2b	3.4a	***	3.3ab	3.3a	3.3b	*	*
dry extract (g/L)	16b	20a	***	17b	20a	17b	***	***
glycerol (g/L)	7.2b	8.4a	***	7.4b	8.7a	7.2b	***	***
anthocyans (mg/L)	10.5b	52.6a	***	28b	31ab	36a	*	ns
tannins (g/L catechin)	0.85a	0.44b	***	0.58b	0.64ab	0.70a	**	***
organic acids (g/L)								
acetic	0.15b	0.31a	***	0.20b	0.28a	0.21b	***	***
citric	0.16a	0.12b	***	0.18a	0.10c	0.14b	***	**
succinic	0.65b	1.34a	***	0.88b	1.29a	0.81b	***	***
tartaric	2.43a	1.41b	***	2.10a	1.69c	1.98b	***	***
malic	0.50a	0.15b	***	0.57a	0.13c	0.28b	***	***
lactic	0.45b	1.72a	***	0.83c	1.36a	1.07b	***	*
metals (mg/L)								
iron	0.54b	0.97a	***	0.64b	0.87a	0.75ab	*	*
copper	0.054a	0.041b	***	0.035b	0.053a	0.055a	***	***
zinc	0.22b	0.26a	**	0.15b	0.44a	0.13b	***	***
calcium	75b	78a	**	80a	78a	73b	***	*
sodium	14.4b	17.6a	***	16	16	16	ns	ns
potassium	772	773	ns	785	764	769	ns	***
major volatile compounds (mg/L)								
acetaldehyde	75b	93a	*	124a	41c	88b	***	**
ethyl acetate	38a	32b	*	32	38	35	ns	**
methanol	79a	61b	***	69	71	70	ns	*
n-propanol	34a	31b	**	32b	35a	30b	**	***
isobutanol	46b	73a	***	30c	91a	58b	***	***
isoamyl alcohols	267b	345a	***	273b	326a	320a	***	***
∑highers alcohols	343b	450a	***	336c	451a	402b	***	***
parameters related to color								
color intensity	0.18b	0.44a	***	0.41a	0.19c	0.32b	***	**
hue	1.66a	0.88b	***	1.03b	1.61a	1.16b	***	ns
% yellow	59a	45b	***	47b	58a	50b	***	ns
% red	36b	52a	***	48a	39b	46a	***	ns
% blue	4.9a	3.2b	***	4.9a	2.8b	4.5a	***	*
L*	91.5a	77.4b	***	79.1c	90.3a	83.9b	***	*
a*	7.3b	29.2a	***	25.2a	10.0b	19.5a	***	ns
b*	11.8b	12.6a	***	14.2a	10.2c	12.3b	***	***
C*ab	14.1b	31.0a	***	30a	15b	22ab	***	ns
hab	61a	26b	***	35b	55a	39b	***	ns

[a]Mean is given for wine enological parameters, organic acids, metals, major volatile compounds, and parameters related to color. [b]*p*-Value of the two-way ANOVA; ns: not significant, *: 0.05 > *p*-value > 0.01, **: 0.01 > *p*-value > 0.001, and ***: *p*-value < 0.001. Mean values with different letters differ significantly. GT: Garnacha tinta; CS: Cabernet Sauvignon; CT: wines fermented with *S. cerevisiae* strains; SI-Td: wines fermented with sequential inoculation of *T. delbrueckii* and *S. cerevisiae* strains; and SI-Mp: wines fermented with sequential inoculation of *M. pulcherrima* and *S. cerevisiae* strains.

fermentation.[15] Previous studies have reported decreases in malic acid due to the *T. delbrueckii* activity during sequential fermentation.[11,29] An increase of succinic acid of about 0.4 g/L was observed in SI-Td wines compared to the *S. cerevisiae* controls, being very close to the increase, of about 0.46 g/L, reported in a similar study.[11] Ciani and Maccarelli[42] also reported a higher production of succinic acid by *T. delbrueckii* than *S. cerevisiae* in pure fermentations that ranged from 0.11 to 0.32 g/L. Meanwhile, lower citric acid was observed in the SI-Td wines (Table 2), in agreement with previous studies.[15,29]

The highest levels of anthocyans and tannins were observed in the sequentially fermented wines, especially the SI-Mp wines (Table 2). Similar results were obtained in a previous study for anthocyans,[43] reporting the highest concentrations in SI-Mp compared to Sc wines and intermediate concentrations in SI-Td, although tannins were in the same or even lower contents in wines sequentially fermented with *M. pulcherrima* strains. Conversely, Del Fresno et al.[12] observed a decrease of about 5 mg/L in anthocyans in wines sequentially fermented with *T. delbrueckii* compared to the control *S. cerevisiae* ones.

https://dx.doi.org/10.1021/acs.jafc.0c06970
J. Agric. Food Chem. 2021, 69, 1598−1609

Journal of Agricultural and Food Chemistry pubs.acs.org/JAFC Article

The fermentation strategy also affected the metal concentration in the rosé wines. Lower concentrations of iron, copper, and zinc were found in the control wines, while the SI-Td ones displayed higher overall concentrations of iron, copper, zinc, and calcium. The presence of iron and copper is known to induce the formation of hazes in wines, although in recent years the metal concentrations in wines have decreased and this phenomenon is becoming less common.[44] Meanwhile, zinc is a micronutrient essential for human, which is a constituent of many enzymes involved in physiological functions, although this metal is toxic in excessive intake.[45] Among the major volatile compounds, the significant reduction in acetaldehyde levels found in the sequentially fermented wines was of interest, being of about 80 mg/L for SI-Td and 40 mg/L for SI-Mp wines. Both Td and Mp strains have been reported to induce a lower production of this metabolite ranging from 4 to 50 mg/L for *T. delbrueckii* in mixed culture fermentations,[7] and about 1 mg/L for *M. pulcherrima* in sequential fermentations.[4] However, González-Royo et al.[4] only observed this behavior in sequential fermentation with Mp but not for Td strains. Acetaldehyde has pleasant fruity descriptors at low concentrations, but excess may induce green, grassy, and apple-like off flavors.[46] Therefore, the use of sequential fermentation with non-Sc yeasts may be an appropriate choice to decrease acetaldehyde production. In contrast with previous studies,[13] no statistical differences were observed for ethyl acetate between the sequentially fermented and the control wines, and their levels were in desirable concentrations below 150 mg/L (Table 2). Finally, all of the parameters related to color measured in the samples were affected by the fermentation strategy. The control and SI-Mp wines showed similar color parameter levels, but with slight differences, mainly in color intensity, perceptual lightness (L*), and blue-yellow color component (b*). Of note were the higher color intensity values found in the control wines, which even doubled the values measured in the SI-Td wines (Table 2). b* was around 2 and 4 points greater in the control wines than in SI-Td and SI-Mp, respectively, revealing a slightly higher trend to yellowness. This trend observed for b* was in accordance with other studies, which compared wines produced with Mp, Td, and Sc strains, reporting about 3 points greater values for *S. cerevisiae* control wines.[43] Meanwhile, the SI-Td wines showed more distinct color parameters, with statistically greater values in Hue (around 0.5 points higher), % Yellow (around 8% higher), L* (between 7 and 11 points higher), and hab (between 16 and 20 points higher). Chen et al.,[43] found higher values of L* (around 4 points) and Hue (around 0.06 points) in wines sequentially fermented with *T. delbrueckii* compared to the control wines with *S. cerevisiae* strains. However, the authors also observed similar or even higher values for these parameters in wines sequentially fermented with *M. pulcherrima*, contrasting with the results of this work. *T. delbrueckii* produced wines with considerably lower values in red-green color component (a*), indicating less redness. In the wines elaborated with Cabernet Sauvignon, the levels of a* in the SI-Td wines were around half those of the control and SI-Mp wines. However, when Garnacha tinta was used to elaborate the rosé wines, this parameter decreased to values close to 0 in the SI-Td wines, while the values ranged between 8.1 and 11.4 in the control and SI-Mp wines (Table S3, Supporting Information). These results are in agreement with those found in a similar work,[43] in which the sequential fermentation with Td and Mp strains produced wines with 3−8 lower values of a*. The higher values obtained for color intensity (around 0.1−0.2 points) and for b* (around 2−4 points) in Sc wines also agree with Chen et al.,[43] who observed an increase of these color parameters in control wines with *S. cerevisiae* strains, although Del Fresno et al.[12] did not observe statistical differences between Sc and SI-Td wines.

The rosé wines elaborated with Garnacha tinta and Cabernet Sauvignon varieties showed significant differences in most of the enological parameters addressed (Table 2). Only ethanol, reducing sugars, and potassium remained unchanged regardless of the grape variety factor. The variation in several parameters with regard to the grape variety factor was noteworthy. Volatile acidity was found to be around 1.7-fold higher in the wines elaborated from Cabernet Sauvignon (0.43 g/L of acetic acid) compared with those elaborated from Garnacha tinta (0.25 g/L). The levels of anthocyans were up to 5-fold higher in the Cabernet Sauvignon wines, while the tannin levels in Garnacha tinta doubled those of Cabernet Sauvignon. Large differences were also observed in organic acids linked to the grape variety from which the wines were elaborated. The greater differences were observed for tartaric and malic acid, around 1.7 and 3.2-fold higher, respectively, in the wines elaborated from Garnacha tinta, while the values found for acetic, succinic, and lactic acids were around 2 or 3-fold higher in the rosé wines from Cabernet Sauvignon. The concentrations of acetaldehyde were higher in the Cabernet Sauvignon wines, while Garnacha tinta produced rosé wines with slightly more ethyl acetate.

Higher Alcohols. Higher alcohols represent an important group of desirable volatile compounds formed by yeasts during the alcoholic fermentation, making a greater contribution to secondary aroma.[47] Sequential fermentations with both *T. delbrueckii* and *M. pulcherrima* produced wines with enhanced concentrations of total higher alcohols of about 90 and 60 mg/L, respectively, compared to the *S. cerevisiae* control wines (Table 2). Some authors have also observed similar results for total higher alcohols, reporting increases that range between 60 and 85 mg/L for SI-Td wines and between 35 and 300 mg/L for SI-Mp wines,[4,9,11,47,48] while other studies reported no statistical differences or even the contrary trend in sequential inoculations with *M. pulcherrima*.[32,48] The differences between authors may be explained by the high variability between several *non-Sc* strains.[41]

Ester Composition. Instrumental and experimental factors may cause systematic intensity drift over long periods of time or multiple batches in GC-MS runs that must be taken into consideration during the data analysis. To this end, the samples spiked with ad hoc internal standards (IS) of the target metabolites are frequently used to normalize the response of each analyte in targeted studies.[49] However, the results are not always as expected since this method assumes the same variance in the signals of the internal standards and the analytes. Other methodologies, used in untargeted approaches, are based on computational techniques to correct the signal of analytes using pooled QC samples repeatedly analyzed throughout the entire experimental sequence.[49] Therefore, to obtain a more comprehensive metabolic profiling after IS normalization, a smoothed cubic spline was fitted to the QC samples to correct for the signal drift of all of the samples analyzed, including those used to build the calibration curves. The results were compared against the just IS normalized data. The quantitation of up to 32 esters was attempted, and respective totals of 27 and 25 esters for the drift-corrected and

https://dx.doi.org/10.1021/acs.jafc.0c06970
J. Agric. Food Chem. 2021, 69, 1598−1609

Journal of Agricultural and Food Chemistry pubs.acs.org/JAFC Article

Table 3. Two-way ANOVA for Grape and Fermentation Strategy Used for Rosé Wine Elaboration[a,b]

	grape			fermentation strategy				interaction
esters (μg/L)	GT	CS	*p*-value	CT	SI-Td	SI-Mp	*p*-value	*p*-value
ethyl butyrate	263a	166b	***	218b	174c	250a	***	ns
ethyl hexanoate	836a	594b	***	777b	441c	926a	***	***
ethyl octanoate	1053a	496b	***	862a	405b	1057a	***	*
ethyl decanoate	119a	43b	***	99a	55b	89a	**	ns
ethyl dodecanoate	131a	99b	**	113ab	89b	142a	**	ns
ethyl myristate	12.9	11.2	ns	12.0ab	9.3b	14.9a	**	**
ethyl palmitate	42	46	ns	38	47	47	ns	ns
ethyl stearate	14	16	ns	15	15	15	ns	***
∑EEFAs	2470a	1471b	***	2134b	1235c	2542a	***	**
propyl acetate	32a	23b	***	30a	27ab	25b	**	**
isobutyl acetate	43a	38b	*	31c	42b	48a	***	***
phenylethyl acetate	85	90	ns	87ab	107a	69b	**	*
isoamyl acetate	1329a	690b	***	1304a	530b	1194a	***	**
hexyl acetate	67a	22b	***	81a	17c	35b	***	ns
∑HAAs	1555a	862b	***	1533a	722b	1371a	***	**
ethyl isobutyrate	184b	292a	***	106b	496a	112b	***	***
ethyl 2-methylbutyrate	15b	26a	***	21a	22a	17b	***	ns
ethyl isovalerate	20b	29a	***	27a	18b	28a	***	***
ethyl phenylacetate	0.50b	1.32a	***	0.82	0.95	0.97	ns	**
∑EEBAs	219b	348a	***	155b	537a	158b	***	***
ethyl cinnamate	0.26b	0.29a	***	0.27b	0.29a	0.27b	*	*
ethyl dihydrocinnamate	2.75b	7.72a	***	1.23b	13.23a	1.26b	***	***
∑cinnamates	3.01b	8.02a	***	1.50b	13.52a	1.53b	***	***
methyl hexanoate	2.72a	1.71b	***	2.27b	1.46c	2.93a	***	**
methyl octanoate	3.3a	2.2b	***	2.8ab	2.2b	3.2a	**	*
methyl decanoate	0.47a	0.34b	**	0.50a	0.25b	0.46a	***	ns
∑MEFAs	6.5a	4.3b	***	5.6b	3.9c	6.6a	***	**
ethyl valerate	1.09	1.03	ns	1.00	1.08	1.10	ns	**
ethyl heptanoate	1.97	2.17	ns	2.56a	1.03b	2.61a	***	ns
ethyl nonanoate	0.51b	0.63a	***	0.60a	0.51b	0.60a	**	ns
∑EEOCNAs	3.6	3.8	ns	4.2a	2.6b	4.3a	***	ns
isoamyl butyrate	0.97b	1.05a	**	0.94b	0.96b	1.13a	***	**
isobutyl hexanoate	0.34	0.36	ns	0.27b	0.29b	0.50a	***	***
∑miscellaneous	1.31b	1.41a	*	1.20b	1.25b	1.62a	***	ns
total esters	4258a	2699b	***	3834a	2516b	4085a	***	***

[a]Mean is given for esters. [b]*p*-Value of the two-way ANOVA; ns: not significant, *: 0.05 > *p*-value > 0.01, **: 0.01 > *p*-value > 0.001, and ***: *p*-value < 0.001. Mean values with different letters differ significantly. GT: Garnacha tinta; CS: Cabernet Sauvignon; CT: wines fermented with *S. cerevisiae* strains; SI-Td: wines fermented with sequential inoculation of *T. delbrueckii* and *S. cerevisiae* strains; and SI-Mp: wines fermented with sequential inoculation of *M. pulcherrima* and *S. cerevisiae* strains.

the noncorrected data were satisfactorily fitted in terms of linearity. For both approaches, isoamyl hexanoate, isoamyl octanoate, octyl acetate, methyl butyrate, and ethyl propanoate displayed highly unstable responses for the current experimental conditions. Meanwhile, ethyl dodecanoate and ethyl palmitate had linear correlation coefficients of 0.899 and 0.963 for the just IS normalized data against 0.991 and 0.983 for the drift-corrected data. Additionally, since the samples were randomly analyzed in analytical duplicates and experimental triplicates, the drift correction made it possible to significantly reduce the standard deviation of the entire dataset. In this sense, several compounds, including ethyl dodecanoate, ethyl palmitate, and other esters such as ethyl decanoate, ethyl phenylacetate, and ethyl nonanoate, were discarded in the just IS normalized approach due to high relative standard deviation (RSD > 30) in the analytical replicates, while low deviations were obtained when the data was drift-corrected. Therefore, a total of 27 esters were successfully quantified by fitting a smoothed cubic spline against 22 without the drift correction. The performances of the calibration curves are compared in Table S1, Supporting Information. A series of PCAs were plotted to check the final quality of the data obtained for both strategies (Figures S1 and S2, Supporting Information) and only subtle differences were observed in the metabolites properly quantified with both approaches. Therefore, the application of drift corrections by means of a smoothed cubic spline proved to be a suitable computer strategy in combination with IS normalization to improve the quality of the data in targeted GC-MS studies.

Subsequently, a two-way analysis of variance (ANOVA) was carried out to study differences in the ester composition due to the fermentation strategy and grape variety used (Table 3). Esters were grouped into different families according to their chemical structure and origin in ethyl esters of fatty acids (EEFAs), higher alcohol acetates (HAAs), ethyl esters of branched acids (EEBAs), cinnamates, methyl esters of fatty acids (MEFAs), ethyl esters of odd carbon-chain fatty acids (EEOCNFA), and miscellaneous (Table 3). Differences in the

https://dx.doi.org/10.1021/acs.jafc.0c06970
J. Agric. Food Chem. 2021, 69, 1598−1609

Journal of Agricultural and Food Chemistry pubs.acs.org/JAFC Article

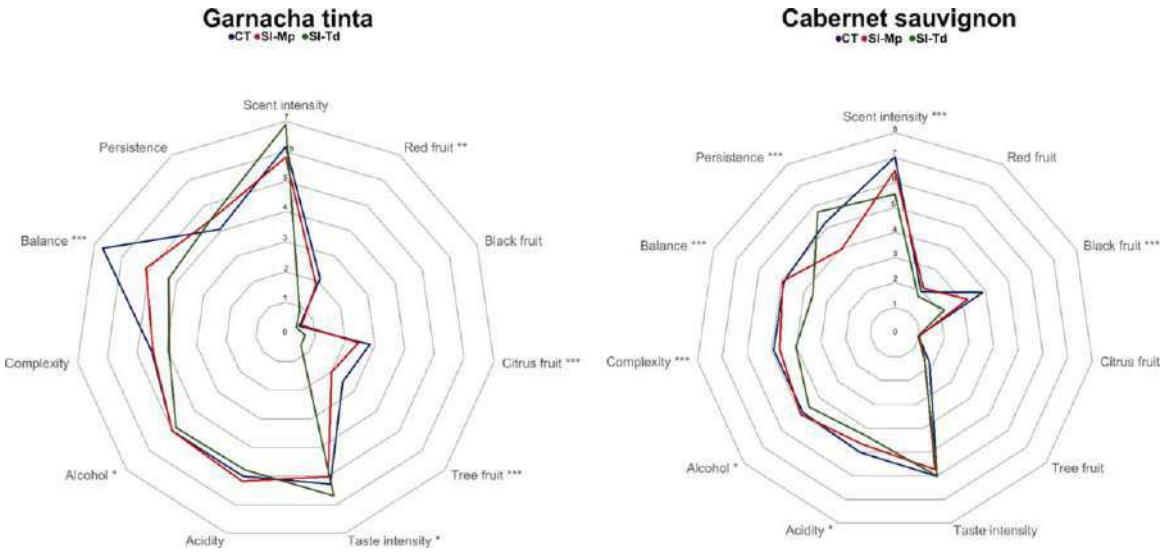

Figure 3. Cobweb diagram of the sensory scores for wines elaborated with Garnacha tinta and Cabernet Sauvignon and different fermentation strategies. CT: wines fermented with *S. cerevisiae* strains; SI-Td: wines fermented with sequential inoculation of *T. delbrueckii* and *S. cerevisiae* strains; SI-Mp: wines fermented with sequential inoculation of *M. pulcherrima* and *S. cerevisiae* strains. *p*-value from the two-way ANOVA. ns: not significant, *: 0.05 > *p*-value > 0.01, **: 0.01 > *p*-value > 0.001, and ***: *p*-value < 0.001.

ester profile were observed due to the fermentation strategy (Table 3). EEFAs and HAAs were the most abundant families, accounting for 95% of the total esters found in the CT and SI-Mp wines. However, different behaviors were found in the SI-Td wines, in which EEFAs and HAAs accounted for only 77% of the total esters and EEBAs for 21%. This trend in the EEBA family was due to a 3-fold (Garnacha tinta wines) and 6-fold (Cabernet Sauvignon wines) increase in ethyl isobutyrate compared to the other fermentation strategies (Table S3, Supporting Information). Similar proportions of these major volatile esters were reported in a previous study.[16] However, SI-Td produced wines with lower overall esters, explained by a decrease in medium-chain fatty acid ethyl esters (C_4–C_{12}), ethyl myristate, and isoamyl acetate (Table 3). Previous studies carried out in white wines sequentially fermented with Td yeasts also observed a clear decrease in esters of C_4–C_{10} fatty acids and isoamyl acetate.[15,50] This behavior may be related to the specific activity of Td yeasts during sequential fermentation since these metabolites were found in the same or even slightly higher levels for the SI-Mp wines (Table 3). Therefore, although some differences were observed for other minor volatile esters, changes in the ester profile linked to the fermentation strategy were far subtler for SI-Mp. Other esters, such as cinnamates, were found in statistically higher concentrations in the SI-Td wines, in particular in the Cabernet Sauvignon wines, reaching close to 20 μg/L (Table S3, Supporting Information). Meanwhile, MEFAs, EEOCNAs, and miscellaneous esters were always observed in lower levels in these wines.

The ester profile was also affected by the grape variety from which the wines were produced. Garnacha tinta produced wines with around 1.5-fold higher levels of total esters than Cabernet Sauvignon. The changes in these volatile compounds were highly linked to their chemical structures. EEFAs, HAAs, and MEFAs were at least equal or higher in the rosé wines elaborated from Garnacha tinta, while the contrary behavior was observed for EEBAs, cinnamates, and EEOCNAs (Table 3).

Sensory. The fermentative strategy impacted the sensory perception of the rosé wines (Figure 3). Independently of the grape variety used to produce them, fruity descriptors were scored lower in the SI-Td rosé wines in agreement with previous studies.[15,50] Meanwhile, although fruity nuances were perceived slightly in the CT and SI-Mp wines, significantly greater scores were given for citrus fruit, tree fruit, and red fruit in the wines elaborated from Garnacha tinta and for black fruit in those elaborated from Cabernet Sauvignon. The differences in the fruitiness linked to the grape variety could be explained by the higher overall esters found in Garnacha tinta wines (Table 3). The current results agree with the decrease in the volatile profile reported above since ethyl esters of medium-chain fatty acids exert strong influences on the fruity scent of wines.[50,51] Among them, the powerful odorant ethyl octanoate with ripe fruits, pear, and sweet notes[51] only remained below its odor perception threshold (580 μg/L[52]) in the rosé wines fermented with Td yeasts (Table 3). The substantial decrease in isoamyl acetate, an active odorant with banana notes,[51] detected in all of the samples at much greater levels (Table 3) than its perception threshold (30 μg/L[53]) may also play an important role in the reduced fruitiness reported in the SI-Td rosé wines. The sensory attribute balance displayed significant differences with regard to the grape variety and fermentation strategy used for winemaking. For both grape varieties, SI-Td produced rosé wines with the lowest balance and alcohol scores, while the former was enhanced in the CT rosé wines elaborated from Garnacha tinta (Figure 3). Additionally, a positive effect on taste intensity was found in the SI-Td wines elaborated with the Garnacha tinta variety. The sensory attribute persistence showed statistical differences between the fermentation strategies only in wines produced from Cabernet Sauvignon, observing an increase in SI-Td wines, which could

https://dx.doi.org/10.1021/acs.jafc.0c06970
J. Agric. Food Chem. 2021, 69, 1598−1609

Journal of Agricultural and Food Chemistry pubs.acs.org/JAFC Article

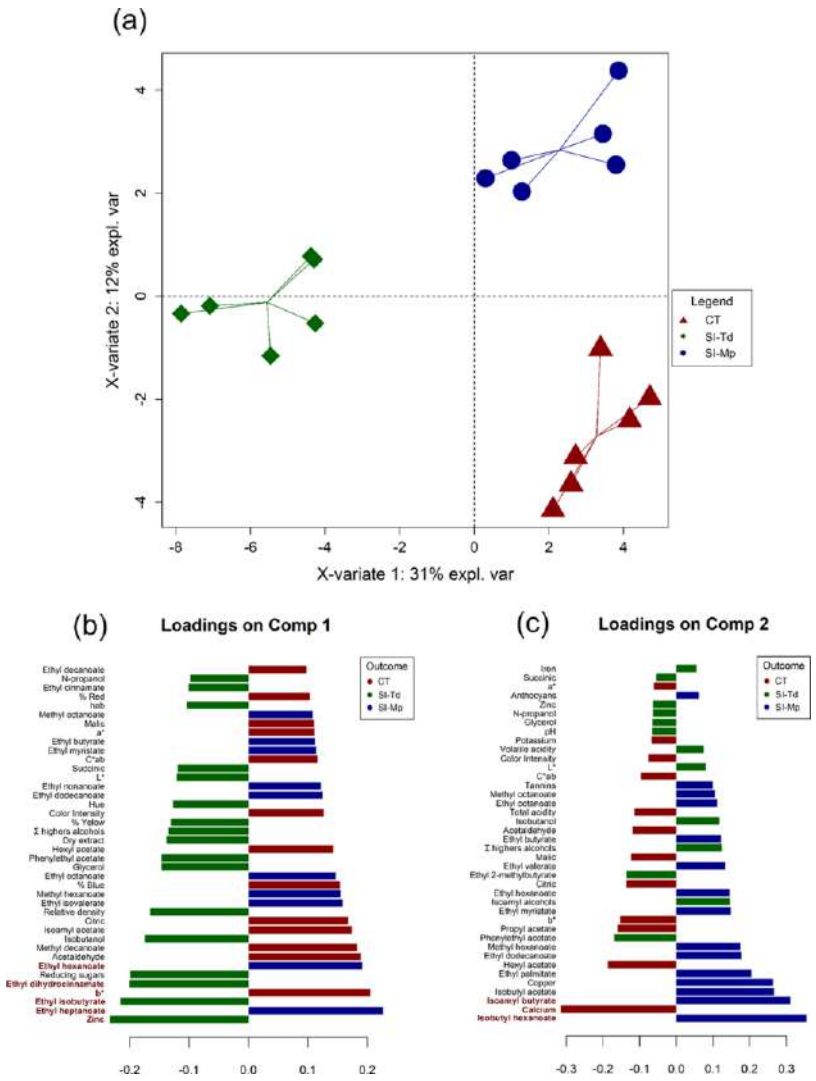

Figure 4. Graphical outputs of the partial least squares discriminant analysis (PLS-DA) performed on the fermentation strategy factor using data from GC-MS and enological analyses. (a) Score plot for components 1 and 2 (X-variate 1 and X-variate 2) and (b, c) loading plots of components 1 and 2, respectively (in red metabolites selected as potential markers during the variable reduction procedure). The color indicates the class for which the compound has a maximal mean value. Bar length represents the multivariate regression coefficient with either a positive or negative sign for that particular feature of each component, i.e., the importance of each variable in the model. CT: wines fermented with *S. cerevisiae* strains; SI-Td: wines fermented with sequential inoculation of *T. delbrueckii* and *S. cerevisiae* strains; and SI-Mp: wines fermented with sequential inoculation of *M. pulcherrima* and *S. cerevisiae* strains.

be explained by the higher polysaccharide contents reported for *T. delbrueckii* compared to *Saccharomyces*.[38]

Multivariate Approach. The data collected from the different sources were fused, and a partial least squares discriminant analysis (PLS-DA) was performed to study the differences related to the fermentation strategy. The PLS-DA model displayed a satisfactory mean overall error of 0.04 ± 0.03 optimized for three components. Disclosed by classes, respective errors of 0.09 ± 0.09, 0.03 ± 0.07, and 0.01 ± 0.06 were obtained for CT, SI-Td, and SI-Mp, and the statistical significance of the model calculated on the basis of a permutation test (N = 1000) was 0.002. The results from the first two components of the PLS-DA model showed the most interesting differences found in the data (Figure 4). The wines produced from each fermentation strategy were grouped into different well-defined scattering regions (Figure 4a). The SI-Td samples were mainly discriminated on the first component of the model (X-variate 1), which explained around the 31% of the total variance found in samples. In addition, the SI-Td wines fell between the CT and SI-Mp samples in the direction of the second component of the model (X-variate 2), which explained 12% of the total variance, highlighting an additional contribution to this component to differentiate wines sequentially fermented with Td yeasts. Therefore, the variables with a high contribution to component 2 were highly related to the fermentation strategy and were

https://dx.doi.org/10.1021/acs.jafc.0c06970
J. Agric. Food Chem. 2021, 69, 1598−1609

also strain dependent. Meanwhile, both the CT and SI-Mp samples were only discriminated in the direction of the component 2. Based on these results, it was to be expected that SI-Td wines had the most distinct metabolic, enological, and sensory profiles. The variables responsible for the groupings of the wine samples can be consulted in the loading bar plots of Figure 4b,c. Only the first 40 variables were displayed in both graphics due to figure margin limitations and the low contribution of the rest of the variables to the sample discrimination. In addition, the potential markers selected in the iterative variable selection procedure are highlighted in bold and red on the loading bar plot of Figure 4. Zinc, ethyl isobutyrate, and ethyl dihydrocinnamate were selected as the main contributors to differentiate the SI-Td samples from the rest (Figure 4b). Ethyl isobutyrate and ethyl dihydrocinnamate are potent odorant compounds observed in much higher concentrations in the SI-Td wines (Table 3) that have already been described as specific markers of Td activity.[15,16] Zinc was found in a mean concentration of 0.44 mg/L in the SI-Td wines, meaning around 3-fold higher levels compared to the wines produced with other fermentation strategies (Table 2). Zinc is an essential micronutrient accumulated by yeasts during fermentation, whose bioavailability in grape must affect the fermentation progress and ethanol yields.[54] Meanwhile, ethyl heptanoate, ethyl hexanoate, and the color parameter for yellowness b* were highlighted as the most discriminative variables of the CT and SI-Mp wines (Figure 4b). In other terms, these variables were found in overall lower contents in the SI-Td wines. Ethyl hexanoate is an ethyl ester of medium-chain fatty acids related to fruity, green apple, brandy, and wine-like smell[55] present in the samples at much greater concentrations (Table 3) than its perception threshold,[52] while ethyl heptanoate is associated with fruity and apple notes.[56] In regard to component 2 of the PLS-DA model, isobutyl hexanoate and isoamyl butyrate were selected as the most discriminative compounds and were found in higher overall concentrations in the SI-Mp wines, while calcium was selected as the marker for the CT wines (Figure 4c). As stated above, since the SI-Td wines fell between the CT and SI-Mp wines, these variables were considered as potential markers for the sequential inoculation. However, the modulation of these compounds was dependent on the grape variety assayed (Table S4, Supporting Information).

The results of this study support the use of sequential inoculation with non-*Saccharomyces* yeasts as a useful tool for modulating the quality and sensory properties of rosé wines. Sequential fermentation with *T. delbrueckii* produced wines with lower ethanol contents and lower concentrations of ethyl esters of medium-chain fatty acids and isoamyl acetate, which reduced its fruitiness perception, but resulted in higher concentrations of other important odorant esters such as cinnamates and ethyl esters of branched acids that may enhance specific sensory descriptors of rosé wines. Sequential inoculation with *M. pulcherrima* enabled rosé wines to be obtained with an enhanced ester profile, reduced acetaldehyde levels, and increased anthocyanins and tannins. The multivariate approach made it possible to assess the contribution of chemicals and sensory attributes to the discrimination of samples, and the most discriminative chemicals were highlighted using a variable reduction procedure.

■ ASSOCIATED CONTENT

Supporting Information

The Supporting Information is available free of charge at https://pubs.acs.org/doi/10.1021/acs.jafc.0c06970.

Calibration curve performances for drift-corrected data using smoothed cubic spline after IS normalized data and just IS normalized data (Table S1); interactions of the two-way ANOVA performed on the relative abundances of the yeast strains present in rosé wines at the end of the alcoholic fermentation (Table S2); interactions of the two-way ANOVA for grape and yeast strategy used for rosé wine elaboration (Table S3); principal component analysis performed for IS normalized and drift-corrected data (Figure S1); and principal component analysis performed for IS normalized data (Figure S2) (PDF)

Modulation of compounds depending on the grape variety (Table S4) (XLSX)

■ AUTHOR INFORMATION

Corresponding Authors

José Manuel Muñoz-Redondo − *Department of Food Science and Health, Andalusian Institute of Agricultural and Fisheries Research and Training (IFAPA), 14004 Córdoba, Spain;* orcid.org/0000-0002-8912-4354; Phone: +34 666 30 66 51; Email: josem.munoz.redondo@juntadeandalucia.es

José Manuel Moreno-Rojas − *Department of Food Science and Health, Andalusian Institute of Agricultural and Fisheries Research and Training (IFAPA), 14004 Córdoba, Spain*; Phone: +34 671 53 27 58; Email: josem.moreno.rojas@juntadeandalucia.es; Fax: +34 957 01 60 43

Authors

Belén Puertas − *Department of Food Science and Health, Andalusian Institute of Agricultural and Fisheries Research and Training (IFAPA), 11471 Jerez de la Frontera, Cádiz, Spain*

Emma Cantos-Villar − *Department of Food Science and Health, Andalusian Institute of Agricultural and Fisheries Research and Training (IFAPA), 11471 Jerez de la Frontera, Cádiz, Spain;* orcid.org/0000-0001-8560-8821

María Jesús Jiménez-Hierro − *Department of Food Science and Health, Andalusian Institute of Agricultural and Fisheries Research and Training (IFAPA), 11471 Jerez de la Frontera, Cádiz, Spain*

María Carbú − *Microbiology Laboratory, Department of Biomedicine, Biotechnology and Heald Public, Faculty of Marine and Environmental Sciences, University of Cádiz, 11510 Puerto Real, Spain*

Carlos Garrido − *Microbiology Laboratory, Department of Biomedicine, Biotechnology and Heald Public, Faculty of Marine and Environmental Sciences, University of Cádiz, 11510 Puerto Real, Spain*

María José Ruiz-Moreno − *Department of Food Science and Health, Andalusian Institute of Agricultural and Fisheries Research and Training (IFAPA), 14004 Córdoba, Spain;* orcid.org/0000-0002-0688-3014

Complete contact information is available at: https://pubs.acs.org/10.1021/acs.jafc.0c06970

https://dx.doi.org/10.1021/acs.jafc.0c06970
J. Agric. Food Chem. 2021, 69, 1598−1609

Funding
J.M.M.-R. was awarded a research contract funded by the Andalusian Institute of Agricultural and Fisheries Research and Training (IFAPA), within the National Youth Guarantee System funded through the European Social Fund (ESF) and the Youth Employment Initiative (YEI). M.J.R.-M. was supported by a research contract funded by IFAPA and ESF (09/2012 to 08/2017). This study has been funded by the Andalusian Institute of Agricultural and Fisheries Research and Training (IFAPA) through the Project "Investigación e Innovación Tecnológica en Vitivinicultura" (PR.AVA.A-VA2019.016) and the European Rural Development Fund (ERDF, EU).

Notes
The authors declare no competing financial interest.

■ ACKNOWLEDGMENTS

The authors are grateful for the collaboration of Lallemand by kindly providing yeasts and technical support.

■ REFERENCES

(1) Roullier-Gall, C.; David, V.; Hemmler, D.; Schmitt-Kopplin, P.; Alexandre, H. Exploring Yeast Interactions through Metabolic Profiling. *Sci. Rep.* **2020**, *10*, No. 6073.
(2) Sieuwerts, S.; De Bok, F. A.; Hugenholtz, J.; van Hylckama Vlieg, J. E. Unraveling Microbial Interactions in Food Fermentations: From Classical to Genomics Approaches. *Appl. Environ. Microbiol.* **2008**, *74*, 4997−5007.
(3) Lee, P.-R.; Chong, I. S.-M.; Yu, B.; Curran, P.; Liu, S.-Q. Effects of Sequentially Inoculated *Williopsis saturnus* and *Saccharomyces cerevisiae* on Volatile Profiles of Papaya Wine. *Food Res. Int.* **2012**, *45*, 177−183.
(4) González-Royo, E.; Pascual, O.; Kontoudakis, N.; Esteruelas, M.; Esteve-Zarzoso, B.; Mas, A.; Canals, J. M.; Zamora, F. Oenological Consequences of Sequential Inoculation with Non-*Saccharomyces* Yeasts (*Torulaspora delbrueckii* or *Metschnikowia pulcherrima*) and *Saccharomyces cerevisiae* in Base Wine for Sparkling Wine Production. *Eur. Food Res. Technol.* **2015**, *240*, 999−1012.
(5) Vicente, J.; Ruiz, J.; Belda, I.; Benito-Vázquez, I.; Marquina, D.; Calderón, F.; Santos, A.; Benito, S. The Genus *Metschnikowia* in Enology. *Microorganisms* **2020**, *8*, No. 1038.
(6) Ramírez, M.; Velázquez, R. The Yeast *Torulaspora delbrueckii*: An Interesting but Difficult-to-Use Tool for Winemaking. *Fermentation* **2018**, *4*, No. 94.
(7) Benito, S. The Impact of *Torulaspora delbrueckii* Yeast in Winemaking. *Appl. Microbiol. Biotechnol.* **2018**, *102*, 3081−3094.
(8) Ciani, M.; Capece, A.; Comitini, F.; Canonico, L.; Siesto, G.; Romano, P. Yeast Interactions in Inoculated Wine Fermentation. *Front. Microbiol.* **2016**, *7*, No. 555.
(9) Loira, I.; Vejarano, R.; Bañuelos, M. A.; Morata, A.; Tesfaye, W.; Uthurry, C.; Villa, A.; Cintora, I.; Suárez-Lepe, J. A. Influence of Sequential Fermentation with *Torulaspora delbrueckii* and *Saccharomyces cerevisiae* on Wine Quality. *LWT—Food Sci. Technol.* **2014**, *59*, 915−922.
(10) Gobbi, M.; Comitini, F.; Domizio, P.; Romani, C.; Lencioni, L.; Mannazzu, I.; Ciani, M. *Lachancea thermotolerans* and *Saccharomyces cerevisiae* in Simultaneous and Sequential Co-Fermentation: A Strategy to Enhance Acidity and Improve the Overall Quality of Wine. *Food Microbiol.* **2013**, *33*, 271−281.
(11) Puertas, B.; Jiménez, M. J.; Cantos-Villar, E.; Cantoral, J. M.; Rodríguez, M. E. Use of *Torulaspora delbrueckii* and *Saccharomyces cerevisiae* in Semi-Industrial Sequential Inoculation to Improve Quality of Palomino and Chardonnay Wines in Warm Climates. *J. Appl. Microbiol.* **2017**, *122*, 733−746.
(12) Del Fresno, J. M.; Morata, A.; Loira, I.; Bañuelos, M. A.; Escott, C.; Benito, S.; Chamorro, C. G.; Suárez-Lepe, J. A. Use of Non-*Saccharomyces* in Single-Culture, Mixed and Sequential Fermentation to Improve Red Wine Quality. *Eur. Food Res. Technol.* **2017**, *243*, 2175−2185.
(13) Oliveira, I.; Ferreira, V. Modulating Fermentative, Varietal and Aging Aromas of Wine Using Non-*Saccharomyces* Yeasts in a Sequential Inoculation Approach. *Microorganisms* **2019**, *7*, No. 164.
(14) Taillandier, P.; Lai, Q. P.; Julien-Ortiz, A.; Brandam, C. Interactions between *Torulaspora delbrueckii* and *Saccharomyces cerevisiae* in Wine Fermentation: Influence of Inoculation and Nitrogen Content. *World J. Microbiol. Biotechnol.* **2014**, *30*, 1959−1967.
(15) Puertas, B.; Jimenez-Hierro, M. J.; Cantos-Villar, E.; Marrufo-Curtido, A.; Carbú, M.; Cuevas, F. J.; Moreno-Rojas, J. M.; González-Rodríguez, V. E.; Cantoral, J. M.; Ruiz-Moreno, M. J. The Influence of Yeast on Chemical Composition and Sensory Properties of Dry White Wines. *Food Chem.* **2018**, *253*, 227−235.
(16) Renault, P.; Coulon, J.; de Revel, G.; Barbe, J.-C.; Bely, M. Increase of Fruity Aroma during Mixed *T. delbrueckii*/*S. cerevisiae* Wine Fermentation Is Linked to Specific Esters Enhancement. *Int. J. Food Microbiol.* **2015**, *207*, 40−48.
(17) Loira, I.; Morata, A.; Comuzzo, P.; Callejo, M. J.; González, C.; Calderón, F.; Suárez-Lepe, J. A. Use of *Schizosaccharomyces pombe* and *Torulaspora delbrueckii* Strains in Mixed and Sequential Fermentations to Improve Red Wine Sensory Quality. *Food Res. Int.* **2015**, *76*, 325−333.
(18) Canonico, L.; Comitini, F.; Oro, L.; Ciani, M. Sequential Fermentation with Selected Immobilized Non-*Saccharomyces* Yeast for Reduction of Ethanol Content in Wine. *Front. Microbiol.* **2016**, *7*, No. 278.
(19) Muñoz-Redondo, J. M.; Ruiz-Moreno, M. J.; Puertas, B.; Cantos-Villar, E.; Moreno-Rojas, J. M. Multivariate Optimization of Headspace Solid-Phase Microextraction Coupled to Gas Chromatography-Mass Spectrometry for the Analysis of Terpenoids in Sparkling Wines. *Talanta* **2020**, *208*, No. 120483.
(20) Ottaviani, D.; Parlani, C.; Citterio, B.; Masini, L.; Leoni, F.; Canonico, C.; Sabatini, L.; Bruscolini, F.; Pianetti, A. Putative Virulence Properties of Aeromonas Strains Isolated from Food, Environmental and Clinical Sources in Italy: A Comparative Study. *Int. J. Food Microbiol.* **2011**, *144*, 538−545.
(21) Vaudano, E.; Garcia-Moruno, E. Discrimination of *Saccharomyces cerevisiae* Wine Strains Using Microsatellite Multiplex PCR and Band Pattern Analysis. *Food Microbiol.* **2008**, *25*, 56−64.
(22) Zapparoli, G.; Reguant, C.; Bordons, A.; Torriani, S.; Dellaglio, F. Genomic DNA Fingerprinting of Oenococcus Oeni Strains by Pulsed-Field Gel Electrophoresis and Randomly Amplified Polymorphic DNA-PCR. *Curr. Microbiol.* **2000**, *40*, 351−355.
(23) OIV (2012). *Compendium of International Methods of Analysis of Wines and Musts*; Office International de La Vigne et Du Vin, Recueil Des Met Hodes Internationales d'analyse Des Vins et Des Mouts: Paris, 1990.
(24) Antalick, G.; Perello, M.-C.; de Revel, G. Development, Validation and Application of a Specific Method for the Quantitative Determination of Wine Esters by Headspace-Solid-Phase Microextraction-Gas Chromatography−Mass Spectrometry. *Food Chem.* **2010**, *121*, 1236−1245.
(25) Kokla, M.; Kl\aavus, A.; Noerman, S.; Koistinen, V. M.; Tuomainen, M.; Zarei, I.; Meuronen, T.; Häkkinen, M. R.; Rummukainen, S.; Babu, A. F. "NoTaMe": Workflow for Non-Targeted LC-MS Metabolic Profiling. *Metabolites* **2020**, No. 135.
(26) Sumner, L. W.; Amberg, A.; Barrett, D.; Beale, M. H.; Beger, R.; Daykin, C. A.; Fan, T. W.-M.; Fiehn, O.; Goodacre, R.; Griffin, J. L.; Hankemeier, T.; Hardy, N.; Harnly, J.; Higashi, R.; Kopka, J.; Lane, A. N.; Lindon, J. C.; Marriott, P.; Nicholls, A. W.; Reily, M. D.; Thaden, J. J.; Viant, M. R. Proposed Minimum Reporting Standards for Chemical Analysis. *Metabolomics* **2007**, *3*, 211−221.
(27) Szymańska, E.; Saccenti, E.; Smilde, A. K.; Westerhuis, J. A. Double-Check: Validation of Diagnostic Statistics for PLS-DA Models in Metabolomics Studies. *Metabolomics* **2012**, *8*, 3−16.

https://dx.doi.org/10.1021/acs.jafc.0c06970
J. Agric. Food Chem. 2021, 69, 1598−1609

(28) Rohart, F.; Gautier, B.; Singh, A.; Le Cao, K.-A. MixOmics: An R Package for 'omics Feature Selection and Multiple Data Integration. *PLoS Comput. Biol.* **2017**, *13*, No. e1005752.
(29) Belda, I.; Navascués, E.; Marquina, D.; Santos, A.; Calderon, F.; Benito, S. Dynamic Analysis of Physiological Properties of *Torulaspora delbrueckii* in Wine Fermentations and Its Incidence on Wine Quality. *Appl. Microbiol. Biotechnol.* **2015**, *99*, 1911−1922.
(30) Constantí, M.; Poblet, M.; Arola, L.; Mas, A.; Guillamón, J. M. Analysis of Yeast Populations during Alcoholic Fermentation in a Newly Established Winery. *Am. J. Enol. Viticult.* **1997**, *48*, 339−344.
(31) Dutraive, O.; Benito, S.; Fritsch, S.; Beisert, B.; Patz, C.-D.; Rauhut, D. Effect of Sequential Inoculation with Non-*Saccharomyces* and *Saccharomyces* Yeasts on Riesling Wine Chemical Composition. *Fermentation* **2019**, *5*, No. 79.
(32) Benito, S.; Hofmann, T.; Laier, M.; Lochbühler, B.; Schüttler, A.; Ebert, K.; Fritsch, S.; Röcker, J.; Rauhut, D. Effect on Quality and Composition of Riesling Wines Fermented by Sequential Inoculation with Non-*Saccharomyces* and *Saccharomyces cerevisiae*. *Eur. Food Res. Technol.* **2015**, *241*, 707−717.
(33) Hranilovic, A.; Gambetta, J. M.; Jeffery, D. W.; Grbin, P. R.; Jiranek, V. Lower-Alcohol Wines Produced by *Metschnikowia pulcherrima* and *Saccharomyces cerevisiae* Co-Fermentations: The Effect of Sequential Inoculation Timing. *Int. J. Food Microbiol.* **2020**, *329*, No. 108651.
(34) García, M.; Esteve-Zarzoso, B.; Cabellos, J. M.; Arroyo, T. Sequential Non-*Saccharomyces* and *Saccharomyces cerevisiae* Fermentations to Reduce the Alcohol Content in Wine. *Fermentation* **2020**, *6*, No. 60.
(35) Belda, I.; Ruiz, J.; Beisert, B.; Navascués, E.; Marquina, D.; Calderón, F.; Rauhut, D.; Benito, S.; Santos, A. Influence of *Torulaspora delbrueckii* in Varietal Thiol (3-SH and 4-MSP) Release in Wine Sequential Fermentations. *Int. J. Food Microbiol.* **2017**, *257*, 183−191.
(36) Ciani, M.; Ferraro, L. Enhanced Glycerol Content in Wines Made with Immobilized *Candida stellata* Cells. *Appl. Environ. Microbiol.* **1996**, *62*, 128−132.
(37) Noble, A. C.; Bursick, G. F. The Contribution of Glycerol to Perceived Viscosity and Sweetness in White Wine. *Am. J. Enol. Viticult.* **1984**, *35*, 110−112.
(38) Domizio, P.; Liu, Y.; Bisson, L. F.; Barile, D. Use of Non-*Saccharomyces* Wine Yeasts as Novel Sources of Mannoproteins in Wine. *Food Microbiol.* **2014**, *43*, 5−15.
(39) Escribano-Viana, R.; Portu, J.; Garijo, P.; López, R.; Santamaría, P.; López-Alfaro, I.; Gutiérrez, A. R.; González-Arenzana, L. Effect of the Sequential Inoculation of Non-*Saccharomyces*/*Saccharomyces* on the Anthocyans and Stilbenes Composition of Tempranillo Wines. *Front. Microbiol.* **2019**, *10*, No. 773.
(40) Jolly, N. P.; Augustyn, O. P. R.; Pretorius, I. S. The Effect of Non-*Saccharomyces* Yeasts on Fermentation and Wine Quality. *S. Afr. J. Enol. Viticult.* **2003**, *24*, 55−62.
(41) Escribano, R.; González-Arenzana, L.; Portu, J.; Garijo, P.; López-Alfaro, I.; López, R.; Santamaría, P.; Gutiérrez, A. R. Wine Aromatic Compound Production and Fermentative Behaviour within Different Non-*Saccharomyces* Species and Clones. *J. Appl. Microbiol.* **2018**, *124*, 1521−1531.
(42) Ciani, M.; Maccarelli, F. Oenological Properties of Non-*Saccharomyces* Yeasts Associated with Wine-Making. *World J. Microbiol. Biotechnol.* **1998**, *14*, 199−203.
(43) Chen, K.; Escott, C.; Loira, I.; del Fresno, J. M.; Morata, A.; Tesfaye, W.; Calderon, F.; Suárez-Lepe, J. A.; Han, S.; Benito, S. Use of Non-*Saccharomyces* Yeasts and Oenological Tannin in Red Winemaking: Influence on Colour, Aroma and Sensorial Properties of Young Wines. *Food Microbiol.* **2018**, *69*, 51−63.
(44) Rousseva, M.; Kontoudakis, N.; Schmidtke, L. M.; Scollary, G. R.; Clark, A. C. Impact of Wine Production on the Fractionation of Copper and Iron in Chardonnay Wine: Implications for Oxygen Consumption. *Food Chem.* **2016**, *203*, 440−447.
(45) Onianwa, P. C.; Adeyemo, A. O.; Idowu, O. E.; Ogabiela, E. E. Copper and Zinc Contents of Nigerian Foods and Estimates of the Adult Dietary Intakes. *Food Chem.* **2001**, *72*, 89−95.
(46) Liu, S.-Q.; Pilone, G. J. An Overview of Formation and Roles of Acetaldehyde in Winemaking with Emphasis on Microbiological Implications. *Int. J. Food Sci. Technol.* **2000**, *35*, 49−61.
(47) Escribano-Viana, R.; González-Arenzana, L.; Portu, J.; Garijo, P.; López-Alfaro, I.; López, R.; Santamaría, P.; Gutiérrez, A. R. Wine Aroma Evolution throughout Alcoholic Fermentation Sequentially Inoculated with Non-*Saccharomyces*/*Saccharomyces* Yeasts. *Food Res. Int.* **2018**, *112*, 17−24.
(48) Varela, C.; Sengler, F.; Solomon, M.; Curtin, C. Volatile Flavour Profile of Reduced Alcohol Wines Fermented with the Non-Conventional Yeast Species *Metschnikowia pulcherrima* and *Saccharomyces uvarum*. *Food Chem.* **2016**, *209*, 57−64.
(49) Thonusin, C.; IglayReger, H. B.; Soni, T.; Rothberg, A. E.; Burant, C. F.; Evans, C. R. Evaluation of Intensity Drift Correction Strategies Using MetaboDrift, a Normalization Tool for Multi-Batch Metabolomics Data. *J. Chromatogr. A* **2017**, *1523*, 265−274.
(50) Azzolini, M.; Tosi, E.; Lorenzini, M.; Finato, F.; Zapparoli, G. Contribution to the Aroma of White Wines by Controlled *Torulaspora delbrueckii* Cultures in Association with *Saccharomyces cerevisiae*. *World J. Microbiol. Biotechnol.* **2015**, *31*, 277−293.
(51) Gómez-Míguez, M. J.; Cacho, J. F.; Ferreira, V.; Vicario, I. M.; Heredia, F. J. Volatile Components of Zalema White Wines. *Food Chem.* **2007**, *100*, 1464−1473.
(52) Ruiz-Moreno, M. J.; Muñoz-Redondo, J. M.; Cuevas, F. J.; Marrufo-Curtido, A.; León, J. M.; Ramírez, P.; Moreno-Rojas, J. M. The Influence of Pre-Fermentative Maceration and Ageing Factors on Ester Profile and Marker Determination of Pedro Ximenez Sparkling Wines. *Food Chem.* **2017**, *230*, 697−704.
(53) Ferreira, V.; Lopez, R.; Cacho, J. F. Quantitative Determination of the Odorants of Young Red Wines from Different Grape Varieties. *J. Sci. Food Agric.* **2000**, *80*, 1659−1667.
(54) Zhao, X.-Q.; Bai, F. Zinc and Yeast Stress Tolerance: Micronutrient Plays a Big Role. *J. Biotechnol.* **2012**, *158*, 176−183.
(55) Welke, J. E.; Zanus, M.; Lazzarotto, M.; Zini, C. A. Quantitative Analysis of Headspace Volatile Compounds Using Comprehensive Two-Dimensional Gas Chromatography and Their Contribution to the Aroma of Chardonnay Wine. *Food Res. Int.* **2014**, *59*, 85−99.
(56) Fan, W.; Qian, M. C. Characterization of Aroma Compounds of Chinese "Wuliangye" and "Jiannanchun" Liquors by Aroma Extract Dilution Analysis. *J. Agric. Food Chem.* **2006**, *54*, 2695−2704.

https://dx.doi.org/10.1021/acs.jafc.0c06970
J. Agric. Food Chem. 2021, 69, 1598−1609

CAPÍTULO 2

CALIDAD AROMÁTICA DEL BRANDY DE JEREZ

Resumen

La calidad aromática del brandy, al igual que en el vino, es uno de los atributos con mayor relevancia para los consumidores. Su resultado depende en gran medida del vino base utilizado para su elaboración, aunque también entra en juego el proceso de destilación, que produce los principales cambios en su composición relacionados con sus propiedades sensoriales únicas.

Los ésteres se encuentran entre los mayores constituyentes de los brandies y son de los compuestos aromáticos con mayor impacto en las características sensoriales de este producto. Sin embargo, no existen muchas referencias bibliográficas que hayan abordado su modulación durante la etapa de producción del Brandy de Jerez.

En este capítulo se optimiza y valida un método basado en HS-SPME-GC-MS para la determinación de 28 ésteres en brandies. Para ello se utilizan herramientas estadísticas multivariante como la metodología de superficie de respuesta, que permiten realizar procesos de optimización con gran precisión y con un número de experimentos reducido. La metodología desarrollada se validó en términos de linealidad, sensibilidad y precisión de acuerdo a los criterios establecidos por AOAC.

Esta metodología fue posteriormente aplicada para investigar la modulación de los ésteres en muestras de Brandy de Jerez provenientes de Solerajes con tiempos de crianza diferentes. Se observaron cambios importantes en esta familia de compuestos con el tiempo de crianza, relacionados previsiblemente con procesos de hidrólisis y efectos de “merma” por evaporación del alcohol y el agua a través de los poros de las barricas de madera.

Por otro lado, esta metodología se aplicó para estudiar el efecto sobre los ésteres de un proceso de estabilización por frio y filtración que se aplica para reducir la neblina que aparece por la suspensión de ciertos compuestos, entre otros, los ésteres etílicos de ácidos grasos de cadena larga (C12-C20). Además, este proceso de estabilización por frío se comparó con una estabilización a temperatura ambiente. Ambos procesos resultaron exitosos para reducir (precipitar) los ésteres etílicos de cadena larga. Sin embargo, la estabilización por frío y filtración provocó menos cambios en el perfil de ésteres de los brandies, resultando un proceso menos agresivo.

ARTÍCULO 6

Multivariate optimization of headspace solid-phase microextraction coupled to gas chromatography-mass spectrometry for the analysis of esters in brandies

José Manuel Muñoz-Redondo, Manuel José Valcárcel-Muñoz, Raquel Rodríguez Solana, Belén Puertas, Emma Cantos-Villar, José Manuel Moreno-Rojas

Food Chemistry

(Enviado)

Multivariate optimization of headspace solid-phase microextraction coupled to gas chromatography-mass spectrometry for the analysis of esters in brandies

José Manuel Muñoz-Redondo[1], Manuel José Valcárcel-Muñoz[2], Raquel Rodríguez Solana[1], Belén Puertas[3], Emma Cantos-Villar[3], José Manuel Moreno-Rojas[1*]

[1]Department of food Science and Health. Andalusian Institute of Agricultural and Fisheries Research and Training (IFAPA). Alameda del Obispo Avda, Menéndez Pidal, s/n. 14071, Córdoba, Spain

[2]Research and Development Department. Bodegas Fundador, S.L.U. Calle San Ildefonso, nº3, 11403, Jerez de la Frontera, Cádiz, Spain

[3]Department of food Science and Health. Andalusian Institute of Agricultural and Fisheries Research and Training (IFAPA). Cañada de la Loba, 11471, Jerez de la Frontera, Cádiz, Spain.

*Corresponding author:

E-mail: josem.moreno.rojas@juntadeandalucia.es

Tel.: +34 671 53 27 58; Fax: +34 957 01 60 43

Abstract

A method based on headspace solid-phase microextraction and gas chromatography coupled to mass spectrometry was optimised and validated to quantify 28 esters in brandies. The optimal extraction conditions using a response surface methodology and a multicriteria desirability function were obtained at 33 ºC with an extraction time of 55 minutes and a sample dilution of 7.2 % v/v ethanol. The method developed for the 28 esters (including ethyl esters of fatty acids, higher alcohol acetates, ethyl esters of branched acids, ethyl esters of odd carbon number fatty acids, methyl esters of fatty acids, cinnamates, and isoamyl esters of fatty acids) was successfully validated in terms of linearity, matrix effect, intra and inter-day precision, detection and quantification limit, and accuracy. This method was tested on Spanish sherry brandies matured through the traditional dynamic ageing system of *Criaderas* and *Solera*. The main differences in the brandy samples related to the ester profile were highlighted by means of multivariate statistical analyses, revealing the main changes as a consequence of the dynamic ageing of the samples in oak barrels.

Keywords: esters, brandy, HS-SPME/GC-MS, method validation, multivariate statistics, multi-response optimization

1. Introduction

Brandy is a spirit beverage elaborated by distilling wine followed by maturation in wooden casks (Regulation (EC) 2019/787). This alcoholic drink is characterized by a complex matrix comprising a large number of metabolites with different chemical natures, including higher alcohols, acids, esters, terpenes and carbonyl compounds (Tsakiris et al., 2014). These compounds are formed at different stages of brandy production, such as the ripening of grapes (primary flavour), wine fermentation (secondary flavour), wine distillation (tertiary flavour), and the maturation or ageing of brandy (quaternary flavour) (Spaho et al., 2013). Among them, esters constitute one of the most important families of volatile compounds, affecting the aroma and quality of brandies, ethyl esters of fatty acids being of special importance due to their abundance in distilled spirits (Guymon, 1974).

The relevance of esters on the sensory properties of distilled beverages comes from their relatively high content and low odour threshold (Nascimento et al., 2008). Although these compounds are present in grapes, they are mainly produced enzymatically during yeast fermentation and through the ethanolysis of acyl-CoA formed during fatty acid synthesis or degradation (Bao Jiang, 2012). Most esters are formed at the beginning of fermentation, but their concentration also varies slightly during wine maturation, the distillation process and brandy ageing (Tsakiris et al., 2014). Thus, increasing contents of ethyl esters of fatty acids such as ethyl decanoate and laurate in brandies can be associated with the preservation of wines with lees before distillation since these compounds are generally retained within yeast cells. The even-numbered fatty acids are known to predominate in natural products, apparently because the acid precursors are synthesized by successive couplings of the acyl-CoA fragment with acetyl-CoA (a C2 addition to the molecule). Thus, the most characteristic esters of distilled alcoholic beverages such as brandy are usually those of even-numbered higher-boiling fatty acids,

particularly caproic (C6), caprylic (C8), capric (C10), lauric (C12), myristic (C14), and palmitic (C16) acids (Guymon & Crowell, 1969; van Jaarsveld et al., 2017).

Many esters have previously been identified and quantified using classical methodologies for general volatile identification including the presence of organic solvents, and less sensitive techniques (determinations > mg/L) such as gas chromatography coupled with a flame ionisation detector (GC-FID) (Steger & Lambrechts, 2000; van Jaarsveld et al., 2017). However, most of the methods are not specific to this family of compounds, and specificities of the method of quantification such as the internal standards may be not suited to all the analytes within the same family, leading to inaccurate quantifications. Previous authors mentioned the importance of the synergism among different aroma compounds, even at levels below their individual perception thresholds, implying the need to look for chromatographic methods to identify as many compounds as possible, even those present at low concentrations (ng/L to mg/L levels), which can contribute greatly to the aroma of the final drink (De-La-Fuente-Blanco et al., 2020; V. Ferreira et al., 2016; Muñoz-Redondo et al., 2017; Niu et al., 2018).

In this sense, headspace solid-phase microextraction (HS-SPME) constitutes an environmentally-friendly strategy for volatiles extraction, characterized by a simple, rapid, accurate, sensitive and easy-to-automate solvent-free technique. It is usually coupled to gas-chromatography with a sensitive mass spectrometry instrument (GC-MS) and commonly used for the identification and quantification of different classes of volatiles in alcoholic beverages (Cardeal et al., 2008; Medina et al., 2020; Rodríguez-Solana et al., 2018; Vázquez-Araújo et al., 2013), including esters (Rodríguez-Solana et al., 2021; Zacaroni et al., 2017; Zhang et al., 2011; Zhao et al., 2009). As changes in experimental parameters can lead to very different extraction efficiencies, HS-SPME requires a previous optimization. Traditionally, the optimization of analytical procedures has been performed by using the so-called one-factor-at-a-time technique, where only

the experimental response of one factor at a time is modified and monitored, the rest remaining constant. This technique makes it possible to study the effect of the chosen factor but does not include interaction effects between factors, often leading to erroneous or suboptimal results. In addition, it requires a large number of experimental runs to determine the optimal conditions, this being extremely time-consuming (Bezerra et al., 2008; Gandolfi et al., 2015). To overcome these problems, response surface methodology (RSM) has emerged as a good statistical-based strategy. RSM is a collection of mathematical and statistical procedures used to fit empirical models to the data obtained from experimental designs with a minimum number of experimental combinations of the factors (Bezerra et al., 2008; Polat & Sayan, 2019). A popular RSM tool widely used for the optimization of experimental trials is the Box-Behnken design. This is a powerful, useful and efficient approach with a rotatable or nearly rotatable quadratic design and treatment combinations at central points and middle points of the edges of a cube (Ferreira et al., 2007). A large number of applications of this method for the optimization of analytical strategies have been reported in recent years (Bezerra et al., 2008; Chmiel et al., 2017; Muñoz-Redondo et al., 2020; Rodríguez-Solana et al., 2017; Sadoughi et al., 2015).

The goal of this study was to optimize and validate a specific, sensitive and accurate analytical method for the simultaneous quantification of a large number of esters in brandy using HS-SPME coupled to GC–MS. First, we determined the optimal experimental conditions of the HS-SPME by means of response surface methodology using a Box-Behnken design. To provide specificity for the method, a total of 8 deuterated ethyl esters were used as internal standards. The method was then validated and applied to real samples of Spanish sherry brandies matured in the *Criaderas* and *Solera* system, and with different average ageing times. The results of this characterization were assessed by means of multivariate statistics and the main differences among the samples were related with their ester profile.

2. Material and methods

2.1. Brandy samples

The brandies used in this study are from Jerez de la Frontera (Spain) and with protected geographical indication (Regulation (EC) 2019/787). They were elaborated following the traditional dynamic ageing system called *Criaderas* and *Solera* as established in the specifications provided by the Technical File of the Geographical Indication of Brandy de Jerez (Boletín Oficial la Junta Andalucía, 2018).

2.1.1. Brandies for method development

Five brandy samples with presumably different volatile profiles were used for the method validation, including the commercial Spanish sherry brandies Fundador Solera Reserva Pedro Domecq (Fundador) and Veterano (Osborne) acquired from a supermarket (Córdoba, Spain), as well as one *Solera* brandy (6-8 months of ageing), one *Solera Reserva* brandy (12-15 months), and one *Solera Gran Reserva* brandy (8-10 years) were provided by Bodegas Fundador (Jerez de la Frontera, Spain).

2.1.2. Brandies for method application

The method developed was used to characterize the ester profile of 21 samples, shown in Table 1. The younger *Criadera* in system A was a mixture of *holandas*, which are wine spirits with alcoholic contents below 70 % v/v. In system B, it was a mixture of wine spirits with alcoholic contents between 70 and 86 % v/v (IGP Brandy de Jerez, 2018). For the remaining systems (C, D, E, F and G), it was a mixture of young brandies. The next levels of *Criaderas* and *Solera* followed the dynamic ageing system by refilling the extracted fraction with the previous *Criadera*, always within the same system. Quality control samples (QCs) were prepared from a pool of these brandies to detect unwanted variations due to potential metabolite degradation processes, analytical and experimental trends.

2.2. Chemicals

High-performance liquid chromatography (HPLC)-grade ethanol was obtained from J.T. Baker Chemicals B.V. (Denventer, Holland). Milli-Q water was produced by a Milli-Q Plus water system (Millipore, Spain). Ethylenediaminetetraacetic acid (EDTA) was supplied by Panreac Applichem (Barcelona, Spain). Sigma-Aldrich (Madrid, Spain) supplied the following: sodium chloride ACS reagent grade (purity ≥ 99.8%), and the standard compounds ethyl butyrate (≥ 99%), ethyl hexanoate (≥ 99%), ethyl octanoate (≥ 99%), ethyl decanoate (≥ 99%), ethyl dodecanoate (≥ 99%), ethyl myristate (≥ 99%), ethyl palmitate (≥ 99%), ethyl stearate (≥ 99%), propyl acetate (≥ 99%), isobutyl acetate (≥ 99%), isoamyl acetate (≥ 99%), hexyl acetate (≥ 99%), phenylethyl acetate (≥ 99%), ethyl isobutyrate (98%), ethyl 2-methylbutyrate (≥ 99%), ethyl isovalerate (≥ 99%), ethyl phenylacetate (98%), ethyl cinnamate (98%), ethyl dihydrocinnamate (98%), methyl hexanoate (≥ 99%), methyl octanoate (≥ 99%), methyl decanoate (≥ 99%), isoamyl butyrate (98%), ethyl heptanoate (98%), ethyl nonanoate (98%), ethyl propanoate (≥ 99%), isobutyl hexanoate (≥ 99%), ethyl valerate (≥ 99.7%), acetaldehyde (≥ 99.5%). The deuterated internal standards [$^2H_3$]-ethyl butyrate, [$^2H_{11}$]-ethyl hexanoate, [$^2H_{15}$]-ethyl octanoate, [$^2H_5$]-ethyl trans-cinnamate, [$^2H_{23}$]-ethyl dodecanoate, [$^2H_{27}$]-ethyl myristate, [$^2H_{31}$]-ethyl palmitate, and [$^2H_{35}$]-ethyl stearate, were supplied by CDN isotopes (Pointe-Claire, Canada).

2.3. HS-SPME conditions

2.3.1. Sample preparation and extraction conditions

A total of 25 mL of brandy sample were spiked with 20 µL of an internal standard mix solution of 8 deuterated ethyl esters at 200 mg/L, since the final concentration was similar to the analytes and it made it possible to obtain repeatable and well-defined peaks over the course of the experimental runs for the internal standards. After careful inspection, considering the chemical structure and the response signal, the peak integration of each analyte was normalized using a specific deuterated standard. Ethyl isobutyrate, ethyl 2-methylbutyrate, ethyl isovalerate, ethyl propanoate, ethyl butyrate, isoamyl acetate, ethyl

valerate, propyl acetate, and isobutyl acetate were normalized with [$^2H_3$]-ethyl butyrate. Ethyl hexanoate, methyl hexanoate, methyl octanoate, isoamyl butanoate, isobutyl hexanoate, ethyl heptanoate, and hexyl acetate were normalized with [$^2H_{11}$]-ethyl hexanoate. [$^2H_{15}$]-Ethyl octanoate was used to normalize ethyl octanoate, methyl decanoate. Phenylethyl acetate, ethyl dihydrocinnamate, and ethyl cinnamate were normalized with [$^2H_5$]-ethyl trans-cinnamate; while ethyl dodecanoate, ethyl decanoate, ethyl nonanoate, and ethyl phenylacetate with [$^2H_{23}$]-ethyl dodecanoate. Finally, [$^2H_{27}$]-ethyl myristate, [$^2H_{31}$]-ethyl palmitate and [$^2H_{35}$]-ethyl stearate were used to normalize ethyl myristate, ethyl palmitate and ethyl stearate, respectively. Then, the spiked samples were diluted in EDTA solution (200 mM and pH adjusted to 7 with NaOH 1 M), which prevents the oxidation of the compounds, thus improving the HS-SPME efficiency (Dziekońska-Kubczak et al., 2020). As sample dilution was a factor selected for optimization, different dilution conditions were assayed as indicated in the following section. Afterwards, 10 mL of this diluted solution were transferred to a 20 mL SPME vial containing 3.5 g of NaCl, this amount being enough to obtain conditions of salt saturation, which is reported to increase the ionic strength of the analytes and drive more volatiles into the headspace (Davis & Qian, 2019; Dziekońska-Kubczak et al., 2020). The vials were capped and the solution was homogenized using a vortex shaker for 30 s and placed in a Combipal autosampler tray (CTC Analytics, Zwingen, Switzerland).

A 100 µm PDMS fibre (Supelco, Bellefont, PA, USA), previously conditioned according to the supplier's recommendation, was used for the extraction of esters via HS-SPME. This fibre has been previously used in ester analysis due to a similar polarity of these analytes and the polymeric coating. For the equilibrium step, the vials were incubated at 500 rpm for 2 minutes at the extraction temperature, while the extraction was performed maintaining agitation at 500 rpm and using the different temperatures and times considered for optimization in the next section.

2.3.2. Optimization of HS-SPME parameters

The headspace solid-phase microextraction parameters were optimized to achieve good chromatographic signals. Optimization was performed by means of a response surface methodology (RSM), using the peak area of seven families of esters as responses (ordered by abundance: ethyl esters of fatty acids, higher alcohol acetates, ethyl esters of branched acids, ethyl esters of odd carbon number fatty acids, methyl esters fatty acids, cinnamates and isoamyl esters of fatty acids). Extraction temperature, extraction time and sample dilution were the factors optimised by means of a response surface methodology (RSM), based on the Box-Behnken design using three levels [-1 (minimum value), 0 (medium value) and 1 (as the highest value tested)], as usually expressed in coded notation. The levels of the three parameters used to build the Box-Behnken design were set as follows: extraction temperature (30, 40 and 50 ºC), extraction time (30, 45 and 60 min) and sample dilution, which was controlled by the final alcohol content (1.8, 5.8 and 9.8 % v/v of ethanol). The responses obtained from the Box-Behnken design were fitted to a second-order (quadratic) function, and the Bayesian information criterion (BIC) was used to select the model coefficients. The lack of fit (considered significant at a p-value < 0.05), adjusted R^2, predicted R^2, predicted vs actual response values and the normal plot of residuals were used for model evaluation. The levels of the extraction temperature, extraction time and sample dilution were finally optimised by using the desirability function (D) of Derringer and Suich (Derringer & Suich, 1980), which enables multicriteria optimization to be handled. The individual responses of each family of esters were transformed from the experimental domain to individual desirability functions, ranging between 0 and 1 for unacceptable and fully desirable response values, respectively. Then, a global desirability function was obtained by determining the geometric average of the individual desirability values. Model fitting and optimization were performed with the Design-Expert v.10 software.

2.4. GC-MS instrumental parameters

The conditions of the gas chromatograph were adapted from a previous method developed by our research group for esters in wines (Ruiz-Moreno et al., 2017). The desorption time and temperature were set at 15 min and 250 °C respectively. This process was performed in a Trace GC ultragas chromatograph (Thermo Fisher Scientific S. p.A., Rodano, Milan, Italy). Afterwards, the desorbed samples passed to an ISQ Single MS spectrometer (Thermo Fisher Scientific, Austin, Texas, USA). The injection was performed in splitless mode, and a BP21 column of 50m × 0.32mm and 0.25 µm film thickness (SGE Analytical Science, UK) was used for the separation. The carrier gas was helium at a constant flow rate of 1.7 mL/min. The oven temperature program was set at 40 °C for 5 min, raised to 220 °C at 3 °C/min and held for 30 min. The MS operated in electron ionization mode at 70 eV using selected-ion-monitoring (SIM) mode. The transfer line and source temperature of the MS were set at 230 °C and 200 °C respectively. The identification procedure was performed by comparing the retention times and mass spectra with those of the pure standards.

2.5. Method validation

The GC-MS method was validated in terms of the linearity of the standard addition curves using commercial brandies spiked with a mixture of the analytes at six levels of concentration, matrix effect, precision, accuracy (recovery at different spiked levels) and limits of detection (LOD) and quantification (LOQ), as in previous similar studies (Antalick et al., 2010; Arcari et al., 2017; D. C. Ferreira et al., 2019; Muñoz-Redondo et al., 2020). For linearity, five standard addition curves were fitted using different brandy samples spiked with the standard compounds at the different concentrations shown in Table 3. In GC-MS analyses, a higher range of variation is typically found at the top levels of the curve (heteroscedasticity) (Li et al., 2002). To prevent domination of the higher levels of concentration, we used a weighting factor aimed at minimizing the sum of the relative errors in the regression to correct the calibration curves (de Bairros et al., 2015). The slope of the five standard addition curves was used to evaluate the matrix effect.

Calculation of the LOD and LOQ of each metabolite was based on the signal-to-noise ratio of the lowest spiked standard concentration which produced a measurable response. Respective ratios of 3:1 and 10:1 were used for the LOD and LOQ. Precision was evaluated in terms of repeatability (intra-day) and reproducibility (inter-day). For repeatability, 9 identical brandy samples were analysed in a one-day sequence, while for inter-day reproducibility, an unspiked sample was measured 12 times over a 1-month period. The accuracy was assessed at two levels of concentration (low and high) by analysing five replicates of the same brandy.

2.6. Application of HS-SPME-GC-MS to real samples.

The ester profile of sherry brandies of different average ages were analysed with the optimal conditions of the HS-SPME (temperature and time of extraction, and sample dilution) and the validated GC-MS method. Quality control samples (QCs) prepared from a pool of brandies of different ageing times were repeatedly analysed throughout the experimentation period to detect unwanted variations due to potential metabolite degradation processes, or analytical and experimental trends, as mentioned before. Only metabolites with stable responses (RSD ≤ 20 in the QCs) and no clear trends in the QCs were considered in the method.

2.7. Statistical analysis

The statistical analyses of the sherry brandies analyzed with the optimized and validated methodology were based on principal component analysis (PCA). This statistic was first used to check the overall quality of the data acquired during processing, fitting a model that included both the quality control (QCs) and real brandy samples. Then, the QCs were removed from the dataset and a new PCA was performed to study the overall differences in the ester profile of the samples regarding the dynamic systems of *Criaderas* and *Solera*. The statistical software R version 4.0.3 using the package *mixOmics* (Rohart et al., 2017) was used to perform the PCAs.

3. Results and discussion

3.1. Optimization of the HS-SPME conditions

The extraction efficiency of volatile compounds by HS-SPME is affected by experimental conditions such as pH, amount of sample, sample dilution, ionic strength (salt addition), time and temperature of sample conditioning, extraction and desorption. The impact of these controlled factors on the final extraction yield varies according to a general pattern known as the Pareto principle, which states that for many events, roughly 80% of the effects (responses) come from 20% of the causes (Politis et al., 2017). Therefore, response surface models (RSM) are usually designed with only those factors with the greatest influence on responses to reduce the number of experimental runs needed to estimate the coefficients of the models to be fitted.

The main factors influencing the yield extraction of volatile compounds by HS-SPME are the extraction temperature and time, which are generally included as the target parameters in optimization attempts (Chmiel et al., 2017; Muñoz-Redondo et al., 2020; Pati et al., 2021; Sadoughi et al., 2015). Higher temperatures affect the diffusion coefficient of the analytes, shortening the extraction time, but lowering the partition coefficient. The samples are, therefore, heated to accelerate the release of volatile compounds into the headspace, and reduce the time at which equilibrium between sample headspace and the stationary phase of the fused-silica fibre is reached (Chmiel et al., 2017; Prosen & Zupančič-Kralj, 1999). The extraction temperature was varied between 30 to 50 ºC for optimization since most studies characterizing esters in alcoholic beverages found the optimum conditions within this range (Antalick et al., 2010; Muñoz-Redondo et al., 2017; Plutowska & Wardencki, 2008; Ruiz-Moreno et al., 2017). The optimal extraction time depends on the partition coefficient of the analytes and sample agitation. The maximum amount of metabolite is extracted when the equilibrium time is reached, but this time may be too long for many analytes (Prosen & Zupančič-Kralj, 1999). Thus, extraction time is usually set at one for which the amount of analyte exceeds the limit of quantification. According to normal operation times used for ester

characterization by HS-SPME in alcoholic beverages in previous studies (Antalick et al., 2010; Muñoz-Redondo et al., 2017; Plutowska & Wardencki, 2008; Ruiz-Moreno et al., 2017), the extraction time tested in this study ranged between 30 and 60 min to prevent the analyses being too time-consuming.

Based on previous experience of our research group, sample dilution is a factor with a strong impact on the extraction of volatile metabolites, and therefore, it was one of the factors included in the experimental design. An important loss of signal can be observed for dilutions above 10 % v/v of ethanol, probably as a result of the fibre becoming saturated with ethanol, which is found in large quantities in samples with a high alcohol content (Rodríguez-Solana et al., 2020). In addition, optimal dilution ratios may reduce the matrix effect in complex samples (Pawliszyn, 2011). The range established for the dilution rate to control the final degree of alcohol of the samples was from 1.8 to 9.8 % v/v of ethanol.

3.2. Response surface methodology

The HS-SPME was optimized by means of a Box-Behnken design (BBD) at three levels (-1,0 and 1 in coded factors) with the level combinations shown in Supplementary Figure S1. This design consisted of 12 experimental runs and 5 central points performed randomly. The esters identified were grouped by families and, as Table 2 shows, ordered according to decreasing peak areas in the following families: ethyl esters of fatty acids, higher alcohol acetates, ethyl esters of branched acids, ethyl esters of odd carbon number fatty acids, methyl esters of fatty acids, cinnamates, isoamyl esters of fatty acids. Then, a second order model including interactions was fitted for each family of esters (response) using a stepwise regression (forward and backward selection) optimised by the Bayesian Information Criterion (BIC), obtaining a total of 7 models with the following mathematical formula:

$$Y_i = \alpha_0 + \sum_{i=1}^{3} \beta_i X_i + \sum_{i=1}^{3} \beta_{ii} X_i^2 + \sum_{i=1}^{3} \beta_{ij} X_i X_j$$

where, Y_i is the predicted response (peak areas of the ester family i), α_0 is the intercept, β_i, β_{ii} and β_{ij} are the coefficients indicating the effect on the responses, and X_i and X_j are the factors.

The response surface models were obtained considering only the coefficients with a p-value ≤ 0.05 and were assessed by means of an analysis of variance (ANOVA). All the single models displayed non-significant lack of fit at a 95% of confidence level and p-value of the model below 0.001. The adjusted determination coefficients (R^2_{Adj}) showed a high percentage of variation in the responses (summation of the ester families) explained by the factors, with values above 0.92. In addition, the predicted determination coefficients (R^2_{Pred}) showed reasonable values with differences less than 0.2 compared to the R^2_{Adj} (Table 2). The actual vs predicted response values showed a good fit to the quadratic models with low prediction errors (Supplementary Figure S2), and the normal distribution of the data was confirmed by the normal plot of residuals (Supplementary Figure S3).

The optimal HS-SPME experimental conditions were determined by the multicriteria desirability function (D) of Derringer and Suich (Derringer & Suich, 1980). The combination of levels for the three factors that produced the highest values in the global desirability function determined the optimal conditions of the HS-SPME. The 3D surface plots of the desirability values as a function of the extraction temperature, extraction time and sample dilution are shown in Figure 1. In each 3D surface plot, the missing factor was set to the optimal value determined from the optimization process. Sample dilution was the most critical experimental factor since different dilution ratios led to high variations in the global desirability values. Moving from higher to lower dilution ratios (i.e., from 1.8 to 9.8 % v/v of ethanol), the extraction yield of esters increased progressively, obtaining desirability values that ranged from 0 to close to 1. The optimal dilution ratio was obtained for a narrow range between 7-8 % v/v of ethanol, regardless of the temperature and time of extraction (Figure 1a and 1b). A slight decrease in sample

dilution (from 8.2 to 9.8 % v/v of ethanol) resulted in a drastic decrease in the extraction yield of esters, probably due to the fibre becoming saturated with ethanol. Meanwhile, after setting the optimal sample dilution, the temperature and time of extraction did not affect the extraction efficiency critically (Figure 1c). However, a combination of lower temperature and a longer extraction time led to slight increases in the extraction of esters, the optimal values of both experimental factors being found for approximately 32 to 34 ºC and 52 to 58 min respectively.

The levels of the three factors that showed the highest extraction yields of esters (obtaining a global desirability value of D = 0.951) were a sample dilution of 7.2% v/v of ethanol, and a temperature and time of extraction of 33 ºC and 55 min, respectively. These optimized parameters were within the experimental range of the Box-Behnken design selected in the initial design.

3.3. Method validation

After HS-SPME optimization, the GC-MS methodology proposed in this study was validated for linearity, matrix effect, intra and inter-day precision, limit of detection and quantification and accuracy as previously described in similar studies (Antalick et al., 2010; Ivanova et al., 2012; Korban et al., 2021; Muñoz-Redondo et al., 2020). The chromatographic program was manually inspected and modified to enable the quantification of the maximum number of peaks from ester compounds. A total of 8 deuterated internal standards were used to normalize the peak areas of esters to improve the precision of quantification. The internal standard used for each ester compound was selected according to similarity of the chemical structure and chromatographic response across the different runs.

3.3.1. Linearity, limits of detection and matrix effect

Using the method of standard addition, five standard addition curves were built with different aged brandies spiked with a mixture of the analytes at six concentration levels and the internal standards for compound normalization. The standard addition curves

were fitted by means of least squares regression. All the esters displayed a satisfactory linearity, with $R^2 \geq 0.981$ (Table 3). Determination of LOD and LOQ was based on the minimum injected concentration of standards that was successfully validated, with a signal-to-noise ratio of 3 and 10 respectively. The calculated LOD and LOQ are shown in Table 3. Meanwhile, the slope of the five standard addition curves built on different brandies was compared, and the relative standard deviation (RSD %) was calculated to evaluate matrix effects. All the ester compounds showed RSD (%) values below 13, except for ethyl phenylacetate (RSD = 21) and ethyl nonanoate (RSD = 30) (Table 3), these results being indicative of no matrix effects.

3.3.2. Precision and accuracy

Precision was assessed for repeatability and reproducibility. The repeatability of the esters included in the method was determined from 9 samples analysed within the same day at two levels (low and high) of injected concentrations. The RSD (%) values calculated for the repeatability at these two levels varied at an acceptable range between 1 to 30 % (Table 3), meaning low intra-day variation. The reproducibility was assessed with an unspiked sample measured 12 times over a 1-month period. The RSD (%) values determined for reproducibility ranged from 1 to 18 % (Table 3), indicating low inter-day variation. The accuracy was calculated in terms of recovery at two levels of concentration (low and high), obtaining good recovery yields varying between 81 and 118% (Table 3), which indicated a high extraction efficiency of esters by the HS-SPME procedure.

3.4. Application to real samples

The optimized and validated methodology was used to characterize the ester profile of 21 samples of sherry brandies (Table 1). These brandies display unique characteristics due to the special production method based on a dynamic system known as *Criaderas* and *Solera* and ageing in American oak casks previously used for Sherry wines of 500-600 L of capacity (Durán-Guerrero et al., 2021). All the samples were analysed in duplicate and the sequence was randomized to avoid misleading results due to

experimental errors and trends. Pooled quality control samples (QCs) were injected throughout the different sequences to check the quality of the data and to correct for experimental and analytical drifts by fitting a smoothed cubic spline onto the QCs, as previously described (Kokla et al., 2020).

Most of the esters studied are present in the brandy as consequence of the wine spirits, that depends on the distilled wines (these could contain a certain amount of fine lees not yet decanted, especially in the first distillations of the year, increasing their concentrations); as well as the distillation processes, influenced by the separation yield of the distillation heads (many esters are eliminated with the heads due to their affinity with ethanol).

During the ageing, the esters have different behaviours, some of them increase its concentration by esterification between ethanol and the free acids present in the distillates and other decrease its concentration by hydrolysis due to the acidity of the brandy (pH around 3.0 - 4.5).

Ethyl esters of fatty acids (EEFAs) were the most abundant family of esters in Brandies due probably to the continuous esterification of fatty acids and ethanol during ageing (Christoph & Bauer-Christoph, 2007), their concentrations ranging between 14.5 and 44.7 mg/L. They were followed by higher alcohol acetates (HAAs; 1.6 to 5.1 mg/L), ethyl esters of branched acids (EEBAs; 365 to 2449 µg/L), ethyl esters of odd carbon number fatty acids (EEOCNFAs; 24 to 478 µg/L), methyl esters of fatty acids (MEFAs; 18 to 63 µg/L), cinnamates (7 to 26 µg/L) and isoamyl esters of fatty acids (IEFAs; 2.5 to 14 µg/L). The remaining miscellaneous esters displayed concentrations between 0.7 and 25.8 mg/L, mainly driven by the high content of ethyl propanoate. Among EEFAs, the ethyl octanoate was the most abundant ester, with concentrations ranging between 9 and close to 23 mg/L, ethyl hexanoate, ethyl decanoate, ethyl dodecanoate and ethyl palmitate also being found in high concentrations compared to the remaining esters (Supplementary Table S1). These concentrations agree with previous findings in brandy

samples (Zhao et al., 2009), ethyl esters of fatty acids being described as the most abundant family of esters in brandy (Guymon & Crowell, 1969).

A multivariate statistical approach based on principal component analysis (PCA) was followed to reveal the main differences in the samples related to their ester profile. The first two principal components accounted for the 67 % of the total variance found in the samples, the main differences related to the ageing being found in PC1, which explained 36 % of the total variance. Samples from the youngest *Criaderas* in all the systems studied were allocated at lower values of PC1 and moved towards more positive values during ageing (oldest *Criaderas* and also in *Solera* samples) (Figure 2a). This trend was related to strong decreases in the ester concentration during ageing. Among the esters that presented a reduction in their concentration with ageing time were phenylethyl acetate, methyl octanoate, ethyl hexanoate, hexyl acetate, isoamyl acetate, isobutyl hexanoate, methyl decanoate, methyl hexanoate, ethyl palmitate, ethyl valerate, ethyl octanoate, and to a lesser extend in ethyl stearate, ethyl myristate, ethyl cinnamate and ethyl butyrate (Figure 2b). By contrast, PC1 revealed increases during ageing in ethyl phenylacetate, ethyl 2-methylbutyrate, ethyl isovalerate, ethyl heptanoate, ethyl decanoate, ethyl nonanoate, and less pronounced increases in propyl acetate, isoamyl butyrate, ethyl isobutyrate and ethyl dodecanoate, which could be explained by the continuous esterification of fatty acids and ethanol during ageing (Christoph & Bauer-Christoph, 2007). Systems A and B presented negative PC1 values even at *Solera* level, displaying an ester profile more similar to the initial points of the remaining systems (corresponding to the younger *Criaderas*). This was expected since the *Solera* from systems A and B are used as raw material in the youngest *Criaderas* of the remaining systems (C, D, E, F and G).

Meanwhile, the ester profile of the brandies obtained from *Solera* with different average ageing and maturation times displayed significant variations, which were explained in PC2. The systems F and G, with average ageing of 25 and 40 years respectively, were

located in negative values of this principal component, with values especially negative in system G. While the systems with lower average ageing (C, D and E), ranging between 10 to 15 years, fell in the positive values of PC2. However, all the systems moved from more positive to more negative values. This meant an increase in most of the esters in the last levels of these systems (1st *Criadera* and *Solera* of systems C, D, E, F and G), except for ethyl valerate, phenylethyl acetate and hexyl acetate (Figure 2a and 2c). Ethyl isobutyrate and ethyl butyrate were reported to increase their contents with ageing in a previous study (Caldeira et al., 2010). This increase in the overall content of esters could be explained by losses of water and ethanol during the ageing of brandies due to evaporation effects and/or perspiration through the pores of the wood (Durán-Guerrero et al., 2021).

4. Conclusions

A multivariate approach was applied to optimize the HS-SPME conditions for the quantification of esters in brandy through GC-MS. Three factors with great influence on the extraction of volatiles from alcoholic beverages using HS-SPME were optimized by means of a second order Box-Behnken design at three levels. The results confirmed that all the factors significantly affected the peak responses of the ester families. The linearity of the method was satisfactory in the range evaluated for each compound, with determination coefficients higher than 0.99. Good precision, accuracy, LOD and LOQ were attained for all the esters included in the method. The optimized methodology was then applied to brandies from Jerez from *Criaderas* and *Solera system*, the main differences in their ester profile being related to the average ageing time of the samples analysed.

Financial funds

J.M.M.-R. was awarded a research contract funded by the Andalusian Institute of Agricultural and Fisheries Research and Training (IFAPA), within the National Youth Guarantee System funded through the European Social Fund (ESF) and the Youth

Employment Initiative (YEI). R.R.S. was supported by Juan de la Cierva —Incorporation contract from the Spanish Ministry of Science, Innovation and Universities (IJC2018-036207-I). This study has been funded by the Andalusian Institute of Agricultural and Fisheries Research and Training (IFAPA) and Bodegas Fundador, S.L.U through the Project FEDER-Innterconecta “Factores que influyen en la calidad del Brandy y nuevos sistemas de elaboración del mismo, desde el viñedo al envasado” (BESTBRANDY).

References

Antalick, G., Perello, M.-C., & de Revel, G. (2010). Development, validation and application of a specific method for the quantitative determination of wine esters by headspace-solid-phase microextraction-gas chromatography–mass spectrometry. *Food Chemistry*, *121*(4), 1236–1245.

Arcari, S. G., Caliari, V., Sganzerla, M., & Godoy, H. T. (2017). Volatile composition of Merlot red wine and its contribution to the aroma: Optimization and validation of analytical method. *Talanta*, *174*, 752–766.

Bao Jiang. (2012). Effect of terrains on the volatiles of Cabernet Sauvignon wines grown in Loess Plateau region of China. *AFRICAN JOURNAL OF BIOTECHNOLOGY*, *11*(33). https://doi.org/10.5897/AJB10.1649

Bezerra, M. A., Santelli, R. E., Oliveira, E. P., Villar, L. S., & Escaleira, L. A. (2008). Response surface methodology (RSM) as a tool for optimization in analytical chemistry. *Talanta*, *76*(5), 965–977.

Boletín Oficial la Junta Andalucía. (2018). *Consejería de Agricultura Pesca y Desarrollo rural. Orden de 28 de junio de 2018, por la que se aprueba el expediente técnico de Indicación Geográfica “Brandy de Jerez”* (127, 19–20).

Caldeira, I., Anjos, O., Portal, V., Belchior, A. P., & Canas, S. (2010). Sensory and chemical modifications of wine-brandy aged with chestnut and oak wood

fragments in comparison to wooden barrels. *Analytica Chimica Acta*, *660*(1–2), 43–52.

Cardeal, Z. L., de Souza, P. P., Silva, M. D. R. G. da, & Marriott, P. J. (2008). Comprehensive two-dimensional gas chromatography for fingerprint pattern recognition in cachaça production. *Talanta*, *74*(4), 793–799. https://doi.org/10.1016/j.talanta.2007.07.021

Chmiel, T., Kupska, M., Wardencki, W., & Namieśnik, J. (2017). Application of response surface methodology to optimize solid-phase microextraction procedure for chromatographic determination of aroma-active monoterpenes in berries. *Food Chemistry*, *221*, 1041–1056.

Christoph, N., & Bauer-Christoph, C. (2007). Flavour of spirit drinks: Raw materials, fermentation, distillation, and ageing. In *Flavours and fragrances* (pp. 219–239). Springer.

Commission of the European Communities (EEC), Council Regulation (EEC) No. 110/2008 of 15 January, 2008. (2008). Official Journal of the European Union, L 39/16 (2008), pp. 17-18.

Davis, P. M., & Qian, M. C. (2019). Effect of Ethanol on the Adsorption of Volatile Sulfur Compounds on Solid Phase Micro-Extraction Fiber Coatings and the Implication for Analysis in Wine. *Molecules*, *24*(18), 3392.

de Bairros, A. V., de Almeida, R. M., Pantaleão, L., Barcellos, T., e Silva, S. M., & Yonamine, M. (2015). Determination of low levels of benzodiazepines and their metabolites in urine by hollow-fiber liquid-phase microextraction (LPME) and gas chromatography–mass spectrometry (GC–MS). *Journal of Chromatography B*, *975*, 24–33.

De-La-Fuente-Blanco, A., Sáenz-Navajas, M.-P., Valentin, D., & Ferreira, V. (2020). Fourteen ethyl esters of wine can be replaced by simpler ester vectors without

compromising quality but at the expense of increasing aroma concentration. *Food Chemistry*, *307*, 125553.

Derringer, G., & Suich, R. (1980). Simultaneous optimization of several response variables. *Journal of Quality Technology*, *12*(4), 214–219.

Durán-Guerrero, E., Castro, R., García-Moreno, M. de V., Rodríguez-Dodero, M. del C., Schwarz, M., & Guillén-Sánchez, D. (2021). Aroma of Sherry Products: A Review. *Foods*, *10*(4), 753.

Dziekońska-Kubczak, U., Pielech-Przybylska, K., Patelski, P., & Balcerek, M. (2020). Development of the method for determination of volatile sulfur compounds (vscs) in fruit brandy with the use of HS–SPME/GC–MS. *Molecules*, *25*(5), 1232.

Ferreira, D. C., Hernandes, K. C., Nicolli, K. P., Souza-Silva, É. A., Manfroi, V., Zini, C. A., & Welke, J. E. (2019). Development of a method for determination of target toxic carbonyl compounds in must and wine using HS-SPME-GC/MS-SIM after preliminary GC$\times$ GC/TOFMS analyses. *Food Analytical Methods*, *12*(1), 108–120.

Ferreira, S. C., Bruns, R. E., Ferreira, H. S., Matos, G. D., David, J. M., Brandão, G. C., da Silva, E. P., Portugal, L. A., Dos Reis, P. S., & Souza, A. S. (2007). Box-Behnken design: An alternative for the optimization of analytical methods. *Analytica Chimica Acta*, *597*(2), 179–186.

Ferreira, V., Sáenz-Navajas, M.-P., Campo, E., Herrero, P., de la Fuente, A., & Fernández-Zurbano, P. (2016). Sensory interactions between six common aroma vectors explain four main red wine aroma nuances. *Food Chemistry*, *199*, 447–456.

Gandolfi, F., Malleret, L., Sergent, M., & Doumenq, P. (2015). Parameters optimization using experimental design for headspace solid phase micro-extraction analysis of short-chain chlorinated paraffins in waters under the European water framework directive. *Journal of Chromatography A*, *1406*, 59–67.

Guymon, J. F. (1974). Chemical aspects of distilling wines into brandy. *Chemistry of Winemaking*, 232–253.

Guymon, J. F., & Crowell, E. A. (1969). Gas chromatographic determination of ethyl esters of fatty acids in brandy or wine distillates. *American Journal of Enology and Viticulture*, *20*(2), 76–85.

IGP Brandy de Jerez. (2018). *El gran libro del Brandy de Jerez. Consejo Regulador IGP Brandy de Jerez. Jerez de la Frontera. Jerez de la Frontera (España)*.

Ivanova, V., Stefova, M., Stafilov, T., Vojnoski, B., Bíró, I., Bufa, A., & Kilár, F. (2012). Validation of a method for analysis of aroma compounds in red wine using liquid–liquid extraction and GC–MS. *Food Analytical Methods*, *5*(6), 1427–1434.

Kokla, M., Kl\aavus, A., Noerman, S., Koistinen, V. M., Tuomainen, M., Zarei, I., Meuronen, T., Häkkinen, M. R., Rummukainen, S., & Babu, A. F. (2020). *"NoTaMe": Workflow for Non-Targeted LC-MS Metabolic Profiling*.

Korban, A., Charapitsa, S., Čabala, R., Sobolenko, L., Egorov, V., & Sytova, S. (2021). Advanced GC–MS method for quality and safety control of alcoholic products. *Food Chemistry*, *338*, 128107.

Li, X.-N., Liang, Y.-Z., & Chau, F.-T. (2002). Smoothing methods applied to dealing with heteroscedastic noise in GC/MS. *Chemometrics and Intelligent Laboratory Systems*, *63*(2), 139–153.

Medina, S., Perestrelo, R., Pereira, R., & Câmara, J. S. (2020). Evaluation of Volatilomic Fingerprint from Apple Fruits to Ciders: A Useful Tool to Find Putative Biomarkers for Each Apple Variety. *Foods*, *9*(12), 1830. https://doi.org/10.3390/foods9121830

Muñoz-Redondo, J. M., Cuevas, F. J., León, J. M., Ramírez, P., Moreno-Rojas, J. M., & Ruiz-Moreno, M. J. (2017). Quantitative profiling of ester compounds using HS-SPME-GC-MS and chemometrics for assessing volatile markers of the second

fermentation in bottle. *Journal of Agricultural and Food Chemistry*, *65*(13), 2768–2775.

Muñoz-Redondo, J. M., Ruiz-Moreno, M. J., Puertas, B., Cantos-Villar, E., & Moreno-Rojas, J. M. (2020). Multivariate optimization of headspace solid-phase microextraction coupled to gas chromatography-mass spectrometry for the analysis of terpenoids in sparkling wines. *Talanta*, *208*, 120483.

Nascimento, E. S. P., Cardoso, D. R., & Franco, D. W. (2008). Quantitative Ester Analysis in Cachaça and Distilled Spirits by Gas Chromatography−Mass Spectrometry (GC−MS). *Journal of Agricultural and Food Chemistry*, *56*(14), 5488–5493. https://doi.org/10.1021/jf800551d

Niu, Y., Yao, Z., Xiao, Z., Zhu, G., Zhu, J., & Chen, J. (2018). Sensory evaluation of the synergism among ester odorants in light aroma-type liquor by odor threshold, aroma intensity and flash GC electronic nose. *Food Research International*, *113*, 102–114.

Pati, S., Tufariello, M., Crupi, P., Coletta, A., Grieco, F., & Losito, I. (2021). Quantification of Volatile Compounds in Wines by HS-SPME-GC/MS: Critical Issues and Use of Multivariate Statistics in Method Optimization. *Processes*, *9*(4), 662.

Pawliszyn, J. (2011). *Handbook of solid phase microextraction*. Elsevier.

Plutowska, B., & Wardencki, W. (2008). Determination of volatile fatty acid ethyl esters in raw spirits using solid phase microextraction and gas chromatography. *Analytica Chimica Acta*, *613*(1), 64–73.

Polat, S., & Sayan, P. (2019). Application of response surface methodology with a Box–Behnken design for struvite precipitation. *Advanced Powder Technology*, *30*(10), 2396–2407. https://doi.org/10.1016/j.apt.2019.07.022

Politis, S., Colombo, P., Colombo, G., & M. Rekkas, D. (2017). Design of experiments (DoE) in pharmaceutical development. *Drug Development and Industrial Pharmacy*, *43*(6), 889–901.

Prosen, H., & Zupančič-Kralj, L. (1999). Solid-phase microextraction. *TrAC Trends in Analytical Chemistry*, *18*(4), 272–282.

Rodríguez-Solana, R., Esteves, E., Mansinhos, I., Gonçalves, S., Pérez-Santín, E., Galego, L., & Romano, A. (2020). Influence of elaboration process on chemical, biological and sensory characteristics of European pennyroyal liqueurs. *Journal of the Science of Food and Agriculture*.

Rodríguez-Solana, R., Esteves, E., Mansinhos, I., Gonçalves, S., Pérez-Santín, E., Galego, L., & Romano, A. (2021). Influence of elaboration process on chemical, biological, and sensory characteristics of E uropean pennyroyal liqueurs. *Journal of the Science of Food and Agriculture*, jsfa.11043. https://doi.org/10.1002/jsfa.11043

Rodríguez-Solana, R., Galego, L. R., Pérez-Santín, E., & Romano, A. (2018). Production method and varietal source influence the volatile profiles of spirits prepared from fig fruits (Ficus carica L.). *European Food Research and Technology*, *244*(12), 2213–2229. https://doi.org/10.1007/s00217-018-3131-3

Rodríguez-Solana, R., Rodríguez-Freigedo, S., Salgado, J. M., Domínguez, J. M., & Cortés-Diéguez, S. (2017). Optimisation of accelerated ageing of grape marc distillate on a micro-scale process using a Box–Benhken design: Influence of oak origin, fragment size and toast level on the composition of the final product. *Australian Journal of Grape and Wine Research*, *23*(1), 5–14.

Rohart, F., Gautier, B., Singh, A., & Lê Cao, K.-A. (2017). mixOmics: An R package for 'omics feature selection and multiple data integration. *PLoS Computational Biology*, *13*(11), e1005752.

Ruiz-Moreno, M. J., Muñoz-Redondo, J. M., Cuevas, F. J., Marrufo-Curtido, A., León, J. M., Ramírez, P., & Moreno-Rojas, J. M. (2017). The influence of pre-fermentative maceration and ageing factors on ester profile and marker determination of Pedro Ximenez sparkling wines. *Food Chemistry*, *230*, 697–704.

Sadoughi, N., Schmidtke, L. M., Antalick, G., Blackman, J. W., & Steel, C. C. (2015). Gas chromatography–mass spectrometry method optimized using response surface modeling for the quantitation of fungal off-flavors in grapes and wine. *Journal of Agricultural and Food Chemistry*, *63*(11), 2877–2885.

Spaho, N., Dürr, P., Grba, S., Velagić-Habul, E., & Blesić, M. (2013). Effects of distillation cut on the distribution of higher alcohols and esters in brandy produced from three plum varieties. *Journal of the Institute of Brewing*, *119*(1–2), 48–56.

Steger, C. L. C., & Lambrechts, M. G. (2000). The selection of yeast strains for the production of premium quality South African brandy base products. *Journal of Industrial Microbiology and Biotechnology*, *24*(6), 431–440.

Tsakiris, A., Kallithraka, S., & Kourkoutas, Y. (2014). Grape brandy production, composition and sensory evaluation. *Journal of the Science of Food and Agriculture*, *94*(3), 404–414.

van Jaarsveld, F. P., Blom, M., Hattingh, S., & Marais, J. (2017). Effect of Juice Turbidity and Yeast Lees Content on Brandy Base Wine and Unmatured Pot-still Brandy Quality. *South African Journal of Enology & Viticulture*, *26*(2). https://doi.org/10.21548/26-2-2126

Vázquez-Araújo, L., Rodríguez-Solana, R., Cortés-Diéguez, S. M., & Domínguez, J. M. (2013). Study of the suitability of two hop cultivars for making herb liqueurs: Volatile composition, sensory analysis, and consumer study. *European Food Research and Technology*, *237*(5), 775–786. https://doi.org/10.1007/s00217-013-2050-6

Zacaroni, L. M., de Sales, P. F., Cardoso, M. das G., Santiago, W. D., & Nelson, D. L. (2017). Response surface optimization of SPME extraction conditions for the analysis of volatile compounds in Brazilian sugar cane spirits by HS-SPME-GC-MS: Response surface optimization of SPME extraction. *Journal of the Institute of Brewing*, *123*(2), 226–231. https://doi.org/10.1002/jib.410

Zhang, C., Ao, Z., Chui, W., Shen, C., Tao, W., & Zhang, S. (2011). Characterization of volatile compounds from Daqu-a traditional Chinese liquor fermentation starter: Characterization of volatile compounds. *International Journal of Food Science & Technology*, *46*(8), 1591–1599. https://doi.org/10.1111/j.1365-2621.2011.02660.x

Zhao, Y., Xu, Y., Li, J., Fan, W., & Jiang, W. (2009). Profile of Volatile Compounds in 11 Brandies by Headspace Solid-Phase Microextraction Followed by Gas Chromatography-Mass Spectrometry. *Journal of Food Science*, *74*(2), C90–C99. https://doi.org/10.1111/j.1750-3841.2008.01029.x

Table 1. Samples of *holandas*, wine spirits and brandies used to characterize the ester profile with the developed method.

System of *Criaderas* and *Solera*	Position	Average ageing in *Solera*
A	1st *Criadera*	
A	*Solera*	5 years
B	2nd *Criadera*	
B	1st *Criadera*	
B	*Solera*	3 years
C	2nd *Criadera*	
C	1st *Criadera*	
C	*Solera*	10-12 years
D	2nd *Criadera*	
D	1st *Criadera*	
D	*Solera*	10-12 years
E	2nd *Criadera*	
E	1st *Criadera*	
E	*Solera*	15 years
F	2nd *Criadera*	
F	1st *Criadera*	
F	*Solera*	25 years
G	3th *Criadera*	
G	2nd *Criadera*	
G	1st *Criadera*	
G	*Solera*	40 years

Table 2. Results of the quadratic models fitted for each family of esters (ordered by abundance in brandies) for the HS-SPME optimization.

Family of esters	Lack of fit (p-value)	R^2_{Adj} [a]	R^2_{Pred} [b]	BIC [c]	Model (p-value)
Ethyl esters of fatty acids	0.59	0.94	0.82	292	<0.001
Higher alcohol acetates	0.83	0.92	0.87	239	<0.001
Ethyl esters of branched acids	0.61	0.95	0.92	210	<0.001
Ethyl esters of odd carbon number fatty acids	0.80	0.93	0.85	223	<0.001
Methyl esters of fatty acids	0.09	0.93	0.74	227	<0.001
Cinnamates	0.44	0.99	0.97	113	<0.001
Isoamyl esters of fatty acids	0.63	0.98	0.96	156	<0.001

[a] Adjusted coefficient of determination; [b] Predicted coefficient of determination; [c] Bayesian information criterion used to optimise coefficients of the quadratic models.

Table 3. Ions, linear retention indexes (LRI), linearity, precision, detection and quantification limits, and accuracy of each ester compound in brandy samples. Esters are grouped in families ordered by abundance in brandies.

Compound	Ions (m/z)[a]	LRI[b]	Linearity[c]					Precision (RSD %)			LOD[f] (µg/L)	LOQ[g] (µg/L)	Accuracy[h]			
			Slope	Intercept	Range (ug/L)	R^2	RSD (%)	Intra-day[d] Level A	Intra-day[d] Level B	Inter-day[e]			Added (µg/L)	Recovery (%)	Added (µg/L)	Recovery (%)
Ethyl esters of fatty acids (EEFAs)																
Ethyl butyrate	**88/**71/60	1023	0.0137	-0.6115	192-4806	0.993	7	2	16	2	58	192	1442	107	4806	87
Ethyl hexanoate	**88/**99/60	1226	0.0156	6.8514	395-9870	0.981	13	3	10	4	119	395	2961	116	9870	86
Ethyl octanoate	**88/**101/27	1435	0.0059	1.4899	809-20236	0.981	6	5	10	8	243	809	6071	106	20236	92
Ethyl decanoate	**88/**101/155	1637	0.0675	14.8919	379-9486	0.982	6	18	29	12	114	379	2846	83	9486	91
Ethyl dodecanoate	**88/**101/183	1839	0.0076	1.0735	203-5086	0.985	7	6	23	14	61	203	1526	110	5086	100
Ethyl myristate	**88/**157/256	2041	0.0234	-0.2748	43-1068	0.983	8	5	24	8	13	43	320	85	1068	84
Ethyl palmitate	**88/**101/157	2249	0.0049	-0.0751	37-937	0.991	8	3	15	15	11	37	281	104	937	104
Ethyl stearate	**88/**157/312	2455	0.0075	0.0091	4.3-109	0.983	5	22	25	14	1.3	4.3	32.6	97	109	106
Higher alcohol acetates (HAAs)																
Propyl acetate	**61/**43	970	0.0048	0.0160	4.2-106	0.980	7	3	18	1	1.3	4.2	31.7	117	106	96
Isobutyl acetate	**56/**43	1004	0.0221	-0.0133	3.6-89	0.984	9	3	17	2	1.1	3.6	26.8	104	89	94
Isoamyl acetate	**70/**55/43	1115	0.0725	3.1188	392-9810	0.981	11	5	17	1	118	392	2943	96	9810	82
Hexyl acetate	**56/**43	1265	0.0161	-0.0190	4.2-105	0.987	7	3	11	6	1.3	4.2	31.6	99	105	98
Phenylethyl acetate	**104/**91/43	1814	0.0566	0.0435	18-459	0.985	10	13	21	18	5	18	138	103	459	83
Ethyl esters of branched acids (EEBAs)																
Ethyl isobutyrate	**116/**88/71	963	0.0054	-0.0748	19-472	0.982	12	1	17	2	6	19	142	81	472	84
Ethyl 2-methylbutyrate	**102/**57/85	1037	0.0615	-0.2960	17-428	0.980	11	6	18	4	5	17	128	100	428	82
Ethyl isovalerate	**88/**85/57	1060	0.0969	-0.6366	17-429	0.990	9	5	21	6		17	129	110	429	82
Ethyl phenylacetate	**91/**105	1781	0.0721	-0.0516	1.1-28	0.984	21	14	11	4	0.3	1.1	8.5	81	28	118
Ethyl esters of odd carbon number fatty acids (EEOCNFAs)																
Ethyl heptanoate	**88/**101	1326	0.0402	-0.0624	7.5-187	0.993	5	7	12	7	2.3	7.5	56.2	105	187	105
Ethyl nonanoate	**101/**88	1529	0.0175	-0.0407	7.2-179	0.984	30	29	30	14	2.2	7.2	53.6	64	179	104
Methyl esters fatty acids (MEFAs)																
Methyl hexanoate	**74/**87/99	1180	0.0120	-0.0104	2.0-50	0.990	5	3	10	6	0.6	2.0	15.0	105	50	104
Methyl octanoate	**74/**87/127	1384	0.0717	-0.0016	2.0-51	0.988	6	5	17	6	0.6	2.0	15.2	86	51	108
Methyl decanoate	**74/**87	1588	0.0301	-0.0318	2.2-54	0.981	13	19	25	13	0.7	2.2	16.2	90	54	82

Cinnamates																
Ethyl cinnamate	**176/**131	2119	0.0166	-0.0034	1.1-27	0.983	9	11	28	15	0.3	1.1	8.1	84	27	81
Ethyl dihydrocinnamate	**104/**91/178	1877	0.1374	0.0458	1.1-29	0.986	9	17	20	17	0.3	1.1	8.6	117	29	104
Isoamyl esters of fatty acids (IEFAs)																
Isoamyl butyrate	**71/**70/55	1258	0.0442	-0.0414	1.8-45	0.991	6	2	11	6	0.5	1.8	13.5	89	45	100
Miscellaneous esters																
Ethyl propanoate	**102/**57/75	968	0.0009	-0.0406	1878-4696	0.993	6	3	16	3	563	1878	1409	110	4696	87
Isobutyl hexanoate	**99/**56/71	1350	0.0195	-0.0153	3.8-96	0.992	6	6	13	7	1.1	3.8	28.9	93	96	98
Ethyl valerate	**85**/88/101	1128	0.0742	0.0159	7.8-194	0.993	5	4	15	3	2.3	7.8	58.4	89	195	84

[a] Ions used for identification. In bold ions used for quantification in SIM mode.

[b] Experimental linear retention indexes in a BP21 chromatographic column.

[c] For linearity, five standard addition curves were fitted.

[d] Intra-day (repeatability) was evaluated using identical samples of spiked brandy at two levels of concentration (n = 9)

[e] Inter-day (reproducibility) was evaluated using an identical non-spiked brandy monitored during one-month period (n = 12).

[f] LOD: limit of detection in brandy.

[g] LOQ: limit of quantification in brandy.

[h] Accuracy in terms of recoveries (%) of ester compounds in brandy samples at two different levels of concentration.

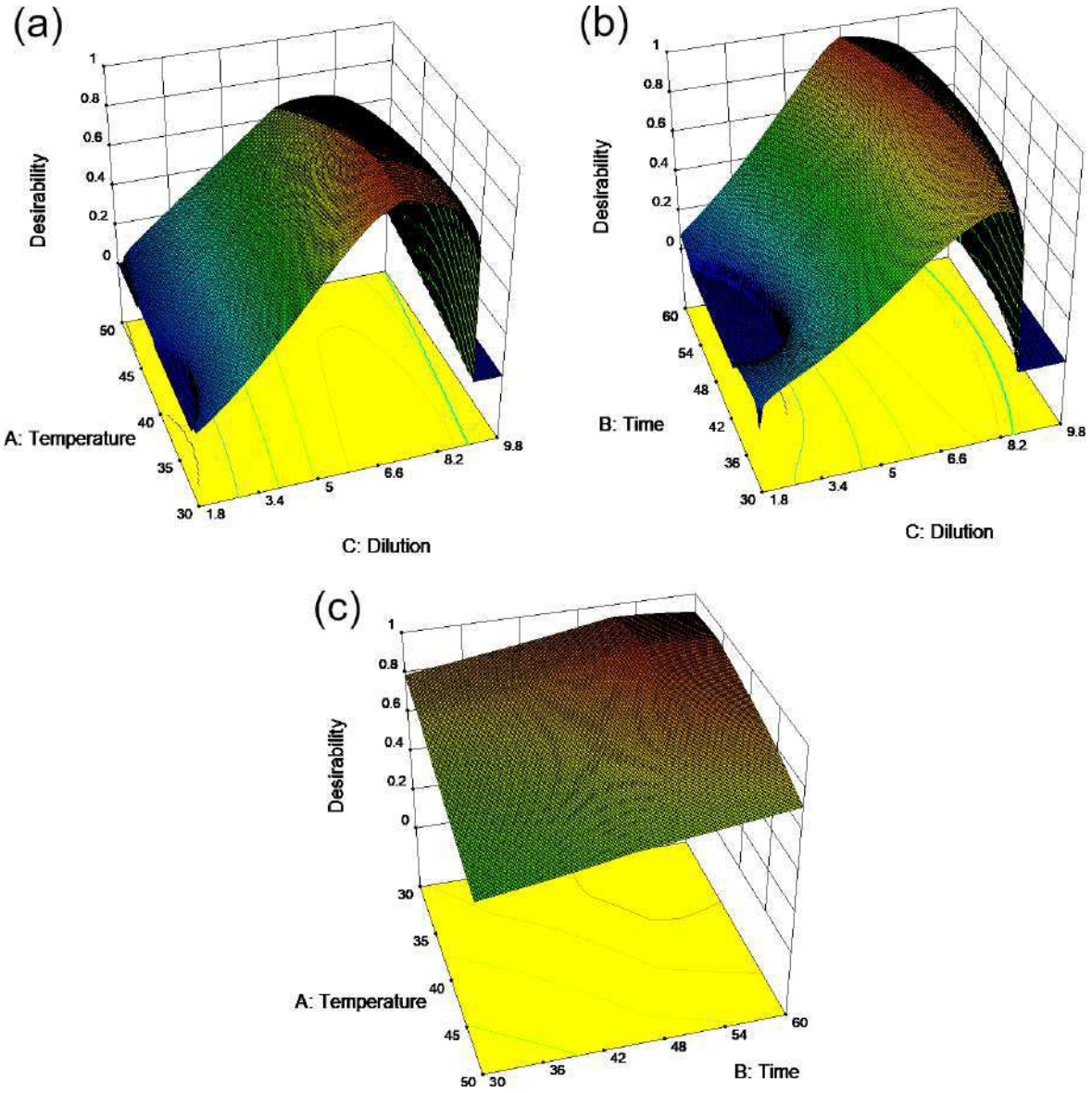

Figure 1. 3D surface plots of the desirability values as function of (a) extraction temperature and extraction time at a fixed optimal sample dilution of 7.2 % v/v in ethanol; (b) extraction time and sample dilution at a fixed optimal extraction temperature of 33 ºC; (c) extraction temperature and sample dilution at a fixed optimal extraction time of 55 min.

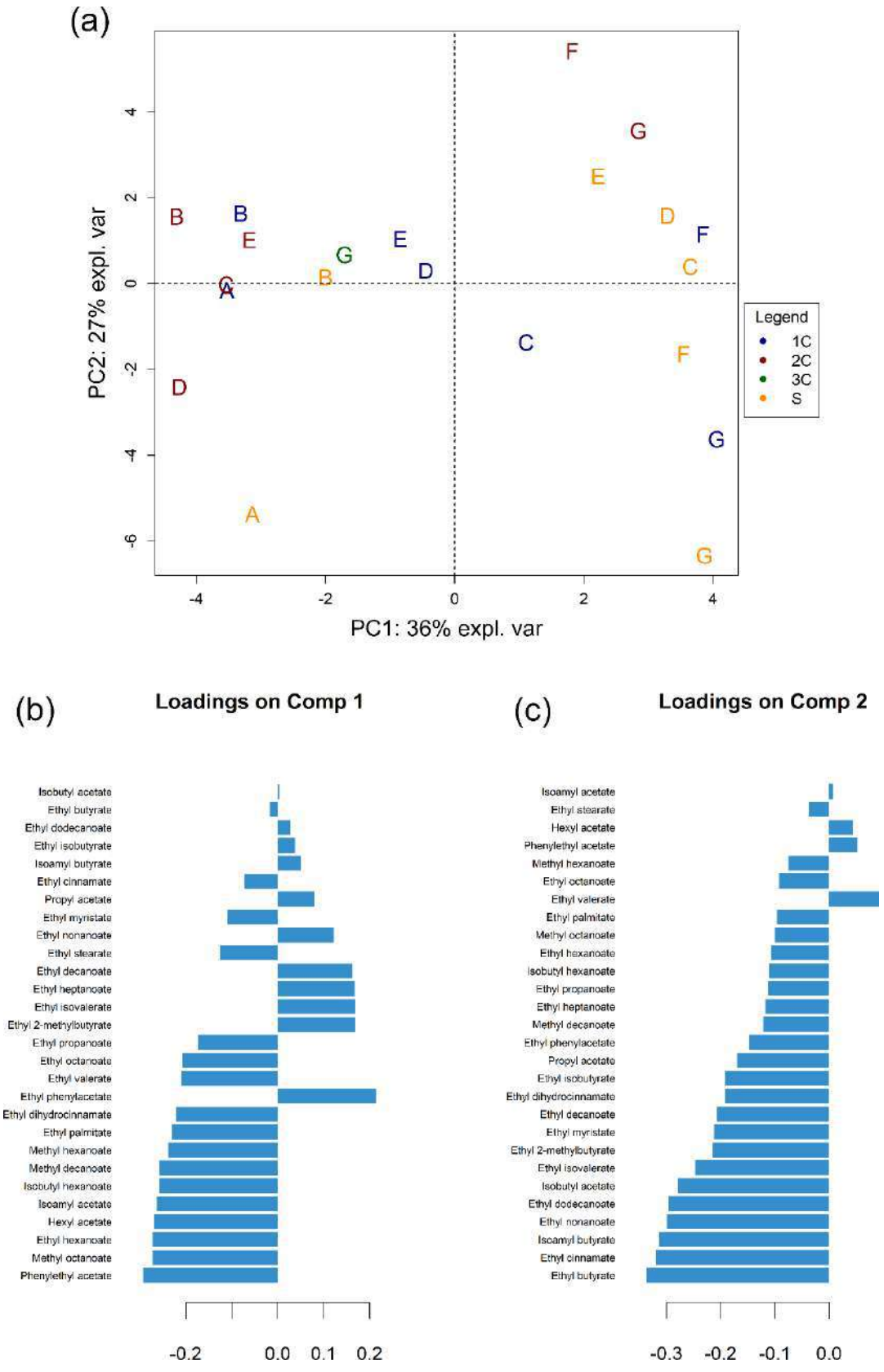

Figure 2. Principal component analysis carried out on the real brandy samples from 7 *Criaderas* and *Solera systems* with different average ageing.

ARTÍCULO 7

Impact of stabilization and filtration on the ester profile of "Brandy de Jerez". A chemometric assessment

José Manuel Muñoz-Redondo, Manuel José Valcárcel-Muñoz, Raquel Rodríguez Solana, Emma Cantos-Villar, Belén Puertas, José Manuel Moreno-Rojas

Journal of Agricultural and Food Chemistry

(Enviado)

Impact of stabilization and filtration on the ester profile of "Brandy de Jerez". A chemometric assessment

José Manuel Muñoz-Redondo[1*], Manuel José Valcárcel-Muñoz[2], Raquel Rodríguez Solana[1], Emma Cantos-Villar[3], Belén Puertas[3], José Manuel Moreno-Rojas[1*]

[1]Department of food Science and Health. Andalusian Institute of Agricultural and Fisheries Research and Training (IFAPA). Alameda del Obispo Avda, Menéndez Pidal, s/n. 14071, Córdoba, Spain

[2]Research and Development Department. Bodegas Fundador, S.L.U. Calle San Ildefonso, nº3, 11403, Jerez de la Frontera, Cádiz, Spain

[3]Department of food Science and Health. Andalusian Institute of Agricultural and Fisheries Research and Training (IFAPA). Cañada de la Loba, 11471, Jerez de la Frontera, Cádiz, Spain.

*Corresponding author:

E-mail: josem.moreno.rojas@juntadeandalucia.es

Tel.: +34 671 53 27 58; Fax: +34 957 01 60 43

Abstract

Brandy stabilization is an important step aimed at decanting the suspended chemical and biological particles that may cause undesirable turbidity in brandies, commonly referred as cloudiness or haze. This phenomenon is originated by high molecular-weight lipids and esters, and ethanol-soluble lignins. Ethyl esters of long-chain fatty acids are associated with haze formation due to decreases in their solubility when brandies are storage at low temperatures. For this reason, producers are recommended to intentionally encourage forming of haze and then remove it before releasing the brandy to the market. The purpose of this study was to study the influence on the ester profile of Brandy de Jerez of two methods of stabilization: room temperature for 1 year and filtration, and 7 days at -10 ºC and filtration. Then, the results were compared with the samples before stabilization. The use of multivariate statistical analyses made it possible to identify the most impacted esters (markers) by the stabilization process. It was observed that stabilization at room temperature yielded the most distinct ester profile, while changes after cold stabilization were more subtle. Meanwhile, both stabilization processes produced a significant decrease in ethyl esters of long-chain fatty acids, achieving the desired effect.

Keywords: esters, brandy, HS-SPME/GC-MS, cold stabilization, multivariate statistics

1. Introduction

Brandy is a spirit obtained by distillation of wine. Its consumption is highly extended throughout the world, being Spain one of the world's leading producers with the so-called "Brandy de Jerez" or "Sherry Brandy". This product is elaborated in the Southern Spanish area known as *Marco de Jerez* under a protected geographical indication (Regulation (EC) 110/2008), following the specification provided by the Technical File (Boletín Oficial la Junta Andalucía, 2018; Off. J. Eur. Union, 2019). "Brandy de Jerez" is produced from holandas (< 70% v/v of ethanol), spirits (70-86% v/v) and wine distillates (86-94.8% v/v), and its organoleptic equilibrium is reached by ageing in American oak (*Quercus alba*) casks of capacity lower than 1000 L, previously seasoned with Sherry wines. This ageing process follows the traditional dynamic system known as *Criaderas* and *Solera* or sometimes, additionally by the static system known as *Añadas* (Schwarz et al., 2009). Three quality categories can be distinguished by the ageing according to the Regulation of the "Brandy de Jerez": Brandy Solera (minimum 6 months), Brandy Solera Reserva (minimum 1 year) and Brandy Solera Gran Reserva (more than 3 years).

The final characteristics of this product are determined by the different steps followed during the production process, such as raw material and winemaking, distillation system (alquitara, charentais alembic, or distillation column), ageing or maturation in American sherry casks, and stabilization (Miljić et al., 2013). Brandy stabilization is an important step aimed at decanting the suspended chemical and biological particles that may cause undesirable turbidity (commonly referred as cloudiness or haze) in brandies, originated by high molecular-weight lipids and esters, and ethanol-soluble lignins (Piggott et al., 1996). Cloudiness often appears in fruit brandies when the alcohol content is below 45 % v/v, as well as temperatures below 7 ºC, usually reached during storage in

transportation (Puškaš et al., 2013). In addition, haze can be slowly formed in the final product after bottling. For this reason, producers are recommended to intentionally encourage forming of haze and then remove it before releasing the brandy on the market (Piggott et al., 1996). In brandies and whiskies, haze formation is known to be related with major volatile components, colourings, and polyphenol substances. Among the volatile metabolites, ethyl and isoamyl esters of long-chain fatty acids, in concrete, ethyl esters of C8-C18 fatty acids such as C12 (ethyl laurate), ethyl-9-hexadecanoate (ethyl palmitoleate), and especially C16 (ethyl palmitate) and C18 (ethyl stearate); as well as phenylethanol, ethyl lactate and long-chain fatty acids are linked to chill haze formation (Balcerek et al., 2019; Bordiga, 2017; Miljić et al., 2013).

There are several ways to reduce the cloudiness in spirit beverages, such as the use of activated carbon, an adsorbent and hydrophobic material that is able to trap volatile compounds and adsorb organic compounds (Mukhin et al., 2009), or based in filtration materials (cellulose, carbon, diatomaceous earth or candle filters) that need to be carefully chosen to prevent loss of flavour compounds (Balcerek et al., 2019). A common practice to remove haze formation in alcoholic beverages (particularly red, sparkling and sweet fortified wines and brandies) is cold stabilization (frozen the spirit at temperatures below -5 ºC for a few days) and subsequent filtration before bottling, this being also referred as cold filtration (Balcerek et al., 2019; Ribéreau-Gayon et al., 2000; Różański et al., 2020).

Previous works carried out in of fruit brandies (apricot, plum and rye) studied different conditions of stabilization such as temperature, and filtration systems (Balcerek et al., 2019; Miljić et al., 2013; Puškaš et al., 2013; Różański et al., 2020). Results showed the influence of these factors on the final turbidity of samples, obtaining the best results with intermediate values of temperature (from -1 to -4 ºC) and filter pore size (filter sheets with higher nominal retention rate, > 0.7 µm, and membranes with 800 nm pore size).

However, to the authors' knowledge, the effect of the cold stabilization and filtration over the ester profile of brandies has not been fully approached before.

The objective of the present work was to study the influence on the ester profile of "Brandy de Jerez" of two methods of stabilization: at room temperature for 1 year followed by filtration, and 7 days at -10 ºC followed by filtration. The ester profile obtained with both stabilization processes was then compared with the ester profile of brandies without stabilization. Brandies used in this work were from different ageing periods: Solera, Solera Reserva and Solera Gran Reserva. The results were analysed by means of multivariate statistical techniques and a multilevel decomposition made it possible to reveal the effect of the stabilization process.

2. Material and methods

2.1. Brandy samples

Brandies used in this work are from Jerez de la Frontera (Spain) and with Protected Geographical Indication (PGI) (Regulation (EC) 110/2008). The samples were elaborated following the traditional dynamic system called *Criaderas* and *Solera* as it is established in the regulations of the Regulatory Council of "Brandy de Jerez" (The Consejo Regulador, 2016). A total of 1 Brandy Solera, 3 Brandies Solera Reserva with a final alcohol content of 36 % v/v, and 5 Brandies Solera Gran Reserva were used, with a final alcohol content of 40 % v/v. Each brandy was stabilized as follow:

- Room temperature for 1 years in darkness followed by filtration with Seitz K-200 filters
- Cold temperature (-10 ºC) for 7 days and filtration at -10ºC with Seitz K-200 filters.

Samples before and after stabilization were storage at 6 ºC and immediately analyzed.

2.2. Chemicals

High-performance liquid chromatography (HPLC)-grade ethanol was obtained from J.T. Baker Chemicals B.V. (Denventer, Holland). Milli-Q water was produced by a Milli-Q Plus

water system (Millipore, Spain). Ethylenediaminetetraacetic acid (EDTA) was supplied by Panreac Applichem (Barcelona, Spain). Sigma-Aldrich (Madrid, Spain) supplied the following: sodium chloride ACS reagent grade (purity ≥ 99.8%), and the standard compounds ethyl butyrate (≥ 99%), ethyl hexanoate (≥ 99%), ethyl octanoate (≥ 99%), ethyl decanoate (≥ 99%), ethyl dodecanoate (≥ 99%), ethyl myristate (≥ 99%), ethyl palmitate (≥ 99%), ethyl stearate (≥ 99%), propyl acetate (≥ 99%), isobutyl acetate (≥ 99%), isoamyl acetate (≥ 99%), hexyl acetate (≥ 99%), phenylethyl acetate (≥ 99%), ethyl isobutyrate (98%), ethyl 2-methylbutyrate (≥ 99%), ethyl isovalerate (≥ 99%), ethyl phenylacetate (98%), ethyl cinnamate (98%), ethyl dihydrocinnamate (98%), methyl hexanoate (≥ 99%), methyl octanoate (≥ 99%), methyl decanoate (≥ 99%), isoamyl butyrate (98%), ethyl heptanoate (98%), ethyl nonanoate (98%), ethyl propanoate (≥ 99%), isobutyl hexanoate (≥ 99%), ethyl valerate (≥ 99.7%), acetaldehyde (≥ 99.5%). The deuterated internal standards [$^2H_3$]-ethyl butyrate, [$^2H_{11}$]-ethyl hexanoate, [$^2H_{15}$]-ethyl octanoate, [$^2H_5$]-ethyl trans-cinnamate, [$^2H_{23}$]-ethyl dodecanoate, [$^2H_{27}$]-ethyl myristate, [$^2H_{31}$]-ethyl palmitate, and [$^2H_{35}$]-ethyl stearate, were supplied by CDN isotopes (Pointe-Claire, Canada).

2.3. HS-SPME GC-MS

2.3.1. Sample preparation and extraction conditions

A total of 25 mL of brandy sample were spiked with 20 µL of an internal standard mix solution of 8 deuterated ethyl esters at 200 mg/L. The peak integration of each ester was normalized using specific deuterated standards as follow: ethyl isobutyrate, ethyl 2-methylbutyrate, ethyl isovalerate, ethyl propanoate, ethyl butyrate, isoamyl acetate, ethyl valerate, propyl acetate, and isobutyl acetate were normalized with [$^2H_3$]-ethyl butyrate. Ethyl hexanoate, methyl hexanoate, methyl octanoate, isoamyl butanoate, isobutyl hexanoate, ethyl heptanoate, and hexyl acetate were normalized with [$^2H_{11}$]-ethyl hexanoate. [$^2H_{15}$]-Ethyl octanoate was used to normalize ethyl octanoate, methyl decanoate. Phenylethyl acetate, ethyl dihydrocinnamate, and ethyl cinnamate were

normalized with [$^2H_5$]-ethyl trans-cinnamate; while ethyl dodecanoate, ethyl decanoate, ethyl nonanoate, and ethyl phenylacetate with [$^2H_{23}$]-ethyl dodecanoate. Finally, [$^2H_{27}$]-ethyl myristate, [$^2H_{31}$]-ethyl palmitate and [$^2H_{35}$]-ethyl stearate were used to normalize ethyl myristate, ethyl palmitate and ethyl stearate, respectively. Then, the spiked samples were diluted in EDTA solution (200 mM and pH adjusted to 7 with NaOH 1 M), since this chemical prevents oxidation of the compounds (Dziekońska-Kubczak et al., 2020). Afterwards, the brandy samples were diluted to reach 7.2 % v/v ethanol, and 10 mL of this solution were transferred to a 20 mL SPME vial containing 3.5 g of NaCl to increase the ionic strength of the analytes and release more volatiles into the headspace (Davis & Qian, 2019; Dziekońska-Kubczak et al., 2020). The vials were capped, and the solution was homogenized using a vortex shaker for 30 s and placed in a Combipal autosampler tray (CTC Analytics, Zwingen, Switzerland).

A 100 µm PDMS fibre (Supelco, Bellefont, PA, USA), previously conditioned according to the supplier recommendation, was used for extraction of esters via HS-SPME. For the equilibrium step, the vials were incubated at 500 rpm for 2 minutes at the extraction temperature, while the extraction was performed at 33 ºC for 55 minutes and maintaining agitation at 500 rpm.

The conditions of the gas chromatograph were as follow: the desorption time and temperature were set at 15 min and 250 °C respectively, performed in a Trace GC ultragas chromatograph (Thermo Fisher Scientific S. p.A., Rodano, Milan, Italy). The desorbed samples passed to an ISQ Single MS spectrometer (Thermo Fisher Scientific, Austin, Texas, USA). The injection was performed in splitless mode in a BP21 column of 50m × 0.32 mm and 0.25 µm film thickness (SGE Analytical Science, UK) for the volatiles separation. The carrier gas was helium at a constant flow rate of 1.7 mL/min. The oven temperature program was set at 40 °C for 5 min, raised to 220 °C at 3 °C/min and held for 30 min. The MS operated in electron ionization mode at 70 eV using selected-ion-monitoring (SIM) mode. The transfer line and source temperature of the MS

were set at 230 °C and 200 °C, respectively. The identification procedure was performed by comparing the retention times and mass spectra with those of the pure standards.

2.4. Statistical analysis

Principal component analysis (PCA) was first used to check the structure of the data and to look for grouping of the brandy samples. Afterwards, the main differences between samples related to the stabilization process were studied by means of a multilevel partial least squares discriminant analysis (PLS-DA). The multilevel decomposition was applied since the data followed a paired structure with two measures for the same samples: before and after cold stabilization and filtration, this allowing to focus on the effect of this treatment regardless the initial composition of each brandy. The model was optimized and validated by means of a double cross-validation scheme described in Szymańska et al., 2012, using the balanced error rate (BER). The p-value of the model was obtained from a permutation test (N = 1000, since it was large enough to sample the tails of the distribution and to attain a p-value up to 0.001) for BER, area under the receiver operating characteristic curve (AUROC), and the average number of misclassified (NMC). The p-value of the model was calculated as follow:

$$p\text{ - }value = 1 + (Diagnostic_P \leq Diagnostic) / N$$

where ($Diagnostic_P \leq Diagnostic$) is the number of elements in the H0 distribution that are smaller or equal to the diagnostic (BER, AUROC or NMC) of the original data.

The most discriminatory metabolites were selected by an iterative process based on variable importance in projection (VIP) scores previously described by Muñoz-Redondo et al., 2020. The statistical analyses were performed using the software R version 4.0.3 and the package *mixOmics* (Rohart et al., 2017).

3. Results and discussion

The most abundant family of esters measured in the brandy samples were ethyl esters of fatty acids, with concentration ranging from 11.6 to 48.8 mg/L in agreement with

previous studies (Nikićević et al., 2011; Zhao et al., 2009). These compounds are known to increase during ageing in alcoholic beverages as a consequence of the slow esterification of organic acids with ethanol (Campo et al., 2007). Among them, ethyl octanoate (from 9 to 18 mg/L) followed by ethyl decanoate (from 0.034 to 20.1 mg/L) displayed the highest concentrations, these being considered as important contributors to the aroma of distilled beverages and identified as odour active compounds in distillates (Genovese et al., 2004; Nikićević et al., 2011). Methyl esters of fatty acids (0.015-14.78 mg/L) were found in high concentrations due to the high contribution of methyl butyrate, that ranged between values close to 0 to 14.74 mg/L. Meanwhile, higher alcohol acetates and ethyl esters of branched acids were found in concentrations between 1.27-3.81 mg/L and 0.14-1.76 mg/L respectively. Isoamyl acetate was the most abundant acetate ester in accordance with literature (Nikićević et al., 2011).

A principal component analysis (PCA) was carried out to study the variation sources in the data and to find sample groupings. The first two principal components of the PCA accounted for the 61 % of the total sample variability (Figure 1), the main variation source being explained by PC1 (39 %), which was related with the ageing of the brandies (Figure 1A). It was observed that brandies Solera and Solera Reserva with a more similar period of ageing averaging 6-9 and 12-18 months respectively, displayed a similar ester profile characterized by higher levels of isoamyl acetate, hexyl acetate, isobutyl acetate, ethyl butyrate, methyl hexanoate, propyl acetate, ethyl octanoate, phenylethyl acetate, ethyl valerate, isobutyl hexanoate, methyl octanoate, isoamyl octanoate, ethyl dihydrocinnamate and ethyl hexanoate. Meanwhile, the ester profile of the Brandies Solera Gran Reserva (averaging 6-12 years of ageing) displayed a more differentiated ester profile with an overall increase of the rest of the esters analyzed (Figure 1A and 1C), including ethyl 2-methylbutyrate, ethyl nonanoate, ethyl phenylacetate, ethyl isovalerate, ethyl isobutyrate, ethyl decanoate, ethyl dodecanoate, ethyl propanoate, ethyl heptanoate, methyl butyrate, isoamyl butanoate, ethyl myristate and ethyl

cinnamate. These results pointed out the distinctive and exclusive character of these brandies. Rodríguez Dodero et al., 2010 also found that "Brandies de Jerez" Solera Gran Reserva displayed a clear different phenolic and furanic derivatives profile from other brandies produced in different regions, indicating their highly specific character. The higher concentrations observed in these esters can be related with continuous esterification of fatty acids and ethanol, and loses of water and ethanol through evaporation effects during ageing (Christoph & Bauer-Christoph, 2007; Durán-Guerrero et al., 2021).

Brandies before and after both stabilization processes were highlighted in the scores plot of Figure 1B. The most distinct ester profile was observed for the brandies submitted to room temperature stabilization, as it was shown by a clear separation in component 2 of the PCA. However, due to the large differences observed between brandies, predominantly related to the ageing, and the paired structure of the data (Westerhuis et al., 2010) with repeated measures to the same samples (before stabilization, after cold stabilization and after room temperature stabilization), the differences related with the stabilization were not clearly highlighted, especially for cold stabilization. Therefore, a multilevel decomposition was applied to focus on the effect of the treatment and a partial least squares discriminant analysis (ML-PLS-DA) was fitted for three-classes: brandies before stabilization, after cold stabilization and filtration, and after room temperature stabilization and filtration (Figure 2). The model was optimized and validated following a double cross-validation scheme. The number of components of the sub-models was predominantly optimized to 2, revealing a low complexity that reduce risk of overfitting (Figure 1B). The ML-PLS-DA displayed a good performance with a BER of 0.09 ± 0.05 (Table 1). Brandies stabilized at room temperature were correctly assigned in all the cases, supporting a more distinct ester profile, while the error of the model was due to incorrect assignment between brandies without stabilization and after cold stabilization. Therefore, this error suggested a lower impact on the ester profile when cold stabilization

was applied. Then, the model was successfully validated with a permutation test. The null distributions calculated from the class label permutation are shown in Figure 3 for three diagnostics statistics: BER, AUROC and NMC, which displayed an expected Gaussian shape. The average performance of the model fell the tail of the null distribution for the three diagnostics, obtaining a p-value of the model below 0.05 in all the cases (Table 1). All these results supported the robustness of the ML-PLS-DA, being this model suitable for analysing and interpreting the dataset.

Differences in the ester profile of brandies related to the stabilization process are shown in the scores and loadings plots of the ML-PLS-DA model (Figure 2A, 2B and 2C). As it was expected from the previous PCA, the brandies submitted to room temperature stabilization and filtration displayed the most distinct ester profile, being separated from the rest in component 1, that explained a high 54 % of the variance. This stabilization process resulted in higher contents of many esters, such as isoamyl octanoate, ethyl isovalerate, ethyl isobutyrate, isobutyl hexanoate, ethyl 2-methylbutyrate, propyl acetate, ethyl butyrate, isoamyl acetate, methyl hexanoate, ethyl hexanoate, ethyl valerate, methyl decanoate and isobutyl acetate. The percentage of change related to the control brandy (before stabilization) is shown in Supplementary Table 1. Meanwhile, other esters such as isoamyl hexanoate, isoamyl butanoate, ethyl octanoate, hexyl acetate, phenylethyl acetate, ethyl cinnamate, methyl butyrate, ethyl decanoate, ethyl heptanoate, ethyl palmitate, ethyl dihydrocinnamate, ethyl stearate, ethyl nonanoate and ethyl myristate displayed a significant decrease concentration.

The brandies submitted to cold stabilization were separated from those before stabilization in component 2, which explained a 11 % of the total variance (Figure 2A and 2D). Differences in the volatile profile were subtler and mainly driven by a decrease in ethyl esters of long-chain fatty acids: ethyl palmitate, ethyl stearate and ethyl myristate. Turbidity of brandies is associated with ethyl esters of long-chain fatty acids due to decreases in their solubility mainly related to low temperatures of storage (Balcerek et

al., 2019). Therefore, reduction of these compounds is beneficial in terms of ensuring the stability of brandies (Carrillo, 2015). These ethyl esters displayed however slightly heavier decrease in brandies stabilized at room temperature, especially for ethyl stearate (decreasing below the detection limit). Meanwhile, both stabilization procedures yielded decreases of ethyl palmitate between 70-98 % of the initial values and ethyl myristate between 11-87 %. A previous study showed a similar reduction of ethyl myristate after brandy stabilization (Balcerek et al., 2019). These results pointed out a low impact on ester profile when cold stabilization was used, compared to room temperature stabilization.

A variable reduction procedure was performed to determine the most impacted esters by the stabilization process, i.e., the markers of this process. This procedure was repeated 100 times, and the compounds selected in at least the 70 % of the iteration were highlighted in Figure 2C and 2D. Ethyl esters of long chain fatty acids were among the largest impacted esters. The ester compounds selected as markers of room temperature stabilization were isoamyl octanoate, isoamyl hexanoate, ethyl isovalerate, ethyl isobutyrate, isobutyl hexanoate, isoamyl butanoate, propyl acetate, ethyl butyrate, ethyl palmitate, ethyl stearate and ethyl myristate. While markers of the cold stabilization were ethyl palmitate, ethyl stearate and ethyl myristate, this treatment being more specific for reduce turbidity in brandies.

4. Conclusions

This study showed the impact of the cold and room temperature stabilization and later filtration on the ester profiles of brandies, some of them being the major cause of turbidity. Stabilization at room temperature yielded the most distinct ester profile, with strong increases of isoamyl octanoate, ethyl isovalerate, ethyl isobutyrate, isobutyl hexanoate, propyl acetate and ethyl butyrate. Meanwhile, brandies submitted to cold stabilization displayed an ester profile more similar to the brandies before stabilization. However, cold stabilization yielded important reduction in ethyl esters of long-chain fatty acids (mainly

ethyl palmitate, ethyl stearate and ethyl myristate), associated with haze formation and highlighting the specificity of this treatment to reduce turbidity without a high impact on the volatile profile.

Financial funds

J.M.M.-R. was awarded a research contract funded by the Andalusian Institute of Agricultural and Fisheries Research and Training (IFAPA), within the National Youth Guarantee System funded through the European Social Fund (ESF) and the Youth Employment Initiative (YEI). R.R.S. was supported by Juan de la Cierva-Incorporation contract from the Spanish Ministry of Science, Innovation and Universities (IJC2018-036207-I). This study has been funded by the Andalusian Institute of Agricultural and Fisheries Research and Training (IFAPA) and Bodegas Fundador, S.L.U through the Project FEDER-Innterconecta “Factores que influyen en la calidad del Brandy y nuevos sistemas de elaboración del mismo, desde el viñedo al envasado” (BESTBRANDY).

References

Balcerek, M., Pielech-Przybylska, K., Dziekońska-Kubczak, U., Patelski, P., & Różański, M. (2019). Effect of filtration on elimination of turbidity and changes in volatile compounds concentrations in plum distillates. *Journal of Food Science and Technology*, *56*(4), 2049–2062.

Boletín Oficial la Junta Andalucía. (2018). *Consejería de Agricultura Pesca y Desarrollo rural. Orden de 28 de junio de 2018, por la que se aprueba el expediente técnico de Indicación Geográfica "Brandy de Jerez"* (127, 19–20).

Bordiga, M. (2017). *Post-fermentation and-distillation technology: Stabilization, aging, and spoilage*. CRC Press.

Campo, E., Cacho, J., & Ferreira, V. (2007). Solid phase extraction, multidimensional gas chromatography mass spectrometry determination of four novel aroma powerful ethyl esters: Assessment of their occurrence and importance in wine and other alcoholic beverages. *Journal of Chromatography A*, *1140*(1–2), 180–188.

Carrillo, J. C. M. (2015). *Feasibility testing of chill filtration of brown spirits to increase product stability*. University of Louisville.

Christoph, N., & Bauer-Christoph, C. (2007). Flavour of spirit drinks: Raw materials, fermentation, distillation, and ageing. In *Flavours and fragrances* (pp. 219–239). Springer.

Commission of the European Communities (EEC), Council Regulation (EEC) No. 110/2008 of 15 January, 2008. (2008). Official Journal of the European Union, L 39/16 (2008), pp. 17-18.

Davis, P. M., & Qian, M. C. (2019). Effect of Ethanol on the Adsorption of Volatile Sulfur Compounds on Solid Phase Micro-Extraction Fiber Coatings and the Implication for Analysis in Wine. *Molecules*, *24*(18), 3392.

Durán-Guerrero, E., Castro, R., García-Moreno, M. de V., Rodríguez-Dodero, M. del C., Schwarz, M., & Guillén-Sánchez, D. (2021). Aroma of Sherry Products: A Review. *Foods*, *10*(4), 753.

Dziekońska-Kubczak, U., Pielech-Przybylska, K., Patelski, P., & Balcerek, M. (2020). Development of the method for determination of volatile sulfur compounds (vscs) in fruit brandy with the use of HS–SPME/GC–MS. *Molecules*, *25*(5), 1232.

Genovese, A., Ugliano, M., Pessina, R., Gambuti, A., Piombino, P., & Moio, L. (2004). Comparison of the aroma compounds in apricot (prunus armeniaca, l. Cv. Pellecchiella) and apple (malus pumila, l. Cv. Annurca) raw distillates. *Italian Journal of Food Science*, *16*(2).

Miljić, U. D., Puškaš, V. S., Vučurović, V. M., & Razmovski, R. N. (2013). The application of sheet filters in treatment of fruit brandy after cold stabilization. *Acta Periodica Technologica*, *44*, 87–94.

Mukhin, V. M., Shubina, N. A., Abramova, I. M., Zubova, I. D., & Lupascu, T. G. (2009). New carbonic adsorbents for industrial sorting purification in vodka production. *Environmental Engineering & Management Journal (EEMJ)*, *8*(5).

Muñoz-Redondo, J. M., Ruiz-Moreno, M. J., Puertas, B., Cantos-Villar, E., & Moreno-Rojas, J. M. (2020). Multivariate optimization of headspace solid-phase microextraction coupled to gas chromatography-mass spectrometry for the analysis of terpenoids in sparkling wines. *Talanta*, *208*, 120483.

Nikićević, N., Velickovic, M., Jadranin, M., Vučković, I., Novaković, M., Vujisić, L. V., Stanković, M., Urosevic, I., & Tešević, V. (2011). The effects of the cherry variety on the chemical and sensorial characteristics of cherry brandy. *Journal of the Serbian Chemical Society*, *76*(9), 1219–1228.

Off. J. Eur. Union. (2019). *European Parliament and of the Council. Regulation (EC) No 2019/787 of 17 April 2019, on the definition, description, presentation and labelling of spirit drinks, the use of the names of spirit drinks in the presentation*

and labelling of other foodstuffs, the protection of geographical indications for spirit drinks, the use of ethyl alcohol and distillates of agricultural origin in alcoholic beverages, and repealing Regulation (EC) No 110/2008. (L130, 17–27).

Piggott, J. R., Gonzalez Vinas, M. A., Conner, J. M., Withers, S. J., & Paterson, A. (1996). Effect of chill filtration on whisky composition and headspace. *SPECIAL PUBLICATION-ROYAL SOCIETY OF CHEMISTRY*, *197*, 319–324.

Puškaš, V., Miljić, U., Vasić, V., Jokić, A., & Manović, M. (2013). Influence of cold stabilisation and chill membrane filtration on volatile compounds of apricot brandy. *Food and Bioproducts Processing*, *91*(4), 348–351.

Ribéreau-Gayon, P., Glories, Y., & Maujean, A. (2000). *Handbook of enology: The chemistry of wine stabilization and treatments*. Wiley.

Rodríguez Dodero, M. C., Guillén Sánchez, D. A., Rodríguez, M. S., & Barroso, C. G. (2010). Phenolic compounds and furanic derivatives in the characterization and quality control of brandy de Jerez. *Journal of Agricultural and Food Chemistry*, *58*(2), 990–997.

Rohart, F., Gautier, B., Singh, A., & Lê Cao, K.-A. (2017). mixOmics: An R package for 'omics feature selection and multiple data integration. *PLoS Computational Biology*, *13*(11), e1005752.

Różański, M., Pielech-Przybylska, K., & Balcerek, M. (2020). Influence of Alcohol Content and Storage Conditions on the Physicochemical Stability of Spirit Drinks. *Foods*, *9*(9), 1264.

Ruiz-Moreno, M. J., Muñoz-Redondo, J. M., Cuevas, F. J., Marrufo-Curtido, A., León, J. M., Ramírez, P., & Moreno-Rojas, J. M. (2017). The influence of pre-fermentative maceration and ageing factors on ester profile and marker determination of Pedro Ximenez sparkling wines. *Food Chemistry*, *230*, 697–704.

Schwarz, M., Rodríguez, Mc., Martínez, C., Bosquet, V., Guillén, D., & Barroso, C. G. (2009). Antioxidant activity of Brandy de Jerez and other aged distillates, and correlation with their polyphenolic content. *Food Chemistry*, *116*(1), 29–33.

Szymańska, E., Saccenti, E., Smilde, A. K., & Westerhuis, J. A. (2012). Double-check: Validation of diagnostic statistics for PLS-DA models in metabolomics studies. *Metabolomics*, *8*(1), 3–16.

The Consejo Regulador. (2016, May 26). Brandy de Jerez. https://www.brandydejerez.es/en/our-philosophy/consejo-regulador

Westerhuis, J. A., van Velzen, E. J., Hoefsloot, H. C., & Smilde, A. K. (2010). Multivariate paired data analysis: Multilevel PLSDA versus OPLSDA. *Metabolomics*, *6*(1), 119–128.

Zhao, Y., Xu, Y., Li, J., Fan, W., & Jiang, W. (2009). Profile of volatile compounds in 11 brandies by headspace solid-phase microextraction followed by gas chromatography-mass spectrometry. *Journal of Food Science*, *74*(2), C90–C99.

Table 1. Multilevel partial least squares discriminant analysis (ML-PLS-DA) performance.

Mean Overall BER	Class	Mean Class Error	Predicted as BS	Predicted as CS	Predicted as RTS	p-value (model)
0.09 ± 0.05	BS	0.15 ± 0.11	765	135	0	BER, AUROC, NMC: 0.001
	CS	0.14 ± 0.10	122	778	0	
	RTS	0.00 ± 0.00	0	0	900	

BER: balanced error rate. BCF: before cold stabilization and filtration; ACF: after cold stabilization and filtration. p-value of the model obtained from a permutation test (N = 1000) for the balanced error rate (BER), area under the receiver operating characteristic curve (AUROC), and the average number of misclassified (NMC).

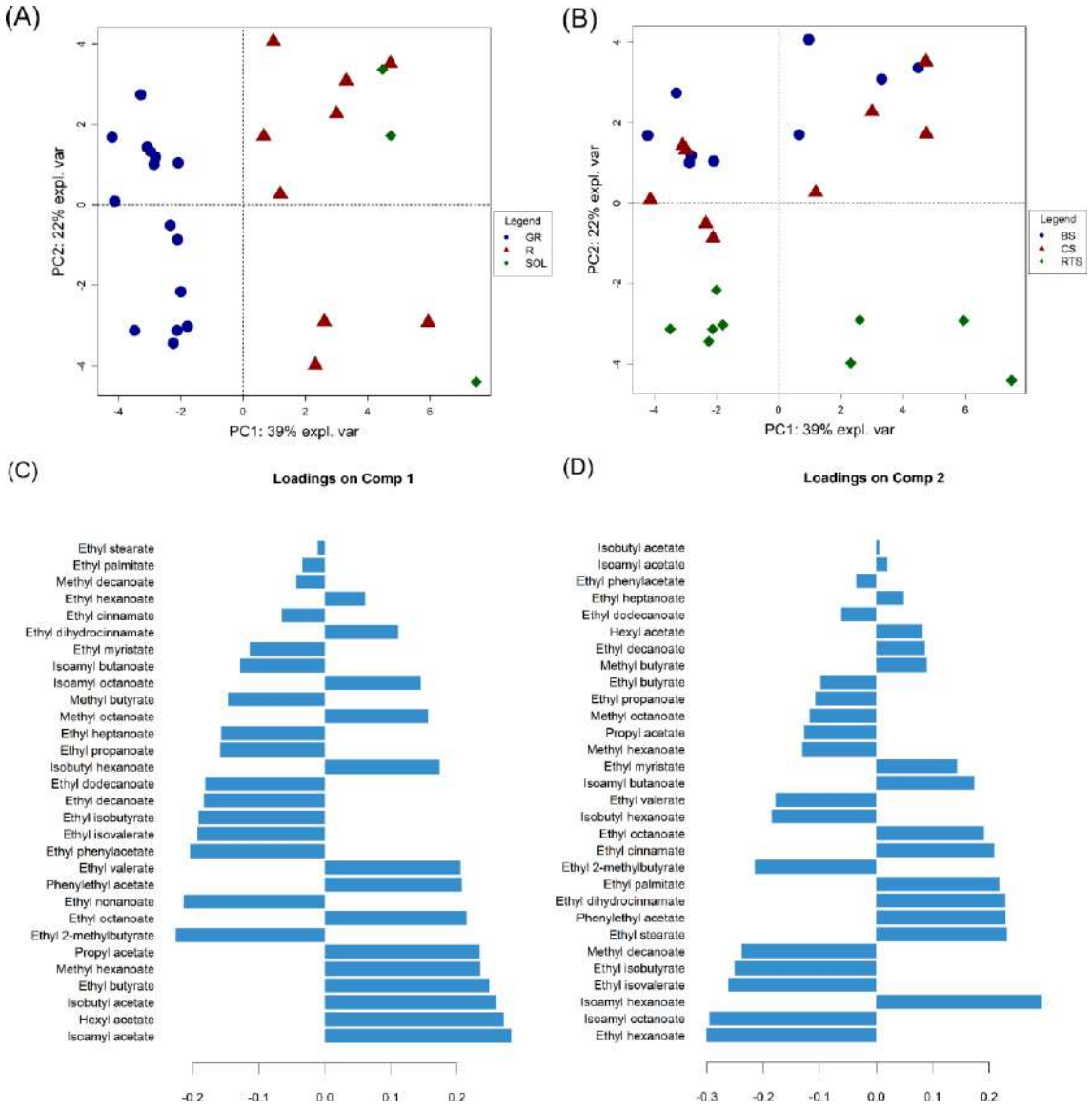

Figure 1. Principal component analysis (PCA) carried out on the brandy samples. Scores plot for the first two principal component highlighting brandies according to the ageing factor (A), and before and after cold stabilization and filtration treatment (B). Loadings bar plot on component 1 (C) and component 2 (D). SOL: Brandy Solera; R: Brandy Solera Reserva; GR: Brandy Solera Gran Reserva. BS: brandy before stabilization; CS: brandy after cold stabilization and filtration; RTS: brandy after room temperature stabilization.

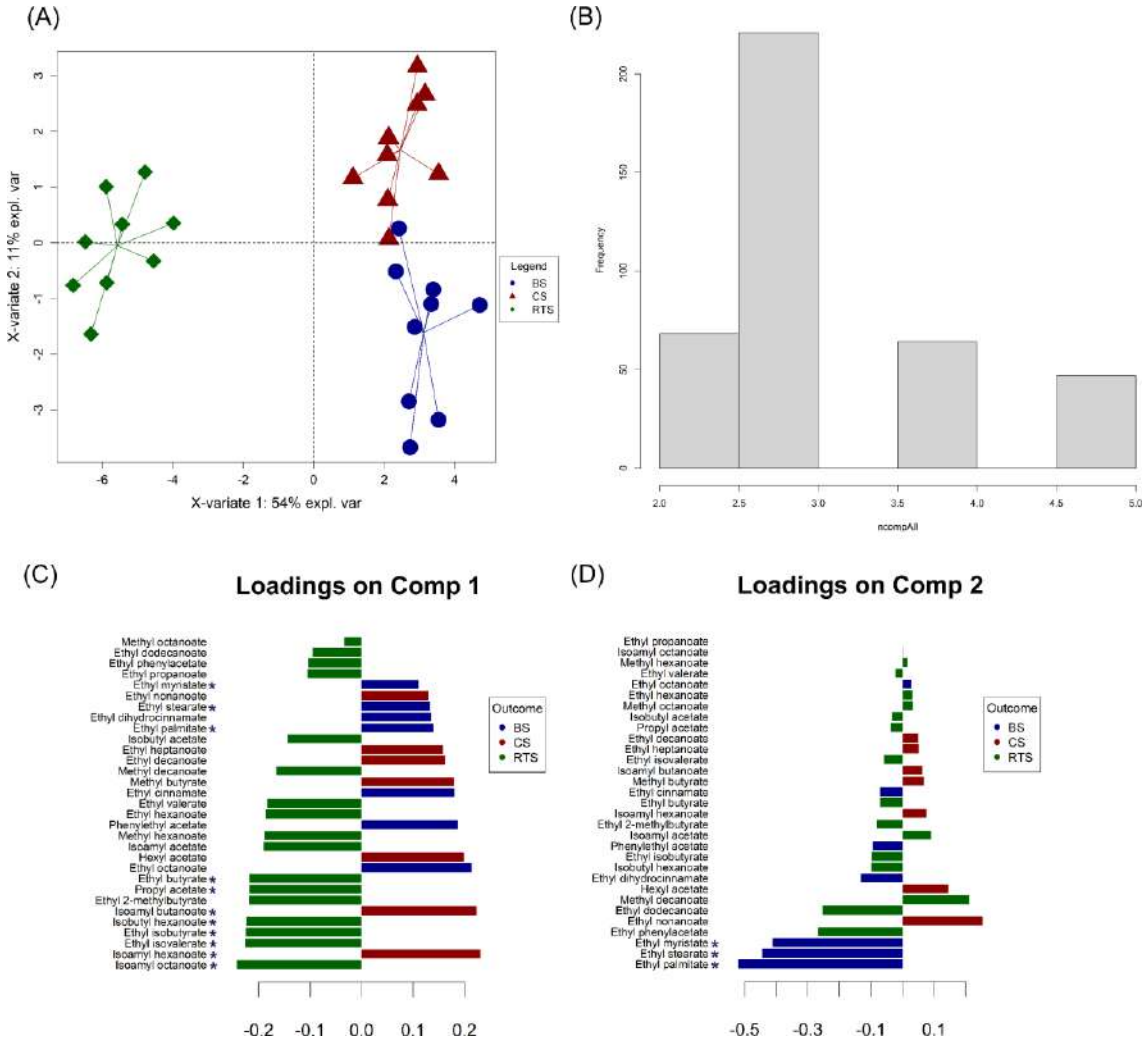

Figure 2. Graphical outputs of the multilevel partial least squares discriminant analysis (ML-PLS-DA) carried out to discriminate brandy samples before and after cold stabilization and filtration. (A) Scores plot for component 1 (X-variate 1), (B) histogram of the number of component optimized for the submodels during the double-cross validation, (C) loadings contribution barplot on component 1 and (D) component 2. Colour indicates the class for which the compound has a maximal mean value. Bar length represents the multivariate regression coefficient with either a positive or negative sign for that particular feature of each component, i.e., the importance of each variable in the model. BS: brandy before stabilization; CS: brandy after cold stabilization and filtration; RTS: brandy after room temperature stabilization.

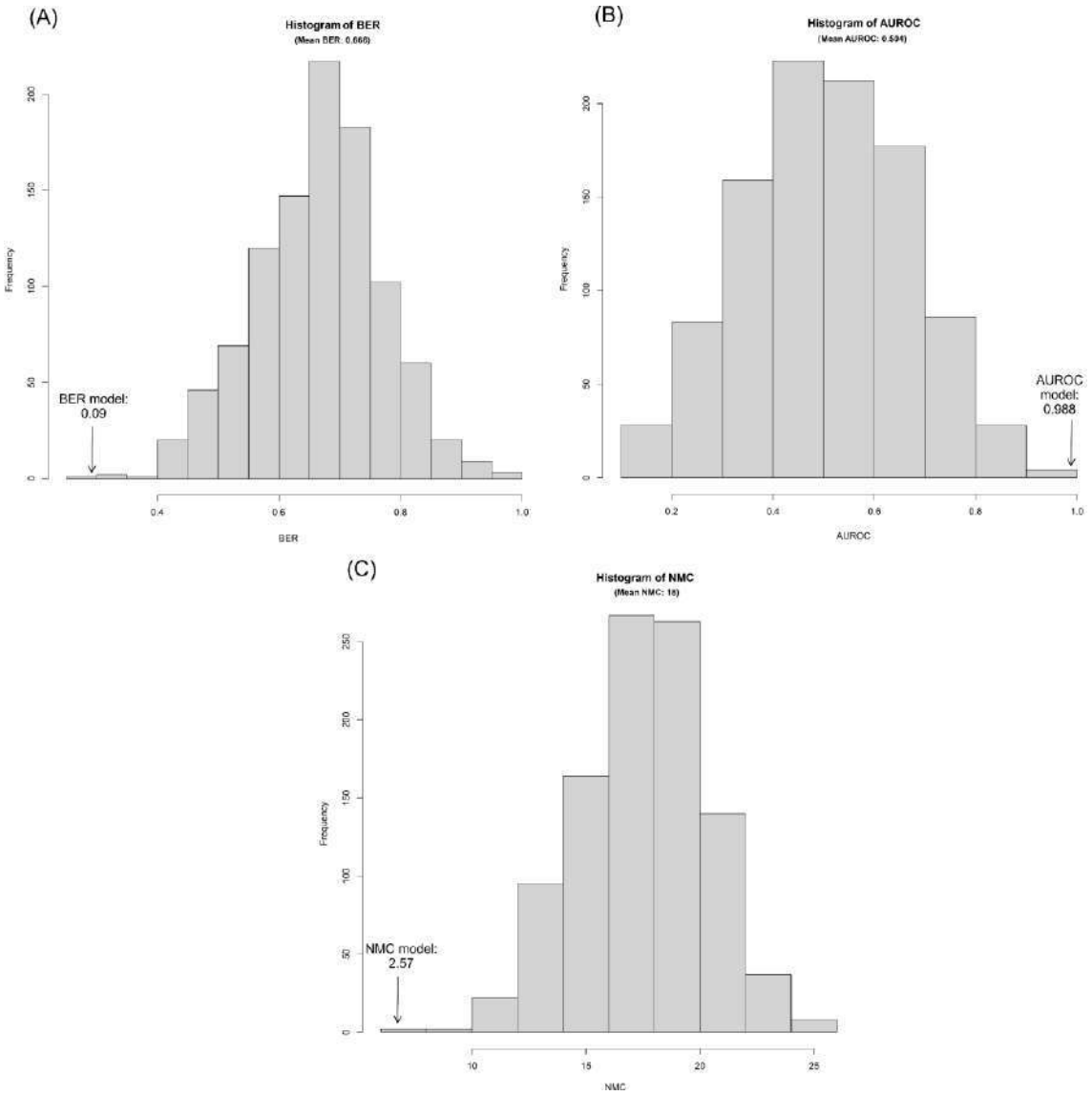

Figure 3. Results from the permutation test (N = 1000) performed on the multilevel partial least squares discriminant analysis (ML-PLS-DA). Histogram obtained from the permutation test for (A) the balanced error rate (BER), (B) area under the receiver operating characteristic curve (AUROC), and (C) the average number of misclassified (NMC). The real average performance of the model for the three statistics obtained from the double cross-validation is shown in each plot.

CAPÍTULO 3

TRAZABILIDAD DE FRUTAS TROPICALES PRODUCIDAS EN LA COSTA DE ANDALUCÍA

Resumen

La trazabilidad alimentaria es un aspecto que ha cobrado fuerza en los últimos años como mecanismo para asegurar a los compradores el origen de un producto, motivado en parte por la creciente preocupación que muestran los consumidores en su alimentación.

Este aspecto cobra especial importancia cuando se trata de productos de alta calidad, cuya mayor retribución económica hace atractiva a otros competidores su falsificación y venta fraudulenta, lo cual puede producir un impacto económico negativo y dañar su imagen. Por esta razón, las empresas que comercializan estos alimentos de calidad diferenciada invierten recursos para desarrollar mecanismos que permitan autentificar sus productos. En este sentido, los productores de frutas tropicales situados a lo largo de la franja costera andaluza han iniciado los trámites para establecer una Indicación Geográfica Protegida para la producción de mangos y aguacates, con el fin de protegerse de sus competidores. Por esta razón, nace la necesidad de establecer metodologías que permitan diferenciar estas frutas producidas en Andalucía de las producidas en otros países.

En este capítulo se desarrolla una metodología basada en los isotopos estables de 5 bioelementos (C, N, S, O y H), el perfil multi-elemental y técnicas quimiométricas para diferenciar los mangos y aguacates producidos en Andalucía de los producidos en otras zonas del mundo. Los resultados mostraron la capacidad de ambas técnicas por separado y de manera conjunta para identificar de manera exitosa las muestras producidas en Andalucía.

ARTÍCULO 8

Tracing the geographical origin of Spanish mango (*Mangifera indica L.*) using stable isotopes ratios and multi-element profiles

J.M. Muñoz-Redondo, D. Bertoldi, A. Tonon, L. Ziller, F. Camin, J.M. Moreno-Rojas

Food Control

125, 107961 (2021)

Q1: 19/139 (Food Science & Technology, 2019)

Impact Factor: 4.258

Food Control 125 (2021) 107961

Contents lists available at ScienceDirect

Food Control

journal homepage: www.elsevier.com/locate/foodcont

Tracing the geographical origin of Spanish mango (*Mangifera indica L.*) using stable isotopes ratios and multi-element profiles

J.M. Muñoz-Redondo [a,**], D. Bertoldi [b], A. Tonon [c], L. Ziller [c], F. Camin [c,d], J.M. Moreno-Rojas [a,*]

[a] Department of Food Science and Health, Andalusian Institute of Agricultural and Fisheries Research and Training (IFAPA), Alameda Del Obispo, Avda, Menéndez Pidal, S/n., 14071, Córdoba, Spain
[b] Department of Experimental and Technological Services, Technology Transfer Centre, Fondazione Edmund Mach, Via E. Mach 1, 38010, San Michele All'Adige, Italy
[c] Department of Food Quality and Nutrition, Research and Innovation Centre, Fondazione Edmund Mach, Via E. Mach 1, 38010, San Michele All'Adige, Italy
[d] Centre Agriculture Food Environment C3A, University of Trento, San Michele All'Adige, Trento, Italy

ARTICLE INFO

Keywords:
IRMS
ICP-MS
Geographical origin
Protected geographical indications
Multivariate analysis
PLS-DA
Stable isotopes

ABSTRACT

The stable isotopes of five bio-elements ($\delta^{13}C$, $\delta^{15}N$, $\delta^{34}S$, $\delta^{2}H$, $\delta^{18}O$) and the elemental composition profile combined with chemometrics were used to differentiate the geographical origin of commercial samples of mango, aimed at contributing to the existence of a Spanish protected geographical indication (PGI). Eighty commercial mangoes from all over the world (Spain, Mexico, Peru, Brazil, Ivory Coast, Equatorial Guinea and Senegal), collected during two consecutive harvests, were analysed and assessed by means of univariate and multivariate data analyses, establishing the main variation sources linked to the origin of the mangoes. The data obtained from each analytical platform were assessed separately and in combination, resulting in three models whose discriminatory power (Spanish vs others) was compared. The model fitted for the stable isotope approach yielded a sensitivity of 100%, meaning that the Spanish mangoes were correctly classified in all the cases, against the 97.6% for multi-element analysis. The combined use of stable isotopes and elemental composition led to the most accurate geographical discrimination of Spanish mangoes, making it possible to select three stable isotope ratios ($\delta^{15}N$, $\delta^{18}O$, $\delta^{34}S$) and six elements (Cd, Se, Cs, As, Pb and Ba) as the main indicators of the geographic origin of mango. The results of this study revealed the feasibility of tracing the provenance of mango through either of the two analytical strategies or by combining them to obtain a more accurate classification.

1. Introduction

Mango (*Mangifera indica L.*) is a predominantly tropical fruit variety whose worldwide production reached 39 million tonnes in 2018, which represented more than half of the total global major tropical fruit production (FAO, 2018). Mango is best cultivated in the intertropical zone, India being the leading producer with around the 40% of the total world production in 2018 (FAO, 2018); UNCTAD, 2016). In recent years, mango cultivation has prospered in Mediterranean regions such as Spain, Morocco and Egypt (UNCTAD, 2016). Among them, Spain plays a key role in the international trade of mango, since it is the only European producer country, giving it a logistical strategic position due to its geographical proximity to this market (Fruittrop, 2020). However, the current market globalization may leave Spanish mango producers in a vulnerable situation if they are not legally protected against mangoes from foreign markets. In this sense, geographical indications such as protected designation of origin (PDO) and protected geographical indications (PGI) have gained importance in recent years. While PDO is a brand used to assure the production, processing and preparation of foodstuffs with strong regional identities, PGI relates to foodstuffs and agricultural products linked to a particular geographical area in at least some of the production, processing or preparation stages (EU Regulation No 1151/2012). Beyond the legal foundations of geographical indications to assure the authenticity and traceability of agricultural and food products, they are being used as a marketing tool, since the restricted geographical location together with the recognized know-how used to elaborate the products implies unique characteristics or qualities (Giovannucci et al., 2009; Martelo-Vidal & Vázquez, 2016, pp. 35–70). This generally results in a greater economic reward and improved social perception, providing added value for those origin-labelled products. In

* Corresponding author.
** Corresponding author.
E-mail addresses: josem.munoz.redondo@juntadeandalucia.es (J.M. Muñoz-Redondo), josem.moreno.rojas@juntadeandalucia.es (J.M. Moreno-Rojas).

https://doi.org/10.1016/j.foodcont.2021.107961
Received 2 November 2020; Received in revised form 20 January 2021; Accepted 1 February 2021
Available online 5 February 2021

this sense, mango producers in southern Spain along the coastal strip of Andalusia (Granada and Malaga) have recently initiated a procedure to register a PGI label with the aim of making their product more competitive and attractive, and to protect their produce from mangoes from foreign markets and reinforce their position as the only European producer (Freshplaza, 2020). However, the potential long-term economic value for origin-labelled products also make them attractive for competitors to imitate and fraudulently sell them as authentic, and this may seriously damage the reputation and income of the geographical indication (Giovannucci et al., 2009). Therefore, a major concern for geographical indications is to assure the traceability and authentication of food and agricultural products. Numerous studies in the last few years have addressed this matter by means of different analytical techniques (Badia-Melis et al., 2015; Camin et al., 2013; Chiesa et al., 2016; Furia et al., 2011; Katerinopoulou et al., 2020). However, only a few studies have dealt with these issues in mangoes, including the impact of geographic location on the volatile composition (Kulkarni et al., 2012) and quality parameters (Hofman et al., 1997) of mangoes, and the authentication of specific mango varieties through the analysis of their volatile profile (Zakaria et al., 2018) and near-infrared spectroscopy (NIR) (Jha et al., 2013), or even the differentiation of organic and conventionally produced mangoes by means of their mineral content (Hernández-Sánchez et al., 2012). Therefore, new tools which make possible simple and accurate geographical traceability of mangoes could be of great value for geographical indications of this fruit.

Stable isotope ratio mass spectrometry (S-IRMS) has demonstrated great potential for tracing the origin of agri-food products, especially when conventional analytical techniques are unable to provide accurate results (Katerinopoulou et al., 2020). This approach is generally based on the stable isotope ratio of light bio-elements ($^{13}C/^{12}C$, $^{15}N/^{14}N$, $^{34}S/^{32}S$, $^{2}H/^{1}H$, $^{18}O/^{16}O$) found in the molecules and compounds of living organisms. Chemical, physical and biochemical processes, influenced by the environmental conditions, agricultural practices and geologic conditions, result in the measurable partitioning of these light stable isotopes (isotopic fractionation) (Crittenden et al., 2007). Therefore, numerous studies have successfully used stable isotope ratios to determine the origin of agri-food products (Badia-Melis et al., 2015; Bertoldi et al., 2014; Bontempo et al., 2009; Camin et al., 2010; Chung et al., 2016; Crittenden et al., 2007; Dasenaki & Thomaidis, 2019; Katerinopoulou et al., 2020; Ocvirk et al., 2018; Opatić et al., 2018; Pianezze et al., 2019; Santato et al., 2012; Wang et al., 2020). The isotopic fingerprint has also been used in conjunction with other techniques such as inductively coupled plasma mass spectrometry (ICP-MS) to determine the geographical origin of foodstuffs (Camin et al., 2010; Katerinopoulou et al., 2020; Opatić et al., 2018; Santato et al., 2012; Wang et al., 2020). This technique makes it possible to determine trace and rare earth elements, which reflect the growth conditions of food products in a particular environment (Katerinopoulou et al., 2020).

The aim of this study was to assess the effectiveness of the stable isotopes of five light bio-elements (C, N, S, H, O) and multi-elemental fingerprinting to determine the geographical origin of commercial mangoes produced in Spain and contribute the existence of a Spanish protected geographical indication of mango. The results from both analytical platforms (IRMS and ICP-MS) were independently and jointly assessed by means of univariate and multivariate statistical analysis. Double cross-validated partial least squares discriminant analysis (PLS-DA) was used to classify the mango samples according to their origin and to compare the prediction abilities of the different approaches.

2. Material and methods

2.1. Samples

Eighty commercial samples of mangoes of different varieties (Osteen, Kent, Palmer, Keitt and Irving) from different geographical origins (Spain N = 43, Senegal N = 8, Ivory Coast N = 2, Equatorial Guinea N = 4, Peru N = 6, Mexico N = 12 and Brazil N = 5) collected at different years (2014 N = 23, 2015 N = 2, 2016 N = 21, 2017 N = 34) were included in the experimental design. The mango pulp samples, without the skin and seed kernel, were freeze dried and homogenized by grinding and milling before analysis. The powdered samples were then placed into 2 mL Eppendorf tubes and stored at −18 °C until analysis.

2.2. Stable isotope ratios measurements

Around 3 mg of the freeze-dried samples were weighed into tin capsules for the determination of $\delta^{13}C$, $\delta^{15}N$ and $\delta^{34}S$ in one run and around 0.3 mg were weighed into silver capsules for the simultaneous determination of $\delta^{2}H$ and $\delta^{18}O$. The $^{15}N/^{14}N$, $^{13}C/^{12}C$ and $^{34}S/^{32}S$ ratios were determined using an IRMS (Isoprime, AP2003, GV Instruments Ltd, Manchester, UK) equipped with an elemental analyser (Vario EL III Elementar Analysensysteme GmbH, Hanau, Germany), while the $^{18}O/^{16}O$ and $^{2}H/^{1}H$ ratios were determined with an IRMS (Flash EATM1112, Thermo Finnigan) equipped with a pyrolyser (FinniganTM TC/EA, ThermoFinnigan). The isotope ratios were expressed as relative to the international standards ratio and denoted in delta notation, although miliurey (mUr) can also be used by comply with the International System of Units (SI), according to the following formula (Brand et al., 2014):

$$\delta(^{i/j}E) = \delta^{i/j}E = \frac{^{i/j}R_P - {}^{i/j}R_{\mathrm{Ref}}}{^{i/j}R_{\mathrm{Ref}}}$$

where superscripts *i* and *j* denote the highest and the lowest atomic mass number of element E, respectively, R_P and R_{Ref} indicate the ratio between the heavier and the lighter isotope ($^{2}H/^{1}H$, $^{13}C/^{12}C$, $^{18}O/^{16}O$, $^{15}N/^{14}N$, $^{34}S/^{32}S$) in the sample and reference material, respectively.

The $\delta^{13}C$ values were reported as relative to the Vienna-Pee Dee Belemnite (V-PDB) standard, $\delta^{15}N$ values relative to the Air standard, $\delta^{34}S$ values to the Vienna Cañon Diablo Troilite (V-CDT) standard and $\delta^{2}H$ and $\delta^{18}O$ values relative to the Vienna-Standard Mean Ocean Water (VSMOW) standard.

The samples were analysed in duplicate. The isotope values were determined by two-point normalization method using international reference materials: L-glutamic acid USGS 40 (IAEA-International Atomic Energy Agency, Vienna, Austria), fuel oil NBS-22 (IAEA) and sugar IAEA–CH–6 for $^{13}C/^{12}C$; L-glutamic acid USGS 40 and potassium nitrate IAEA-NO3 for $^{15}N/^{14}N$; barium sulphates IAEA–SO–5 and NBS 127 (IAEA) for $^{34}S/^{32}S$. International reference materials USGS 54 and 56 (wood) were used for calculating $^{18}O/^{16}O$ and $^{2}H/^{1}H$ of the samples. The analytical uncertainty (2 std dev) was 0.3 for $\delta^{13}C$ and $\delta^{15}N$, 0.6 for $\delta^{18}O$ and $\delta^{34}S$ and 3 for $\delta^{2}H$.

2.3. Elemental analysis

For the acid ultrawave-assisted digestion of samples by means of an UltraWAVE System (Milestone, Shelton, CT, USA) equipped with quartz vials, an aliquot of about 400 mg of homogenized and lyophilized mango was used. Mineralization and subsequent element profile analysis with ICP-MS (Agilent 7500ce, Agilent Technologies, Tokyo, Japan) were performed as detailed in Bertoldi et al. (Bertoldi et al., 2014). A total of 53 macro-micro and trace elements were quantified: Li, Be, B, Na, Mg, Al, P, K, Ca, V, Cr, Mn, Fe, Co, Ni, Cu, Zn, Ga, Ge, As, Se, Rb, Sr, Y, Mo, Pd, Ag, Cd, In, Sn, Sb, Te, Cs, Ba, La, Ce, Pr, Nd, Sm, Eu, Gd, Dy, Er, Tm, Yb, Re, Ir, Pt, Au, Hg, Pb, Th and U. All the materials used for the preparation and analysis of the samples were accurately washed with a nitric acid 5% solution and thoroughly rinsed with ultrapure MilliQ® water (18.2MWcm, Millipore, Bedford, MA, USA). Accuracy was assured by analysing in each analytical batch a certified reference material (NIST 1572 'citrus leaves', National Institute of Standards and Technology Gaithersburg, MD, USA). The obtained recovery for certified and non-certified elements was in the range 78–111%. The detection limit of

each element was calculated as 3-times the standard deviation of the signals obtained by analysing 10 blank samples in a sequence. Precision in terms of reproducibility (sample prepared and analysed 3 times in 3 different batches) and expressed as RSD % was better than 5% for all the detectable elements except for some trace elements (Ag, Be, Co, Eu, Er, Ge, Se, Yb, V, U) for which the reproducibility was between 5 and 10%.

2.4. Statistical analysis

Univariate analyses were carried out to reveal differences in the samples. First, the Levene's and Shapiro Wilk's tests were used to check the normality and heteroscedasticity of the data, and the variables that failed the parametric assumptions were box-cox transformed. Subsequently, differences in the data were assessed by means of a one-way ANOVA and post-hoc Tukey's HSD tests with regard to the geographical origin, which were considered statistically significant at a p-value $\leq$ 0.05. To check the correlations between all the elements and stable isotope ratios analysed, a Spearman correlation test was performed. The distribution of the stable isotope ratios along the geographical origin was shown in a density plot.

Table 1
One-way analysis of variance (ANOVA) for the geographical origin of mangos based on the isotope and element profiles. Stable isotope ratios are expressed in δ-values (‰). B, Na, Mg, Al, P, Ca, Mn, Fe, Cu, Zn, Rb, Sr, Ba are expressed in mg/g, K is expressed in g/L and the rest of elements are expressed in μg/kg.

Isotope/ Element	Brazil (N = 5)	Equatorial Guinea (N = 4)	Ivory Coast (N = 2)	Mexico (N = 12)	Peru (N = 6)	Senegal (N = 8)	Spain (N = 43)	p-value*
$\delta^{15}N$	4.70 ± 1.02 a	3.43 ± 0.50 a	5.21 ± 1.10 a	1.98 ± 1.60 a	5.07 ± 3.48 a	3.58 ± 1.15 a	0.25 ± 1.66 b	***
$\delta^{13}C$	−27 ± 1 ab	−27 ± 1 ab	−25 ± 1 a	−28 ± 1 b	−28 ± 1 ab	−26 ± 1 a	−26 ± 1 a	***
$\delta^{34}S$	9.7 ± 0.9 ab	10.9 ± 0.9 ab	8.5 ± 2.4 abc	4.8 ± 1.4 c	7.2 ± 3.1 bc	11.8 ± 1.8 a	4.8 ± 1.9 c	***
$\delta^{18}O$	36 ± 2 a	35 ± 1 a	34 ± 1 a	30 ± 1 b	29 ± 2 b	31 ± 1 b	34 ± 1 a	***
$\delta^{2}H$	32.0 ± 4.0 ab	24.1 ± 8.6 ab	5.0 ± 2.8 bc	15.8 ± 21.3 bc	−8.3 ± 5.1 c	43.6 ± 5.2 a	21.7 ± 18.3 b	***
Li	5.2 ± 1.8 b	6.3 ± 2.9 b	2.1 ± 0.7 b	20.6 ± 28.9 a	7.6 ± 1.4 ab	14.1 ± 5.3 ab	7.6 ± 4.3 b	*
Be	0.59 ± 0.61 b	0.33 ± 0.20 b	0.58 ± 0.26 b	<0.33 ± 0.12 b	0.45 ± 0.70 b	2.32 ± 2.23 a	<0.33 ± 0.3 b	***
B	4.6 ± 2.0 bcd	2.0 ± 0.5 d	8.1 ± 1.4 ab	4.3 ± 1.3 cd	8.7 ± 1.2 a	3.2 ± 0.6 d	5.8 ± 1.8 bc	***
Na	27 ± 14 b	16 ± 7 b	40 ± 8 ab	25 ± 13 b	70 ± 27 a	48 ± 34 ab	28 ± 17 b	***
Mg	548 ± 170 ab	647 ± 97 ab	551 ± 44 ab	562 ± 130 ab	669 ± 203 a	403 ± 99 b	623 ± 166 ab	*
Al	4.66 ± 3.73 a	1.38 ± 0.33 a	0.87 ± 0.10 a	5.79 ± 7.50 a	7.14 ± 0.97 a	2.18 ± 1.77 a	3.13 ± 2.37 a	*
P	489 ± 85 ab	464 ± 62 ab	565 ± 20 ab	549 ± 120 ab	653 ± 188 a	388 ± 127 b	417 ± 96 b	***
K	9.4 ± 2.8 ab	8.1 ± 1.7 ab	7.7 ± 2.0 ab	9.5 ± 2.2 a	9.5 ± 2.0 ab	6.6 ± 1.6 b	7.0 ± 1.7 b	***
Ca	558 ± 224	751 ± 259	885 ± 163	812 ± 390	1039 ± 210	423 ± 133	857 ± 475	ns
V	8.3 ± 5.8 ab	2.6 ± 0.7 b	5.5 ± 6.1 b	9.5 ± 9.5 ab	14.3 ± 3.3 a	3.3 ± 2.4 b	5.6 ± 4.1 b	**
Cr	608 ± 748 a	345 ± 152 a	1199 ± 1583 a	560 ± 385 a	762 ± 336 a	315 ± 308 a	306 ± 342 a	*
Mn	40.0 ± 48.4 a	16.5 ± 11.6 ab	18.1 ± 3.4 ab	2.9 ± 1.0 b	2.8 ± 0.5 b	8.3 ± 4.5 b	4.5 ± 2.7 b	***
Fe	12.7 ± 4.0	9.3 ± 3.2	11.2 ± 5.8	11.9 ± 4.0	16.9 ± 2.6	12.2 ± 8.8	11.4 ± 4.0	ns
Co	22.8 ± 23.6 a	10.1 ± 4.2 ab	29.5 ± 1.9 a	11.8 ± 6.4 ab	14.3 ± 2.3 ab	20.4 ± 22.0 a	7.9 ± 3.5 b	***
Ni	533 ± 350 a	260 ± 23 ab	701 ± 725 a	255 ± 151 ab	336 ± 178 ab	498 ± 197 a	208 ± 178 b	***
Cu	3.0 ± 1.0	3.8 ± 0.5	5.1 ± 0.8	3.2 ± 0.6	5.0 ± 1.0	3.4 ± 0.7	3.9 ± 1.9	ns
Zn	3.0 ± 0.2 ab	2.8 ± 0.6 ab	3.2 ± 0.0 ab	2.4 ± 0.6 ab	3.9 ± 1.4 a	2.0 ± 0.4 b	2.7 ± 1.1 ab	*
Ga	<1.6 ± 0.9	<1.6	<1.6	<1.6 ± 1.8	1.7 ± 0.5	<1.6	<1.6 ± 0.37	ns
Ge	<0.33 ± 0.10 ab	<0.33 b	<0.33 b	<0.33 ± 0.17 a	<0.33 b	<0.33 ± 0.13 a	<0.33 b	***
As	1.7 ± 1.5 b	<1.6 b	<1.6 b	66.1 ± 42.5 a	41.8 ± 20.7 a	<1.6 ± 0.9 b	1.9 ± 4.1 b	***
Se	5.7 ± 2.8 c	17.4 ± 20.4 bc	6.1 ± 0.9 c	66.6 ± 65.8 ab	13.6 ± 6.2 c	91.6 ± 49.9 a	2.6 ± 1.5 c	***
Rb	41.2 ± 23.8 a	26.0 ± 4.4 ab	12.6 ± 1.6 bc	19.6 ± 7.6 b	3.6 ± 4.1 c	18.3 ± 9.5 b	7.4 ± 5.1 c	***
Sr	1.24 ± 0.80 b	2.41 ± 1.31 ab	3.94 ± 0.58 ab	3.64 ± 1.45 ab	6.16 ± 2.80 a	1.48 ± 0.54 b	3.33 ± 2.95 ab	*
Y	7.27 ± 9.47 a	9.62 ± 10.63 a	10.50 ± 3.24 a	1.57 ± 1.59 b	2.29 ± 1.12 ab	6.29 ± 2.69 a	1.44 ± 1.09 b	***
Mo	26 ± 24 b	16 ± 10 b	33 ± 44 ab	89 ± 78 a	57 ± 41 ab	19 ± 13 b	21 ± 17 b	***
Pd	<0.33 b	<0.33 b	<0.33 b	<0.33 ± 0.16 a	<0.33 ± 0.13 ab	<0.33 ± 0.17 ab	<0.33 ± 0.03 b	ns
Ag	0.97 ± 0.50	1.05 ± 0.46	1.26 ± 0.70	8.28 ± 24.59	1.41 ± 0.57	4.32 ± 10.31	3.43 ± 10.14	ns
Cd	2.37 ± 0.85 b	1.87 ± 1.03 b	6.06 ± 2.44 ab	10.31 ± 5.62 a	12.56 ± 3.02 a	11.75 ± 6.85 a	1.59 ± 1.40 b	***
In	0.16 ± 0.00	0.16 ± 0.00	0.16 ± 0.00	0.16 ± 0.00	0.16 ± 0.00	0.16 ± 0.00	0.19 ± 0.14	ns
Sn	15.7 ± 12.2	9.2 ± 3.0	<3.3 ± 1.8	10.3 ± 19.6	9.8 ± 8.1	15.9 ± 26.7	19.6 ± 48.9	ns
Sb	1.77 ± 0.95	0.94 ± 0.50	0.92 ± 0.03	0.93 ± 0.49	1.69 ± 0.55	1.16 ± 1.44	1.12 ± 1.24	ns
Cs	260 ± 171 ab	246 ± 89 ab	146 ± 9 ab	593 ± 799 a	16 ± 17 b	110 ± 92 b	22 ± 19 b	***
Ba	1.57 ± 2.04 ab	1.64 ± 1.27 ab	3.25 ± 0.75 a	1.13 ± 0.43 b	0.94 ± 1.03 b	1.59 ± 1.05 ab	0.57 ± 0.56 b	***
La	17.63 ± 22.12 a	4.83 ± 4.59 b	1.06 ± 0.07 b	2.61 ± 2.46 b	6.14 ± 7.54 b	2.24 ± 1.50 b	1.94 ± 1.33 b	***
Ce	28.7 ± 31.9 a	4.7 ± 3.7 b	2.2 ± 0.1 b	4.8 ± 5.1 b	12.2 ± 15.0 b	5.1 ± 3.4 b	3.2 ± 2.5 b	***
Pr	3.37 ± 4.17 a	1.02 ± 0.93 b	0.39 ± 0.05 b	0.56 ± 0.61 b	1.39 ± 1.77 ab	0.67 ± 0.44 b	0.42 ± 0.30 b	***
Nd	11.75 ± 14.71 a	4.03 ± 4.19 ab	1.76 ± 0.03 b	1.99 ± 2.13 b	4.94 ± 6.26 ab	3.20 ± 2.02 b	1.44 ± 1.08 b	***
Sm	2.40 ± 2.93 a	1.30 ± 0.99 ab	0.59 ± 0.00 ab	0.42 ± 0.48 b	0.97 ± 1.13 ab	0.99 ± 0.65 ab	0.31 ± 0.23 b	***
Eu	0.64 ± 0.74 a	0.50 ± 0.51 ab	0.38 ± 0.01 ab	0.17 ± 0.12 b	0.23 ± 0.11 ab	0.40 ± 0.21 ab	<0.16 ± 0.08 b	***
Gd	2.31 ± 2.83 a	1.55 ± 1.62 ab	0.96 ± 0.25 ab	0.44 ± 0.45 b	0.93 ± 0.97 ab	1.28 ± 0.77 ab	0.35 ± 0.23 b	***
Dy	1.39 ± 1.67 a	1.34 ± 1.41 a	0.89 ± 0.24 abc	0.34 ± 0.34 bc	0.57 ± 0.33 abc	0.94 ± 0.51 ab	0.27 ± 0.20 c	***
Ho	0.29 ± 0.26 a	0.30 ± 0.25 a	0.25 ± 0.09 ab	<0.16 ± 0.08 b	<0.16 ± 0.07 ab	0.22 ± 0.09 ab	<0.16 ± 0.03 b	***
Er	0.71 ± 0.76 a	0.69 ± 0.71 a	0.62 ± 0.22 ab	0.18 ± 0.21 b	0.31 ± 0.12 ab	0.46 ± 0.21 ab	0.16 ± 0.11 b	***
Yb	0.49 ± 0.60 a	0.48 ± 0.47 ab	0.38 ± 0.03 abc	<0.16 ± 0.16 bc	0.20 ± 0.07 abc	0.28 ± 0.13 abc	<0.16 ± 0.08 c	***
Hg	0.79 ± 0.10	0.76 ± 0.26	0.63 ± 0.09	1.01 ± 0.34	1.73 ± 0.59	0.81 ± 0.79	1.73 ± 1.43	ns
Pb	33.20 ± 7.96 a	14.36 ± 8.75 abc	0.80 ± 0.67 c	19.22 ± 16.07 ab	34.19 ± 18.35 a	10.23 ± 14.71 bc	4.43 ± 6.22 c	***
U	0.40 ± 0.33 bc	<0.16 ± 0.11 c	<0.16 c	0.60 ± 0.39 b	1.04 ± 0.44 a	<0.16 ± 0.11 c	<0.16 ± 0.09 c	***

p-value of the One-Way ANOVA; ns: p-value > 0.05, *: 0.05 > p-value > 0.01, **: 0.01 > p-value > 0.001, ***: p-value ≤ 0.001. Different letters on each variable denote differences between samples from different geographical origin.

The exploratory statistical principal component analysis (PCA) was used to check the structure of the data and to establish the main variation sources, since it is a variable reduction technique that allows for highly correlated variables to be transported to a fewer-dimensional domain containing the uncorrelated information (built by the principal components (PCs)). Afterwards, the most discriminative variables were selected by means of an iterative procedure repeated 30-times, based on variable importance in projection (VIP) scores from the double cross-validated PLS-DA model (30-fold for outer loop, leave-one-out for inner loop). Finally, the variables selected as the most discriminative (potential markers) were used to fit a new double cross-validated model, as described in (Muñoz-Redondo et al., 2020).

All the statistical analyses were performed using the statistical software R v. 4.0.0. The multivariate analyses were carried out by applying in-house routines based on the *mixOmics* R package (Rohart et al., 2017).

3. Results and discussion

3.1. Stable isotope ratio analysis

The mean values with standard deviation of $\delta^{13}C$, $\delta^{15}N$, $\delta^{34}S$, $\delta^{2}H$ and $\delta^{18}O$ determined in the mango samples and a one-way analysis of variance (ANOVA) are shown in Table 1. Statistically significant differences related to the geographical origin of the mango samples were found for all the five stable isotope ratios after applying the Tukey's HSD pairwise comparison. The $\delta^{13}C$ values ranged from −29.74 to −22.79‰, which is consistent with previous results reported in the literature for C_3 plants, values generally ranging between −33 and −23‰ (Pianezze et al., 2019). Significant differences related to $\delta^{13}C$ were found between mangoes cultivated in Mexico and those cultivated in the Ivory Coast, Senegal and Spain (Table 1). Differences in the $\delta^{13}C$ values are usually linked to varietal differences, due to distinct CO_2 fixation pathways during photosynthesis. However, the geographical effect, implying different latitude, altitude, elevation, precipitations, hydric stress and light exposure, as well as management practices could also affect the efficiency of CO_2 fixation, even within the same variety (Diefendorf et al., 2010; Lagad et al., 2013; Wang et al., 2020). The values of $\delta^{15}N$ measured in the mangoes from different countries varied between −3.65 and 7.91‰. The $\delta^{15}N$ signature is highly dependent on the soil properties and agricultural practices such as soil nutrition and fertilisation, since it reflects the nitrogen source of the plants, so this stable isotope ratio is not directly linked to the geographical origin of the samples (Dasenaki & Thomaidis, 2019; Wang et al., 2020). However, previous studies have found relationships between cheeses elaborated at higher latitudes and the $\delta^{15}N$ in casein (Camin et al., 2004). Statistically significant lower values of $\delta^{15}N$ were observed for the Spanish mangoes, averaging 0.25 ± 1.66‰, compared to the foreign mangoes (Table 1). A depletion in the stable nitrogen isotope ratio may reflect intensive agricultural practices using mineral fertilisers involving Spanish mango cultivars, since they tend to reduce the $\delta^{15}N$ signature (Bateman et al., 2007; Cuevas et al., 2019; Wang et al., 2020). This could be explained by a depletion on the ^{15}N in the mango samples, since soil organic N is generally enriched in ^{15}N compared with atmospheric N_2, from which many synthetic fertilizers are produced by the Haber-Bosch process (Inácio et al., 2015). Meanwhile, the $\delta^{34}S$ values were distributed in the range from 1.92 to 14.11‰ among the different mangoes analysed. The $\delta^{34}S$ values of the soil, plants and foods are mainly linked to the geological characteristics of a place (Chung et al., 2016). However, anthropogenic sources such as industrial emissions or the use of S-containing fertilizers, proximity to the coast and climatic conditions may also induce important changes in the $\delta^{34}S$ values (Chung et al., 2016; Pianezze et al., 2020; Rummel et al., 2010). Previous studies have used $\delta^{34}S$ to trace the origin of food products (Chung et al., 2016; Pianezze et al., 2020) and plants (Ocvirk et al., 2018), but to date, this isotope ratio has been less investigated in spite of its potential for geographical traceability (Pianezze et al., 2020). Statistical differences linked to their geographical origin were found in the mangoes for $\delta^{34}S$ (Table 1). The mangoes produced in Brazil, Equatorial Guinea and Senegal displayed higher sulphur isotope values than those produced in Spain and Mexico, revealing higher $\delta^{34}S$ values with decreasing latitudes of the mango cultivation regions. The same behaviour was observed in a previous study with rice cultivars (Chung et al., 2016). In addition, the $\delta^{34}S$ signature is influenced by the so-called sea-spray, which are aerosol particles formed by crashing marine waves, containing high concentrations of inorganic salts, particularly chloride anions, but also SO_4^{2-}, and the greater the distance from the sea, the lower is the amount of sea-spray sulphates deposited on land (Perini et al., 2009). Since marine water displays uniform $\delta^{34}S$ values, of around 20‰ at low and medium latitudes (Richards et al., 2001), the distance from the sea of the different mango cultivars could also explain the higher $\delta^{34}S$ values observed in the mangoes produced in Brazil, Equatorial Guinea and Senegal. Moreover, the $\delta^{2}H$ and $\delta^{18}O$ signatures ranged from −17.78 to 58.75‰ and from 28.00 to 38.03‰ respectively. These stable isotopes are conventionally used in the geographic traceability of food due to their close links with the geographical location and climatic conditions, as their values depend on in the isotopic signature of the consumed water and the climatic characteristics of the area (Camin et al., 2016; Pianezze et al., 2020). This is based on the fractionation of hydrogen and oxygen that occurs during the evaporation and condensation processes of the water cycle. On plant level, also evapotranspiration, impacted by the climatic conditions, plays an important role on defining the isotopic ratios of H and O (Xiao et al., 2018). In addition, unlike the isotopic ratio of hydrogen, for which water is its only source, oxygen is taken by plants from additional sources, such as atmospheric oxygen and carbon dioxide (De Rijke et al., 2016). Both isotopic signatures displayed differences related to the geographical origin of the mangoes (Table 1). The samples from Senegal, Spain and Peru, with respective mean values of 43.6 ± 5.2‰, 21.7 ± 18.3‰ and −8.3 ± 5.1‰, showed statistically significant differences in the $\delta^{2}H$ values. Meanwhile, $\delta^{18}O$ made it possible to differentiate mangoes produced in Brazil, Equatorial Guinea, Ivory Coast, and Spain, with mean values between 34 and 36‰, from the mangoes produced in Mexico, Peru and Senegal, which ranged from 29 to 31‰ (Table 1).

To determine the main variation sources in the data from the stable isotope ratio profile, a PCA was constructed and the subspace spanned by the first two principal components (PCs), which explained the 68% of the total variance, was plotted (Supplementary Fig. S1). Different clusters related to the geographical origin of the samples were observed. In the direction of PC1, which explained around the 38% of the total variance, the mangoes from Mexico and Peru were clearly separated from the ones produced in Brazil, Equatorial Guinea, Ivory Coast and Senegal. The main isotope ratios involved in such differences were $\delta^{13}C$, $\delta^{2}H$ and $\delta^{18}O$. Meanwhile, the variance explained in PC2 made it possible to separate the mangoes produced in Spain from the rest (Supplementary Fig. S1). These results were supported by over 30% of the total variance explained by the PC2, so a good classification performance on the subsequent discriminant analysis is to be expected. Additional information given by this principal component made it possible to differentiate Mexican from Peruvian mangoes, mainly due to changes in the $\delta^{15}N$, $\delta^{34}S$ and $\delta^{18}O$ isotope ratios. The contribution of $\delta^{18}O$ to both components linked to the geographical character of this isotope ratio highlights its potential to trace the origin of mangoes. To assess the effectiveness of the five isotope ratios considered in this study to identify whether a sample of mango was produced in Spain, a partial least squares discriminant analysis (PLS-DA) was fitted considering two groups: authentic mangoes from Spain and foreign market mangoes. The double cross-validated model yielded a satisfactory overall mean balanced error rate (BER) of 0.04 ± 0.01 (Table 2). Interestingly, all the Spanish mangoes were correctly assigned in all cases (i.e. the sensitivity was 100%) and the error of the predictive model was due to incorrect assignments of foreign market mangoes. The graphical outputs of the

Table 2
Performance and dummy matrix of the PLS-DA models carried out to discriminate mangos using the different analytical techniques.

Model	Mean overall BER [a]	Class	Mean class Error [b]	Predicted as Foreign	Predicted as Spain	p-value [c]
Isotope ratios	0.04 ± 0.01	Foreign	0.07 ± 0.02	1004	76	<0.001
		Spain	0.00 ± 0.00	0	1260	
Multielement	0.04 ± 0.01	Foreign	0.06 ± 0.02	1014	66	<0.001
		Spain	0.02 ± 0.00	30	1230	
Isotope ratios + Multielement	0.01 ± 0.00	Foreign	0.03 ± 0.00	1050	30	<0.001
		Spain	0.00 ± 0.00	0	1260	

[a] Mean overall balanced error rate (BER) values with the standard deviation and.
[b] Mean class error values with the standard deviation calculated on the basis of 30 PLS-DA sub-models in a double-cross validation scheme.
[c] Model statistical significance was calculated on the basis of a permutation test (N = 1000) using the mean overall BER, number of misclassifications (NMC) and the area under receiver operating characteristic curve (AUROC) as diagnostic statistics.

PLS-DA model are given in Fig. 1. Although a strict threshold rule set at 0.5 was used for prediction of the test samples, the overall quality of the model was checked by means of the Ypredict plot (Fig. 1c) to overcome inherent limitations of discriminant analyses compared to class modelling. The Ypredict plot shows the Y predicted values for each sample during the 30 repetitions (outer loop) of the double cross-validation (Fig. 1c). Good predictions were considered in ranges from −0.5 to 0.5 for the Spanish samples and from 0.5 to 1.5 for the foreign samples. Additionally, Y predicted values with little scatter along the validation and close to 0 or 1 for the Spanish and foreign samples respectively are expected for more robust models. The error of the model was mainly due to three mangoes from foreign markets that were incorrectly assigned as Spanish ones, highlighted with a red circle in Fig. 1c. Two of these were wrongly classified in all the repetitions of the validation. An additional foreign sample, highlighted in a blue circle in Fig. 1c, displayed Y predicted values outside of the cut-off value 1.5, meaning a poor capability of the model to predict this sample as foreign. As could be expected, the Spanish samples presented less scatter and deviation from the target value (0) of the Y predicted values along the cross-validation. The main differences found in the samples were explained by higher levels of $\delta^{18}O$ and $\delta^{13}C$ in the Spanish mangoes and higher values of $\delta^{15}N$ and $\delta^{34}S$ in the foreign mangoes (Fig. 1a and b). Meanwhile, the $\delta^{2}H$ signature was the least effective stable isotope for differentiating Spanish from foreign mangoes. This was due to a wide variation of this isotope ratio for mangoes produced in Spain, as the density plot of Supplementary Fig. S2 shows.

3.2. Multi-element analysis

Potassium was the most abundant element, the mangoes always presenting concentrations higher than 3 g/kg. The other mean concentrations found were: Ca, Mg and P between 100 mg/kg and 1000 mg/kg; Na and Fe between 100 and 10 mg/kg; Rb, B, Mn, Cu, Al, Zn and Sr between 10 and 1 mg/kg; Ba, Cr and Ni between 1 mg/kg and 100 μg/kg; Cs, Mo and As between 100 and 10 μg/kg; Co, Sn, Li, Pb, V, Se, Ce, Cd, Ga, La, Y and Nd between 10 and 1 μg/kg; and other elements were between 1 and 0.1 μg/kg. These results were in accordance with the concentrations reported in the literature (Habte et al., 2017; Hassan et al., 2019; Liao et al., 2014), except for Pb that was about 10 times lower in these samples than values showed in (Hassan et al., 2019).

K (LOD < 0.03 g/kg), Al (LOD < 0.16 mg/kg), B (LOD < 0.1 mg/kg), Ba (LOD < 0.001 mg/kg), Ca (LOD < 30 mg/kg), Cu (LOD < 0.003 mg/kg), Fe (LOD < 0.3 mg/kg), Mg (LOD < 1.6 mg/kg), Mn (LOD < 0.03 mg/kg), Na (LOD < 1.6 mg/kg), P (LOD < 3.2 mg/kg), Rb (LOD < 0.003 mg/kg), Sr (LOD < 0.003 mg/kg), Zn (LOD < 0.003 mg/kg), Co (LOD < 0.33 mg/kg), Cr (LOD < 1.6 mg/kg), Ce (LOD < 0.16 mg/kg), Cs (LOD < 0.2 mg/kg), Hg (LOD < 0.26 mg/kg), La (LOD < 0.16 mg/kg), Li (LOD < 0.3 mg/kg), Ni (LOD < 3.2 mg/kg), Nd (LOD < 0.16 mg/kg), V (LOD < 1.6 mg/kg), were quantified in all samples. Se (LOD < 0.33 μg/kg) and Cd (LOD <0.33 μg/kg) were present in detectable amounts in 99% of the samples, Y (LOD < 0.33 μg/kg) in 98%, Mo (LOD < 3.25 μg/kg) in 91%, Pr (LOD < 0.16 μg/kg) in 90%, Gd (LOD < 0.16 μg/kg) in 89%, Ag (LOD < 0.33 μg/kg) and Sm (LOD < 0.16 μg/kg) in 86%, Dy (LOD < 0.16 μg/kg) and Pb (LOD < 0.65 μg/kg) in 85%, Sn (LOD < 3.3 μg/kg) in 76%, Er (LOD < 0.16 μg/kg) in 61%, U (LOD < 0.16 μg/kg) in 59%, Eu (LOD < 0.16 μg/kg) in 56%, As (LOD < 1.6 μg/kg) in 45%, Yb (LOD < 0.16 μg/kg) in 42%, Be (LOD < 0.33 μg/kg) and Ho (LOD < 0.16 μg/kg) in 24%, Ge (LOD < 0.33 μg/kg) and Pd (LOD <0.33 μg/kg) in 16%, Ga (LOD <1.6 μg/kg) in 10%, In (LOD < 0.33 μg/kg) and Tm (LOD < 0.16 μg/kg) in 3%, whereas Re (LOD < 0.16 μg/kg), Ir (LOD < 0.33 μg/kg), Pt (LOD < 0.33 μg/kg), Au (LOD < 1.6 μg/kg) and Te (LOD < 0.26 μg/kg) were never detectable.

Data were recalculated assuming an average dry matter content on mango of 14% (Owens & Moore, 2013). The concentrations of the toxic elements Pb and Cd in the analysed mangoes were always decidedly lower than the maximum levels in fruits reported in Regulation EC N°1881/2006 and subsequent amendments (i.e. 0.1 mg/kg fresh weight for Pb and 0.05 mg/kg fresh weight for Cd). In particular, Spanish mangoes show very low levels of Pb and Cd, with respective values about 20 and 30 times lower than the abovementioned limits.

Considering only elements present in at least 20% of the samples, a one-way ANOVA test was performed to highlight significant differences in the contents of mineral elements in the fruits produced in the seven countries under consideration (Table 1). This highlighted the significant differences between mangoes produced in Spain and those produced in foreign countries. The Be, Cd, Co, Dy, Ni, Rb, Se and Y contents were significantly lower in the Spanish mangoes than in those produced in Senegal, whereas the values for B were higher. The Spanish mangoes were richer in B and presented lower contents of Dy, Er, Ho, Rb, Y and Yb than those from Equatorial Guinea. As, B, Cd, Na, P, Pb, V and U were present in significantly lower amounts in the Spanish mangoes than in those from Peru. The Mexican samples were richer in As, Cd, Cs, K, Li, Mo, Pb, Rb, Se and U than those from Spain. Co, Mn, Ni Pb, Rb and rare earths (Ce, Dy, Er, Eu, Gd, Ho, La, Pr, Nd, Sm, Y and Yb) were lower in the mangoes produced in Spain than in Brazil. Finally, Spanish mangoes were lower in Ba, Co, Ni and Y than the fruits from the Ivory coast.

Afterwards, a PCA was performed to study the main variation sources in the samples based on their elemental profile (Supplementary Fig. S3 a and b). Although the African samples were mostly separated from the rest, it was not possible to establish clear differences between the Spanish and foreign samples. This may be explained by the high dimensionality of the data, which include non-informative and noisy elements with low geographical discriminatory potential, making the interpretation and understanding of the system studied more difficult. Hence, robust variable selection methods are frequently used to remove the irrelevant variables and improve the performance of the model. In this sense, an iterative variable selection procedure was performed to select the most discriminative elements (potential markers) of Spanish mangoes. To check the quality of the new reduced data set, a new PCA was again fitted with the selected variables (Supplementary Fig. S3 c and d). The Spanish samples were clearly separated from the rest in the direction of the PC1, which explained 44% of the total variance found in the samples, highlighting the potential of Pb, Sm, Cs, As, Cd, Ba and Se to discriminate these samples. Subsequently, the selected elements were

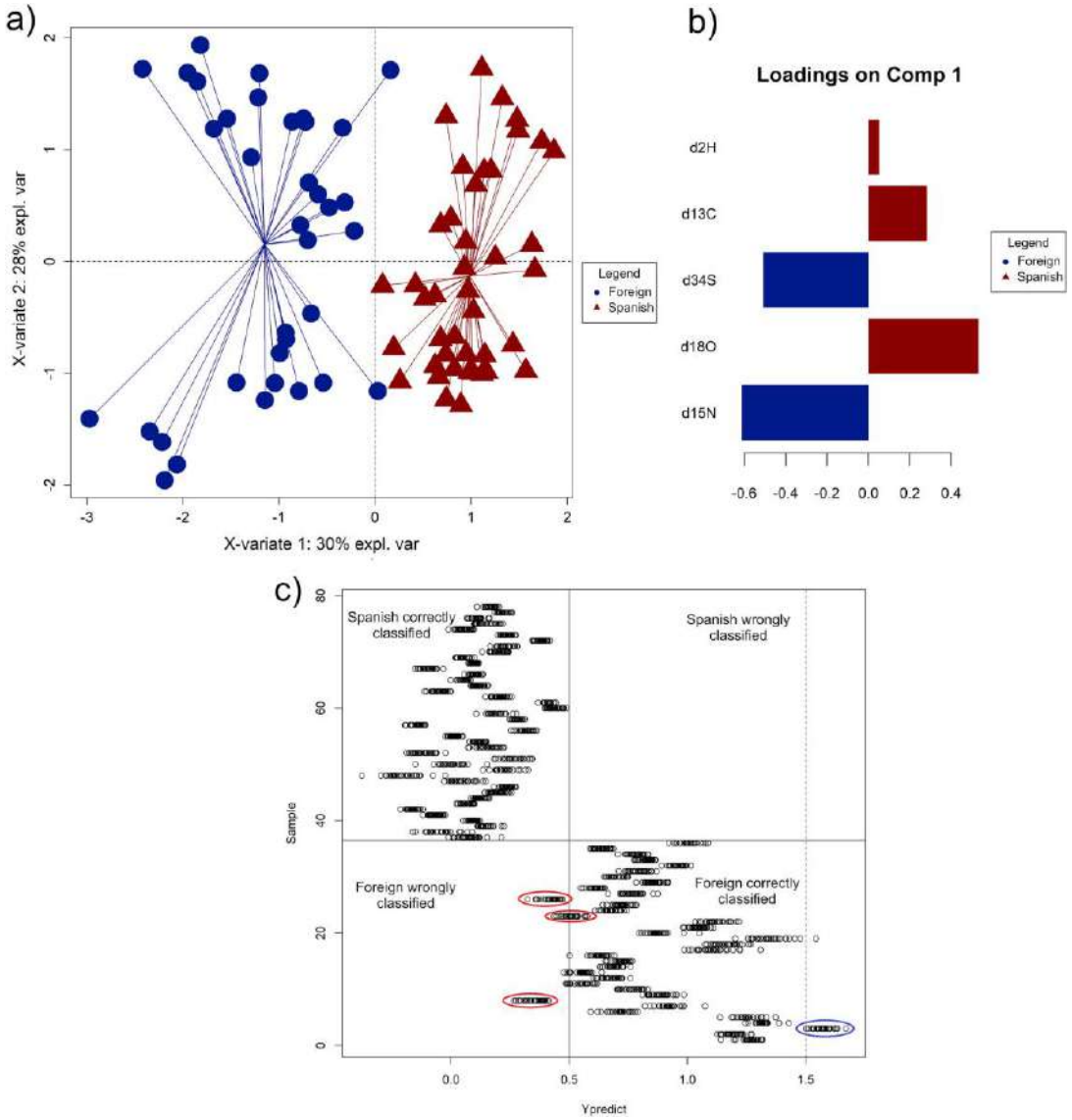

Fig. 1. Graphical outputs of the partial least squares discriminant analysis (PLS-DA) performed to discriminate Spanish from the foreign market mangoes using the stable isotopes of five bio-elements ($\delta^{13}C$, $\delta^{15}N$, $\delta^{34}S$, $\delta^{2}H$, $\delta^{18}O$). [(a)] Scores plot for components 1 and 2 (X-variate 1 and X-variate 2); [(b)] loading contribution barplot on component 1. Colour indicates the class for which the compound has a maximal mean value. Bar length represents the multivariate regression coefficient with either a positive or negative sign for that particular feature of each component, i.e., the importance of each variable in the model. [(c)] Ypredict plot that shows Y predicted values for each sample during the 30 repetitions (outer loop) of the double-cross validation. (For interpretation of the references to colour in this figure legend, the reader is referred to the Web version of this article.)

further used to fit a PLS-DA model to discriminate the Spanish and foreign mangoes (Fig. 2), obtaining the same mean overall BER of 0.04 ± 0.01 (Table 2) as the model from the stable isotope ratios approach. However, one Spanish mango was incorrectly assigned as foreign (Fig. 2c), thus reducing slightly the sensitivity of the model to 97.6%. The scatter of the Y predicted values along the double cross-validation obtained for Spanish mangoes (Fig. 2c) was also slightly higher than the same values obtained in the model fitted with the isotope ratios approach. The elements selected from the iterative variable reduction and highlighted as the main indicators of geographic origin of mango (Pb, Sm, Cs, As, Cd, Ba, Se) were already reported to be useful for geographic traceability for different commodities. In detail, Bontempo, Camin, et al., 2011 reported significant differences in As, Se, Cd, Ba and Pb composition of tomatoes of different geographic provenance. Se, Cd and rare earth elements were used to discriminate green coffee beans from different production areas (Santato et al., 2012), while As, Ba, Cd, Cs, Se and rare earth elements were shown to differentiate cacao beans sampled worldwide (Bertoldi et al., 2016). Ba and Cs were identified as suitable indicators for geographic traceability of wines of 23 estates in South Africa (Coetzee et al., 2014) and these two elements together with Sm were reported to discriminate Saffron spices produced in three Italian regions (D'Archivio et al., 2014). Ba was one of the elements used to characterize wheat samples from different Argentinian sites (Podio et al., 2013). Regarding grapes and wines, rare earth elements have

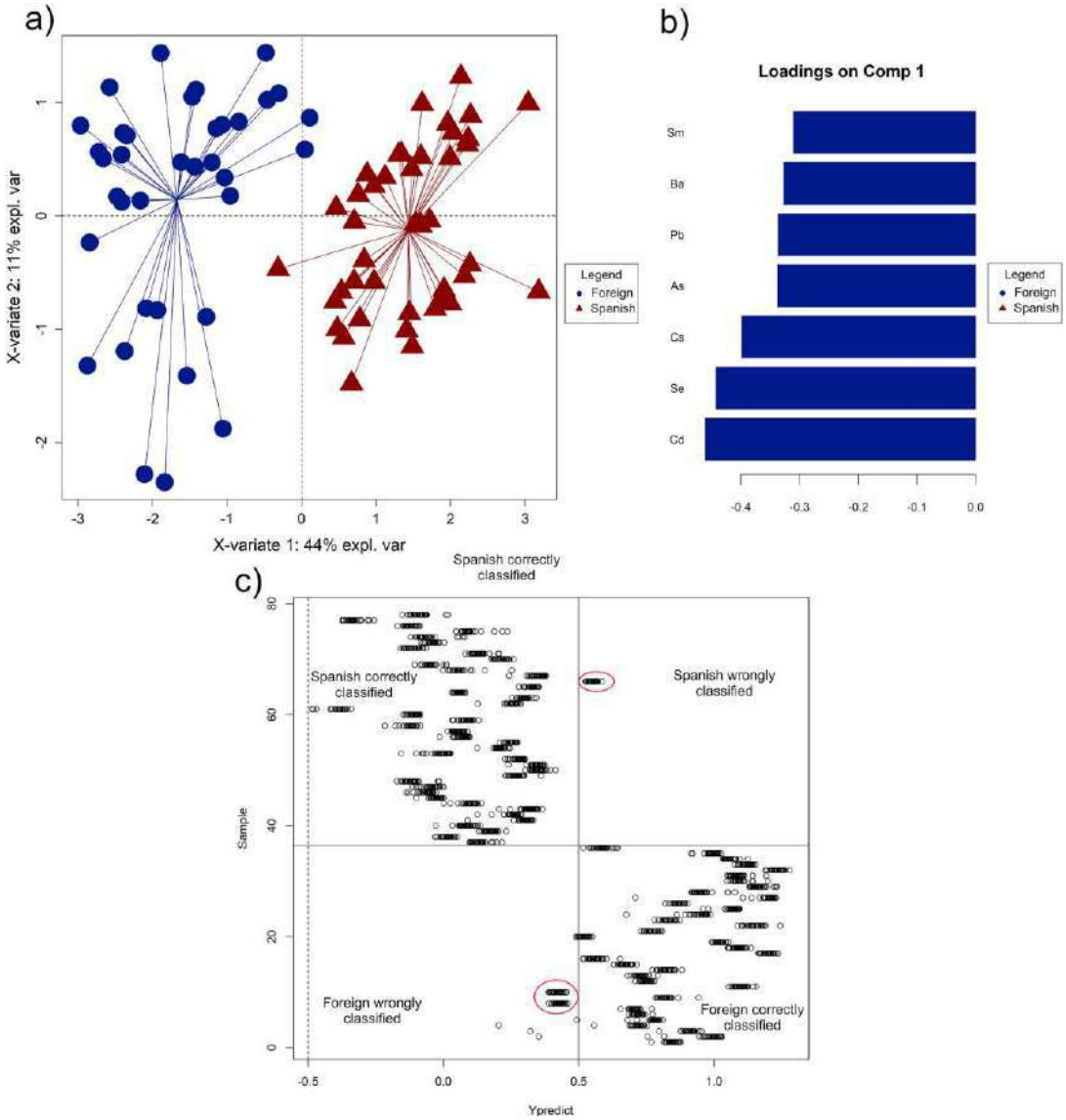

Fig. 2. Graphical outputs of the partial least squares discriminant analysis (PLS-DA) performed to discriminate Spanish from the foreign market mangoes using their elemental composition profile. [(a)] Scores plot for components 1 and 2 (X-variate 1 and X-variate 2); [(b)] loading contribution barplot on component 1. Colour indicates the class for which the compound has a maximal mean value. Bar length represents the multivariate regression coefficient with either a positive or negative sign for that particular feature of each component, i.e., the importance of each variable in the model. [(c)] Ypredict plot that shows Y predicted values for each sample during the 30 repetitions (outer loop) of the double-cross validation. (For interpretation of the references to colour in this figure legend, the reader is referred to the Web version of this article.)

often been used for their classification on the basis of geographic origin (Aceto et al., 2013; Pepi et al., 2016). These elements also showed significantly different concentrations in goji berries grown in China and Italy (Bertoldi et al., 2019). More recently, Cs was also highlighted to be a useful element for geographic characterization of other types of commodities of vegetal (gum Arabic (Perini et al., 2020)) and animal (milk (Luana Bontempo et al., 2011)) origin.

The mineral element composition of mango fruits derives mostly from the minerals present in the soil. Xiangjun and coworkers (Liao et al., 2014) stated that the concentration of As in mango is influenced by the chemical characteristics of the growing soil. Fruits from acid soil usually have a higher As content, whereas the presence of Al–Fe–Mn oxides limits As bioavailability leading to a lower concentration in fruits.

3.3. Stable isotope ratio and multi-element analysis

Data originating from the stable isotope ratio analysis and multi-element profile were concatenated sample-wise into a unique matrix to jointly assess the discrimination abilities of both analytical platforms. As in the previous section, a PCA including all the measures was fitted and the Spanish mangoes were not clearly distinguished from the foreign ones (Fig. 3a and b). The non-informative variables were again removed through an iterative selection procedure. The variables selected during this procedure as the most discriminative (potential

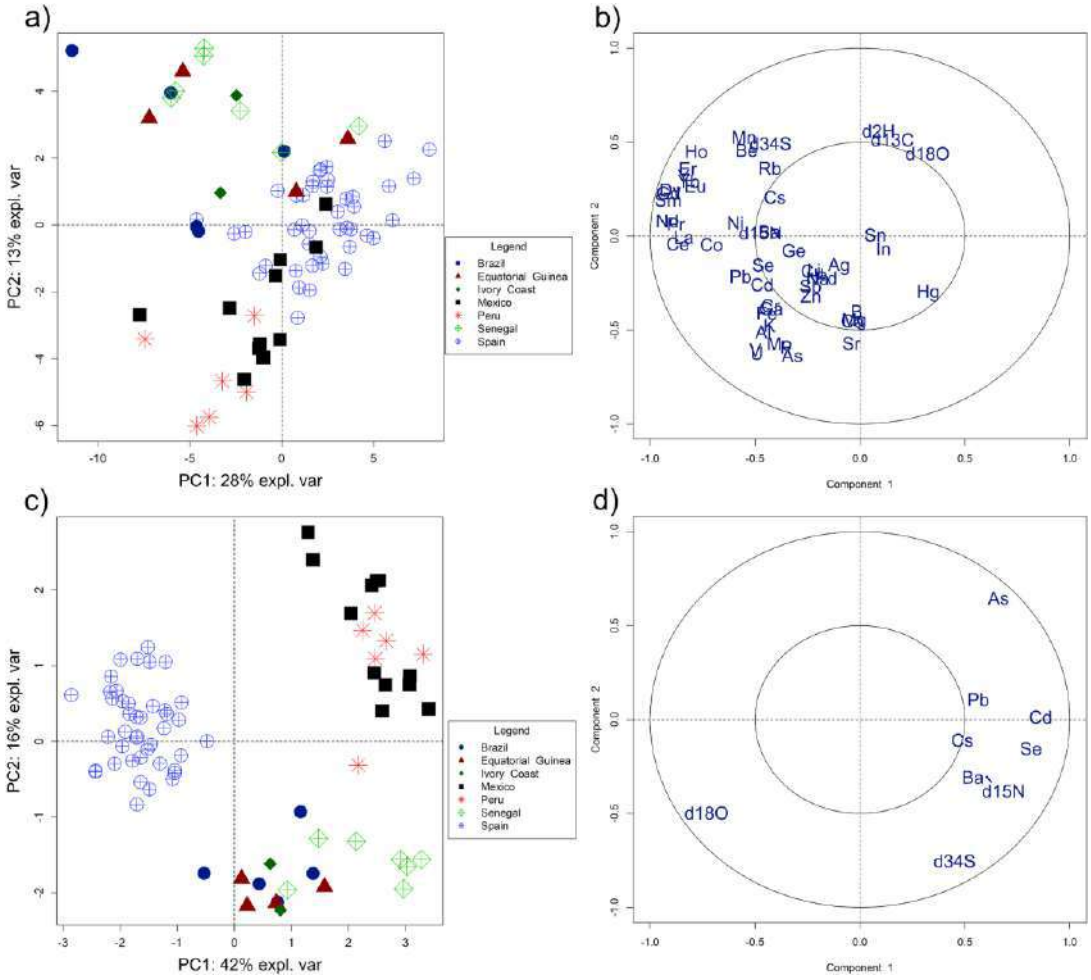

Fig. 3. [a] Scores and [b] loadings plot of the principal component analysis (PCA) carried out on the mango samples using the data from the two analytical platforms: stable isotope ratios and elemental composition profile. [c] Scores and [d] loadings plot of the PCA carried out on the mango samples using the main discriminatory variables from both analytical platforms selected in an iterative variable reduction procedure.

markers) included three stable isotope ratios ($\delta^{15}N$, $\delta^{18}O$ and $\delta^{34}S$) and six elements (Cd, Se, Cs, As, Pb and Ba) (Fig. 3 d). Afterwards, a new PCA was fitted (Fig. 3c and d), achieving a major improvement to differentiate the Spanish from the foreign mangoes. This was observed in the first two principal components of the PCA, since the mangoes produced in Spain were allocated in a narrow and well-defined area (Fig. 3c). In addition, even though the variable reduction procedure was set to find the elements and stable isotopes that maximize differences between the Spanish samples and the rest, two additional clusters were observed, one corresponding to samples from Peru and Mexico and the other to the rest of the foreign mangoes. Finally, a PLS-DA was performed on the reduced data set (Fig. 4) and a mean overall BER of 0.01 ± 0.00 was obtained (Table 2). The prediction error of the model was due to one foreign sample incorrectly assigned as Spanish in all the repetitions of the cross-validation, corresponding to a commercial mango from Equatorial Guinea. The Ypredict plot obtained from this model (Fig. 4c) also showed an increased overall quality, with lower scattering of the predicted samples along the 30 repetitions of the cross-validation and Y predicted values closer to the target values (0 and 1), especially for the mangoes produced in Spain. These results supported the robustness of combining elemental and isotopic data to improve the geographical discrimination of Spanish mangoes, as was previously found in other studies using foodstuffs aimed at, for instance, authenticating PDO cheeses (Bontempo et al., 2011, 2019; Camin et al., 2012) and verifying the geographical provenience of Slovenian milk (Potočnik et al., 2020) and commercial tomato (Opatić et al., 2018).

4. Conclusions

In this study, we investigated the effectiveness of two analytical strategies based on the analysis of the stable isotope ratios of five light bio-elements ($\delta^{13}C$, $\delta^{15}N$, $\delta^{34}S$, $\delta^{2}H$, $\delta^{18}O$) and a multi-element analysis to trace the geographical origin of commercial mangoes. The results from the PLS-DA models fitted for each strategy showed satisfactory overall classification performances to discriminate Spanish mangoes from those from foreign markets. For both analytical platforms, a balanced error rate of 0.04 ± 0.01 was obtained. However, the model fitted for the stable isotope approach yielded a sensitivity of 100%, meaning that the Spanish mangoes were correctly classified in all the cases, against the 97.6% for multi-element analysis. Subsequently, the data from the two analytical sources were combined and jointly assessed. After selecting the most discriminative variables by means of an iterative reduction procedure, a model with a balanced error rate of 0.01 ± 0.00 and 100% sensitivity was obtained, improving the

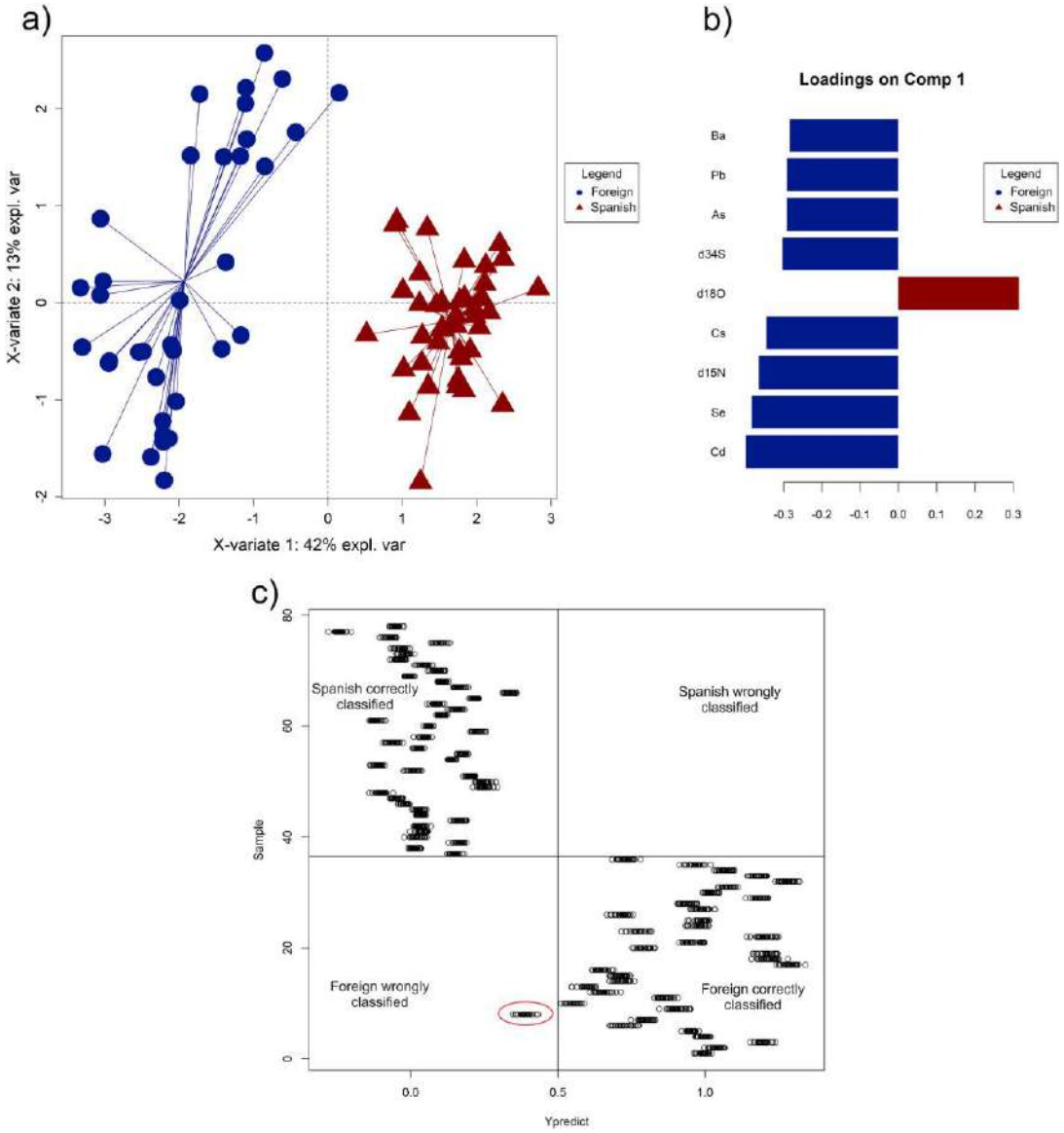

Fig. 4. Graphical outputs of the partial least squares discriminant analysis (PLS-DA) performed to discriminate Spanish from the foreign market mangoes using the main discriminatory variables from the two analytical platforms (stable isotope ratios and elemental composition profile) selected in an iterative variable reduction procedure. [(a)] Scores plot for components 1 and 2 (X-variate 1 and X-variate 2); [(b)] loading contribution barplot on component 1. Colour indicates the class for which the compound has a maximal mean value. Bar length represents the multivariate regression coefficient with either a positive or negative sign for that particular feature of each component, i.e., the importance of each variable in the model. [(c)] Ypredict plot that shows Y predicted values for each sample during the 30 repetitions (outer loop) of the double-cross validation. (For interpretation of the references to colour in this figure legend, the reader is referred to the Web version of this article.)

performance of the independent assessment models. The main potential markers involved in the discrimination of Spanish from foreign market mangoes included three stable isotope ratios ($\delta^{15}N$, $\delta^{18}O$ and $\delta^{34}S$) and six elements (Cd, Se, Cs, As, Pb and Ba). The results of this study revealed the main differences in the stable isotope ratios and trace element profiles between mangoes produced in Spain and those from some leading producer countries, addressing an essential issue towards supporting the existence of a potential Spanish protected geographical indication (PGI) of mango. These results are rather explorative and the potential establishment of a robust PGI would need to be supported by a sampling extended and maintained over time.

Financial funds

J. M. Muñoz-Redondo was awarded a research contract funded by the Andalusian Institute of Agricultural and Fisheries Research and Training (IFAPA), within the National Youth Guarantee System funded through the European Social Fund (ESF) and the Youth Employment Initiative (YEI). This study was funded by the Andalusian Institute of Agricultural and Fisheries Research and Training (IFAPA) and the European Rural Development Fund (ERDF, EU) through the Project 'Caracterización de alimentos y nuevos productos elaborados: potential saludable, organoléptico y trazabilidad alimentaria. Estrategias de

diversificación y reclamo competitivo" (PR.AVA.AVA201601.20). This work has been partially funded within the framework of Accordo di Programma, traceability unit of Fondazione Edmund Mach.

CRediT authorship contribution statement

J.M. Muñoz-Redondo: Methodology, Software, Validation, Formal analysis, Investigation, Writing - original draft, Writing - review & editing, Visualization. **D. Bertoldi:** Methodology, Validation, Resources, Investigation, Writing - original draft, Writing - review & editing. **A. Tonon:** Resources, Investigation. **L. Ziller:** Resources, Investigation. **F. Camin:** Project administration, Writing - review & editing, Supervision. **J.M. Moreno-Rojas:** Term, Conceptualization, Writing - review & editing, Supervision, Project administration, Funding acquisition.

Declaration of competing interest

The authors declare that they have no known competing financial interests or personal relationships that could have appeared to influence the work reported in this paper.

Acknowledgements

The authors thank the "Asociación Española de Productores de Frutas Tropicales".

Appendix A. Supplementary data

Supplementary data to this article can be found online at https://doi.org/10.1016/j.foodcont.2021.107961.

References

Aceto, M., Robotti, E., Oddone, M., Baldizzone, M., Bonifacino, G., Bezzo, G., Di Stefano, R., Gosetti, F., Mazzucco, E., & Manfredi, M. (2013). A traceability study on the Moscato wine chain. *Food Chemistry, 138*(2–3), 1914–1922.

Badia-Melis, R., Mishra, P., & Ruiz-García, L. (2015). Food traceability: New trends and recent advances. A review. *Food Control, 57*, 393–401.

Bateman, A. S., Kelly, S. D., & Woolfe, M. (2007). Nitrogen isotope composition of organically and conventionally grown crops. *Journal of Agricultural and Food Chemistry, 55*(7), 2664–2670.

Bertoldi, D., Barbero, A., Camin, F., Caligiani, A., & Larcher, R. (2016). Multielemental fingerprinting and geographic traceability of Theobroma cacao beans and cocoa products. *Food Control, 65*, 46–53.

Bertoldi, D., Cossignani, L., Blasi, F., Perini, M., Barbero, A., Pianezze, S., & Montesano, D. (2019). Characterisation and geographical traceability of Italian goji berries. *Food Chemistry, 275*, 585–593.

Bertoldi, D., Santato, A., Paolini, M., Barbero, A., Camin, F., Nicolini, G., & Larcher, R. (2014). Botanical traceability of commercial tannins using the mineral profile and stable isotopes. *Journal of Mass Spectrometry, 49*(9), 792–801.

Bontempo, L., Barbero, A., Bertoldi, D., Camin, F., Larcher, R., Perini, M., Sepulcri, A., Zicarelli, L., & Piasentier, E. (2019). Isotopic and elemental profiles of Mediterranean buffalo milk and cheese and authentication of Mozzarella di Bufala Campana PDO: An initial exploratory study. *Food Chemistry, 285*, 316–323.

Bontempo, L. U. A. N. A., Camin, F., Larcher, R., Nicolini, G., Perini, M., & Rossmann, A. (2009). Coast and year effect on H, O and C stable isotope ratios of Tyrrhenian and Adriatic Italian olive oils. *Rapid Communications in Mass Spectrometry: An International Journal Devoted to the Rapid Dissemination of Up-to-the-Minute Research in Mass Spectrometry, 23*(7), 1043–1048.

Bontempo, L., Camin, F., Manzocco, L., Nicolini, G., Wehrens, R., Ziller, L., & Larcher, R. (2011). Traceability along the production chain of Italian tomato products on the basis of stable isotopes and mineral composition. *Rapid communications in mass spectrometry, 25*(7), 899–909.

Bontempo, L. U. A. N. A., Larcher, R., Camin, F., Hölzl, S., Rossmann, A., Horn, P., & Nicolini, G. (2011). Elemental and isotopic characterisation of typical Italian alpine cheeses. *International Dairy Journal, 21*(6), 441–446.

Brand, W. A., Coplen, T. B., Vogl, J., Rosner, M., & Prohaska, T. (2014). Assessment of international reference materials for isotope-ratio analysis (IUPAC Technical Report). *Pure and Applied Chemistry, 86*(3), 425–467.

Camin, F., Bontempo, L., Perini, M., & Piasentier, E. (2016). Stable isotope ratio analysis for assessing the authenticity of food of animal origin. *Comprehensive Reviews in Food Science and Food Safety, 15*(5), 868–877.

Camin, F., Bontempo, L., Perini, M., Tonon, A., Breas, O., Guillou, C., Moreno-Rojas, J. M., & Gagliano, G. (2013). Control of wine vinegar authenticity through δ18O analysis. *Food Control, 29*(1), 107–111.

Camin, F., Larcher, R., Nicolini, G., Bontempo, L., Bertoldi, D., Perini, M., Schlicht, C., Schellenberg, A., Thomas, F., & Heinrich, K. (2010). Isotopic and elemental data for tracing the origin of European olive oils. *Journal of Agricultural and Food Chemistry, 58*(1), 570–577.

Camin, F., Wehrens, R., Bertoldi, D., Bontempo, L., Ziller, L., Perini, M., Nicolini, G., Nocetti, M., & Larcher, R. (2012). H, C, N and S stable isotopes and mineral profiles to objectively guarantee the authenticity of grated hard cheeses. *Analytica Chimica Acta, 711*, 54–59.

Camin, F., Wietzerbin, K., Cortes, A. B., Haberhauer, G., Lees, M., & Versini, G. (2004). Application of multielement stable isotope ratio analysis to the characterization of French, Italian, and Spanish cheeses. *Journal of Agricultural and Food Chemistry, 52*(21), 6592–6601.

Chiesa, L., Panseri, S., Bonacci, S., Procopio, A., Zecconi, A., Arioli, F., Cuevas, F. J., & Moreno-Rojas, J. M. (2016). Authentication of Italian PDO lard using NIR spectroscopy, volatile profile and fatty acid composition combined with chemometrics. *Food Chemistry, 212*, 296–304.

Chung, I.-M., Kim, J.-K., Prabakaran, M., Yang, J.-H., & Kim, S.-H. (2016). Authenticity of rice (oryza sativa L.) geographical origin based on analysis of C, N, O and S stable isotope ratios: A preliminary case report in korea, China and philippine. *Journal of the Science of Food and Agriculture, 96*(7), 2433–2439.

Coetzee, P. P., Van Jaarsveld, F. P., & Vanhaecke, F. (2014). Intraregional classification of wine via ICP-MS elemental fingerprinting. *Food Chemistry, 164*, 485–492.

Crittenden, R. G., Andrew, A. S., LeFournour, M., Young, M. D., Middleton, H., & Stockmann, R. (2007). Determining the geographic origin of milk in Australasia using multi-element stable isotope ratio analysis. *International Dairy Journal, 17*(5), 421–428.

Cuevas, F. J., Pereira-Caro, G., Muñoz-Redondo, J. M., Ruiz-Moreno, M. J., Montenegro, J. C., & Moreno-Rojas, J. M. (2019). A holistic approach to authenticate organic sweet oranges (Citrus Sinensis L. cv Osbeck) using different techniques and data fusion. *Food Control, 104*, 63–73.

Dasenaki, M. E., & Thomaidis, N. S. (2019). Quality and authenticity control of fruit juices-a review. *Molecules, 24*(6), 1014.

De Rijke, E., Schoorl, J. C., Cerli, C., Vonhof, H. B., Verdegaal, S. J. A., Vivó-Truyols, G., Lopatka, M., Dekter, R., Bakker, D., & Sjerps, M. J. (2016). The use of δ2H and δ18O isotopic analyses combined with chemometrics as a traceability tool for the geographical origin of bell peppers. *Food Chemistry, 204*, 122–128.

Diefendorf, A. F., Mueller, K. E., Wing, S. L., Koch, P. L., & Freeman, K. H. (2010). Global patterns in leaf 13C discrimination and implications for studies of past and future climate. *Proceedings of the National Academy of Sciences, 107*(13), 5738–5743.

D'Archivio, A. A., Giannitto, A., Incani, A., & Nisi, S. (2014). Analysis of the mineral composition of Italian saffron by ICP-MS and classification of geographical origin. *Food Chemistry, 157*, 485–489.

Food and Agriculture Organization of the United Nations (FAO). (2018). Major tropical fruits. *Market review*. http://www.fao.org/3/ca5692en/CA5692EN.pdf.

Fruittrop, 2020. Spanish mango. Retrieved September 15, 2020, from https://www.fruitrop.com/en/Articles-by-subject/Full-country-profile/2016/Spanish-mango, 15 September.

Freshplaza, 2020. Spanish mangoes from Malaga and Granada seek PGI designation. Retrieved September 20, 2020, from https://www.freshplaza.com/article/9081187/spanish-mangoes-from-malaga-and-granada-seek-pgi-designation/.

Furia, E., Naccarato, A., Sindona, G., Stabile, G., & Tagarelli, A. (2011). Multielement fingerprinting as a tool in origin authentication of PGI food products: Tropea red onion. *Journal of Agricultural and Food Chemistry, 59*(15), 8450–8457.

Giovannucci, D., Josling, T., Kerr, W., O'Connor, B., & Yeung M, T. (2009). *Guide to geographical indications*. Internation Tracde Centre.

Habte, G., Choi, J. Y., Nho, E. Y., Jamila, N., Khan, N., Hwang, I. M., & Kim, K. S. (2017). Determination of essential and toxic elements in tropical fruit by microwave-assisted digestion and inductively coupled plasma–mass spectrometry. *Analytical Letters, 50*(6), 1025–1039.

Hassan, S., Mazhar, W., Farooq, S., Ali, A., & Musharraf, S. G. (2019). Assessment of heavy metals in calcium carbide treated mangoes by inductively coupled plasma-mass spectrometry (ICP-MS). *Food Additives & Contaminants: Part A, 36*(12), 1769–1776.

Hernández-Sánchez, C., Luis, G., Moreno, I., Cameán, A., González, A. G., González-Weller, D., Castilla, A., Gutiérrez, A., Rubio, C., & Hardisson, A. (2012). Differentiation of mangoes (Magnifera indica L.) conventional and organically cultivated according to their mineral content by using support vector machines. *Talanta, 97*, 325–330.

Hofman, P. J., Smith, L. G., Meiburg, G. F., & Giles, J. E. (1997). Production locality affects mango fruit quality. *Australian Journal of Experimental Agriculture, 37*(7), 801–808.

Inácio, C. T., Chalk, P. M., & Magalhães, A. M. (2015). Principles and limitations of stable isotopes in differentiating organic and conventional foodstuffs: 1. Plant products. *Critical Reviews in Food Science and Nutrition, 55*(9), 1206–1218.

Jha, S. N., Jaiswal, P., Narsaiah, K., Kumar, R., Sharma, R., Gupta, M., Bhardwaj, R., & Singh, A. K. (2013). Authentication of mango varieties using near-infrared spectroscopy. *Agricultural Research, 2*(3), 229–235.

Katerinopoulou, K., Kontogeorgos, A., Salmas, C. E., Patakas, A., & Ladavos, A. (2020). Geographical origin authentication of agri-food products: A review. *Foods, 9*(4), 489.

Kulkarni, R. S., Chidley, H. G., Pujari, K. H., Giri, A. P., & Gupta, V. S. (2012). Geographic variation in the flavour volatiles of Alphonso mango. *Food Chemistry, 130*(1), 58–66.

Lagad, R. A., Alamelu, D., Laskar, A. H., Rai, V. K., Singh, S. K., & Aggarwal, S. K. (2013). Isotope signature study of the tea samples produced at four different regions in India. *Analytical Methods, 5*(6), 1604–1611.

Liao, X., Fu, Y., He, Y., & Yang, Y. (2014). Occurrence of arsenic in fruit of mango plant (Mangifera indica L.) and its relationship to soil properties. *Catena, 113*, 213–218.

Martelo-Vidal, M. J., & Vázquez, M. (2016). Advances in ultraviolet and visible light spectroscopy for food authenticity testing. *En Advances in food authenticity testing*. Elsevier.

Muñoz-Redondo, J. M., Ruiz-Moreno, M. J., Puertas, B., Cantos-Villar, E., & Moreno-Rojas, J. M. (2020). Multivariate optimization of headspace solid-phase microextraction coupled to gas chromatography-mass spectrometry for the analysis of terpenoids in sparkling wines. *Talanta, 208*, 120483.

Ocvirk, M., Ogrinc, N., & Košir, I. J. (2018). Determination of the geographical and botanical origin of hops (Humulus lupulus L.) using stable isotopes of C, N, and S. *Journal of Agricultural and Food Chemistry, 66*(8), 2021–2026.

Opatić, A. M., Nečemer, M., Lojen, S., Masten, J., Zlatić, E., Šircelj, H., Stopar, D., & Vidrih, R. (2018). Determination of geographical origin of commercial tomato through analysis of stable isotopes, elemental composition and chemical markers. *Food Control, 89*, 133–141.

Owens, G., & Moore, C. (2013). *Mango Dry matter instructions* (Vol. 2).

Pepi, S., Sansone, L., Chicca, M., Marrocchino, E., & Vaccaro, C. (2016). Distribution of rare earth elements in soil and grape berries of Vitis vinifera cv. "Glera". *Environmental Monitoring and Assessment, 188*(8), 477.

Perini, M., Bertoldi, D., Nardin, T., Pianezze, S., Ferrari, G., & Larcher, R. (2020). Combined use of elemental profiles and stable isotope ratios for the botanical and commercial discrimination of gum Arabic. *Food Hydrocolloids, 105*, Article 105773.

Perini, M., Camin, F., Bontempo, L., Rossmann, A., & Piasentier, E. (2009). Multielement (H, C, N, O, S) stable isotope characteristics of lamb meat from different Italian regions. *Rapid Communications in Mass Spectrometry: An International Journal Devoted to the Rapid Dissemination of Up-to-the-Minute Research in Mass Spectrometry, 23*(16), 2573–2585.

Pianezze, S., Bontempo, L., Perini, M., Tonon, A., Ziller, L., Franceschi, P., & Camin, F. (2020). $\delta^{34}S$ for tracing the origin of cheese and detecting its authenticity. *Journal of Mass Spectrometry, 55*(7), Article e4451.

Pianezze, S., Perini, M., Bontempo, L., Ziller, L., & D'Archivio, A. A. (2019). Geographical discrimination of garlic (Allium Sativum L.) based on Stable isotope ratio analysis coupled with statistical methods: The Italian case study. *Food and Chemical Toxicology, 134*, Article 110862.

Podio, N. S., Baroni, M. V., Badini, R. G., Inga, M., Ostera, H. A., Cagnoni, M., Gautier, E. A., García, P. P., Hoogewerff, J., & Wunderlin, D. A. (2013). Elemental and isotopic fingerprint of Argentinean wheat. Matching soil, water, and crop composition to differentiate provenance. *Journal of Agricultural and Food Chemistry, 61*(16), 3763–3773.

Potočnik, D., Nečemer, M., Perišić, I., Jagodic, M., Mazej, D., Camin, F., Eftimov, T., Strojnik, L., & Ogrinc, N. (2020). Geographical verification of Slovenian milk using stable isotope ratio, multi-element and multivariate modelling approaches. *Food Chemistry*, Article 126958.

Regulation (EU) No 1151/2012 of the European Parliament and of the Council of 21 November 2012 on quality schemes for agricultural products and foodstuffs. Vol. 29.

Richards, M. P., Fuller, B. T., & Hedges, R. E. (2001). Sulphur isotopic variation in ancient bone collagen from Europe: Implications for human palaeodiet, residence mobility, and modern pollutant studies. *Earth and Planetary Science Letters, 191*(3–4), 185–190.

Rohart, F., Gautier, B., Singh, A., & Le Cao, K.-A. (2017). mixOmics: An R package for 'omics feature selection and multiple data integration. *PLoS Computational Biology, 13*(11), Article e1005752.

Rummel, S., Hoelzl, S., Horn, P., Rossmann, A., & Schlicht, C. (2010). The combination of stable isotope abundance ratios of H, C, N and S with 87Sr/86Sr for geographical origin assignment of orange juices. *Food Chemistry, 118*(4), 890–900.

Santato, A., Bertoldi, D., Perini, M., Camin, F., & Larcher, R. (2012). Using elemental profiles and stable isotopes to trace the origin of green coffee beans on the global market. *Journal of Mass Spectrometry, 47*(9), 1132–1140.

UNCTAD trust fund on market information on agricultural commodities. (2016). *Mango. An INFOCOMM comodity profile*.

Wang, Z., Erasmus, S. W., Dekker, P., Guo, B., Stoorvogel, J. J., & van Ruth, S. M. (2020). Linking growing conditions to stable isotope ratios and elemental compositions of Costa Rican bananas (Musa spp.). *Food Research International, 129*, Article 108882.

Xiao, W., Wei, Z., & Wen, X. (2018). Evapotranspiration partitioning at the ecosystem scale using the stable isotope method—a review. *Agricultural and Forest Meteorology, 263*, 346–361.

Zakaria, S. R., Saim, N., Osman, R., Abdul Haiyee, Z., & Juahir, H. (2018). Combination of sensory, chromatographic, and chemometrics analysis of volatile organic compounds for the discrimination of authentic and unauthentic harumanis mangoes. *Molecules, 23*(9), 2365.

ARTÍCULO 9

Multi-element and stable isotopes characterization of commercial avocado fruit (Persea americana Mill) with origin authentication purposes

J.M. Muñoz-Redondo, D. Bertoldi, A. Tonon, L. Ziller, F. Camin, J.M. Moreno-Rojas

Food Chemistry

Bajo revisión

Multi-element and stable isotopes characterization of commercial avocado fruit (*Persea americana Mill*) with origin authentication purposes

J. M. Muñoz-Redondo[1], D. Bertoldi[2], A. Tonon[3], L. Ziller[3], F. Camin[3, 4], J. M. Moreno-Rojas[1*]

[1]Department of Food Science and Health. Andalusian Institute of Agricultural and Fisheries Research and Training (IFAPA). Alameda del Obispo. Avda, Menéndez Pidal, s/n. 14071, Córdoba, Spain.

[2]Department of Experimental and Technological Services, Technology Transfer Centre, Fondazione Edmund Mach, Via E. Mach 1, 38098 San Michele all'Adige, Italy

[3]Department of Food Quality and Nutrition, Research and Innovation Centre, Fondazione Edmund Mach, Via E. Mach 1, 38098 San Michele all'Adige, Italy

[4]Centre Agriculture Food Environment C3A, University of Trento, San Michele all'Adige, Trento, Italy

*Corresponding authors:

E-mail: josem.moreno.rojas@juntadeandalucia.es

Tel.: +34 671 53 27 58; Fax: +34 957 01 60 43

E-mail: josem.munoz.redondo@juntadeandalucia.es

Tel.: +34 666 30 66 51

Abstract

Avocado (*Persea americana Mill*) is a fruit consumed worldwide due to its valuable organoleptic and health-promoting properties. To date, no information is available about the isotopic composition of this foodstuff and this study determines the stable isotope composition of five bio-elements (C, N, S, H and O) and the composition profile of 46 macro, micro and trace elements. The stable isotope and elemental profiles were determined in 131 avocados from different producing regions (Spain, Brazil, Chile, Colombia, Kenya, Mexico, Peru, South Africa) collected over three years to study the main geographical differences. A PLS-DA model was performed combining the stable isotopes with the elemental profile, making it possible to distinguish the Spanish from the non-Spanish avocados with a high prediction accuracy (98 % correct classification). The results of this study highlight the potential of stable isotope ratios and elemental profiles for tracing the geographical origin of avocados.

Keywords: IRMS, ICP-MS, stable isotopes, traceability, chemometrics, avocado

1. Introduction

Avocados (*Persea americana Mill*) are mainly produced in regions with a tropical climate. They are rich in essential nutrients, several potential cancer-preventing phytochemicals, proteins, unsaturated fatty acids, natural antioxidants, and fat-soluble vitamins less common in other fruits, but contain small amounts of calories, sodium, and fats (Duarte et al., 2016; Pleguezuelo et al., 2018). Several studies have related avocado consumption with being part of a healthy diet due to benefits such as preventing cardiovascular diseases and diabetes, and reducing cholesterol (Bhuyan et al., 2019; Duarte et al., 2016). The unique nutritional and phytochemical composition linked to these health benefits have earned avocado the title of "superfood", although this term can be vague and misleading and often involves unrealistic health claims (Bhuyan et al., 2019). In the last decade, the worldwide production of avocado has increased at a faster rate than all other tropical fruits, with an annual average rate of 6%. The production volume of avocados reached 6.3 million tonnes and the export volume 2.13 million tonnes in 2018 (FAO, 2018), accounting for 30% of the global trade of major tropical fruits. The main export destinations of avocados are the United States of America (around 50 % of global exports) and the European Union (around 28 %) with France, United Kingdom and Germany being the largest avocado-consuming markets (FAO, 2018; Moreno-Ortega et al., 2019). Spain is the only European country that produces and exports avocados, making possible the rapid distribution of this high-quality product to this market (Moreno-Ortega et al., 2019). Approximately 90 % of the avocado cultivars are distributed along the southern coastal strip of Andalusia (Malaga, Granada and Cadiz) and the rest in the Canary Islands, avocados being the main tropical fruit in terms of production, surpassing the mango (*Mangifera indica L.*) and cherimoya (*Annona cherimola Mill.*) (Fruittoday, 2019).

Consumers are increasingly interested in the quality parameters and provenance of food, as well as the sustainability and environmental impact involved in their production. In this

sense, European Union quality schemes identify products with unique characteristics linked to a geographical location or a traditional know-how, allowing products to be granted “geographical indications”. This recognition enables consumers to trust and recognize quality products and is used as a marketing tool by producers to add value to their crops (EU Regulation No 1151/2012). Recently, the Spanish tropical fruit producers formed an association, seeking to obtain a protected geographical indication (PGI) for the avocados produced on the coastal strip of Andalusia (Fruittoday, 2019). PGI emphasises the link between a product and a particular geographical area in at least some of the production, processing or preparation stages (Regulation (EU) No 1151/2012). In this sense, traceability is of essential importance to ensure the geographical origin, quality and safety of this product, several studies having been performed into this matter. Liu et al., 2020 determined several quality traits of avocados of different origins such as moisture levels and the content of ascorbic acid, oil, total flavonoid, soluble protein and soluble sugar, but found no significant differences according to their geographical origin. Carvalho et al., 2015 reported geographical differences in the fatty acid contents of avocados from different latitudes in Colombia, and highlighted the importance of considering these compounds in a potential PDO due to their health benefits. Donetti & Terry, 2014 found differences in the main bioactive compounds present in the avocado mesocarp related to their geographical origin and harvest-time. Besides seasonal variations and maturity, it was possible to distinguish avocados produced in Chile, Peru and Spain by their oleic acid, palmitic acid, palmitoleic acid, dry matter and oil content. Among these, the authors suggested oleic acid as a potential marker for tracing the geographical growing area of avocados. These results were based on unsupervised analysis (PCA), and no classification rates were available. Martín-Torres et al., 2020 and Jiménez-Carvelo et al., 2021 combined lipid fingerprints, acquired by HPLC-DAD and GC-FID, with chemometrics to successfully authenticate the origin and the botanical variety of avocados. The authors were able to discriminate

avocados produced in Spain from those from other countries, including Peru, Mexico, South Africa and Kenya. However, all the Spanish samples were collected from Granada, while avocados from Malaga, which is the main production area in Spain, were not included. Although stable isotope ratios of light bio-elements ($\delta^{13}C$, $\delta^{15}N$, $\delta^{34}S$, $\delta^{2}H$, $\delta^{18}O$) have long been used to trace the geographical origin of agro-food products (Katerinopoulou et al., 2020) no studies have characterized the isotopic profile of avocados. In addition, a great deal of progress has been made in recent years verifying the geographical origin of foodstuffs by combining multi-isotope analyses with multi-elemental fingerprinting and chemometrics (Wang et al., 2020).

In this study, the isotopic composition of five light bio-elements (C, N, S, H, O) was assessed for the first time in avocado samples from eight producing regions (Spain, Mexico, Colombia, Peru, Brazil, Chile, Kenya and South Africa) and combined with the characterization of their mineral content and chemometrics to trace their geographical origin.

2. Material and methods

2.1. Samples and preparation

A total of 131 avocado samples were collected from Spain (N = 49) and different worldwide producing regions (Brazil N = 4, Chile N 15, Colombia N = 9, Kenya N = 4, Mexico N = 20, Peru N = 26, South Africa N = 4), and different years (2015 N = 30, 2016 N = 29, 2017 N = 72). The avocado was peeled, and the pulp was freeze-dried, homogenized by grinding and milling, placed into 2 mL Eppendorf tubes and stored at -18 ºC for elemental analyses. For the stable isotope analyses, the dry powder was extracted with a solution of hexane:isopropanol at a ratio of 3:2 as described by Feng et al., 2004. The defatted dry matter (protein fractions) and the lipid fractions were stored at -20 ºC until the stable isotope analysis.

2.2. Stable isotope ratio analysis

Around 3 mg of the freeze-dried protein fraction of avocados were weighed into tin capsules for the simultaneous determination of $\delta^{13}C$, $\delta^{15}N$ and $\delta^{34}S$. The $\delta^{2}H$ and $\delta^{18}O$ were analysed simultaneously using 0.2 mg of samples weighed into silver capsules. The $^{15}N/^{14}N$, $^{13}C/^{12}C$ and $^{34}S/^{32}S$ ratios were determined using an IRMS (Isoprime, AP2003, GV Instruments Ltd, Manchester, UK) equipped with an elemental analyser (Vario EL III Elementar Analysensysteme GmbH, Hanau, Germany), while the $^{18}O/^{16}O$ and $^{2}H/^{1}H$ ratios were determined with an IRMS (Flash EATM1112, Thermo Finnigan) equipped with a pyrolizer (FinniganTM TC/EA, ThermoFinnigan).

For the analysis of $\delta^{13}C$ in the lipid fraction, around 1.5 mg of the freeze-dried avocado samples were weighed into tin capsules. The $\delta^{2}H$ and $\delta^{18}O$ in the lipid fraction were analysed using around 0.3 and 1 mg of sample respectively weighed into silver capsules. The $^{13}C/^{12}C$ ratio was determined by continuous flow (ConfloII) elemental analysis isotope ratio mass spectrometry (CF-EA-IRMS) using an EA 1108 CHN elemental analyser (ThermoFisher, Milan, Italy). The $^{18}O/^{16}O$ and $^{2}H/^{1}H$ ratios were determined by continuous flow (ConfloII) total combustion elemental analysis isotope ratio mass spectrometry (CF-TC-IRMS) using a TC/EA (ThermoFisher, Milan, Italy).

The isotope ratios were expressed as relative to the international standards ratio and denoted in delta notation in accordance with the following formula (Brand et al., 2014):

$$\delta(^{i/j}E) = \delta^{i/j}E = \frac{^{i/j}R_P - ^{i/j}R_{\mathrm{Re}f}}{^{i/j}R_{\mathrm{Re}f}}$$

where superscripts *i* and *j* denote the highest and the lowest atomic mass number of element E, respectively, R_P and R_{Ref} indicate the ratio between the heavier and the lighter isotope ($^{13}C/^{12}C$, $^{15}N/^{14}N$, $^{34}S/^{32}S$, $^{2}H/^{1}H$, $^{18}O/^{16}O$) in the sample and reference material, respectively.

The delta values were multiplied by 1000 and expressed in units “per mil” (‰), although miliurey (mUr) can also be used to comply with the International System of Units (SI).

The $\delta^{13}C$ values were expressed as relative to Vienna-Pee Dee Belemnite (V-PDB), $\delta^{15}N$ to Air, $\delta^{34}S$ to Vienna Cañon Diablo Troilite (V-CDT), while $\delta^{2}H$ and $\delta^{18}O$ were expressed relative to Vienna-Standard Mean Ocean Water (VSMOW), by using the reference materials listed below. The samples were analysed at least in duplicate, and the isotope values were calculated and normalised against international reference materials: L-glutamic acid USGS 40 (IAEA-International Atomic Energy Agency, Vienna, Austria), fuel oil NBS-22 (IAEA) and sugar IAEA–CH–6 for $^{13}C/^{12}C$ in the defatted avocado; caffeine IAEA 600, casein protein IVA33802155, razorbill feathers LIE-PA and cow horn powder EBD-23 for $^{13}C/^{12}C$ in the lipid fraction; L-glutamic acid USGS 40 and potassium nitrate IAEA-NO3 for $^{15}N/^{14}N$; barium sulphates IAEA–SO–5 and NBS 127 (IAEA) for $^{34}S/^{32}S$; whole wood USGS 54 and 56 for $^{2}H/^{1}H$ and $^{18}O/^{16}O$ in the defatted avocado; fuel oil NBS-22 (IAEA) and Tibetan human hair powder USGS-42 for $^{2}H/^{1}H$; caffeine IAEA 600, benzoic acid IAEA 601 and benzoic acid IAEA 602 for $^{18}O/^{16}O$ in the lipid fraction.

The analytical uncertainty (2 std dev) was 0.3 for $\delta^{13}C$ and $\delta^{15}N$, 0.6 for $\delta^{18}O$ and $\delta^{34}S$ and 3 for $\delta^{2}H$.

2.3. Elemental analysis

A total of 500 mg of homogenized and lyophilized avocado sample were used for the acid ultrawave-assisted digestion with an UltraWAVE System (Milestone, Shelton, CT, USA) equipped with quartz vials. For acid mineralization, the samples were added with 2 ml of ultrapure HNO3 (67-69%, Carlo Erba, Milan, Italy), 1 ml of H_2O_2 (30%, Merck, Darmstadt, Germany), 4 ml of ultrapure water (18.2 MΩ-cm, Millipore, Bedford, MA, USA) and 0.5 ml of internal standard solution (In 1.6 mg/l) prepared starting from the certified standard solution of Indium 1000 mg/l (Merck, Darmstadt, Germany). The digestion temperature programme was as follows: from room temperature to 100°C in 12 minutes, increasing to 240°C in 13 minutes before being kept at 240°C for 10 minutes. After mineralization, the samples were accurately transferred into a PP 13ml-vial and

brought to volume with ultrapure water. Mineral element analyses were performed with an ICP-MS (Agilent 7500ce, Agilent Technologies, Tokyo, Japan), as detailed in Bertoldi et al., 2016. A total of 46 macro, micro and trace elements were quantified: Li, Be, B, Na, Mg, Al, P, K, Ca, Cr, Mn, Fe, Co, Ni, Cu, Zn, Ga, Ge, As, Se, Rb, Sr, Y, Mo, Pd, Ag, Cd, Sn, Sb, Cs, Ba, La, Ce, Pr, Nd, Sm, Eu, Gd, Dy, Ho, Er, Tm, Yb, Hg, Pb, and U.

A solution of diluted ultrapure HNO3 (5 %) followed by ultrapure water was used to wash and rinse all the materials used for the preparation and analysis of the standard and samples. Accuracy was evaluated by analysing the certified reference material NIST 1572 'citrus leaves' (National Institute of Standards and Technology Gaithersburg, MD, USA) in each analytical batch with a result, expressed as recovery%, ranging from 76 to 107% for all the certified and non-certified elements. The cleanliness of the whole procedure was verified by preparing and analyzing a blank sample in each analytical batch. The preparation and analysis of 10 blank samples in the same sequence made it possible to calculate the detection limit (LOD) as three times the standard deviation of the signals obtained.

2.4. Statistical analysis

A one-way analysis of variance (ANOVA) followed by the post-hoc Tukey's HSD (honest significance test) were used to study the differences in the samples related to their geographical origin, which were considered statistically significant at a p-value ≤ 0.05. Before these parametric tests, the heteroscedasticity of the data was assessed by means of Levene's test and normality by the Shapiro-Wilk and Kolmogorov-Smirnov tests. The variables failing these parametric assumptions were box-cox transformed. The correlations between the variables were also analysed by means of a Pearson correlation test. Partial least squares discriminant analysis (PLS-DA) was performed on the data for the classification of the samples according to the geographical origin. A double cross-validation was used to optimize and calculate the errors of the PLS-DA models, using the balanced error rate (BER) as the diagnostic statistic. The most

discriminative variables were selected by means of an iterative procedure based on the variable importance in projection (VIP), repeated 100 times. The variables selected as the most discriminative (potential markers for the geographical discrimination of avocado samples) were further used to fit a new double cross-validated model and the classification performance was compared to the initial model. The statistical principal component analysis (PCA) was used to study the structure of the data before and after the variable reduction. All the statistical analyses were carried out with the statistical software R v. 4.0.3. In-house routines based on the *mixOmics* R package were used for the multivariate analyses.

3. Results and discussion

A one-way analysis of variance (ANOVA) with Tukey's HSD pairwise comparison for the geographical origin of the avocado samples is given in Table 1. A total of 54 variables were examined, 8 different isotopic variables and 46 trace elements. The stable isotope ratios of carbon, nitrogen, sulphur, hydrogen and oxygen were analysed in the lipid-free fraction of the avocado. Additional stable isotope measurements of carbon, hydrogen and oxygen were performed on the lipid extraction to determine whether the information obtained could be redundant. Finally, the trace elements in the bulk avocados were analysed to avoid any treatment that could contaminate the samples due to the lower values of certain elements.

3.1. Carbon and nitrogen stable isotope ratios

According to FoodData Central of the US Department of Agriculture, avocados are composed of 14.66 g of total lipids. Lipids in plants tend to be depleted in heavier ^{13}C isotopes relative to proteins and carbohydrates by fractionation during the oxidation of pyruvate to acetyl coenzyme A (DeNiro & Epstein, 1978). Therefore, comparisons of $\delta^{13}C$ values between samples with a high lipid content may be confounded by variations in lipid contents, the extraction of this organic constituent therefore being recommended

(DeNiro & Epstein, 1978). The mean values determined for $\delta^{13}C$ in both fractions according to the geographical origin are given in Table 1. The $\delta^{13}C_L$ values ranged from -36.9 to -28.7 ‰ with an average value of -31.9 ± 1.5 ‰, while $\delta^{13}C_P$ varied between -31.7 to -23.9 ‰ with an average value of -27.6 ± 1.7 ‰. A depletion in ^{13}C during the lipid synthesis may explain the lower $\delta^{13}C_L$ values (on average 4.3 ‰) compared to $\delta^{13}C_P$. Previous studies have also reported lower $\delta^{13}C$ values in fat fractions, e.g. for animal products of about 4.31 ‰ in sea bass tissues (Tulli et al., 2020) or 5.2 ‰ in lamb meat (Perini et al., 2009). The $\delta^{13}C$ values measured in the lipid and protein fractions displayed a similar variation according to the geographical origin of the avocados (Table 1), as highlighted by the relatively high correlation coefficient of 0.713 (Supplementary Table S1), but with some differences. Regarding $\delta^{13}C_P$, values about 1 ‰ lower were observed in the avocados from Spain and Chile compared to the rest, while the lowest $\delta^{13}C_L$ signature values were found in the samples from Chile (around -33.8 ± 1.8 ‰), followed by Spain (-31.9 ± 0.9 ‰), Brazil (-32.0 ± 0.8 ‰) and Colombia (-32.4 ± 1.1 ‰) (Table 1). This geographical variation observed in the $\delta^{13}C$ values of the avocados may be explained by the impact of management practices or geographical characteristics (elevation, altitude, latitude, precipitations, hydric stress or even light exposure) on the efficiency of CO_2 fixation (Lagad et al., 2013). Differences in the relative humidity of the different regions may also explain the variations in the $\delta^{13}C$ signature, as previously described in garlic (Choi et al., 2020).

The $\delta^{15}N$ values were determined in the defatted fraction ($\delta^{15}N_P$) of the avocados, variations between -2.4 to 6.4 ‰ being found. A similar range of variation was previously described in other fruit matrixes such as pulp mango (between -3.65 and 7.91 ‰; Muñoz-Redondo et al., 2021), and apple juice pulp (between 0 and 4.3 ‰; Bat et al., 2016). The $\delta^{15}N$ signature has been reported to be affected by geographical/climate factors such as mean annual precipitations (Inácio et al., 2015), making it possible to differentiate the geographical origin of different foodstuffs in combination with $\delta^{13}C$. However, the $\delta^{15}N$

values in plants are mainly influenced by soil properties and agricultural practices, being highly dependent on the available nitrogen sources (Inácio et al., 2015). Previous studies have shown that the $\delta^{15}N$ values of organic matter is generally within the range of 6.4 to 11.2 ‰, since organic soils are usually more enriched in ^{15}N compared to the atmospheric N_2, but the use of organic or synthetic fertilizers can alter the $\delta^{15}N$ values of soil organic nitrogen (Inácio et al., 2015). Fertilizers display different $\delta^{15}N$ values depending on their origin, conventional fertilizers presenting values between -3.9 to 5.7 ‰, while the $\delta^{15}N$ signature of organic fertilizers has been reported to present greater variation, with values between 2.5 to 45.2 ‰ (Bateman & Kelly, 2007; Inácio et al., 2015). Therefore, low $\delta^{15}N$ values in plants may be the result of agricultural intensification processes. For instance, the $\delta^{15}N$ values of the avocados produced in Brazil, Chile, Mexico, Peru, South Africa and Spain had average ranges of 0.4-2.0 ‰, while those from Colombia and Kenya, averaging $\delta^{15}N$ values of 3.9 ± 1.5 and 4.5 ± 2.1 ‰ respectively, were most likely produced with less intensive agricultural practices.

3.2. Sulphur stable isotope ratio

The $\delta^{34}S$ content was also determined in the defatted fraction of the avocado samples, values ranging between 3.4 and 8.8 ‰. The sulfur isotopic ratio in plant materials is mainly influenced by the $\delta^{34}S$ of soil, which depends on the geological characteristics of a location, proximity to the coast, anthropogenic sources, climatic conditions and the deposition of sea-spray (aerosolised seawater containing sulphates) in areas and crops close to the sea (Pianezze et al., 2020). Since avocados are mainly produced in coastal regions, the sea-spray effect may have a strong influence on the sulfur isotopic signature. In this study, the highest $\delta^{34}S$ values were found for the avocados produced in Kenya, Brazil and South Africa, with an average value of 11.7 ± 1.6, 8.8 ± 0.3 and 7.7 ± 1.4 ‰ respectively. On the other hand, the avocados from Peru, Spain, Mexico and Chile had the lowest $\delta^{34}S$ values, averaging 3.4 ± 4.6, 3.5 ± 2.8, 4.4 ± 1.1 and 4.7 ± 3.0 ‰ respectively. A high variation in the $\delta^{34}S$ values was also observed within countries,

especially for Chile (0.5 to 9.6 ‰), Colombia (3.1 to 13.4 ‰), Peru (-3.0 to 12.7 ‰) and Spain (-0.8 to 9.8 %). This may be an indicator of different geographical areas of avocado production within these countries, as observed for the Spanish samples, which were collected from Malaga and Granada and displayed respective $\delta^{34}S$ values of 6.3 ± 1.2 and 1.2 ± 1.3 %. Previous studies have also found large variations in sulphur isotope ratios in lamb meat within single European regions (Camin et al., 2007).

3.3. Hydrogen and oxygen stable isotope ratios

The ratios of the stable isotopes of hydrogen and oxygen are conventionally used for determining provenance. These ratios are the result of the isotope fractionation produced during the meteorological water cycle of evaporation, condensation and precipitation that constitutes groundwater and shows a systematic geographical isotope variation (Drivelos & Georgiou, 2012). Groundwater is consumed by plants and animals, this isotopic variation being reflected in their composition. Another factor affecting the $\delta^{2}H$ and $\delta^{16}O$ signatures in plants is evapotranspiration, which is in turn influenced by climate conditions (Xiao et al., 2018). Oxygen is also taken from atmospheric O_2 by plants at leaf level by transpiration through stomata (Farquhar et al., 1993). During the metabolism of water, biochemical isotope fractionation, which depends on the composition of organisms such as proteins, lipids and carbohydrates, also plays a key role in defining the isotopic ratios of hydrogen and oxygen. Previous studies have reported a depletion in ^{2}H for lipids (Tulli et al., 2020), differences in the fat fraction and fat content of samples thus producing variations in the overall stable isotope values for hydrogen. To clarify the effect of the delipidization process on the isotopic signature of hydrogen and oxygen and to determine whether additional information could be obtained, we analysed the $\delta^{2}H$ and $\delta^{18}O$ in both the delipidized and lipid-free fractions of the avocados. The mean $\delta^{2}H$ values determined in the protein and lipid fractions of avocados according to the geographical origin are given in Table 1. Important differences were found between the isotopic values of $\delta^{2}H_P$ and $\delta^{2}H_L$ (Table 1), the Pearson correlation test showing a weak correlation of

0.164 (Supplementary Table S1). While the isotopic signature of hydrogen varied between -76 to -3 ‰ in the lipid-free fraction of avocados, in the extracted lipids it ranged between -174 to -146 ‰ (Table 1). In addition, the δ^2H signatures of avocados of different geographical origins presented notable differences (Table 1). The δ^2H_P signatures were higher (less negative) in the samples from Brazil, Kenya, and South Africa, averaging -15 ± 6, -3 ± 12 and -26 ± 7 ‰, respectively. Meanwhile, Spanish avocados presented the lowest statistically significant δ^2H_P values, with an average of -76 ± 30 ‰. This signature, therefore, shows great potential as a discriminator for the geographical origin of Spanish avocados. The δ^2H_P values of the avocado samples were linked to north/south and east/west trends and consistent with the global map of hydrogen isotope ratios in precipitation given in waterisotopes.org. In general, the avocados from countries located at higher latitudes displayed lower δ^2H_P values, especially those from Spain (Table 1). In Kenya and in the coastal strip of South Africa and Brazil, the δ^2H values in precipitation water are reported to be higher according to the global map, ranging from -13 to 41 ‰. This is in accordance with the higher δ^2H_P values observed in the avocados from those countries (Table 1). The stable isotope ratios of hydrogen determined in the fat fraction did not show such a geographical discriminatory capability for the Spanish avocados, which presented similar statistically significant values (-153 ± 12 ‰ on average) as those from South Africa (-146± 3 ‰) and Kenya (-156 ± 11 ‰). The difference between the $\delta^{18}O$ values in the defatted and lipid fractions was less significant (Table 1), as highlighted by the high correlation coefficient of 0.887 (Supplementary Table S1), although the $\delta^{18}O$ values from the lipid fraction showed a slightly better differentiation capability than those from the protein fraction. While the $\delta^{18}O_L$ values were higher in the avocados from Spain (on average 25.1 ± 1.3 ‰) compared to those from the other countries, higher $\delta^{18}O_P$ values were found in the avocados from both Spain and Kenya, with respective average values of 29.2 ± 1.7 and 30.6 ± 1.2 ‰ (Table 1). The $\delta^{18}O$ in both the protein and lipid fractions in all the samples ranged between 3.2 and 26.1 ‰,

these values differing from those reported in precipitations (-2.3 to -50.4 ‰). This may be explained by the influence of atmospheric O_2 that is taken by plants at leaf level (Farquhar et al., 1993), as described above. However, a similar $\delta^{18}O$ trend was observed in the avocados and precipitation (global map of $\delta^{18}O$ in precipitation provided by waterisotopes.org). Kenya and the coastal strip of Brazil and South Africa display higher $\delta^{18}O$ values in precipitations (between -2.3 to 4.5 ‰), which would correlate with the higher values for this isotope in the protein and lipid fractions of the avocados produced in those countries (Table 1). Meanwhile, on the coast of Mexico, Peru, Chile and Colombia lower $\delta^{18}O$ values in precipitation were reported (between -22.9 to -9.2 ‰), this being in line with the lower stable isotope ratio values obtained for the avocados produced in these countries. In contrast, $\delta^{18}O$ in precipitation given for Spain were reported to vary between -9.2 to 2.3 ‰, lower $\delta^{18}O$ values therefore being expected in the avocados from this country, but in fact we observed that the avocados produced in this country had a $\delta^{18}O$ signature equal or even higher than those from Kenya, Brazil and South Africa probably due to the influence of atmospheric O_2.

3.4. Elemental profile

Potassium was the most abundant element in the avocados, with concentrations ranging between 10 and 40 g/kg, followed by P, Mg and Ca, presenting concentrations between 100 mg/kg and 5000 mg/kg. Na was observed in very different concentrations in the avocado samples, varying between 4 to over 1000 mg/kg. The concentration of B was found to be between 10 and 400 mg/kg; Mn, Fe, Cu, Zn and Rb between 1 and 100 mg/kg; Al and Sr between 100 µg/kg and 30 mg/kg; Li, Ba and Ni between 1 µg/kg and 20 mg/kg; Cr, Mo, Cd, Co, As and Cs between 0.5 µg/kg and 4 mg/kg; Be, Ga, Ge, Se, Y, Pd, Ag, Sn, La, Ce, Nd, Pb and U between 0.1 and 200 µg/kg and the remaining elements between <LOD and 10 µg/kg. These results are in accordance with previous studies performed in avocado samples (Hardisson et al., 2001; Reddy et al., 2014),

although Cd, Co, Cr, Cu, Pb and Se were below the limits of detection in Reddy et al., 2014.

All the samples contained the following elements: K (LOD < 0.03 g/kg), Al (LOD < 0.1 mg/kg), B (LOD < 0.1 mg/kg), Ba (LOD < 0.001 mg/kg), Ca (LOD < 30 mg/kg), Cu (LOD < 0.003 mg/kg), Fe (LOD < 0.03 mg/kg), Mg (LOD < 1.6 mg/kg), Mn (LOD < 0.03 mg/kg), Na (LOD < 1.6 mg/kg), P (LOD < 3.2 mg/kg), Rb (LOD < 0.003 mg/kg), Sr (LOD < 0.003 mg/kg), Zn (LOD < 0.003 mg/kg), Co (LOD < 0.33 µg/kg), Cr (LOD < 1.6 µg/kg), Ce (LOD < 0.03 µg/kg), Cs (LOD < 0.2 µg/kg), La (LOD < 0.03 µg/kg), Li (LOD < 0.3 µg/kg), Ni (LOD < 3.2 µg/kg), Nd (LOD < 0.03 µg/kg), Mo (LOD < 3.25 µg/kg), Cd (LOD <0.33 µg/kg), Sm (LOD < 0.03 µg/kg), Gd (LOD < 0.03 µg/kg), and Pb (LOD < 0.16 µg/kg). Meanwhile, Dy (LOD < 0.03 µg/kg) was present at detectable amounts in the 99 % of the samples, Sb (LOD < 0.26 µg/kg) in 98 %, Pr (LOD < 0.03 µg/kg) in 97 %, Se (LOD < 1.6 µg/kg) in 96 %, Eu (LOD < 0.03 µg/kg) in 95 %, Yb (LOD < 0.03 µg/kg) in 91 %, Hg (LOD < 0.3 µg/kg) in 89 %, Ga (LOD < 0.2 µg/kg) in 88 %, Ge (LOD < 0.2 µg/kg) in 86 %, As (LOD < 1.6 µg/kg) in 83 %, Er (LOD < 0.03 µg/kg) in 79 %, Y (LOD < 0.33 µg/kg) in 74 %, Pd (LOD < 0.33 µg/kg) in 68 %, Sn (LOD < 2.6 µg/kg) in 64 %, U (LOD < 0.16 µg/kg) in 63 %, Ag (LOD < 0.33 µg/kg) in 48 %, Be (LOD < 0.33 µg/kg) in 44 %, Ho (LOD < 0.03 µg/kg) in 41 %, and Tm (LOD < 0.03 µg/kg) in 15 %.

A one-way ANOVA was performed to study the differences in the elemental profiles related to the geographical origin of the avocados. Statistically significant differences linked to the geographical origin of the samples were found for all the elements except Cr, Sn and Hg (Table 1). However, the random selection of avocados from different origins implies different agricultural practices such as fertilization and may lead to variations in the elemental profile. The Spanish avocados displayed low concentrations overall for most of the elements compared to the non-Spanish avocados. Only B and P were found in significantly higher concentrations compared to the rest, with respective

average values of 126 and 2412 mg/kg (Table 1). High concentrations of Li and Na were also found in the Spanish avocados, with average values of 1289 µg/kg and 142 mg/kg. The avocados from Kenya, Brazil and South Africa displayed similar elemental profiles, although several differences related to some elements were found (Table 1). The avocados produced in Brazil had higher concentrations of P, K, Co, Cu, Zn, La, Pr, Nd, Sm, Eu and Gd, while those produced in Kenya displayed higher contents of Be, Al, Ga, Ag, Ce, Er, Tm and Yb. Meanwhile, the samples collected from South Africa showed significantly higher contents of Ni, Rb and Cs and lower concentrations of Sr, Y, Dy and Ho. The avocados from Peru were richer in B, Na, Mg, P, Zn, Ge, As, Se, Mo, Pd, Cd and Sb, and in particular Li, with average concentrations of 2654 µg/kg. Finally, the elemental profiles of avocados produced in Chile, Colombia and Mexico were also similar (Table 1). However, higher concentrations of Na, Ca and Ga, and lower concentrations of Ba and Eu were observed in the avocados produced in Chile. Meanwhile the samples from Colombia were richer in Pd.

3.5. Multivariate analysis

The samples were classified according to their geographical origin by means of a partial least squares discriminant analysis (PLS-DA) model including the elemental and stable isotope ratio profiles. The PLS-DA model yielded a low balanced error rate (BER) of 0.02 ± 0.01 (Table 2), making it possible to discriminate avocados produced in Spain from those produced in other countries. The first two latent variables explained respectively 20 % and 15 % of the total variance found in the samples, displaying the main differences between the Spanish and non-Spanish avocados related to the stable isotope ratios and trace elements (Figure 1a and 1b). The overall quality of the PLS-DA model was also evaluated with the Ypredict plot in Figure 1c. It shows the predicted Y values for each avocado sample during the 50 repetitions (in outer loop) of the double cross-validation. Good predictions were considered to range from -0.5 to 0.5 for the non-Spanish samples and from 0.5 to 1.5 for the Spanish samples. Respective values closer to 0 and 1 for

non-Spanish and Spanish avocados and little scattering in the predicted values of Y for the 50 repetitions are expected for more robust models. The PLS-DA model displayed very scattered predicted Y values, especially for the non-Spanish samples (Figure 1c). Five non-Spanish samples were wrongly classified as Spanish in several repetitions of the cross-validation, while four other samples had predicted Y values below -0.5, indicating a low prediction capability for these samples. However, since the target class was the Spanish avocados, this result may not be considered to worsen the quality of our model. The noisy contribution of non-explicative variables may explain these results and a variable reduction procedure was used to select the most discriminative stable isotope ratios and elements (potential markers). Principal component analysis (PCA) was performed with all the data and with the selected markers to evaluate the suitability of eliminating the non-informative variables in tracing the geographical origin of the avocados (Figure 2). This approach also allowed us to observe the distribution of the samples according to the country of provenance. The PCA including all the data (Figure 2a and 2b) did not enable clear differences in the samples according to their geographical origin to be established, although the avocados produced in Kenya, Brazil and South Africa were slightly separated from the rest in component 1, and some avocados from Peru and Colombia seemed to be separated from the Spanish ones in component 2. Meanwhile, the PCA constructed with the potential markers from the variable reduction procedure, including 6 stable isotope ratios ($\delta^{18}O_L$, $\delta^{18}O_P$, $\delta^{2}H_L$, $\delta^{13}C_P$, $\delta^{2}H_P$, $\delta^{15}N_P$) and 8 elements (Fe, Ca, Mn, Sr, Rb, Eu, Ba and Mg), improved the separation of the Spanish avocados (Figure 2c and 2d), which were allocated in a narrow and well-defined area separate from the non-Spanish samples and mainly defined by component 1. This result was expected since the goal of the variable reduction procedure was to find the most powerful discriminators involved in the differentiation of Spanish from non-Spanish avocados. Nonetheless, additional clusters were observed in the samples from Kenya, Brazil and South Africa, which were separated from the avocados

produced in Peru, Colombia, Chile and Mexico in component 2. Subsequently, a new PLS-DA model was performed with the selected markers, showing a BER of 0.02 ± 0.00 and displaying a similar classification error to the previous model including all the variables (Table 2). However, the overall quality of the model increased, since the range of predicted Y values was smaller and its complexity was reduced from 2-3 to 1 component (Figure 1d and Figure 3d). The classification error of the PLS-DA was explained by two Spanish avocados, one of which was wrongly classified in all the repetitions of the cross-validation, and two non-Spanish avocados that were always classified as being Spanish. Meanwhile, one non-Spanish sample displayed lower predicted Y values than -0.5 (Figure 3c). The one latent variable optimized for this new model explained 44 % of the total variance found in the samples. The stable isotope of oxygen for the protein ($\delta^{18}O_P$) and lipid ($\delta^{18}O_L$) fractions were the main geographical discriminators (Figure 3a and 3b), these being found in higher overall values in the Spanish samples. The stable isotope of hydrogen measured in the lipid fraction ($\delta^{2}H_L$) was also selected as potential marker for the geographical differentiation and it was found in higher overall values in the Spanish avocados (Figure 3b). As mentioned in the univariate approach, the opposite was observed for the $\delta^{2}H_P$, displaying higher values in the non-Spanish avocados. Additionally, the stable isotopes of carbon and nitrogen determined in the lipid-free fraction ($\delta^{13}C_P$ and $\delta^{15}N_P$) were also selected as important discriminators for the geographical origin of avocados. On this basis, we recommend determining the stable isotopes of carbon and hydrogen in the protein and lipid fractions separately to avoid misleading variations due to differences in lipid and protein contents. All the elements selected as potential markers (Fe, Ca, Mn, Sr, Rb, Eu, Ba and Mg) were found in lower concentrations in the Spanish avocados. Previous studies have described the usefulness of these elements for tracing the origin of different foodstuffs. Fe was the most discriminative element selected in the variable reduction procedure (Figure 3b). Sun et al., 2011 showed significant geographical differences in the Fe contents of

de-fatted mutton samples, while Guo et al., 2007 selected this element as a good tracer of beef origin. Fe, Ca, Mn, Ba and Mg have been successfully used for verifying the geographical provenance of olive-pomace and olive oils (Beltrán et al., 2015). Mottese et al., 2018 reported a strong correlation between the concentration of several minerals and the geographical area of production of *Opuntia ficus indi*a L. Miller fruits, selecting Fe, Ca, Mn and Mg as the markers of provenance. Regarding fruits, Sr, Mg were found to be the most suitable elements for discriminating their geographical origin by Benabdelkamel et al., 2012. Rb has also been reported to be a marker for the geographical characterization of Italian goji berries (Bertoldi et al., 2019). This element was also used, together with Fe, Ca, Mn, Sr, Ba and Mg, for the successful classification of coca beans from different countries (Bertoldi et al., 2016). Coetzee et al., 2014 identified Sr, Rb, Ba and Mg as suitable indicators for the geographical determination of wines produced in 23 estates in South Africa. In a recent study, Ba was selected as a potential geographical marker for mangoes (Muñoz-Redondo et al., 2021). Ba has also been used in combination with Sr, Mn and Eu for the correct classification of wheat samples from different Argentinian regions (Podio et al., 2013).

4. Conclusions

In this study, we characterized for the first time the isotopic composition of avocados from different geographical origins. We evaluated the effect of the delipidization procedure on the isotopic signatures of C, H and O, finding important differences due to different isotopic fractionations occurring during the metabolism of different compounds in the avocado plants. The elemental profile of avocados was also assessed and statistical differences related to their geographical location were observed for most of the minerals analysed. Potassium was the most abundant element in avocados, followed by P, Mg and Ca. Then, the geographical origin of the avocados was assessed by means of a PLS-DA model including the stable isotope ratios and the elemental composition, and the potential markers selected during a variable selection procedure included six

stable isotope measurements ($\delta^{18}O_L$, $\delta^{18}O_P$, $\delta^{2}H_L$, $\delta^{13}C_P$, $\delta^{2}H_P$, $\delta^{15}N_P$) and eight elements (Fe, Ca, Mn, Sr, Rb, Eu, Ba and Mg). The PLS-DA model yielded a high classification ratio of 98 %, revealing the potential of stable isotopes and elemental profiles to trace the provenance of Spanish avocados.

5. Acknowledgements

The authors thank the “Asociación Española de Tropicales” for supplying the samples.

6. Financial funds

J. M. Muñoz-Redondo was awarded a research contract funded by the Andalusian Institute of Agricultural and Fisheries Research and Training (IFAPA), within the National Youth Guarantee System funded through the European Social Fund (ESF) and the Youth Employment Initiative (YEI). This study was funded by the Andalusian Institute of Agricultural and Fisheries Research and Training (IFAPA) and the European Rural Development Fund (ERDF, EU) through the Project 'Caracterización de alimentos y nuevos productos elaborados: potencial saludable, organoléptico y trazabilidad alimentaria. estrategias de diversificación y reclamo competitivo” (PR.AVA.AVA201601.20). This work has been partially funded within the framework of Accordo di Programma 2018-2019, Traceability unit of Fondazione Edmund Mach.

References

Bat, K. B., Eler, K., Mazej, D., Vodopivec, B. M., Mulič, I., Kump, P., & Ogrinc, N. (2016). Isotopic and elemental characterisation of Slovenian apple juice according to geographical origin: Preliminary results. *Food chemistry*, *203*, 86-94.

Bateman, A. S., & Kelly, S. D. (2007). Fertilizer nitrogen isotope signatures. *Isotopes in environmental and health studies*, *43*(3), 237-247.

Beltrán, M., Sánchez-Astudillo, M., Aparicio, R., & García-González, D. L. (2015). Geographical traceability of virgin olive oils from south-western Spain by their multi-elemental composition. *Food Chemistry*, *169*, 350-357.

Benabdelkamel, H., Di Donna, L., Mazzotti, F., Naccarato, A., Sindona, G., Tagarelli, A., & Taverna, D. (2012). Authenticity of PGI "Clementine of Calabria" by multielement fingerprint. *Journal of agricultural and food chemistry*, *60*(14), 3717-3726.

Bertoldi, D., Barbero, A., Camin, F., Caligiani, A., & Larcher, R. (2016). Multielemental fingerprinting and geographic traceability of Theobroma cacao beans and cocoa products. *Food Control*, *65*, 46-53.

Bertoldi, D., Cossignani, L., Blasi, F., Perini, M., Barbero, A., Pianezze, S., & Montesano, D. (2019). Characterisation and geographical traceability of Italian goji berries. *Food chemistry*, *275*, 585-593.

Bertoldi, D., Santato, A., Paolini, M., Barbero, A., Camin, F., Nicolini, G., & Larcher, R. (2014). Botanical traceability of commercial tannins using the mineral profile and stable isotopes. *Journal of Mass Spectrometry*, *49*(9), 792-801.

Bhuyan, D. J., Alsherbiny, M. A., Perera, S., Low, M., Basu, A., Devi, O. A., Barooah, M. S., Li, C. G., & Papoutsis, K. (2019). The odyssey of bioactive compounds in avocado (Persea americana) and their health benefits. *Antioxidants*, *8*(10), 426.

Brand, W. A., Coplen, T. B., Vogl, J., Rosner, M., & Prohaska, T. (2014). Assessment of international reference materials for isotope-ratio analysis (IUPAC Technical Report). *Pure and Applied Chemistry*, *86*(3), 425-467.

Camin, F., Bontempo, L., Heinrich, K., Horacek, M., Kelly, S. D., Schlicht, C., Thomas, F., Monahan, F. J., Hoogewerff, J., & Rossmann, A. (2007). Multi-element (H, C, N, S) stable isotope characteristics of lamb meat from different European regions. *Analytical and Bioanalytical Chemistry*, *389*(1), 309-320.

Carvalho, C. P., Bernal E, J., Velásquez, M. A., & Cartagena V, J. R. (2015). Fatty acid content of avocados (Persea americana Mill. Cv. Hass) in relation to orchard altitude and fruit maturity stage. *Agronomía Colombiana*, *33*(2), 220-227.

Choi, S.-H., Bong, Y.-S., Park, J. H., & Lee, K.-S. (2020). Geographical origin identification of garlic cultivated in Korea using isotopic and multi-elemental analyses. *Food Control*, *111*, 107064.

Coetzee, P. P., Van Jaarsveld, F. P., & Vanhaecke, F. (2014). Intraregional classification of wine via ICP-MS elemental fingerprinting. *Food Chemistry*, *164*, 485-492.

DeNiro, M. J., & Epstein, S. (1978). Influence of diet on the distribution of carbon isotopes in animals. *Geochimica et Cosmochimica Acta*, *42*(5), 495-506.

Donetti, M., & Terry, L. A. (2014). Biochemical markers defining growing area and ripening stage of imported avocado fruit cv. Hass. *Journal of Food Composition and Analysis*, *34*(1), 90-98.

Drivelos, S. A., & Georgiou, C. A. (2012). Multi-element and multi-isotope-ratio analysis to determine the geographical origin of foods in the European Union. *TrAC Trends in Analytical Chemistry*, *40*, 38-51.

Duarte, P. F., Chaves, M. A., Borges, C. D., & Mendonça, C. R. B. (2016). Avocado: Characteristics, health benefits and uses. *Ciência Rural*, *46*(4), 747-754.

FruitToday, 2019. El aguacate y el mango andaluz, un paso más cerca de obtener la IGP. Retrieved March 1, 2021 from https://fruittoday.com/el-aguacate-y-el-mango-andaluz-un-paso-mas-cerca-de-obtener-la-igp.

Farquhar, G. D., Lloyd, J., Taylor, J. A., Flanagan, L. B., Syvertsen, J. P., Hubick, K. T., Wong, S. C., & Ehleringer, J. R. (1993). Vegetation effects on the isotope composition of oxygen in atmospheric CO 2. *Nature*, *363*(6428), 439-443.

Feng, S., Lock, A. L., & Garnsworthy, P. C. (2004). A rapid lipid separation method for determining fatty acid composition of milk. *Journal of dairy science*, *87*(11), 3785-3788.

Food and Agriculture Organization of the United Nations (FAO), 2018. *Major tropical fruits. Market Review*. Retrieved March 11, 2021 from http://www.fao.org/3/ca5692en/CA5692EN.pdf

Guo, B. L., Wei, Y. M., Pan, J. R., & Li, Y. (2007). Determination of beef geographical origin based on multi-element analysis. *Scientia Agricultura Sinica*, *12*.

Hardisson, A., Rubio, C., Báez, A., Martín, M. M., & Alvarez, R. (2001). Mineral composition in four varieties of avocado (Persea gratissima, L.) from the island of Tenerife. *European Food Research and Technology*, *213*(3), 225-230.

Inácio, C. T., Chalk, P. M., & Magalhães, A. M. (2015). Principles and limitations of stable isotopes in differentiating organic and conventional foodstuffs: 1. Plant products. *Critical reviews in food science and nutrition*, *55*(9), 1206-1218.

Jiménez-Carvelo, A. M., Martín-Torres, S., Ortega-Gavilán, F., & Camacho, J. (2021). PLS-DA vs sparse PLS-DA in food traceability. A case study: Authentication of avocado samples. *Talanta*, *224*, 121904.

Katerinopoulou, K., Kontogeorgos, A., Salmas, C. E., Patakas, A., & Ladavos, A. (2020). Geographical Origin Authentication of Agri-Food Products: A Review. *Foods*, *9*(4), 489.

Lagad, R. A., Alamelu, D., Laskar, A. H., Rai, V. K., Singh, S. K., & Aggarwal, S. K. (2013). Isotope signature study of the tea samples produced at four different regions in India. *Analytical Methods*, *5*(6), 1604-1611.

Liu, Y., Ge, Y., Zhan, R., Lin, X., Zang, X., Li, Y., Yang, Y., & Ma, W. (2020). Molecular markers and a quality trait evaluation for assessing the genetic diversity of avocado landraces from China. *Agriculture*, *10*(4), 102.

Martín-Torres, S., Jiménez-Carvelo, A. M., González-Casado, A., & Cuadros-Rodríguez, L. (2020). Authentication of the geographical origin and the botanical variety of avocados using liquid chromatography fingerprinting and deep learning methods. *Chemometrics and Intelligent Laboratory Systems*, *199*, 103960.

Moreno-Ortega, G., Pliego, C., Sarmiento, D., Barceló, A., & Martínez-Ferri, E. (2019). Yield and fruit quality of avocado trees under different regimes of water supply in the subtropical coast of Spain. *Agricultural Water Management*, *221*, 192-201.

Mottese, A. F., Naccari, C., Vadalà, R., Bua, G. D., Bartolomeo, G., Rando, R., Cicero, N., & Dugo, G. (2018). Traceability of Opuntia ficus-indica L. Miller by ICP-MS multi-element profile and chemometric approach. *Journal of the Science of Food and Agriculture*, *98*(1), 198-204.

Muñoz-Redondo, J. M., Bertoldi, D., Tonon, A., Ziller, L., Camin, F., & Moreno-Rojas, J. M. (2021). Tracing the geographical origin of Spanish mango (Mangifera indica L.) using stable isotopes ratios and multi-element profiles. *Food Control*, 107961.

Perini, M., Camin, F., Bontempo, L., Rossmann, A., & Piasentier, E. (2009). Multielement (H, C, N, O, S) stable isotope characteristics of lamb meat from different Italian regions. *Rapid Communications in Mass Spectrometry: An International Journal Devoted to the Rapid Dissemination of Up-to-the-Minute Research in Mass Spectrometry*, *23*(16), 2573-2585.

Pianezze, S., Bontempo, L., Perini, M., Tonon, A., Ziller, L., Franceschi, P., & Camin, F. (2020). δ34S for tracing the origin of cheese and detecting its authenticity. *Journal of Mass Spectrometry*, *55*(7), e4451.

Pleguezuelo, C. R. R., Martínez, J. R. F., Tejero, I. F. G., Ruíz, B. G., Tarifa, D. F., & Zuazo, V. H. D. (2018). Avocado (Persea americana Mill.) Trends in Water-Saving Strategies and Production Potential in a Mediterranean Climate, the Study Case of SE Spain: A Review. *Water Scarcity and Sustainable Agriculture in Semiarid Environment*, 317-346.

Podio, N. S., Baroni, M. V., Badini, R. G., Inga, M., Ostera, H. A., Cagnoni, M., Gautier, E. A., García, P. P., Hoogewerff, J., & Wunderlin, D. A. (2013). Elemental and isotopic fingerprint of Argentinean wheat. Matching soil, water, and crop composition to differentiate provenance. *Journal of agricultural and food chemistry*, *61*(16), 3763-3773.

Reddy, M., Moodley, R., & Jonnalagadda, S. B. (2014). Elemental uptake and distribution of nutrients in avocado mesocarp and the impact of soil quality. *Environmental monitoring and assessment*, *186*(7), 4519-4529.

Sun, S., Guo, B., Wei, Y., & Fan, M. (2011). Multi-element analysis for determining the geographical origin of mutton from different regions of China. *Food Chemistry*, *124*(3), 1151-1156.

Tulli, F., Moreno-Rojas, J. M., Messina, C. M., Trocino, A., Xiccato, G., Muñoz-Redondo, J. M., Santulli, A., & Tibaldi, E. (2020). The Use of Stable Isotope Ratio Analysis to Trace European Sea Bass (D. labrax) Originating from Different Farming Systems. *Animals*, *10*(11), 2042.

Wang, J., Chen, T., Zhang, W., Zhao, Y., Yang, S., & Chen, A. (2020). Tracing the geographical origin of rice by stable isotopic analyses combined with chemometrics. *Food Chemistry*, *313*, 126093.

Xiao, W., Wei, Z., & Wen, X. (2018). Evapotranspiration partitioning at the ecosystem scale using the stable isotope method—A review. *Agricultural and Forest Meteorology*, *263*, 346-361.

Table 1. One-way analysis of variance (ANOVA) for the geographical origin of avocados based on the isotope and element profiles. B, Na, Mg, Al, P, Ca, Mn, Fe, Cu, Zn, Rb, Sr, Ba are expressed in mg/g, K is expressed in g/L and the rest of elements are expressed in µg/kg.

Variable	Spain (N=49)	Brazil (N=4)	Chile (N=15)	Colombia (N=9)	Mexico (N=20)	Peru (N=26)	Kenya (N=4)	South Africa (N=4)	p-value
$\delta^{13}C_P$	-28.4±1.4b	-26.8±0.8a	-28.5±1.7b	-26.8±1.2a	-27.1±1.9a	-26.4±1.0a	-26.3±1.9a	-27.2±1.1ab	***
$\delta^{15}N_P$	0.4±1.6c	1.4±0.4c	1.2±1.8c	3.9±1.5ab	1.3±1.7c	1.8±1.9c	4.5±2.1a	2.0±1.0bc	***
$\delta^{34}S_P$	3.5±2.8d	8.8±0.3ab	4.7±3.0cd	5.9±3.4bc	4.4±1.1cd	3.4±4.6d	11.7±1.6a	7.7±1.4abc	***
$\delta^{2}H_P$	-76±30d	-15±6a	-51±10bc	-49±17bc	-56±30bc	-58±37c	-3±12a	-26±7ab	***
$\delta^{18}O_P$	29.2±1.7a	24.9±0.3bc	24.3±1.1c	22.1±2.8d	23.5±2.6c	24.1±1.3c	30.6±1.2a	26.7±0.7b	***
$\delta^{13}C_L$	-31.9±0.9b	-32.0±0.8b	-33.8±1.8c	-32.4±1.1b	-31.6±1.9ab	-30.8±1.0a	-31.2±1.9ab	-31.4±1.1ab	***
$\delta^{2}H_L$	-153±12a	-163±2bc	-162±12b	-172±17bc	-173±16c	-174±17c	-156±11ab	-146±2a	***
$\delta^{18}O_L$	25.1±1.3a	21.6±0.5bc	19.9±1.4d	18.2±2.1e	19.1±2.0de	19.1±1.5de	23.7±1.6ab	20.6±0.6cd	***
Li	1289±2798b	3±1c	104±103bc	57±115bc	19±19c	2654±3408a	115±119bc	85±57bc	**
Be	0.18±0.16d	1.06±0.42bcd	0.38±0.23cd	0.75±0.68bcd	1.80±2.82bc	0.33±0.15d	7.95±13.94a	3.38±0.51b	***
B	126±62a	106±46ab	67±42b	60±35b	72±65b	138±94a	44±18b	56±26b	***
Na	142±126b	14±5c	256±90a	20±25c	118±110bc	284±212a	15±6c	25±5bc	***
Mg	923±212b	1153±121ab	1084±195ab	1194±246a	1045±185ab	1163±308a	1151±116ab	1082±282ab	***
Al	1.16±0.91c	0.66±0.10c	2.02±1.43b	1.03±0.81c	1.00±0.47c	1.67±1.56bc	4.44±3.58a	0.77±0.14c	***
P	2412±603abc	3031±1049a	2496±843ab	2786±566a	2106±617bc	2792±894a	1692±421c	1875±655bc	**
K	20±4c	28±9a	17±5c	21±2bc	20±4c	24±6ab	19±3c	18±3c	***
Ca	375±131c	611±129b	880±308a	567±130bc	573±265bc	673±254b	589±106bc	459±202bc	***
Cr	97±196	158±89	63±29	110±138	61±43	141±173	138±159	61±26	ns
Mn	4.6±1.1d	11.0±3.0abc	9.2±5.5bc	12.4±7.3ab	7.2±2.5c	8.2±6.5c	16.7±4.2a	14.1±3.6a	***
Fe	11.7±3.6c	17.8±4.0ab	19.2±5.1ab	21.6±8.9a	19.7±5.4ab	16.6±6.4b	21.2±5.9ab	18.9±5.1ab	***
Co	46±23c	482±156a	75±150c	64±55c	53±29c	41±24c	74±29c	284±56b	***
Ni	519±262e	2885±1553b	596±851de	1758±733bc	586±834de	1168±2186cd	3084±4229b	6294±2104a	***
Cu	6.6±2.8c	18.1±8.6a	7.5±3.2bc	8.9±2.5bc	8.6±2.8bc	9.3±3.1b	5.0±2.5c	9.2±2.4bc	***
Zn	18±5b	28±11a	17±5b	22±3ab	18±7b	25±10a	17±2b	15±4b	***
Ga	0.41±0.21cd	0.26±0.07d	0.59±0.30b	0.38±0.23cd	0.36±0.11d	0.55±0.43bc	1.37±0.97a	0.28±0.06d	***
Ge	0.28±0.11b	0.31±0.11b	0.32±0.12b	0.39±0.10ab	0.30±0.07b	0.42±0.18a	0.39±0.09ab	0.30±0.05b	**
As	10.9±10.8b	3.8±0.2b	34.4±39.2b	5.2±11.4b	5.1±6.1b	268.3±240.6a	2.1±1.2b	2.5±1.3b	***
Se	5.8±3.1b	2.7±0.4b	4.3±2.4b	21.3±21.4ab	5.7±4.0b	23.2±37.0a	22.5±18.9ab	13.5±10.9ab	**
Rb	10.3±5.8d	34.9±11.3b	15.8±10.2cd	20.9±15.9c	20.8±9.2c	16.8±9.0c	26.0±17.1bc	65.4±29.1a	***
Sr	1.91±1.12d	5.71±1.59abc	4.28±1.48bc	5.75±1.74ab	6.88±5.67a	3.42±1.81c	6.47±4.14ab	2.77±1.57cd	***
Y	0.49±0.35d	7.02±2.45ab	1.31±0.86cd	0.75±0.63d	1.90±1.58c	0.76±0.67d	8.65±8.95a	5.20±1.65b	***
Mo	73±45b	38±16b	102±70ab	139±152a	70±39b	106±76a	60±85b	58±40b	*
Pd	1.10±1.70b	0.40±0.10b	0.51±0.34b	3.01±2.28a	0.77±1.47b	2.61±2.62a	1.60±1.23ab	0.17±0.06b	***
Ag	0.44±0.51b	0.36±0.08b	0.49±0.36b	0.22±0.14b	0.28±0.09b	0.44±0.37b	1.99±1.42a	0.63±0.26b	***
Cd	55±96b	14±7b	20±17b	159±126a	34±78b	135±145a	82±71ab	3±1b	***
Sn	7.13±19.47	3.62±2.05	5.11±4.06	1.75±1.91	3.47±1.80	5.76±6.69	4.15±2.18	3.65±1.94	ns
Sb	0.60±0.24b	0.62±0.25ab	1.80±1.31a	0.44±0.27b	0.91±0.38ab	1.67±1.84a	1.75±0.84a	1.97±1.03a	***
Cs	29±42c	17±10c	24±26c	28±42c	36±45bc	195±312b	31±38bc	1449±1715a	***
Ba	0.23±0.14b	2.77±1.21a	0.49±0.31b	3.20±1.81a	2.48±2.57a	0.38±0.35b	3.22±3.01a	2.02±0.65a	***
La	1.21±2.89d	29.65±14.80a	1.59±0.92d	1.62±1.67d	3.46±3.04cd	1.45±1.14d	21.89±25.59b	8.23±4.24c	***
Ce	2.09±5.18bc	5.84±2.54b	1.97±1.21bc	2.09±2.96bc	1.28±0.66c	2.21±1.65bc	13.19±7.67a	4.04±1.17bc	***
Pr	0.21±0.53d	4.28±1.96a	0.26±0.16cd	0.23±0.23cd	0.40±0.29cd	0.21±0.19d	3.04±3.32b	0.95±0.36c	***
Nd	0.70±1.19d	16.19±7.16a	1.05±0.58cd	0.87±0.87cd	1.50±0.99cd	0.84±0.80d	10.78±11.06b	3.58±1.46c	***
Sm	0.13±0.10d	2.30±1.05a	0.23±0.12cd	0.19±0.11d	0.28±0.16cd	0.19±0.14d	1.72±1.62b	0.56±0.19c	***
Eu	0.052±0.024d	0.878±0.370a	0.091±0.031d	0.274±0.115c	0.245±0.188c	0.077±0.047d	0.430±0.255b	0.327±0.096bc	***
Gd	0.14±0.12e	2.31±1.10a	0.25±0.11de	0.21±0.13de	0.32±0.20d	0.20±0.13de	1.69±1.60b	0.77±0.25c	***
Dy	0.09±0.06c	1.00±0.40a	0.18±0.11c	0.12±0.10c	0.20±0.12c	0.13±0.09c	1.21±1.20a	0.55±0.22b	***
Ho	0.019±0.010d	0.189±0.069a	0.038±0.022cd	0.027±0.019cd	0.045±0.027c	0.028±0.019cd	0.247±0.246a	0.117±0.041b	***
Er	0.050±0.033d	0.504±0.180b	0.107±0.077cd	0.079±0.068cd	0.129±0.084c	0.075±0.058cd	0.746±0.722a	0.322±0.142b	***
Tm	0.008±0.004e	0.047±0.015b	0.011±0.010de	0.012±0.012de	0.019±0.014cd	0.010±0.008de	0.094±0.091a	0.035±0.014bc	***
Yb	0.057±0.027e	0.304±0.108b	0.100±0.071de	0.096±0.068de	0.154±0.129cd	0.089±0.046e	0.629±0.523a	0.237±0.096bc	***
Hg	89 ±230	2 ±1	1±1	2±1	49±204	4±6	2±0	1±1	ns
Pb	3.8±2.9c	11.1±7.0ab	5.3±2.4bc	4.4±3.7bc	4.7±2.0bc	9.2±12.2b	16.1±4.7a	5.7±1.4bc	***
U	0.363±0.365b	0.073±0.036b	0.680±0.784a	0.123±0.137b	0.206±0.135b	0.510±0.412ab	0.519±0.422ab	0.131±0.090b	**

Table 2. Performance and dummy matrix of the PLS-DA models performed to discriminate avocados using all the variables and the selected markers after a variable reduction procedure. Results are given on the basis of a double cross-validation repeated 50 times.

Model	Mean overall BER [(a)]	Class	Mean class Error [(b)]	Predicted as Spanish	Predicted as non-Spanish	p-value [(c)]
All variables	0.02 ± 0.01	Spanish	0.02 ± 0.01	2389	61	< 0.001
		Non-Spanish	0.02 ± 0.02	102	3998	
Potential markers	0.02 ± 0.00	Spanish	0.02 ± 0.00	2391	59	< 0.001
		Non-Spanish	0.02 ± 0.00	100	4000	

[(a)] Mean overall balanced error rate (BER) values with the standard deviation and [(b)] mean class error values with the standard deviation calculated on the basis of 50 PLS-DA sub-models in a double-cross validation scheme. [(c)] Model statistical significance calculated from a permutation test (N=1000) using the number of misclassifications (NMC) as diagnostic statistics.

Figure captions

Figure 1. Graphical outputs of the partial least squares discriminant analysis (PLS-DA) performed to discriminate Spanish from non-Spanish avocados using all the stable isotope measurements and element profile. (a) Scores plot for components 1 and 2 (X-variate 1 and X-variate 2); (b) loadings plot for components 1 and 2; (c) Ypredict plot that shows predicted Y values for each sample during the 50 repetitions (outer loop) of the double-cross validation. (d) Histogram of the components optimized for the 50 PLS-DA models during the double cross validation.

Figure 2. (a) Scores and (b) loadings plot of the principal component analysis (PCA) performed on the avocado samples using all the stable isotopes and elements analysed. (c) Scores and (d) loadings plot of the PCA performed on the avocado samples using the main discriminatory variables selected in an iterative variable reduction procedure.

Figure 3. Graphical outputs of the partial least squares discriminant analysis (PLS-DA) performed to discriminate Spanish from non-Spanish avocados using the stable isotopes and elements selected as markers. (a) Scores plot for component 1 (X-variate 1); (b) loading contribution barplot on component 1. Colour indicates the class for which the compound has a maximal mean value. Bar length represents the multivariate regression coefficient with either a positive or negative sign for that particular feature of each component, i.e., the importance of each variable in the model. (c) Ypredict plot that shows predicted Y values for each sample during the 50 repetitions (outer loop) of the double-cross validation. (d) Histogram of the components optimized for the 50 PLS-DA models during the double cross validation.

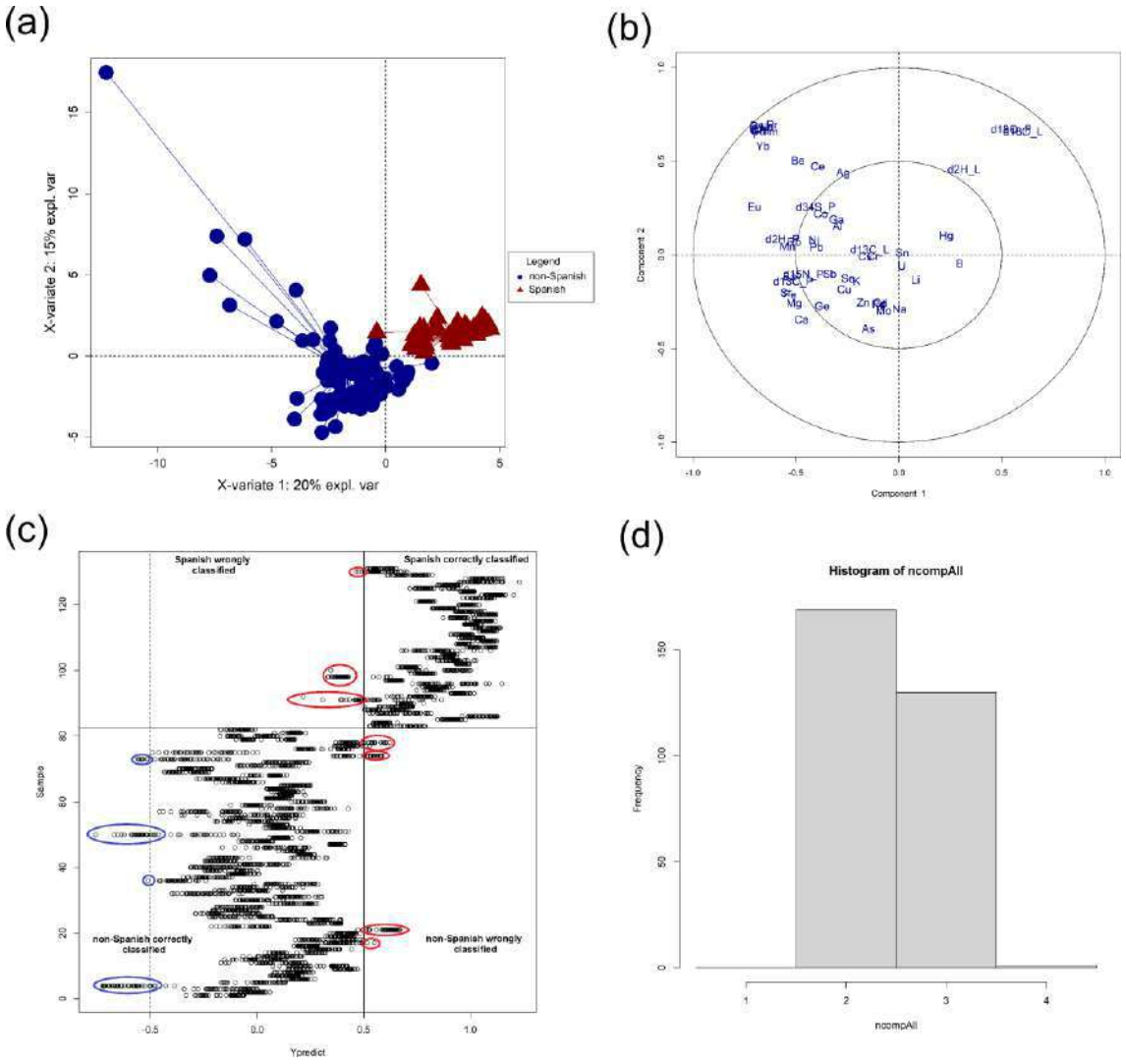
(a)
X-variate 2: 15% expl. var
X-variate 1: 20% expl. var
Legend
non-Spanish
Spanish
(b)
Component 2
Component 1
(c)
Spanish wrongly classified
Spanish correctly classified
non-Spanish correctly classified
non-Spanish wrongly classified
Sample
Ypredict
(d)
Histogram of ncompAll
Frequency
ncompAll

Figure 1.

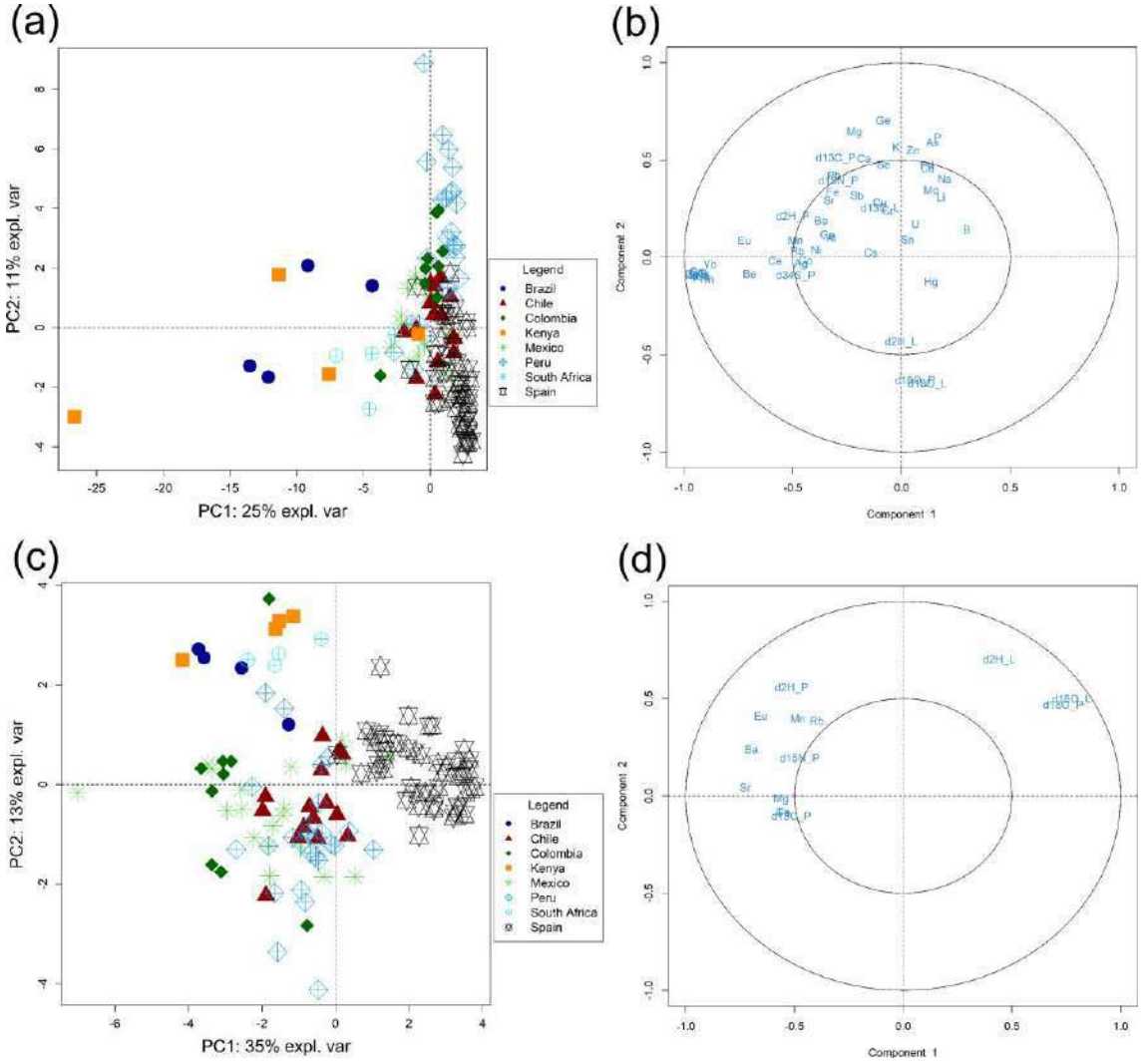
(a)
PC2: 11% expl. var
PC1: 25% expl. var
Legend
Brazil
Chile
Colombia
Kenya
Mexico
Peru
South Africa
Spain
(b)
Component 2
Component 1
(c)
PC2: 13% expl. var
PC1: 35% expl. var
Legend
Brazil
Chile
Colombia
Kenya
Mexico
Peru
South Africa
Spain
(d)
Component 2
Component 1

Figure 2.

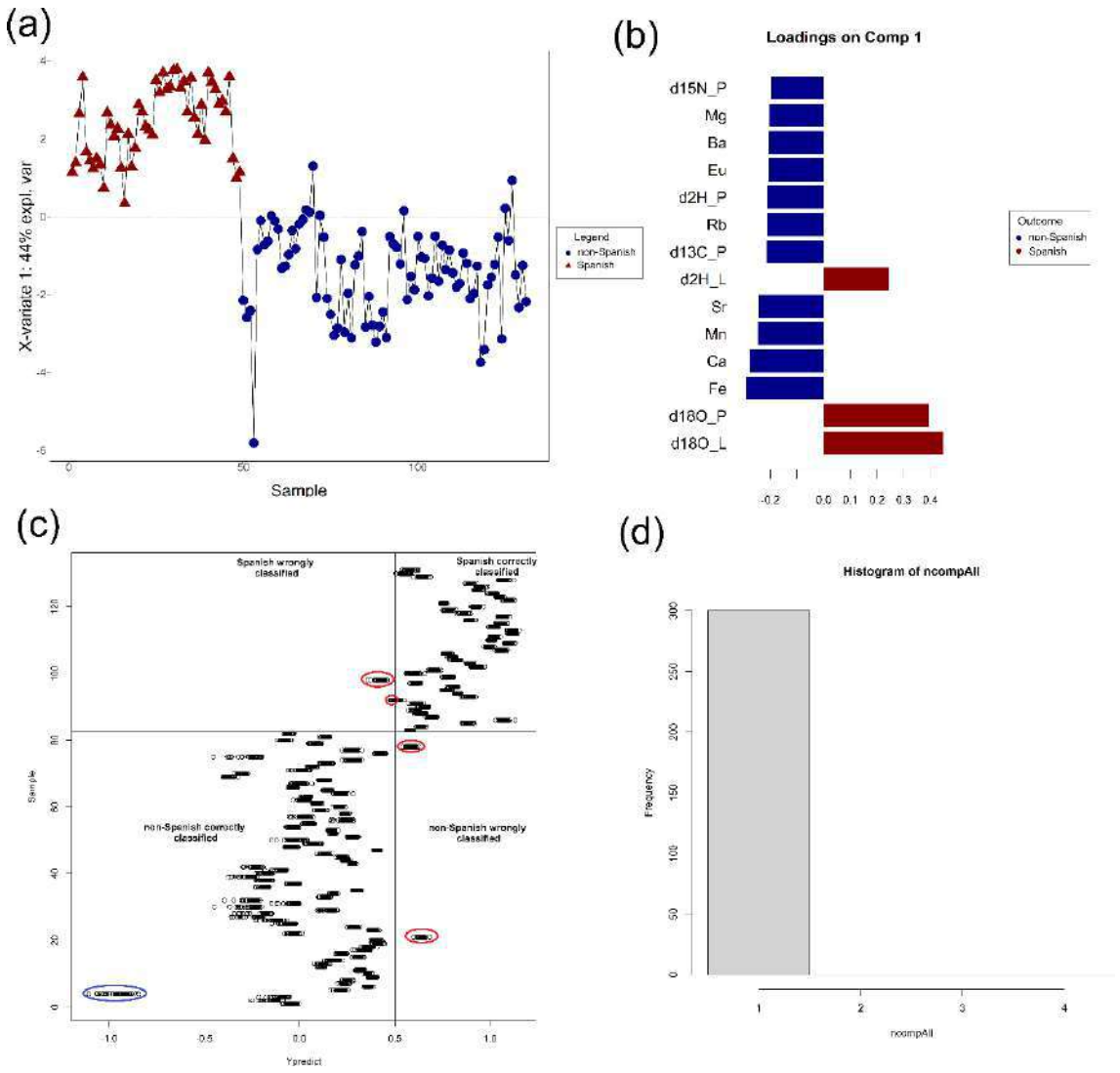
(a)
X-variate 1: 44% expl. var
Sample
Legend
non-Spanish
Spanish
(b)
Loadings on Comp 1
d15N_P
Mg
Ba
Eu
d2H_P
Rb
d13C_P
d2H_L
Sr
Mn
Ca
Fe
d18O_P
d18O_L
Outcome
non-Spanish
Spanish
(c)
Spanish wrongly classified
Spanish correctly classified
non-Spanish correctly classified
non-Spanish wrongly classified
Sample
Ypredict
(d)
Histogram of ncompAll
Frequency
ncompAll

Figure 3.

Conclusiones

De los resultados obtenidos en la presente Tesis Doctoral se ha llegado a las siguientes conclusiones:

- Se optimizó y validó exitosamente un método para determinar un total de 26 terpenos en vinos espumosos mediante HS-SPME-GC-MS. Los resultados mostraron buena linealidad, sensibilidad y precisión para todos los terpenos evaluados. Asimismo, la metodología desarrollada demostró su utilidad al ser aplicada a muestras de Champagne, Cava y vinos espumosos andaluces, revelando las principales diferencias relativas a estos compuestos.
- Los resultados de esta investigación mostraron el efecto de la segunda fermentación en botella sobre el perfil de ésteres de vinos espumosos. Se estableció el potencial del vino base de partida como mecanismo para para producir vinos espumosos con un carácter distintivo. Asimismo, la combinación de HS-SPME-GC-MS con métodos estadísticos supervisados demostró ser una potente herramienta para estudiar el aroma desde un punto de vista holístico, teniendo en cuenta las interacciones entre los distintos compuestos.
- Se demostró el impacto de la maceración pre-fermentativa sobre el perfil de ésteres de vinos espumosos y se identificaron los ésteres que sufrieron un mayor cambio. Este proceso se caracterizó principalmente por producir vinos espumosos con mayores niveles de ésteres etílicos de ácidos grasos ramificados, cinamatos y ésteres metílicos de ácidos grasos, así como menores niveles de ésteres etílicos de ácidos grasos, acetatos de alcoholes superiores y ésteres isoamílicos de ácidos grasos. Por otro lado, se puso de manifiesto el efecto de la crianza sobre lías durante los nueve primeros meses y se establecieron interacciones entre el proceso de crianza y la maceración pre-fermentativa, encontradas principalmente en los acetatos de alcoholes superiores y los ésteres etílicos de ácidos grasos ramificados.
- Se establecieron los principales cambios en el perfil químico, de ésteres y sensorial de vinos rosados fermentados mediante inoculación secuencial, usando una combinación de levaduras *Saccharomyces* y *no Saccharomyces*. Los resultados pusieron de manifiesto el uso de este tipo de estrategias de fermentación como alternativa a la convencional, para producir vinos con propiedades sensoriales distintivas.
- Se estableció una metodología de procesado de datos y análisis estadístico para estudiar la modulación del metaboloma de vinos rosados y su relación

con los descriptores sensoriales. Esta metodología permitió estudiar los cambios más importantes en el perfil metabólico (volátil y no volátil) de los vinos sometidos a distintos procesos de fermentación y se demostró la importancia de utilizar métodos estadísticos integrativos para comprender los complejos efectos de interacción.

- Se optimizó y validó exitosamente un método para determinar un total de 28 ésteres en brandies mediante HS-SPME-GC-MS. Los resultados mostraron buena linealidad, sensibilidad y precisión para todos los terpenos evaluados. Asimismo, la metodología desarrollada demostró su utilidad al ser aplicada a muestras de Brandy de Jerez de *Solerajes* con distintos tiempos de crianza, poniendo de manifiesto la modulación de los ésteres durante este proceso.
- Se estableció el impacto sobre el perfil de ésteres del proceso de estabilización por frío y filtración del Brandy de Jerez, y se comparó con la estabilización a temperatura ambiente. Se determinó que la estabilización por frío modificó más levemente el perfil de ésteres, pero redujo con éxito las concentraciones de los ésteres etílicos de ácidos grasos de cadena larga, implicados en la formación de neblinas indeseadas.
- Se desarrolló una metodología analítica basada en isotopos estables y análisis multi-elemental, en combinación con técnicas quimiométricas, con la capacidad de discriminar los mangos y aguacates producidos en la zona de la costa andaluza, de los producidos en otras zonas mundiales. Los resultados abordan un tema esencial para apoyar la existencia de una Indicación Geográfica Protegida de mangos y aguacates españoles.

Conclusions

The main conclusions obtained from the research of this Doctoral Thesis are listed below:

- A method for the determination of 26 terpenes in sparkling wines based on HS-SPME-GC-MS was successfully optimized and validated. The results showed good linearity, sensitivity and precision for all the terpenes evaluated. Then, the developed methodology was successfully applied to characterize the terpene profile of Champagnes, Cavas and Andalusian sparkling wines, revealing the main differences related to these compounds.

- The results of this research showed the effect of the second fermentation in bottle on the ester profile of sparkling wines. The potential of the base wine as a mechanism to produce sparkling wines with a distinctive character was established. The combination of HS-SPME-GC-MS with supervised statistical methods proved to be a powerful tool to study the aroma from a holistic point of view, by considering the interactions among the different compounds.

- The impact of the pre-fermentative maceration on the ester profile of sparkling wines was revealed and the esters that underwent the greatest changes were identified. This process was linked to higher contents in the sparkling wines of ethyl esters of branched fatty acids, cinnamates and methyl esters of fatty acids, as well as lower levels of ethyl esters of fatty acids, higher alcohol acetates and isoamyl esters fatty acids. On the other hand, the effect of ageing on lees was revealed during the first nine months and interactions were established between this ageing process and the pre-fermentative maceration, mainly found in higher alcohol acetates and ethyl esters of branched fatty acids.

- The main changes related to the sequential fermentation, using a combination of *Saccharomyces* and *non-Saccharomyces* yeasts, over the chemical, ester and sensory profile of rosé wines were established. The results revealed the use of this type of fermentation strategy as an alternative to the conventional one, to produce wines with distinctive sensory properties.

- A data processing and statistical analysis pipeline was established to study the modulation of the rosé wine metabolome and its relationship with the sensory descriptors. This methodology made it possible to study the most important changes in the metabolic profile (volatile and non-volatile) of the wines subjected to different fermentation processes and the importance of

using integrative statistical methods to understand the complex interaction effects was demonstrated.

- A method to determine 28 esters in brandies using HS-SPME-GC-MS was successfully optimized and validated. The results showed good linearity, sensitivity and precision for all the terpenes evaluated. Then, the developed methodology successfully applied to characterize samples of Brandy de Jerez from *Solerajes* with different aging times, showing the modulation of the esters during this process of ageing.

- The impact of the cold stabilization and filtration process on the ester profile of Brandy de Jerez was established and compared with the stabilization at room temperature. The cold stabilization process results in a lower impact on the ester profile of the brandies while successfully reducing the concentrations of the ethyl esters of long chain fatty acids, which are involved in the unwanted haze formation.

Bibilografía

Antalick, G., Perello, M.-C., & de Revel, G. (2010). Development, validation and application of a specific method for the quantitative determination of wine esters by headspace-solid-phase microextraction-gas chromatography–mass spectrometry. *Food Chemistry*, *121*(4), 1236–1245.

Antalick, G., Perello, M.-C., & de Revel, G. (2014). Esters in wines: New insight through the establishment of a database of French wines. *American Journal of Enology and Viticulture*, *65*(3), 293–304.

AvoGo Consulting. (2020, November 8). Principales variedades de mango en España. *AvoGo Consulting*. https://avogoconsulting.com/subtropicales/principales-variedades-de-mango-en-espana/

Bertrand, A. (1983). Volatiles from grape must fermentation. *Flavour of Distilled Beverages: Origin and Development/Editor, JR Piggott*.

Bhuyan, D. J., Alsherbiny, M. A., Perera, S., Low, M., Basu, A., Devi, O. A., Barooah, M. S., Li, C. G., & Papoutsis, K. (2019). The odyssey of bioactive compounds in avocado (Persea americana) and their health benefits. *Antioxidants*, *8*(10), 426.

Bill, M., Sivakumar, D., Thompson, A. K., & Korsten, L. (2014). Avocado fruit quality management during the postharvest supply chain. *Food Reviews International*, *30*(3), 169–202.

Black, C. A., Parker, M., Siebert, T. E., Capone, D. L., & Francis, I. L. (2015). Terpenoids and their role in wine flavour: Recent advances. *Australian Journal of Grape and Wine Research*, *21*, 582–600.

Boletín Oficial la Junta Andalucía. (2018). *Consejería de Agricultura Pesca y Desarrollo rural. Orden de 28 de junio de 2018, por la que se aprueba el expediente técnico de Indicación Geográfica "Brandy de Jerez"* (127, 19–20).

Brereton, R. G., Jansen, J., Lopes, J., Marini, F., Pomerantsev, A., Rodionova, O., Roger, J. M., Walczak, B., & Tauler, R. (2018). Chemometrics in analytical

chemistry—part II: Modeling, validation, and applications. *Analytical and Bioanalytical Chemistry*, *410*(26), 6691–6704.

Câmara, J., Alves, M. A., & Marques, J. C. (2006). Changes in volatile composition of Madeira wines during their oxidative ageing. *Analytica Chimica Acta*, *563*(1–2), 188–197.

Câmara, J. de S., Herbert, P., Marques, J. C., & Alves, M. A. (2004). Varietal flavour compounds of four grape varieties producing Madeira wines. *Analytica Chimica Acta*, *513*(1), 203–207.

Campo, E., Ferreira, V., Escudero, A., & Cacho, J. (2005). Prediction of the wine sensory properties related to grape variety from dynamic-headspace gas chromatography- olfactometry data. *Journal of Agricultural and Food Chemistry*, *53*(14), 5682–5690.

Cantagrel, R., Lurton, L., Vidal, J. P., & Galy, B. (1990). La distillation charentaise pour l'obtention des eaux-de-vie de Cognac. *Les Eaux-de-Vie Traditionnelles d'origine Viticole*, 60–69.

Carpena, M., Fraga-Corral, M., Otero, P., Nogueira, R. A., Garcia-Oliveira, P., Prieto, M. A., & Simal-Gandara, J. (2021). Secondary Aroma: Influence of Wine Microorganisms in Their Aroma Profile. *Foods*, *10*(1), 51.

Cerdán, T. G., Goñi, D. T., & Azpilicueta, C. A. (2004). Accumulation of volatile compounds during ageing of two red wines with different composition. *Journal of Food Engineering*, *65*(3), 349–356.

Cerri, J., Thøgersen, J., & Testa, F. (2019). Social desirability and sustainable food research: A systematic literature review. *Food Quality and Preference*, *71*, 136–140.

Charters, S., & Pettigrew, S. (2007). The dimensions of wine quality. *Food Quality and Preference*, *18*(7), 997–1007.

Cortés-Diéguez, S., Rodriguez-Solana, R., Domínguez, J. M., & Díaz, E. (2015). Impact odorants and sensory profile of young red wines from four Galician (NW of Spain) traditional cultivars. *Journal of the Institute of Brewing*, *121*(4), 628–635.

Cubero-Leon, E., Peñalver, R., & Maquet, A. (2014). Review on metabolomics for food authentication. *Food Research International*, *60*, 95–107.

Cunningham, P., Cord, M., & Delany, S. J. (2008). Supervised learning. In *Machine learning techniques for multimedia* (pp. 21–49). Springer.

Danezis, G. P., Tsagkaris, A. S., Camin, F., Brusic, V., & Georgiou, C. A. (2016). Food authentication: Techniques, trends & emerging approaches. *TrAC Trends in Analytical Chemistry*, *85*, 123–132.

De-La-Fuente-Blanco, A., Sáenz-Navajas, M.-P., Valentin, D., & Ferreira, V. (2020). Fourteen ethyl esters of wine can be replaced by simpler ester vectors without compromising quality but at the expense of increasing aroma concentration. *Food Chemistry*, *307*, 125553.

Duarte, P. F., Chaves, M. A., Borges, C. D., & Mendonça, C. R. B. (2016). Avocado: Characteristics, health benefits and uses. *Ciência Rural*, *46*(4), 747–754.

Durán-Guerrero, E., Castro, R., García-Moreno, M. de V., Rodríguez-Dodero, M. del C., Schwarz, M., & Guillén-Sánchez, D. (2021). Aroma of Sherry Products: A Review. *Foods*, *10*(4), 753.

Ebeler, S. E., & Thorngate, J. H. (2009). Wine chemistry and flavor: Looking into the crystal glass. *Journal of Agricultural and Food Chemistry*, *57*(18), 8098–8108.

Escudero, A., Campo, E., Fariña, L., Cacho, J., & Ferreira, V. (2007). Analytical characterization of the aroma of five premium red wines. Insights into the role of odor families and the concept of fruitiness of wines. *Journal of Agricultural and Food Chemistry*, *55*(11), 4501–4510.

Ferrandino, A., & Lovisolo, C. (2014). Abiotic stress effects on grapevine (Vitis vinifera L.): Focus on abscisic acid-mediated consequences on secondary metabolism and berry quality. *Environmental and Experimental Botany*, *103*, 138–147.

Food and Agriculture Organization of the United Nations (FAO). (2018). *Major tropical fruits. Market Review*. http://www.fao.org/3/ca5692en/CA5692EN.pdf

Gamero, A., Manzanares, P., Querol, A., & Belloch, C. (2011). Monoterpene alcohols release and bioconversion by Saccharomyces species and hybrids. *International Journal of Food Microbiology*, *145*(1), 92–97.

Gatfield, I. L. (1992). Bioreactors for industrial production of flavours: Use of enzymes. *Bioformation of Flavours. The Royal Society of Chemistry*, 171–195.

Gonzalez, R., & Morales, P. (2017). Wine secondary aroma: Understanding yeast production of higher alcohols. *Microbial Biotechnology*, *10*(6), 1449.

González-Barreiro, C., Rial-Otero, R., Cancho-Grande, B., & Simal-Gándara, J. (2015). Wine aroma compounds in grapes: A critical review. *Critical Reviews in Food Science and Nutrition*, *55*(2), 202–218.

Grané, A., & Jach, A. (2014). *Applications of principal component analysis (PCA) in food science and technology*. John Wiley & Sons, Chichester, UK.

Guitart, A., Orte, P. H., Ferreira, V., Peña, C., & Cacho, J. (1999). Some observations about the correlation between the amino acid content of musts and wines of the Chardonnay variety and their fermentation aromas. *American Journal of Enology and Viticulture*, *50*(3), 253–258.

Guth, H. (1997). Identification of character impact odorants of different white wine varieties. *Journal of Agricultural and Food Chemistry*, *45*(8), 3022–3026.

Hirst, M. B., & Richter, C. L. (2016). Review of aroma formation through metabolic pathways of Saccharomyces cerevisiae in beverage fermentations. *American Journal of Enology and Viticulture*, *67*(4), 361–370.

Ivanović, S., Simić, K., Tešević, V., Vujisić, L., Ljekočević, M., & Go\djevac, D. (2021). GC-FID-MS Based Metabolomics to Access Plum Brandy Quality. *Molecules*, *26*(5), 1391.

Jiménez-Carvelo, A. M., González-Casado, A., Bagur-González, M. G., & Cuadros-Rodríguez, L. (2019). Alternative data mining/machine learning methods for the analytical evaluation of food quality and authenticity–A review. *Food Research International*, *122*, 25–39.

Jones, J. E., Kerslake, F. L., Close, D. C., & Dambergs, R. G. (2014). Viticulture for sparkling wine production: A review. *American Journal of Enology and Viticulture*, *65*(4), 407–416.

Khan, S. S., & Madden, M. G. (2014). One-class classification: Taxonomy of study and review of techniques. *The Knowledge Engineering Review*, *29*(3), 345–374.

Killian, E., & Ough, C. S. (1979). Fermentation esters—Formation and retention as affected by fermentation temperature. *American Journal of Enology and Viticulture*, *30*(4), 301–305.

Kotseridis, Y., & Baumes, R. (2000). Identification of impact odorants in Bordeaux red grape juice, in the commercial yeast used for its fermentation, and in the produced wine. *Journal of Agricultural and Food Chemistry*, *48*(2), 400–406.

Kuhn, N., Guan, L., Dai, Z. W., Wu, B.-H., Lauvergeat, V., Gomès, E., Li, S.-H., Godoy, F., Arce-Johnson, P., & Delrot, S. (2013). Berry ripening: Recently heard through the grapevine. *Journal of Experimental Botany*, *65*(16), 4543–4559.

Lauricella, M., Emanuele, S., Calvaruso, G., Giuliano, M., & D'Anneo, A. (2017). Multifaceted health benefits of Mangifera indica L.(Mango): The inestimable value of orchards recently planted in Sicilian rural areas. *Nutrients*, *9*(5), 525.

Les vins rosés aux Etats-Unis, une révolution—Business France. (2018). https://www.businessfrance.fr/decouvrir-la-France-article-les-vins-roses-aux-etats-unis#

Longo, M. A., & Sanromán, M. A. (2006). Production of food aroma compounds: Microbial and enzymatic methodologies. *Food Technology and Biotechnology*, *44*(3), 335–353.

Loscos, N., Hernandez-Orte, P., Cacho, J., & Ferreira, V. (2007). Release and formation of varietal aroma compounds during alcoholic fermentation from nonfloral grape odorless flavor precursors fractions. *Journal of Agricultural and Food Chemistry*, *55*(16), 6674–6684.

Lytra, G., Tempere, S., Le Floch, A., de Revel, G., & Barbe, J.-C. (2013). Study of sensory interactions among red wine fruity esters in a model solution. *Journal of Agricultural and Food Chemistry*, *61*(36), 8504–8513.

Makhotkina, O., & Kilmartin, P. A. (2012). Hydrolysis and formation of volatile esters in New Zealand Sauvignon blanc wine. *Food Chemistry*, *135*(2), 486–493.

Moreno-Ortega, G., Pliego, C., Sarmiento, D., Barceló, A., & Martínez-Ferri, E. (2019). Yield and fruit quality of avocado trees under different regimes of water supply in the subtropical coast of Spain. *Agricultural Water Management*, *221*, 192–201.

OIV. (2015). *The rosé wine market*.

OIV. (2019). *Statistical Report on World Vitiviniculture. The International Organisation of Vine and Wine*. : http: //www.oiv.int/public/medias/6782/oiv-2019-statistical-report-on-world-vitiviniculture.pdf

OIV. (2020). *Producción de vino en 2020. Primeras estimaciones OIV*.

Oliveri, P. (2017). Class-modelling in food analytical chemistry: Development, sampling, optimisation and validation issues–a tutorial. *Analytica Chimica Acta*, *982*, 9–19.

Oliveri, P., & Forina, M. (2012). Chapter 2—Data Analysis and Chemometrics. In Y. Picó (Ed.), *Chemical Analysis of Food: Techniques and Applications* (pp. 25–57). Academic Press. https://doi.org/10.1016/B978-0-12-384862-8.00002-9

Omar, C. M. Z. C. (2013). Challenges and marketing strategies of Halal products in Malaysia. *Interdisciplinary Journal of Research in Business ISSN*, *2046*, 7141.

Oms-Oliu, G., Odriozola-Serrano, I., & Martín-Belloso, O. (2013). Metabolomics for assessing safety and quality of plant-derived food. *Food Research International*, *54*(1), 1172–1183.

Ortega-Heras, M., González-Huerta, C., Herrera, P., & González-Sanjosé, M. L. (2004). Changes in wine volatile compounds of varietal wines during ageing in wood barrels. *Analytica Chimica Acta*, *513*(1), 341–350.

Peres, S., Giraud-Heraud, E., Masure, A.-S., & Tempere, S. (2020). Rose Wine Market: Anything but Colour? *Foods*, *9*(12), 1850.

Perestrelo, R., Silva, C., & Câmara, J. S. (2019). Madeira wine volatile profile. A platform to establish madeira wine aroma descriptors. *Molecules*, *24*(17), 3028.

Pineau, B., Barbe, J.-C., Van Leeuwen, C., & Dubourdieu, D. (2009). Examples of perceptive interactions involved in specific "red-" and "black-berry" aromas in red wines. *Journal of Agricultural and Food Chemistry*, *57*(9), 3702–3708.

Pleguezuelo, C. R. R., Martínez, J. R. F., Tejero, I. F. G., Ruíz, B. G., Tarifa, D. F., & Zuazo, V. H. D. (2018). Avocado (Persea americana Mill.) Trends in Water-Saving Strategies and Production Potential in a Mediterranean Climate, the Study Case of SE Spain: A Review. *Water Scarcity and Sustainable Agriculture in Semiarid Environment*, 317–346.

Polášková, P., Herszage, J., & Ebeler, S. E. (2008). Wine flavor: Chemistry in a glass. *Chemical Society Reviews*, *37*(11), 2478–2489.

Pons, M., Dauphin, B., La Guerche, S., Pons, A., Lavigne-Cruege, V., Shinkaruk, S., Bunner, D., Richard, T., Monti, J.-P., & Darriet, P. (2011). Identification of impact odorants contributing to fresh mushroom off-flavor in wines: Incidence of their reactivity with nitrogen compounds on the decrease of the olfactory defect. *Journal of Agricultural and Food Chemistry*, *59*(7), 3264–3272.

Ramey, D. D., & Ough, C. S. (1980). Volatile ester hydrolysis or formation during storage of model solutions and wines. *Journal of Agricultural and Food Chemistry*, *28*(5), 928–934.

Ribéreau-Gayon, P., Glories, Y., & Maujean, A. (2000). *Handbook of enology: The chemistry of wine stabilization and treatments*. Wiley.

Rodríguez, I., Cámara-Martos, F., Flores, J. M., & Serrano, S. (2019). Spanish avocado (Persea americana Mill.) honey: Authentication based on its composition criteria, mineral content and sensory attributes. *LWT*, *111*, 561–572.

Rodríguez-Bencomo, J. J., Muñoz-González, C., Andújar-Ortiz, I., Martín-Álvarez, P. J., Moreno-Arribas, M. V., & Pozo-Bayón, M. Á. (2011). Assessment of the effect of the non-volatile wine matrix on the volatility of typical wine aroma compounds by headspace solid phase microextraction/gas chromatography analysis. *Journal of the Science of Food and Agriculture*, *91*(13), 2484–2494.

Ruiz, J., Kiene, F., Belda, I., Fracassetti, D., Marquina, D., Navascués, E., Calderón, F., Benito, A., Rauhut, D., & Santos, A. (2019). Effects on varietal aromas during wine making: A review of the impact of varietal aromas on the flavor of wine. *Applied Microbiology and Biotechnology*, *103*(18), 7425–7450.

Santos, J. P., Arroyo, T., Aleixandre, M., Lozano, J., Sayago, I., Garcıa, M., Fernández, M. J., Ares, L., Gutierrez, J., & Cabellos, J. M. (2004). A comparative study of sensor array and GC–MS: Application to Madrid wines characterization. *Sensors and Actuators B: Chemical*, *102*(2), 299–307.

Spaho, N., Dürr, P., Grba, S., Velagić-Habul, E., & Blesić, M. (2013). Effects of distillation cut on the distribution of higher alcohols and esters in brandy produced from three plum varieties. *Journal of the Institute of Brewing*, *119*(1–2), 48–56.

Styger, G., Prior, B., & Bauer, F. F. (2011). Wine flavor and aroma. *Journal of Industrial Microbiology and Biotechnology*, *38*(9), 1145.

Sumby, K. M., Grbin, P. R., & Jiranek, V. (2010). Microbial modulation of aromatic esters in wine: Current knowledge and future prospects. *Food Chemistry*, *121*(1), 1–16.

Tsakiris, A., Kallithraka, S., & Kourkoutas, Y. (2014). Grape brandy production, composition and sensory evaluation. *Journal of the Science of Food and Agriculture*, *94*(3), 404–414.

Ubeda, C., Kania-Zelada, I., del Barrio-Galán, R., Medel-Marabolí, M., Gil, M., & Peña-Neira, Á. (2019). Study of the changes in volatile compounds, aroma and sensory attributes during the production process of sparkling wine by traditional method. *Food Research International*, *119*, 554–563.

Villamor, R. R., & Ross, C. F. (2013). Wine matrix compounds affect perception of wine aromas. *Annual Review of Food Science and Technology*, *4*, 1–20.

Visan, L., Tamba-Berehoiu, R.-M., Popa, C. N., Danaila-Guidea, S. M., & Culea, R. (2018). Aromatic compounds in wines. *Scientific Papers Series-Management, Economic Engineering in Agriculture and Rural Development*, *18*(4), 423–430.

Westerhuis, J. A., Hoefsloot, H. C., Smit, S., Vis, D. J., Smilde, A. K., van Velzen, E. J., van Duijnhoven, J. P., & van Dorsten, F. A. (2008). Assessment of PLSDA cross validation. *Metabolomics*, *4*(1), 81–89.